THE ROLE OF NEUTROPHILS IN ORAL BIOFILM FORMATION

by

Basmah Mohammed Almaarik

A thesis submitted to the University of Birmingham for the degree of

DOCTOR OF PHILOSOPHY

Periodontal Research Group

School of Dentistry

College of Medical and Dental Sciences

University of Birmingham

November 2024

Abstract

Biofilms are complex multicellular communities embedded in an extracellular polymeric substance (EPS). EPS contains extracellular DNA (eDNA), which contributes to its stability and complexity. There are many types of *in vivo* biofilms; the periodontal biofilm is one example. Bacterial biofilms are a leading cause of periodontitis, but host inflammatory responses against these are essential factors contributing to periodontal disease occurrence and severity.

The primary protective leukocyte type against oral pathogens is neutrophil. This innate immune cell constantly surveils the periodontal tissues and migrates into the gingival crevice. Neutrophils express a variety of antimicrobial mechanisms in response to pro-inflammatory signals, including degranulation, phagocytosis, and the production of web-like extracellular DNA referred to as neutrophil extracellular traps (NETs). NET production is closely related to reactive oxygen species (ROS) production. An imbalance in neutrophil antimicrobial responses in the oral cavity is thought to contribute to periodontitis.

This thesis describes the interactions of neutrophils with representative bacteria of early colonisers of periodontal biofilms, namely the streptococci *S. oralis*, *S. mitis*, and *S. intermedius* in single and mixed species scenarios. It also assesses several *in vitro* models for biofilm formation and evaluates neutrophil retention in these. Furthermore, the dynamics of neutrophils and the periodontal pathogenic strain *A. actinomycetemcomitans* were analysed and compared to the streptococcal species.

The evaluated biofilm growing methods included two dynamic models (flow cell and flow chamber) and one static model (multiwell plate) for biofilm development. The dynamic

models were found to be prone to contamination, challenging to set up, disinfect, and operate. The multiwell static system did not show these issues.

While static models do not accurately represent all aspects of the *in vivo* environment, such as fluid flow and shear stress, it was applied in this study because it addresses some of the disadvantages of the dynamic models, such as contamination, lack of reproducibility, and access to CO_2.

This work hypothesised that neutrophil NET production contributes to biofilm development by enhancing the bacterial eDNA scaffold within biofilms. On the contrary, neutrophils affected the three-species biofilms as well as *S. oralis* biofilms by decreasing biomass and eDNA content. On the other hand, the number of live bacterial cells in the biofilms increased after interacting with neutrophils. The streptococcal biofilm-activated neutrophils produced ROS. Bacterial DNA was found to activate neutrophils.

A. actinomycetemcomitans biofilm was introduced in this study because this bacterium is associated with the rapidly progressing form of periodontitis. In contrast to the tested streptococci, neutrophils failed to battle *A. actinomycetemcomitans*. There was no change in biofilm mass, thickness, or eDNA after neutrophil engagement. On the neutrophil level, a slight activity in intracellular ROS rapidly decreased. This decrease was attributed to the LtxA production in increased biofilm concentration.

In conclusion, NETs did not enhance the tested streptococcal biofilm, but neutrophils decreased the biofilm mass and its eDNA content. The pathogenic *A. actinomycetemcomitans* biofilm was not affected by neutrophils. A thorough understanding of the specific effects of neutrophils on commensal, pathogenic, and mixed biofilms and vice versa could help develop novel anti-biofilm strategies targeting neutrophils or the biofilms themselves.

Acknowledgements

First and foremost, I want to express my heartfelt gratitude to Dr Josefine Hirschfeld, my supervisor, for accepting me, a mother of four, into the split-side program scheme and managing all the difficulties that come with the program. Her essential mentorship, constant support, and insightful critiques guided me throughout my research journey.

I am also grateful to my co-supervisors, Prof. Paul Cooper and Prof. Michael Milward, for their wise and expert suggestions, which were invaluable in refining my research.

My most tremendous gratitude goes to my parents and my family, especially my husband and children, who have been a continual source of affection for me. They have made several personal sacrifices to see me succeed and have encouraged me every step of the way. This PhD would not have been possible without their understanding and support.

Sincere appreciation also goes to the University of Birmingham Dental Hospital research team for supporting me and creating an environment that always felt like home. Their kind hospitality made me feel welcome every time I returned to Birmingham. In addition, I am deeply grateful to King Saud University for their financial support through the EJSP programme, which was critical in making my PhD journey a reality rather than a possibility. Finally, I'd like to thank all of my coworkers, the EJSP team, and the entire Clinical Laboratory Sciences department staff, especially Samah Alamri and Dr. Reem Alrshoudi, for their support and friendship. The shared wisdom and collaborative moments have immensely aided my personal and intellectual development. Thank you to everyone who has contributed to this process.

Table of contents

Table of Figures

List of Tables

Abbreviations

AFU	arbitrary fluorescent units
ATCC	American type culture collection
BHI	brain heart infusion
BSA	bovine serum albumin
C3aR1	complement receptor 1 for C3a protein
CF	cystic fibrosis
CFU	colony forming unit
CLSM	confocal laser scanning microscope
CV	crystal violet
DMSO	dimethyl sulphoxide
DNAse	deoxyribonuclease
eDNA	extracellular DNA
EPS	extracellular polymeric substances
FBS	foetal bovine serum
fMLP	N-formyl-methionyl-leucyl-phenylalanine
GCF	gingival crevicular fluid
H2O2	hydorgen peroxide
HClO	hydrogen hypochlorite
HOCl	hypochlorous acid
IADR	international Association for Dental Research
ICAM	intercellular adhesion molecules
IL	interleukin
LPS	lipopolysaccharide
LtxA	leukotoxin A
MMP	matrix metalloproteinase
MNase	micrococcal nuclease
MPO	myeloperoxidase
NADPH	nicotinamide adenine dinucleotide phosphate
OD	optical density
PBS	phosphate buffered saline
PFA	paraformaldehyde
PMA	phorbol myristate acetate
PMNs	polymorpolymorphonuclear neutrophils
PRR	pattern recognition receptors
rcf	relative centrifugal force
RLU	relative light units
ROS	reactive oxygen species
SD	standard deviation
SEM	scanning electron microscopy
SOD	superoxide dismutase
TLRs	toll-like receptors

1 CHAPTER ONE: Introduction and Background

1.1 Biofilms

Biofilms are complex, well-organised communities of microorganisms that are embedded in a self-produced extracellular polymeric substance (EPS). Biofilms can be found adhering to surfaces or can be non-surface attached aggregates (Sauer et al., 2022, Alhede et al., 2011). The clustering of microorganisms leads to group behaviour which aids in surviving hostile environments (Yin et al., 2019). Bacteria and fungi are the most common microorganisms found in biofilms, followed by protozoa and algae (Raghupathi et al., 2018, Costa-Orlandi et al., 2017, Bogino et al., 2013). Within the biofilm, microorganisms are organised into compartmentalised microenvironments of diverse nutrient and oxygen levels, which can support a wide variety of microbial species.

One of the essential properties of biofilms is the ability to withstand a range of external stressors, including antimicrobial agents and immune system defences (Donlan and Costerton, 2002). The EPS is vital to biofilm survival and accounts for up to 90% of its biomass (Flemming and Wingender, 2010). The type of microorganisms, local shear stress, availability of nutrients/substrates, and the host environment are all factors that can change the composition and structure of EPS (Flemming et al., 2016). The EPS matrix can consist of exopolysaccharides, which serve as a scaffold for surface adhesion and cell cohesion; it also protects the bacteria that live within from physical and mechanical stresses (Costerton, 1999, Mulcahy et al., 2008). An EPS component that can be present in a biofilm is extracellular DNA (eDNA), which acts as an adhesive between bacterial cells to promote bacterial surface attachment and maintain biofilm structural integrity (Okshevsky and Meyer, 2015). The EPS matrix also absorbs and traps nutrients from the surrounding environment to be used by resident bacteria; it efficiently retains water through hydrogen bond interactions with hydrophilic

polysaccharides. The trapped water forms a hydrated gel structure around the microbial cells, allowing them to grow and survive. (Conrad et al., 2003, Flemming and Wingender, 2010). Despite the ability of EPS to sequester and store nutrients, biofilm cells have limited access to resources due to factors such as diffusion limitations, nutrient gradients, competition, and waste accumulation (Stewart and Franklin, 2008, Aparna and Yadav, 2008). Because of nutrient limitations, these bacterial strains within the biofilm, termed sessile bacteria, exist in a dormant or stationary phase and differ from the previous planktonic (free-floating) state by phenotypic properties, such as growth rate, metabolism, or gene expression. These properties are understood to exert an anti-immune property and play a role in biofilm survival (Stoodley et al., 2002, Vilain et al., 2004). Because of the protective EPS matrix, changing metabolic states, varied microenvironments, immune evasion techniques, intercellular communication, and direct suppression of immune cell function, sessile bacteria display resistance to host immunological responses (Boisvert et al., 2016). Another potential biofilm component are small colony variants, a subpopulation of bacteria that differ from sessile bacterial cells by their small colony size on solid agar. They are distinguished from the normal phenotype by a mutation in metabolic genes, resulting in decreased metabolic activity (Oliver et al., 2000, Besier et al., 2007, Besier et al., 2008). Under specific situations, small colony variants have the ability to revert to the normal or wild-type phenotype, a process known as phenotypic switching. This switching can occur spontaneously or in response to environmental factors (Proctor et al., 2006). The capacity of bacteria to transition between various phenotypes provides flexibility and can contribute to the persistence and chronicity of bacterial illnesses (Kahl, 2014).

1.2 Biofilms: Their Influence on Human Diseases

Biofilms have been found to play significant roles in various human diseases, as they are responsible for around 65% of chronic infections in humans (Yadav et al., 2020). Several chronic infections are associated with biofilm formation caused by *Staphylococcus aureus* (*S. aureus*). *S. aureus* is a common pathogenic bacterium that persists on host tissues such as bone and heart valves, causing endocarditis and osteomyelitis, or on medical devices such as catheters, prosthetic joints, and pacemakers (Kiedrowski and Horswill, 2011). *Candida* species are widespread fungi that create biofilms *in vivo*, particularly on medical devices and in immunocompromised patients and are frequently associated with systemic fungal infections (Chandra and Mukherjee, 2015).

Another clinically relevant example of human pathogenic biofilms *in vivo* is formed by *P. aeruginosa* in cystic fibrosis (CF) patients. *P. aeruginosa* is considered the primary cause of morbidity and mortality in CF patients (Cantin, 1995, Doggett et al., 1964).

CF is a genetic condition caused by a mutation in the CF transmembrane regulator gene, encoding an ion channel for mucus clearance on the epithelial cell surface (Riordan et al., 1989). As a result, the defective protein leads to the accumulation of thick mucoid secretions in the lungs and a decrease in airway surface liquid, leading to failure in mucociliary clearance (Matsui et al., 1998, Smith et al., 1996). This inspissated mucus offers a suitable rich environment for bacterial growth. Airway colonisation with *P. aeruginosa* in CF patients accrues early in life (Hoiby, 1974), causing impaired lung function (Emerson et al., 2002, Schaedel et al., 2002). Due to the environment of CF patients' lungs, *P. aeruginosa* undergoes a phenotypic switch to a mucoid phenotype (Doggett, 1969), which protects the bacteria from oxidative stress and immune system attacks (Krieg et al., 1988, Simpson et al., 1988).

Furthermore, *P. aeruginosa* forms a thick biofilm, which confers another protective advantage for the bacteria (Lam et al., 1980, Speert et al., 1987). Decades-long infections with *P. aeruginosa* biofilms in the lungs of CF patients provide natural models for studying biofilm adaptation under antibiotic and immune system pressure.

1.2.1 Stages of Biofilm Development on Surfaces: A Sequential Process

The initial step of biofilm synthesis is the attachment of planktonic bacteria, followed by the colonisation of a solid surface (Claessen et al., 2014). Biofilm growth can occur on a submerged surface or at an air-liquid interface (Wu et al., 2012).

Reversible attachment, irreversible attachment, micro-colony formation, maturation, and dispersal are the five stages of biofilm formation (Monds and O'Toole, 2009) (**Figure 1.1**). Bacterial contact with a surface initiates attachment, and such interaction is influenced by cell surface appendages and charge (Tuson and Weibel, 2013). In this reversible stage, bacteria can detach and re-join the planktonic population if perturbed by hydrodynamic forces (sloughing bacteria off the surface), repulsive forces (Dunne Jr, 2002), or nutrient availability (Wu and Outten, 2009). Irreversible attachment is achieved by bacteria that can withstand shear forces. The biofilm then shifts to the irreversible attachment stage, which is mediated by quorum-sensing (QS) signalling molecules, that allow bacteria to communicate and coordinate gene expression and behaviour within the biofilm (Hancock and Perego, 2004, Spoering and Gilmore, 2006). The growth of small bacterial clusters then forms micro-colonies. The microorganisms secrete EPS during this stage, which aids in forming a matrix that anchors micro-colonies to surfaces. During the maturation stage, micro-colonies grow and mature, forming a three-dimensional structure containing thicker EPS and many porous layers with water channels, providing bacteria with essential nutrients. At this stage, the

biofilm differentiates and forms specialised microenvironments. The biofilm will eventually detach from the surface and disperse as individual cells or small aggregates. Mechanical disruption, enzymatic degradation of the EPS matrix, and the release of QS molecules are all mechanisms involved in bacterial dispersal (Annous et al., 2009, Kostakioti et al., 2013).

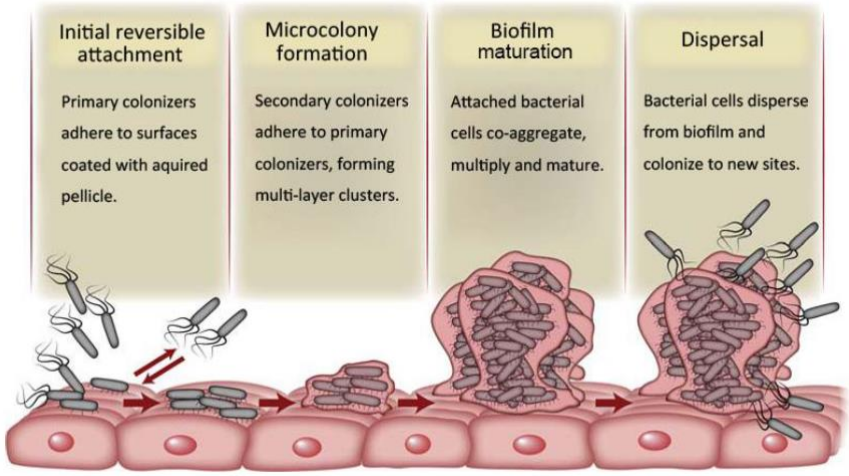

Figure 1.1: Biofilm formation steps. Biofilm formation on surfaces begins with the initial reversible attachment of planktonic cells, followed by surface adhesion (1). The attached bacteria create a microcolony monolayer and adhere irreversibly by secreting an extracellular matrix (2), followed by the emergence of multilayers (3). The biofilm matures in later stages, creating distinctive "mushroom" structures due to the presence of polysaccharides. (4). Finally, dispersal takes place when bacterial cells detach (Mansab Ali et al., 2018).

Biofilm-associated human infections can be classified into two types, depending on the surface on which the biofilms grow (Høiby et al., 2015). Biotic biofilms form on living surfaces like host tissues (e.g. mucosal surfaces, teeth), leading to diseases such as pulmonary infections in CF, diabetic foot ulcer infections, chronic otitis media and rhinosinusitis, recurrent urinary tract infections, as well as dental caries and periodontitis. Other biofilms can grow on prosthetic surfaces and are referred to as

abiotic biofilms. Such surfaces include central venous or urinary catheters, joint or dental prostheses, heart valves, endotracheal tubes, intrauterine devices and dental implants. Device-associated biofilms can spread to the surrounding tissues through biofilm cell detachment and re-localisation. Infections caused by microbial biofilms are an increasing medical concern, and biofilms are involved in 80% of human bacterial infections (Scharnow et al., 2019).

Biofilm has the potential to spread beyond the medical field. They can be found in natural ecosystems (river rock surfaces and soil ecosystems'), industrial settings (water pipes, cooling towers, and food processing equipment), marine environments (on ship hulls and coral reefs), and household surfaces (drain pipes and shower curtains). Depending on the circumstances, the influence of biofilms can be both beneficial and detrimental. While biofilms can cause corrosion, decreased efficiency, and product contamination in industrial settings, they can also be advantageous in wastewater treatment and soil nutrient cycling (Flemming and Wuertz, 2019).

1.2.2 Biofilm eDNA

The EPS can comprise DNA released by bacterial cells, which becomes incorporated into the extracellular matrix that surrounds and supports the biofilm. Whitchurch and colleagues discovered the presence of eDNA in biofilms when studying eDNA involvement in *Pseudomonas aeruginosa* (*P. aeruginosa*) biofilms (Whitchurch et al., 2002). This finding was demonstrated by the ability of the enzyme DNase 1 to destroy mature biofilm and inhibit biofilm formation. Several investigations followed to determine the origin of eDNA. The presence of eDNA in the biofilm was achieved through QS-independent and -dependent cell lysis or by cellular secretions of DNA (Thomas et al., 2008, Whitchurch et al., 2002, Allesen-Holm et al., 2006, De Kievit,

2009). Basal levels of eDNA release are caused by prophage-induced cell lysis independent of QS (Allesen-Holm et al., 2006, Webb et al., 2003). In Gram-positive bacteria, eDNA released through QS-dependent mechanisms is mediated mainly by the production of autolysins, including oral bacterial strains such as *Streptococcus oralis (S. oralis)* and *Streptococcus mutans (S. mutans)*. Autolysins, or peptidoglycan hydrolases, are endogenous bacterial enzymes involved in various cellular processes, including programmed cell death (Vollmer et al., 2008). Autolysins are essential for EPS production as they degrade cell walls and release intracellular components such as DNA and proteins that contribute to forming the EPS matrix. Autolysins also encourage biofilm detachment and dispersal by cleaving the EPS matrix and weakening cell cohesion (Paganelli et al., 2013).

Extracellular DNA provides structural support to biofilm architecture through stable filamentous networks (Böckelmann et al., 2006). It frequently forms complex networks, which may include Holliday junctions stabilised by protein anchors. These connections are crucial for sustaining the three-dimensional structure of the biofilm matrix (Devaraj et al., 2019). Furthermore, histone-like proteins, which are physically and functionally similar to eukaryotic histones, play an important role in DNA organisation inside biofilms (Stojkova et al., 2019). These proteins aid in the bending and compaction of eDNA, which is required for the dense packing found in biofilm matrices (Devaraj et al., 2019).

Furthermore, eDNA can exist in many forms in the biofilm, particularly the B- and Z-forms, which are important for biofilm architecture (Buzzo et al., 2021, Flemming and Wingender, 2010). The B-form of DNA is the most prevalent right-handed helix seen in biological systems, and it adds to the biofilm's overall structural framework (Kulkarni and Mukherjee, 2017). In contrast, the Z-form is a left-handed helix that can develop

in response to biological stress or when impacted by specific ions and proteins (Rich and Zhang, 2003). The presence of Z-form DNA in biofilms may impact the biofilm's physical qualities and its interactions with some antibacterial drugs, impacting its stability under various environmental conditions (Buzzo et al., 2021).

In the oral biofilm, studies have shown that DNase can disrupt biofilm formation in single or mixed species *in vitro* biofilms, strengthening the role of eDNA in the structural integrity of biofilms (Jakubovics and Burgess, 2015). These findings align with Whitchurch's early study, which found that eDNA is required for biofilm formation (Whitchurch et al., 2002). This was particularly evident with *S. mutans*, where adding DNA increased biofilm strength, viscoelasticity, and adhesion to hydrophobic surfaces (Das et al., 2011a, Das et al., 2011b, Peterson et al., 2013).

Extracellular DNA was proven to be specifically vital during the initial stages of biofilm formation as the concentration of eDNA in *S. mutans* biofilms peaks during the early growth phase, and DNase effectiveness in biofilm disruption decreases after the first 8 h of biofilm life (Schlafer et al., 2017, Liao et al., 2014). Moreover, in the early stages of *Enterococcus faecalis* biofilm formation, this bacterium binds to abiotic surfaces due to interactions between its eDNA and specific bacterial cell wall proteins as well as these surfaces (Bhatty et al., 2015). Isolated eDNA from endodontic infection bacteria (*Enterococcus faecalis* and *P. aeruginosa*) was suggested to trigger inflammatory responses from macrophages, indicating a potential role in exacerbating oral inflammation (Ramirez et al., 2019).

Additionally, there is evidence that eDNA may interact synergistically with glucans produced by streptococci, specifically in *S. mutans*; insoluble glucans were found to colocalise with eDNA within the biofilm matrix (Rainey et al., 2019). This colocalisation

may contribute to the biofilm's structural stability and lead to further bacterial adhesion and aggregation.

Apart from its structural importance for the biofilm, eDNA can induce antibiotic resistance by binding and chelating cations from the surrounding environment (Mulcahy et al., 2008), restricting antimicrobial diffusion (Chiang et al., 2013, Doroshenko et al., 2014), and by acidifying the local environment promoting aminoglycoside resistance (Wilton et al., 2016). In addition, eDNA mediates horizontal gene transfer (Molin and Tolker-Nielsen, 2003). It has anti-immune properties, including neutralising important cationic antimicrobial peptides (Jones et al., 2013). Furthermore, eDNA can facilitate biofilm spreading (Gloag et al., 2013) and act as a nutrient source during starvation (Finkel and Kolter, 2001). Given the prevalence of this critical EPS component, eDNA offers an ideal broad-spectrum molecular target for preventing and treating biofilm infections.

1.3 Periodontal Diseases

Oral prevalent illnesses involving inflammation affecting the gingivae and supporting tissues of the teeth (periodontium) are referred to as periodontal diseases. Plaque-induced gingivitis and periodontitis are the most prevalent types. Gingivitis occurs when bacterial biofilm accumulates (dental plaque) on the teeth adjacent to the gingiva, causing a reversible inflammatory response. Periodontitis develops when the inflammatory zone spreads to include the periodontium, resulting in the creation of periodontal pockets. If left untreated, such inflammation leads to the loss of collagen and bone tissue attachment around the tooth, resulting in tooth loosening and, eventually, tooth loss (Loesche and Grossman, 2001).

According to the World Health Organisation, periodontal diseases are the 11th most prevalent disease globally (Vos et al., 2017). It is the main cause of tooth loss and one of the two leading threats to oral health, the other being untreated dental caries (Benjamin, 2010, de Pablo et al., 2009).

Periodontitis was classified as either aggressive or chronic. Since 2018, both types have been grouped into a single category defined based on a stage and grade system, with 'grade' describing the risk or proof of progression rate (Papapanou et al., 2018, Tonetti et al., 2018).

The periodontal biofilm, consisting of approximately 700 species (Dewhirst et al., 2010), can resist and evade the host immune system via various mechanisms, contributing to periodontitis's chronic and destructive nature. Periodontitis destructive factors include the secretion of enzymes by macrophages and neutrophils, leading to the distruction of host proteins and immunoglobulins, as well as the formation of the protective EPS that isolates bacteria from the host immune response (Leid, 2009).

However, bacterial biofilm is not the sole factor of periodontitis. Host inflammatory responses against dental plaque, influenced by genetic and environmental modifiers, are also essential determinants of periodontal disease onset and severity (Page et al., 1997). The primary protective cell for innate host defence in periodontitis is the neutrophil, and this is found in relatively large numbers within the gingival crevice and epithelium. Neutrophil influx towards the dental plaque and the ability of oral bacteria to trigger the intra-biofilm release of neutrophil extracellular traps (NET) and antimicrobial proteins have been reported previously (Hirschfeld et al., 2015).

1.3.1 Biofilm Formation in Periodontitis

Biofilms are dynamic habitats that can form in various areas of the oral cavity, including the tooth and root surfaces (both supra- and sub-gingival). Early colonisers of supragingival biofilms are *Streptococcus* species accounting for 60-80% of all primary colonisers (Diaz and Valm, 2020). Streptococci have mechanisms for adhering to the salivary pellicle and can metabolise salivary components (Fernández-Babiano et al., 2022) as well as tolerating high oxygen concentrations and salivary flow (Gibbons et al., 1990). Recent research indicates that the aggregation of specific oral bacteria can act as an initiator for forming complex biofilm structures (Simon-Soro et al., 2022). These aggregates are not random but rather structured microbial communities that can attach to dental surfaces and facilitate subsequent colonisation by other microorganisms. *S. oralis*, *S. mitis biovar 1*, and *S. salivarius* were identified as the first bacterial species to attach as early as 4 hours after professional cleaning (Pearce et al., 1995, Teles et al., 2012). Hence, streptococci are essential for the spatial and temporal development and maintenance of oral biofilms (Bacali et al., 2022). Streptococci then become colonised with other bacteria, such as *Actinomyces* species and *Veillonella*. The plaque accumulation is highest at the gingival margins and often leads to gingival inflammation. If plaque remains undisturbed, secondary colonisers attach in the subgingival areas (Lamont and Jenkinson, 1998, Bradshaw et al., 1998). Due to reduced oxygen levels in this area, several anaerobes, including spirochetes and Gram-negative bacteria (such as black-pigmented *Bacteroides*), can thrive there (Kumar et al., 2005). During subgingival biofilm development, gingival crevicular fluid (GCF) proteins and glycoproteins are a primary source of nutrients (Donlan and Costerton, 2002). The GCF flow through the epithelial tissue is illustrated in **Figure 1.2**.

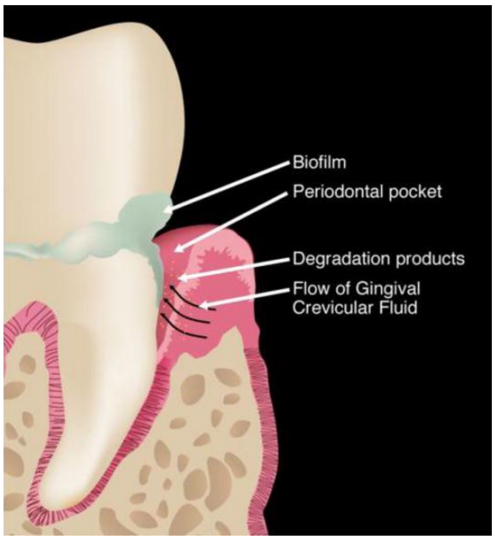

Figure 1.2: Gingival crevicular fluid (GCF) flow through oral epithelial cells in the presence of a biofilm and a periodontal pocket .(Barros et al., 2016)

Various compounds are produced from plaque bacteria adjacent to the tissue, such as hydrogen sulfide, ammonia, amines, endotoxins, and enzymes such as collagenases, all of which penetrate the gingival tissue and evoke an inflammatory response (Dahlen et al., 2019). The resulting immune response is responsible for the loss of periodontal tissue attachment (Eke et al., 2012, Meyle and Chapple, 2015, Gaffen and Hajishengallis, 2008).

1.3.2 Bacteria Causing Periodontitis

Socransky and colleagues proposed the "Socransky-microbial complexes" hypothesis (**Table 1.1**) to explain the interactions of oral bacteria in the subgingival plaque biofilm and their association with periodontitis (Socransky et al., 1998). In this hypothesis, oral bacteria were grouped into colour complexes according to the strength of their association with periodontitis. Red and orange complexes are considered the pathogenic microbial consortium associated with periodontitis.

Table 1.1: Socransky microbial complexes in the subgingival plague. *The table is adapted from (Socransky et al., 1998).*

Microbial complexes in subgingival plaque	Species
Red complex	*Porphyromonas gingivalis*
	Tannerella forsythensis
	Treponema denticola
Orange complex	*Campylobacter gracilis*
	Campylobacter rectus
	Campylobacter showae
	Eubacterium nodatum
	Fusobacterium nucleatum ssp. *nucleatum*
	Fusobacterium nucleatum ssp. *polymorphum*
	Fusobacterium nucleatum ssp. *vincentii*
	Fusobacterium periodonticum
	Peptostreptococcus micros
	Prevotella intermedia
	Prevotella nigrescens
	Streptococcus constellatus
Green complex	*Actinobacillus actinomycetemcomitans* serotype a
	Campylobacter concisus
	Capnocytophaga gingivalis
	Capnocytophaga ochracea
	Capnocytophaga sputigena
	Eikenella corrodens
Yellow complex	*Streptococcus gordonii*
	Streptococcus intermedius
	Streptococcus mitis
	Streptococcus oralis
	Streptococcus sanguis
Purple complex	*Actinomyces odontolyticus*
	Veillonella parvula
Other species	*Actinobacillus actinomycetemcomitans* serotype b *Actinomyces naeslundii* genospecies 2 (*A. viscosus*) *Selenomonas noxia*

The so-called "red complex" are bacteria found in deep pockets in the periodontium that are ‘strongly’ associated with severe forms of periodontitis (Mohanty et al., 2019). Species from the "orange complex" are hypothesised to play a role in the progression of gingivitis to periodontitis and are intermediately related to periodontal disease (Socransky et al., 1998). Some oral bacteria species cannot adhere directly to biofilms without an intermediate bacterial species being present. This specific cell-cell interaction between genetically distinct cells is known as co-aggregation and is critical in forming oral biofilms (Kolenbrander et al., 2002). The dominant species in the orange complex cluster is *Fusobacterium* species because of its versatile ability to co-aggregate and mediate the co-aggregation and communication of periodontal pathogens that do not co-aggregate intrinsically. This species is regarded as a key "bridging" organism (Oettinger-Barak et al., 2014).

The study of oral microbiota and dental plaque production has progressed from the first conceptions of Socransky complexes to more nuanced and precise explanations that use molecular and microbiological approaches. This evolution has been characterised by a better understanding of microbial community dynamics and the roles of bacteria within these communities.

Socransky classified complexes based on their cooccurrence in subgingival plaque. This model proved influential in demonstrating dental biofilms' organised nature and the species' interdependence. Recent studies have extended this work by discovering relationships and the precise roles these bacteria play (Hajishengallis and Lamont, 2016). In this article, oral communities were divided into keystone pathogens, such as *Porphyromonas gingivalis*, that, despite their low prevalence, have a disproportionate impact on their communities by dysregulating the host immune system and providing a more favourable environment for other pathogens. Their existence is critical to the

pathogenicity of the whole community. Second, accessory pathogens have been described, which may not cause disease but can worsen its severity and course. They frequently work with keystone pathogens and include *S. gordonii S. parasanguinis* (Whitmore and Lamont, 2011, Duan et al., 2016). Third, pathobionts, usually harmless microorganisms, can become pathogenic under particular conditions, such as changes in the local environment or the host immune system. These are, for example, *Fusobacterium nucleatum* (Jauregui et al., 2013).

Streptococcus species comprise the majority of the "yellow complex". The yellow complex bacteria include members of the *viridans* group streptococci, which are human commensal organisms capable of colonising the genitourinary tract and oral cavity, and they are classified based on phenotypic characteristics (Doern and Burnham, 2010). In the oral cavity, the development of the oral microbiota is strongly influenced by these streptococci as they are considered early colonisers of dental plaque, which comprise over 80% of early biofilm constituents (Kreth et al., 2009). Although the bacteria in the yellow complex are not pathogenic, their presence can contribute to the formation of dental plaque and lay the groundwork for colonisation by more pathogenic species by aggregating with other bacteria and aiding in dental biofilm formation. *S. oralis, S. mitis, S. gordonii, S. sanguinis*, and *S. intermedius* are the five organisms that represent the yellow complex in the oral cavity (Socransky et al., 1998). These streptococci have key physiological and functional characteristics that allow them to thrive in the oral cavity environment: adhesion, acid generation, and the ability to live in an environment with a wide pH range, osmolarity, and oxygen changes (Krzyściak et al., 2013, Abranches et al., 2018).

Aggregatibacter actinomycetemcomitans (*A. actinomycetemcomitans)* serotype b is one of two distinct strains that do not belong to any of the aforementioned complexes;

it is a low-abundance oral pathobiont that is highly associated with periodontitis (Fine et al., 2019). Furthermore, *A. actinomycetemcomitans* is found in more rapidly progressing forms of periodontitis (Armitage, 2010, Fine et al., 2007).

1.3.3 Oral Streptococci: The Early Colonisers

Streptococci are Gram-positive facultative anaerobic cocci. They prefer anoxic environments but can survive in the presence of oxygen. Oral streptococci are divided into four categories (Whiley and Beighton, 1998). Subsequently, a more rigorous phylogenetic approach was applied, and oral streptococci were recently classified into six different groups: *S. mitis*, *S. sanguinis*, *S. anginosus*, *S. salivarius*, *S. downei*, and *S. mutans* (Richards et al., 2014). The mitis group, which now has 20 species, is the largest of the oral cavity groups. Species within the mitis group, particularly *S. oralis* and *S. mitis*, have been difficult to distinguish based solely on 16S RNA sequences. Recent efforts to reclassify many species in this group have revealed that many strains have been misclassified and need to be described under new classifications (Jensen et al., 2016). Members of the mitis group are the first organisms discovered in newborn infants' mouths and are regarded as pioneer species (primary colonisers) that allow for the formation of a complex microbiota (Abranches et al., 2018).

One of the distinguished criterial of streptococci is their capacity to ferment a wide range of carbohydrates from salivary and food substrates. This metabolic activity, while providing them with an energy source, also has the unintended consequence of establishing an acidic environment (Abranches et al., 2018). *Streptococcus* have specific strategies to tolerate the acidic pH environment, which enables them to survive and proliferate in the oral cavity. A competitive advantage of some oral streptococci against oral pathogens is the generation of hydrogen peroxide (H_2O_2) as a byproduct

of carbohydrate metabolism. *S. oralis, S. mitis, S. sanguinis, S. gordonii*, and *S. oligofermentans* are among the recognised peroxigenic commensals (Garcia-Mendoza et al., 1993).

The majority of the oral mitis group streptococci have cell wall polysaccharides rather than capsular polysaccharides. *S. oralis* antigen is a polysaccharide consisting of glucose, galactose, rhamnose, and N-acetylgalactosamine, with N-acetylgalactosamine serving as the primary antigenic determinant (Koga et al., 1983). Intra- and inter-species horizontal gene transfer has occurred in *S. oralis* and *S. mitis* (Zähner et al., 2011). *Mitis* group streptococci possess the innate ability to achieve genetic transformation, a process known as natural competence (Ronda et al., 1988).

In addition, this group's members utilise horizontal gene transfer, including virulence gene exchange (Whatmore et al., 2000). Oral mitis streptococci, especially *S. oralis* and *S. mitis*, have anti-immune properties enabling the degradation of IgA immunoglobulin by expressing a family of IgA1 proteases, allowing bacteria to evade the functions of the predominant IgA in saliva and oral mucosal surfaces. This property promotes their colonisation and blocks their local agglutination by IgA (Cole et al., 1994, Mistry and Stockley, 2006). *S. oralis* produce enzymes, including glucosyltransferases, which catalyse glucose polymerisation, resulting in an accumulation of insoluble matrix on the teeth surface. This, in turn, creates a suitable environment for dental plaque accumulation (Koo et al., 2013, Hoshino et al., 2004). In addition, the streptococcal enzymes neuraminidases, which break down sialic acids from carbohydrates and glycoproteins, are hypothesised to contribute to plaque formation and extra-oral infections caused by oral streptococci. These enzymes enable the host sialo-glycoconjugates to degrade, revealing the underlying carbohydrate

structure and allowing the bacteria to bind more effectively. This enhanced adherence contributes to the production of biofilm and plaque on teeth (Sudhakara et al., 2019).

In conclusion, despite being commensals, oral streptococci, such as *S. oralis, S. mitis*, and *S. intermedius,* demonstrate a variety of virulence features that contribute to their pathogenicity.

1.3.4 *Aggregatibacter actinomycetemcomitans* and Its Role in Periodontitis

A. actinomycetemcomitans is a Gram-negative bacterium (formerly known as *Actinobacillus actinomycetemcomitans*) that induces a host response and has been connected to the aetiology of periodontitis (Fine et al., 2019). An *A. actinomycetemcomitans* highly virulent clone has been associated with severe periodontal deterioration in young West African populations (Haubek et al., 2008).

Several virulence factors in *A. actinomycetemcomitans* contribute to its pathogenicity. Among the most important virulence factors are: the highly toxic lipopolysaccharide (LPS) comprised of lipid A, core oligosaccharide, and O-antigen polysaccharide, which can induce inflammation and tissue destruction (Belibasakis et al., 2019). The bacterium's LPS structure differences in the O-antigen part are used for *A. actinomycetemcomitans* serotyping. At least six serotypes, labelled a-f, have been identified, with some evidence pointing to the existence of additional serotypes. These serotypes can differ in virulence and are crucial for understanding the bacterium's epidemiology (Kaplan et al., 2001).

A. actinomycetemcomitans secrete Leukotoxin (LtxA), which is highly selective for leukocytes, particularly neutrophils. LtxA can cause neutrophil and other leukocyte cytolysis, resulting in tissue injury and inflammation (Vega et al., 2019). Another toxin produced by *A. actinomycetemcomitans* is cytolethal distending toxin (Cdt) that can

cause cell cycle arrest and apoptosis in a range of host cell types and is hypothesised to contribute to the tissue death seen in periodontitis.

(Belibasakis et al., 2005). *A. actinomycetemcomitans* attaches to the host tissues by a variety of fimbriae. Fimbriae bind to extracellular matrix proteins such as fibronectin and laminin (Yoshimoto et al., 2016, Alugupalli et al., 1996). These virulence factors enable *A. actinomycetemcomitans* to bypass host defences and cause tissue injury, which can progress into periodontitis.

1.4 Biofilm Hydrodynamics

The initial and most crucial step of biofilm formation on surfaces is its attachment to a surface. This step depends on the surface type and medium hydrodynamic properties, such as flow rates and shear forces (Krsmanovic et al., 2021). The medium hydrodynamic environment influences biofilm formation, attachment, spread, and survival (Shen et al., 2015). The flow of the medium is essential during the biofilm formation phase. Fluid flow transports nutrients, oxygen, and waste products through the biofilm, whereas shear stress can cause biofilm detachment and damage. Fluid flow can impact microbial interaction within the biofilm (Liu et al., 2017). Cells in a static environment, whether in a planktonic or attached state, have limited interaction with other cells (Rijnaarts et al., 1993). The forces generated by fluid motion in the medium promote convection and cell migration (Krsmanovic et al., 2021).

Biofilms have complicated mechanical behaviours that can be defined as viscoelastic, which implies they have both fluid-like (viscous) and solid-like (elastic) qualities. When stress is applied to a biofilm, it deforms, and its reaction can be linear or nonlinear viscoelastic (Barai et al., 2016). In the biofilm linear viscoelastic response, the traction force is relatively small, and the biofilm can recover and return to its original shape

after the force is removed. While the traction forces are extensive in the non-linear viscoelastic response, the biofilm may undergo significant deformation (Krsmanovic et al., 2021). Biofilms grown under high shear stress have a dense flat or monolayer structure that resists shear due to its compactness. In contrast, biofilms grown in low shear develop a non-dense multilayer structure, allowing for better nutrient exchange, but cannot withstand mechanical impacts compared with the flat structure (Paul et al., 2012). Shear stress can enhance adhesion by increasing cell residence times on microfluidic surfaces, regardless of surface chemistry (Lecuyer et al., 2011). Whilst high-velocity flow detaches weakly adhesive cells, favouring their dispersal and the formation of small colonies elsewhere, low-velocity flow allows both highly and weakly adhesive cells to attach, promoting the formation of larger colonies (Martínez-García et al., 2018).

Moreover, bacterial surface adhesion catch bonds are known to increase their bond with increased shear stress (Nilsson et al., 2006, Mathelié-Guinlet et al., 2021). Catch bonds have been observed in various bacterial adhesins, including *Escherichia coli* FimH and staphylococcal adhesins (Huang et al., 2022, Sokurenko et al., 2008, Mathelié-Guinlet et al., 2021). This unique property enables bacteria to adhere more securely to surfaces in flow conditions typical of biofilm environments. Strengthening their adhesion in response to mechanical forces enhances bacterial colonisation and biofilm formation, contributing to the stability and resilience of these complex microbial communities. Similarly, bacteria possessing slip-bond pili can demonstrate catch-bond behaviour when subjected to simultaneous force exposure on multiple pili (Björnham and Axner, 2010).

Understanding biofilm hydrodynamics and catch bonds provides insights into bacterial biofilm formation and is critical for developing preventive and therapeutic measures to control biofilm growth.

1.5 Biofilms Models *in vitro*: Static vs Dynamic

Various in vitro biofilm models mimicking oral biofilms in periodontal disease have been described and studied (Azeredo et al., 2017). Since the first biofilm model systems were described in the mid-1900s (Pigman et al., 1952), methodologies have subsequently been modified to reflect the oral environment better. Several models have been used to grow biofilms *in vitro*. They are classified according to nutrient availability in static and dynamic models. In the static models (agar or multiwell plates), nutrients are limited over time, whereas in the dynamic models, nutrients are supplied continually by drip-fed or flow-fed systems (Santos et al., 2019). In drip-fed systems, nutrients are delivered in a semi-continuous fashion, whereas flow-fed systems provide nutrients in a continuous flow. The drip-fed systems have many examples which have been created over time and include the constant-depth film fermenter, the Sorbarod perfusion system and the drip-flow biofilm reactor (Luo et al., 2022). The flow-fed system includes the modified Robbins device (Kharazmi et al., 1999), flow cells, flow chambers, tubular flow cells, and microfluidic systems (Mosier and Cady, 2011). Biofilm models are illustrated in **Figure** 1.3. Dynamic biofilms have an advantage over static biofilms as they more closely resemble *in vivo* biofilms, as fluids circulate through the biofilm, mimicking the passage of physiological fluids *in vivo*. Furthermore, they enable live monitoring of biofilm development (Azeredo et al., 2017). One disadvantage, however, is the potential for airlock formation in closed flow channels, which alters biofilm consistency (Gomez-Suarez et al., 2001).

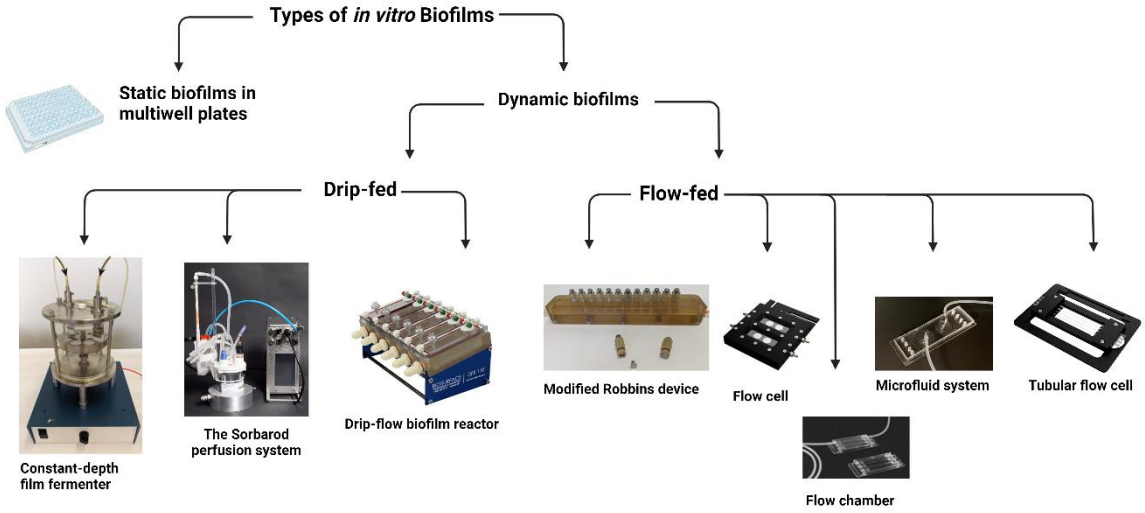

Figure 1.3: Overview of *in vitro* biofilm growth models based on nutrient availability. Static models are depicted and are characterised by limited and decreasing nutrient availability over time as well as by accumulation of bacterial waste productions. In contrast, dynamic models are shown, where nutrients are supplied continuously or semi-continuously. The dynamic models are further subdivided into drip-fed systems, including the constant-depth film fermenter, Sorbarod perfusion system, and drip-flow biofilm reactor, which deliver nutrients in a semi-continuous manner. Flow-fed systems, such as the modified Robbins device, flow cells, flow chambers, tubular flow cells, and microfluidic systems, provide a continuous nutrient flow ensuring constant availability. (Adapted from Luo et al., 2022).

While it is challenging to replicate the complexity of the *in vivo* environment when studying biofilms *in vitro,* establishing and validating *in vitro* models that capture essential aspects of biofilm behaviour is a critical unmet need. When studying the interaction of neutrophils with biofilms, the findings should be interpreted with caution because they may not be accurate for biofilms of other species or even biofilms of the same species. After all, culture conditions change biofilm features. The type of surface used for biofilm cultivation, whether culture dishes, polystyrene, glass, or metal, can significantly impact the outcome, especially in terms of bacterial adhesion. Also, applying *in vitro* findings to *in vivo* situations or from animal models to human disease is complex as biofilm models cannot accurately reflect naturally occurring diseases *in vivo*.

1.6 Neutrophils: Frontline Warriors of the Immune System

Neutrophils or polymorphonuclear neutrophils (PMNs) are the most abundant type of leukocyte in human blood, comprising up to two-thirds of all leukocytes (Dancey et al., 1976). The high number of neutrophils reflects their role as a first line of defence against microbial invaders. The name neutrophil arises from its ability to be stained by neutral dyes. Its diameter is between 9 and 15 µm, and the cell is characterised by a segmented nucleus with 2 to 5 lobules (**Figure 1.4**). Neutrophils play a crucial role in innate immunity, resolution or amplification of various pathologies such as infections, chronic inflammation, autoimmunity, and cancer (Jaillon et al., 2013). Furthermore, they directly and indirectly influence the maturation and effector functions of other leukocytes, including those of the acquired immune response (Li et al., 2019).

The production of neutrophils occurs in the bone marrow. They are then released into the blood circulation, typically remaining for less than 24 hours (Lahoz-Beneytez et al., 2016). From the circulation, they migrate to the site of infection following chemotactic gradients. Chemokines are released by other immunocompetent cells, as well as invading pathogens (Kolaczkowska and Kubes, 2013).

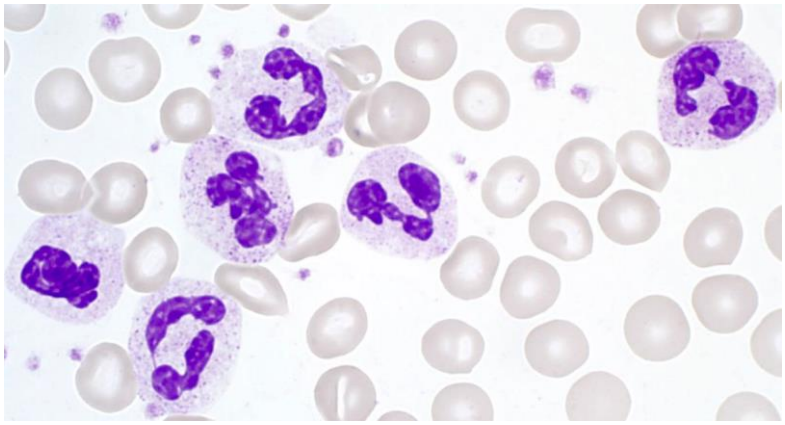

Figure 1.4: Morphology of neutrophils. Segmented granular neutrophils with red blood cells in Pappenheim-stained blood cell smears (Kraus and Gruber, 2021)

Neutrophil movement occurs via pseudopodia, which are cell surface protrusions (Roberts and Hallett, 2019). The segmented nucleus aids neutrophils in chemotactic migration from the circulation through narrow spaces of the extracellular matrix (Carvalho et al., 2015, Hoffmann et al., 2007).

1.6.1 Neutrophil Receptors

The activation of neutrophils is dependent on the effective recognition of microbial pathogens. Pathogens are recognised directly by neutrophils via innate immune receptors known as pattern recognition receptors (PRRs) which recognise pathogen-associated molecular patterns (PAMP), and subsequently activate and initiate intracellular signalling cascades (Li and Wu, 2021). G-protein-coupled seven-transmembrane receptors, Fc-receptors, adhesion molecules such as selectins/selectin ligands and integrins, various cytokine receptors, and innate immune receptors such as Toll-like receptors (TLRs) and C-type lectins are all expressed on the surface of neutrophils (Futosi et al., 2013). TLRs are type-1 transmembrane PRRs that recognise invading microbial components. For example, TLR2 allows the

neutrophil to detect peptidoglycans of Gram-positive bacteria and TLR4 detects LPS present in Gram-negative bacteria (Takeuchi et al., 1999). An illustration of neutrophil TLRs and their ligands is provided in **Figure 1.5**.

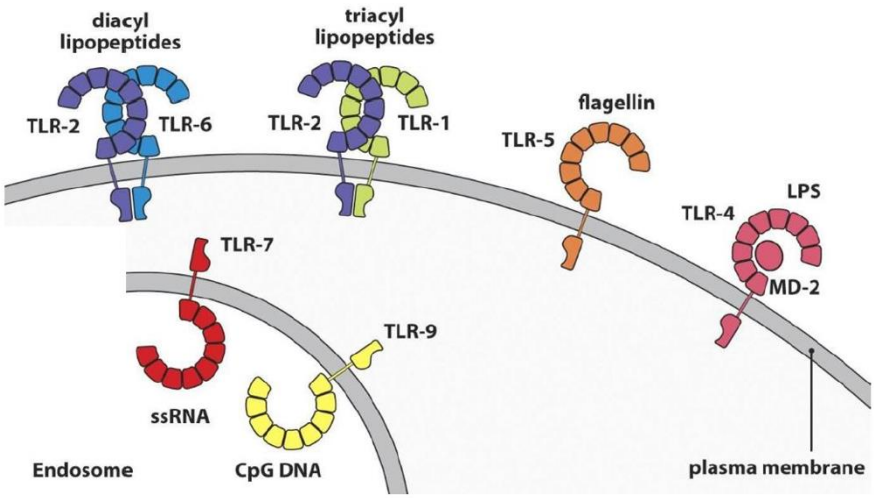

Figure 1.5: Neutrophil TLRs and their respective ligand (Vijay, 2016).

Among all TLRs, TLR-2, 4 and 9 are the neutrophil's most common receptors. TLRs are classified into two types based on their functionality and location in the host cell (Takeuchi and Akira, 2010, Behzadi et al., 2021):

The first type of TLR is expressed on the cell surface in its active form, with the external pathogen recognition ectodomain facing outside, enabling sensing and binding with alien ligands. TLR1, 2, 4, 5, 6, and 10 are included in this category. The second type of TLR class is expressed within the host cell on organelle bio-membranes such as the endoplasmic reticulum (ER), endosomes, and lysosomes. TLR3, 7, 8, and 9 are included in this group (Chang, 2010). All endosomal TLRs recognise nucleic acid ligands (Miyake et al., 2022). This endosomal compartmentalisation of TLRs limits the recognition of self-derived ligands released by dying cells which are found primarily in the extracellular space (Barton et al., 2006). Apart from this, the external pathogen

recognition domain of TLR3, 7, 8, and 9 must be cleaved by endosome-resident proteases before they can function as a receptor (Ishii et al., 2014).

1.6.2 Antimicrobial Functions of Neutrophils

Neutrophils secrete or produce proinflammatory substances that are derived from intracellular stored granules or synthesised *de novo* upon receptor stimulation. These granule-derived molecules are released by degranulating or exocytosing secretory granules. The neutrophil can also secrete a wide range of antimicrobial proteins and enzymes into phagosomes containing engulfed microorganisms or particles. Simultaneously, neutrophils expel reactive oxygen species (ROS) and cytokines to kill extracellular bacteria and recruit additional leukocytes to the site of infection or inflammation, respectively (Sheshachalam et al., 2014).

The abundance of granules of varying sizes is a distinguishing feature of neutrophils; these granules render neutrophil members of the granulocyte family. Granule formation (granulopoiesis) occurs sequentially during myeloid cell differentiation and is regulated by several myeloid transcription factors that are active at different stages of neutrophil development (Lawrence et al., 2018). There are three categories of neutrophil granules (**Figure 1.6**) based on their enzyme content and function and these are described below.

1) Azurophilic (primary) granules contain the most potent antipathogenic agents and are only released in response to relatively strong stimuli. These granules contain hydrolytic enzymes, including myeloperoxidase (MPO), antimicrobial peptides (e.g., defensins), lysozyme, and serine proteases (e.g., neutrophil elastase, cathepsin G, and proteinase 3) (Faurschou and Borregaard, 2003). Azurophilic granules are considered the microbicidal compartment mobilised during phagocytosis due to their

array of acidic hydrolases and antimicrobial proteins. Because azurophil granules lack lysosome-associated membrane proteins (LAMP), they cannot be classified as lysosomes. Instead, they appear to have the functional characteristics of a regulated secretory granule (Cieutat et al., 1998).

2) Specific granules (secondary), which contain the collagenase matrix metalloproteinase 8 (MMP8) and high levels of lactoferrin, which prevent bacterial growth by segregating the free iron required for bacterial growth.

3) Gelatinase granules (tertiary) contain metalloproteinases such as gelatinase (MMP9) and leukolysin (Borregaard, 2010).

Both secondary and tertiary granules contain nicotinamide adenine dinucleotide phosphate (NADPH) oxidase as well as the cell adhesion molecule β_2-integrin CD11b/CD18 (Mayadas et al., 2014, Lo et al., 1989). In addition to granules, human neutrophils contain secretory vesicles that contain human serum albumin, such extracellular fluid is possibly derived from endocytosis of the circulating blood plasma (Amulic et al., 2012).

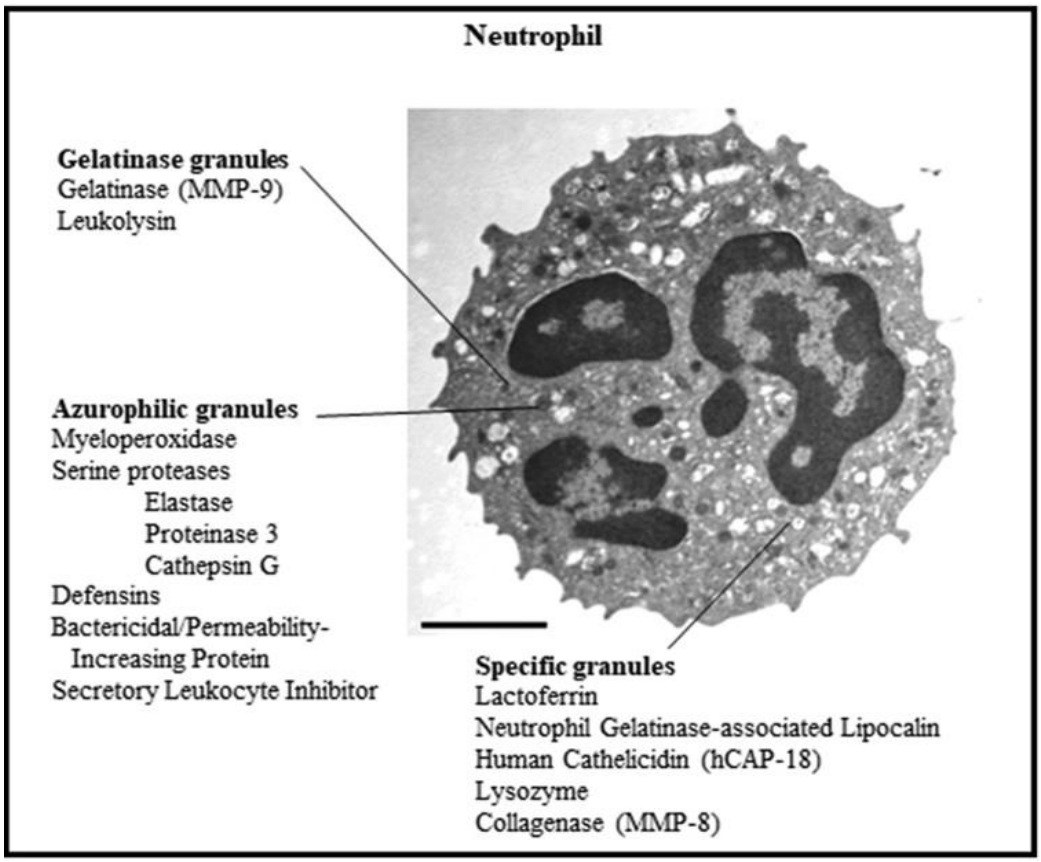

Figure 1.6: Electron micrograph of a neutrophil showing granules and their contents. Neutrophil granules have three subsets defined by their morphology, their time of biosynthesis, and their protein content. (Gigon et al., 2021)

1.6.2.1 Neutrophil Degranulation

The process by which neutrophils release granules containing antimicrobial proteins and other enzymes to target invading pathogens is known as degranulation. Subsequently to neutrophil activation, granules move towards the plasma membrane or microbe-loaded phagosomes. The granule membranes become fused either intracellularly to the phagosome or through exocytotic fusion with the plasma membrane, leading to the complete release of its contents into the extracellular environment (Borregaard and Cowland, 1997). The released mediators containing pro-inflammatory mediators (e.g., proteases), which are stored inside the granules, do not only kill invading microorganisms but also lead to host tissue collateral damage.

Different granule types are released sequentially. Tertiary granules are released first, followed by secondary granules. Finally, primary granules containing the most proinflammatory and antimicrobial proteins are secreted (Kolaczkowska and Kubes, 2013).

1.6.2.2 Neutrophil Phagocytosis

Phagocytosis is the internalisation of a microorganism or particle. Neutrophils are specialised phagocytes that are activated by a receptor-mediated process. Neutrophils phagocytose faster and have a more robust oxidative respiratory response than other innate immunity cells, such as macrophages (Nordenfelt and Tapper, 2011). The process of phagocytosis enables the clearance of microbes, dead cells and tissue debris (Jaumouillé and Waterman, 2020). For the internalisation of various particulate materials, two distinct mechanisms have been identified: 1) the trigger mechanism, in which discrete signalling initiates the formation of actin-shaped plasma membrane protrusions that surround the nearby material, and 2) the zipper mechanism, in which cell surface receptors sequentially bind to ligands on the target particle, resulting in the particle being entirely enclosed by the plasma membrane (Nordenfelt and Tapper, 2011). Phagocytosis of microbes is initiated through the recognition of opsonised foreign bodies. The recognition process can be either via the FCγR on pseudopod extensions on the neutrophil surface or by complement receptor 3 (αMβ2 integrin) uptake. The FCγR on pseudopod extension binds to the Fc portion of IgG bound to a target epitope (Nordenfelt and Tapper, 2011). TLRs and NOD receptors are not phagocytic receptors, but their activation may increase phagocytosis (Zhou et al., 2018)

Receptor activation triggers signalling cascades that re-model lipids in the cell membrane and cause actin cytoskeleton rearrangement to extend the cell membrane around the particle. After foreign bodies are internalised in phagosomes, the plasma membrane is rebuilt (Fairn and Grinstein, 2012). The neutrophil phagosome is considered mature when fused with cytoplasmic granules (Nordenfelt and Tapper, 2011). The recruitment of NADPH oxidase enables granule activation (Johansson et al., 1995). It has been proposed that the oxidative burst in neutrophil phagosomes is preceded by early alkalisation of the phagosomes (Segal et al., 1981).

1.6.2.3 Neutrophil Oxidative Burst

Oxidative burst is an oxygen-dependent process characterised by the prompt production of ROS. In fact, activated neutrophils are the most potent physiological superoxide radical producers (Silva, 2010). During activation, neutrophils' oxygen consumption can be 100 times that of their basal metabolic activity (Winterbourn et al., 2016).

In neutrophils, ROS are produced via a complex pathway involving several proteins and molecular reactions. Upon neutrophil activation, the multi-protein complex NADPH oxidase 2 (NOX_2) is assembled on the plasma membrane. NOX_2 is a membrane-bound enzyme complex that faces the extracellular space (**Figure 1.7**). Oxygen (O_2) is then converted to the highly reactive free radical superoxide anion (O_2^-) by the action of NOX_2 along with the NADPH substrate (Dahlgren and Karlsson, 1999, Roos et al., 2003).

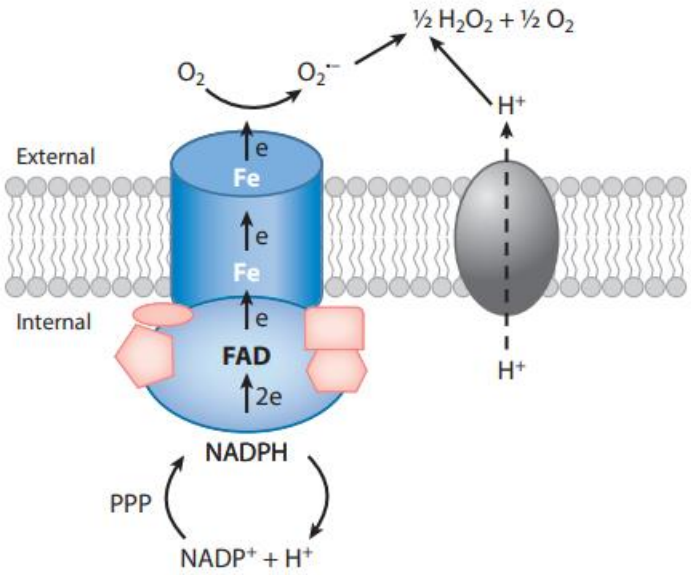

Figure 1.7: Membrane assembly of NOX_2 on the neutrophil cell membrane and ROS production. NOX_2 oxidase catalyses the directed movement of electrons from NADPH from the cytoplasm to the membrane's exterior surface. The electrons move to molecular oxygen O_2 to produce superoxide (O_2^-), which is then transformed into hydrogen peroxide (H_2O_2). H^+: hydrogen ion, NADPH: Nicotinamide adenine dinucleotide phosphate (Winterbourn et al., 2016).

NOX_2 is highly reactive; it can oxidise the total amount of NADPH present within the neutrophil (approximately 50 μM) in less than one second (Decoursey and Ligeti, 2005). When NOX_2 is active on the cell surface, superoxide is released extracellularly. However, when activity is localised to internal membranes, such as phagosomes, superoxide is released into the enclosed vesicle (Winterbourn et al., 2016). Soluble stimuli can activate NOX2 and this does not require the formation of phagosomes. An example of such stimuli is phorbol myristate acetate (PMA), which crosses the plasma membrane without the aid of a membrane receptor (Belambri et al., 2018).

As illustrated in **Figure 1.8**, the produced superoxide anion is rapidly converted to another less toxic non-radical agent H_2O_2, by the antioxidant scavenging enzyme superoxide dismutase (SOD). This occurs in order to minimise host cell damage by the

superoxide. Granule-localised MPO produces hypochlorous acid (HOCl) from H_2O_2, which can aid in clearing invading pathogens which, in turn, is converted into hydroxyl radicals HO^- (Chapple, 1996). H_2O_2 is also converted into less harmful products by SODs, catalases and peroxiredoxins (Imlay, 2008).

ROS action is not restricted to killing internally trapped or extracellular organisms. ROS can also boost the neutrophil's overall antimicrobial response by activating granule release, inducing the formation of NETs, and increasing the production of proinflammatory cytokines like tumour necrosis factor-alpha (TNF-α) and macrophage inflammatory protein 2 (MIP-2) (Brinkmann et al., 2010, Naik and Dixit, 2011, Sheshachalam et al., 2014).

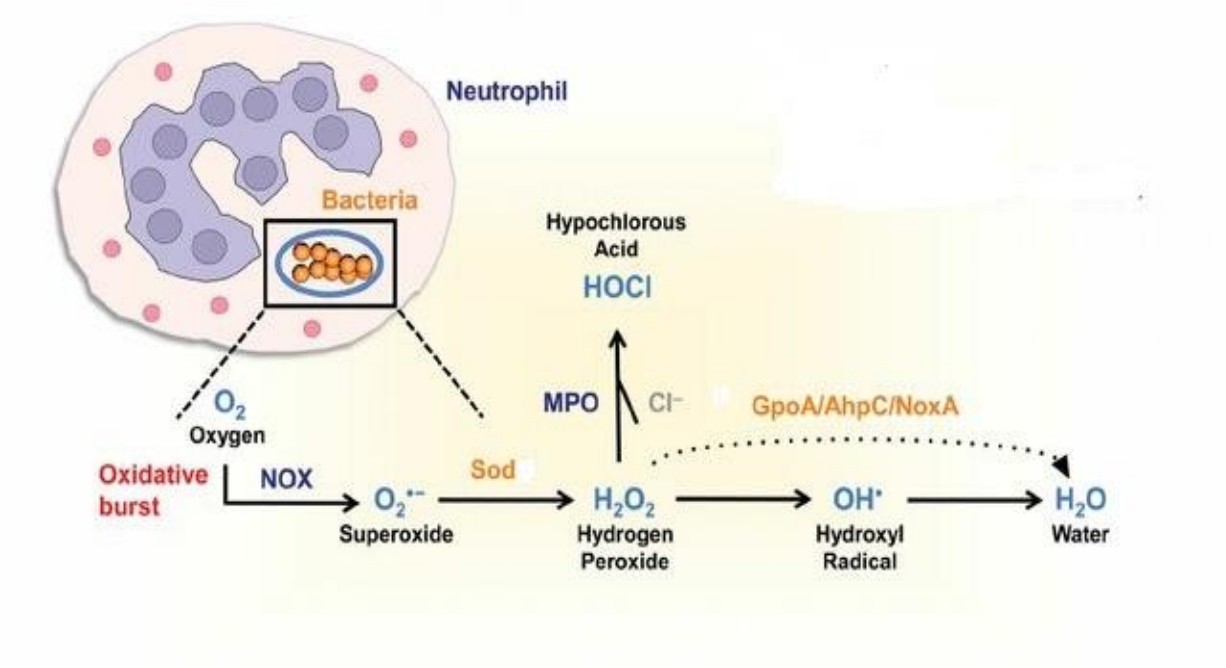

Figure 1.8: ROS generation in human neutrophils following phagocytosis of bacteria. When NADH oxidase (NOX) is activated, superoxide (O_2^-) is formed from oxygen O_2. The enzyme superoxide dismutase (SOD) converts superoxide to hydrogen peroxide (H_2O_2). During the Fenton reaction, both superoxide and H_2O_2 can be converted into hydroxyl radicals (OH). During the oxidative burst, the neutrophil enzyme MPO catalyses the formation of bactericidal hypochlorous acid HOCl from H_2O_2 and the chloride anion Cl. The enzymes Gpo, AhpC, and NoxA can detoxify H_2O_2 into water, whilst hydroxyl radicals can be converted to water after gaining an electron. (Henningham et al., 2015).

Excessive or prolonged ROS production causes local tissue damage and inflammation. In addition, chronic ROS release is also thought to contribute to the development of systemic diseases and autoimmune diseases such as chronic kidney disease (Sharma et al., 2016) and rheumatoid arthritis (Rasheed, 2008).

1.6.2.4 Neutrophil Extracellular Traps

Neutrophils have long been known for their phagocytic activity and degranulation. In 2004, Brinkmann and colleagues reported fibres released by neutrophils in response to infection; these fibres consisted of granular proteins and chromatin that form neutrophil extracellular traps (NETs). The process of NET production was referred to as NETosis. Neutrophil nuclear shape loss preceding NETosis was reported by Fuchs in 2007. Fuchs subsequently described the homogenisation of euchromatin and heterochromatin followed by a distinct change in the nuclear envelope and fragmentation of the nuclear membrane, allowing the mixing of NET constituents. Fuchs also found that NET production was reliant on ROS and NOX activity. Furthermore, NET-related cell death (suicidal NETosis) was reported to be distinct from apoptosis and necrosis (Fuchs et al., 2007).

The process of NET formation begins after neutrophil activation by inflammatory stimuli. The first step is the activation of ROS, followed by the migration of neutrophil elastase (NE) and MPO from granules to the nucleus. Peptidyl Arginine Deiminase 4 (PAD4) is a calcium dependent enzyme which participates in NET formation by converting positively charged arginine residues in chromatin-bound histones to citrulline, thereby releasing the ionic bonds that normally confine nuclear DNA to nucleosomes. The loss of positive charge on the guanidino group of arginine caused

by PAD4 action allows the DNA strands to unfurl and relax the chromatin structure, allowing NE to gain access (Li et al., 2010). NE enters the nucleus, degrades the linker histone H1 and processes core histones (Papayannopoulos et al., 2010), while MPO promotes chromatin decondensation. As a result, the nucleus loses its distinctive lobular shape, and chromatin becomes decondensed, in parallel with granular disintegration, followed by rupture of the plasma membrane and the expel of the NETs (Björnsdottir et al., 2015, Brinkmann and Zychlinsky, 2012). NETs are composed of DNA and histones as well as the before mentioned granular proteins and several cytoplasmic proteins (Brinkmann et al., 2004, Fuchs et al., 2007, Urban et al., 2006). The ejected cloudy structure observed microscopically can occupy up to 15 times the volume of the original cell (Brinkmann and Zychlinsky, 2012).

NOX-generated ROS are essential in NET formation, as NOX inhibitors have been shown to reduce NET formation (Arai et al., 2014). However, it has been reported that neutrophils can extrude NETs in response to stimuli such as calcium ionophores via NOX-independent mechanisms (Konig and Andrade, 2016, Kenny et al., 2017). Furthermore, calcium ionophore-induced NOX-independent NET formation was reported to occur via small-conductance calcium-activated potassium channel protein 3 (SK3) and mitochondrial ROS (Douda et al., 2015).

However, neutrophil destruction is not the inevitable outcome of NET formation. NETs can reportedly be produced via mitochondrial DNA extrusion instead of nuclear DNA (vital NETosis), in which neutrophils lose their mitochondrial DNA material but retain their ability to phagocytose microorganisms. This process is also ROS-dependent and is triggered through the recognition of complement component 5a (C5a) or LPS (Anderson et al., 2008, Yousefi et al., 2009, Kumar and Sharma, 2010). Unlike nuclear DNA, mitochondrial DNA binds to granular proteins after release into the extracellular

space (Yousefi et al., 2009, Yousefi et al., 2008). Another type of vital NETosis has been discovered, which is independent of ROS and includes the release of nuclear DNA in response to stimulation (Branitzki-Heinemann et al., 2016, Pilsczek et al., 2010) and activation via TLRs, as well as the complement receptor for C3 protein (C3aR1) (Clark et al., 2007, Byrd et al., 2013, Yipp et al., 2012, Douda et al., 2015). Neutrophil activation is often stimulated through the use of non-physiological chemicals such as PMA, which directly stimulates protein kinase C (PKC), resulting in the production of ROS. NETs can also be induced by host cytokines (e.g., IL-8), microbes, and microbial products such as LPS. (Björnsdottir et al., 2015, Mohanty et al., 2015). In contrast, phagocytosis of small microorganisms mediated by C-type lectin receptor Dectin-1 can obstruct NET formation, as Dectin-1 inhibits the translocation of elastase to the nucleus (Branzk et al., 2014). In addition, neutrophils can lose their capacity to produce NETs after phagocytosis of substrates, such as apoptotic cells and activated platelets (Manfredi et al., 2015). The neutrophils' fate determination between phagocytosis and NET production is influenced by many factors, including environmental conditions, the metabolic, adhesive and activation state of the phagocyte, and the type and magnitude of signals associated with the tethered phagocytic cargo (Manfredi et al., 2015).

1.6.2.5 Priming of Neutrophils

Neutrophils are the first cells to arrive at the infection site during a microbial challenge. Triggered by chemotactic factors, neutrophils transmigrate the endothelium of local capillary blood vessel walls, followed by their migration through connective tissue along the chemotactic gradient. Upon arrival, they phagocytose and kill invading microbes intracellularly via oxidative (e.g., ROS) or non-oxidative (e.g., defensins and lysozyme)

pathways. The final and most crucial step in the neutrophils battle against invading pathogens is degranulation. This occurs in two stages, the first is termed “priming”, and the second is activation. According to recent research, degranulation by secretagogue agonists occurs only if the neutrophil has been previously primed (Cowburn et al., 2008). Priming is essential for controlling the neutrophil response, and primed cells can return to the quiescent (inactive) state if no further stimuli are applied (Kitchen et al., 1996). However, if neutrophils are primed by proinflammatory cytokines, bacterial components, or ionophores, their functional response to subsequent stimulation is amplified by eliciting a pre-activation state and greater NOX activation (Condliffe et al., 1998). This pre-activation allows neutrophils to respond to subsequent stimuli more rapidly and effectively. Primed neutrophil amplified functions include boosted oxidative burst, activated actin polymerisation, and enhanced degranulation of secretory vesicles and subsets of granules (Hallett and Lloyds, 1995). The priming agent does not typically cause a noticeable functional response, except following very high concentrations of the priming agent (Swain et al., 2002). Priming is not an on/off state but rather a continuum of different activation states depending on the quantity and identity of the priming agent (Swain et al., 2002).

For priming, two distinct mechanisms have been proposed. Within minutes of being stimulated, rapid priming occurs. This type of priming is characterised by a short response time due to the transfer and release of preformed intracellular granules with pre-existing receptors to the plasma membrane. There is no active protein synthesis in this type of priming, only an increase in the number and affinity of cell surface receptors. On the other hand, delayed priming can occur. In this case, the priming agent activates transcription factors, actively synthesising new molecules including receptors and cytokines (Shah et al., 2017).

However, excessive or prolonged neutrophil priming can cause tissue damage and inflammation both locally and systemically (Shah et al., 2017).

1.7 Neutrophils and Biofilm Interactions

The intricate interaction between biofilms and neutrophils is essential for host defence and the development of numerous infectious and inflammatory disorders. Microorganisms use biofilm formation as a survival strategy to defend themselves from environmental stressors such as antimicrobial chemicals and the host's immunological response. Neutrophils interact with EPS which encloses the biofilm components. The EPS composition varies quite diversely between species and may even fluctuate depending on environmental and growth conditions. Furthermore, different species use different quorum-sensing molecules, whereas others share some molecules (Hänsch, 2012). Notably, the majority of evidence on neutrophil (or other phagocytic cell) interactions with biofilms comes from research on *P. aeruginosa or Staphylococci* biofilms.

In CF, chronic airway infection often develops in childhood, caused by pathogens such as *S. aureus* and *P. aeruginosa* (Lund-Palau et al., 2016). The infection is characterised by a neutrophil-dominant inflammation featuring elevated IL-8 levels, in which neutrophils increase 1500-fold in bronchoalveolar lavage (Khan et al., 1995, Armstrong et al., 2005, Britigan et al., 1993). The combination of infection and inflammation plays a role in recurring acute pulmonary deterioration, resulting in progressive loss of lung function (Stenbit and Flume, 2011). CF excessive and thick mucus was found to contain extracellular DNA, primarily caused by NET release (Papayannopoulos et al., 2011). Isolated strains of *P. aeruginosa* from patients were found to acquire resistance to NET-mediated killing in the chronic state of the disease

(Young et al., 2011). Although NETs do not affect CF bacterial biofilms, they contain the infection and prevent its dissemination (Thanabalasuriar et al., 2019).

Unlike *P. aeruginosa* biofilms, *S. aureus* biofilms are not intrinsically protected against attack by neutrophils or macrophages. A study found that the neutrophil phagocytes form ROS, produce NETs, and clear *S. aureus* biofilm (Meyle et al., 2010). The phagocytosis of *S. aureus* biofilms occurred without the need for opsonisation. However, an extra signal provided by immunoglobulin binding is required for ROS bacterial killing, suggesting that the cells detect biofilm components (Stroh et al., 2011, Thurlow et al., 2011).

The interaction of host defence with biofilms is also evident in the quorum-sensing system, which governs biofilm production as well as the expression of virulence factors. In *P. aeruginosa* biofilms, one of the major QS molecules, N-3-oxo-dodecanoyl-l-homoserine lactone (C12), causes neutrophil death (Singh et al., 2019). In *S. aureus* biofilm, the agr QS system induced neutrophil chemotaxis, indicating that the QS operon may also be involved in host defence regulation (Mullarky et al., 2001).

1.8 Neutrophils and Periodontitis

Neutrophils play a vital role in the oral cavity's innate immune response. They are present in large numbers within the gingival crevice and oral epithelium (Scott and Krauss, 2012). Under normal conditions, the junctional epithelium continuously secretes an IL-8 gradient to actively recruit neutrophils into the gingival crevice, as this tissue is in close contact with the oral biofilm (Curtis et al., 2011). This constant recruitment creates a symbiotic relationship between the oral microbiome and the host immune system. When dental plaque accumulates on the tooth surface near the gumline, an imbalance in the oral microbial community (dysbiosis) triggers the immune

system reaction. Subsequently, more neutrophils are attracted to the site of infection by chemokines such as IL-8, complement factors C5a, and N-formyl-peptides derived from bacteria (Dorward et al., 2015, Herrmann and Meyle, 2015). Activated neutrophils in the bloodstream start to express integrins, which bind to cell adhesion molecules (ICAMs) on the surface of endothelial cells and establish a tight adhesion that prepares the neutrophils for transmigration (Brinkmann and Zychlinsky, 2007). As a result, neutrophils migrate through the endothelium and the periodontal connective tissues towards the gingival crevice. When neutrophils reach the site of infection, they release inflammatory mediators that can damage gingival tissue and elicit an inflammatory response, aggravating gingival inflammation and contributing to the redness, swelling, and bleeding characterising gingivitis (Scott and Krauss, 2012). In a healthy immune response, the inflammation resolves once the bacterial challenge is controlled (Barton, 2008). Neutrophils undergo apoptosis (programmed cell death) and are cleared by macrophages via efferocytosis, contributing to the resolution of inflammation and tissue repair. However, in persistent gingivitis, inflammatory resolution may be hampered, resulting in continuous tissue damage and the possibility of the development to periodontitis (Chang et al., 2021).

Periodontitis is characterised by excessive and chronic activation of oral neutrophils, contributing to the periodontal tissue damage (Nussbaum and Shapira, 2011). The interaction of systemic neutrophils with greater quantities of circulating bacterial metabolites and pro-inflammatory cytokines emerging from the inflamed periodontium is related to their hyperactivity (Hirschfeld, 2019). The formed periodontal pocket has a near neutral pH at most sites and an oxygen tension of approximately 1%; these conditions are suitable for neutrophils to generate ROS, demonstrating the potential for excess ROS production in the periodontal pocket leading to tissue injury (Chapple

and Matthews, 2007). However, despite this inflammatory response, the oral bacterial infection is not contained, and hyperactive neutrophils instead contribute to a worsening of the infection state. One possible explanation is that periodontal inflammation strengthens microbial dysbiosis by creating a nutritionally favourable environment due to the accumulation of inflammatory tissue breakdown products that bacteria can use to obtain essential nutrients, including amino acids and iron (Lamont et al., 2018). This, in turn, activates neutrophils further, leading to a chronic cycle of infection and inflammation. When circulating neutrophils isolated from periodontitis patients are exposed to either a soluble stimulus, such as PMA or a bacterial stimulus, such as *Porphyromonas gingivalis*, they produce more ROS than neutrophils isolated from healthy individuals (Matthews et al., 2007a). This elevation in ROS production in the test group compared with the control group is highly dependent upon the type of stimulus used for priming neutrophils (Chapple and Matthews, 2007). Furthermore, neutrophils isolated from the oral cavity of periodontitis patients have higher plasma membrane expression of several CD markers found in neutrophil granules derived from healthy donors. This increase in granule markers, such as adhesion markers CD11b and CD66b, as well as the activation and degranulation marker CD63, suggests that neutrophils are activated for exocytosing granules (Fine et al., 2016).

Circulating and oral neutrophils in periodontitis patients share a primed phenotype as a consequence of the adhesive interactions with vascular endothelium and pro-inflammatory mediators during the neutrophil trafficking process (Lakschevitz et al., 2016). In addition, neutrophils are continuously released into the gingival crevice and the oral cavity. GCF in disease is an inflammatory exudate loaded with neutrophils, which was found to have elevated amounts of NETs in chronic periodontitis patients (Vitkov et al., 2009). Furthermore, MPO-positive NET structures were found in gingival

connective tissue following inflammation in substantial numbers compared with healthy tissue (Cooper et al., 2013).

Periodontal pathogens have developed a variety of defence mechanisms to withstand neutrophil attacks. *Treponema denticola* and *Porphyromonas gingivalis* disrupt neutrophil cytoskeleton pathways, thereby limiting neutrophil phagocytosis and protecting other bacteria in the biofilm. They also generate proteases that can destroy complement components, allowing them to avoid opsonisation and phagocytosis (Miralda and Uriarte, 2021).

In addition, Periodontal pathogens decrease neutrophil recruitment by four primary mechanisms: reducing IL-8 production, impeding chemokine detection, inhibiting E-selectin expression, and inhibiting neutrophil actin cytoskeleton rearrangement (Jiang et al., 2021). These mechanisms are illustrated in **Figure 1.9**. Moreover, several oral bacteria have the ability to produce DNase to degrade NETs (Palmer et al., 2012) as well as producing catalytic and metabolic enzymes to resist ROS mediated killing (Jiang et al., 2021).

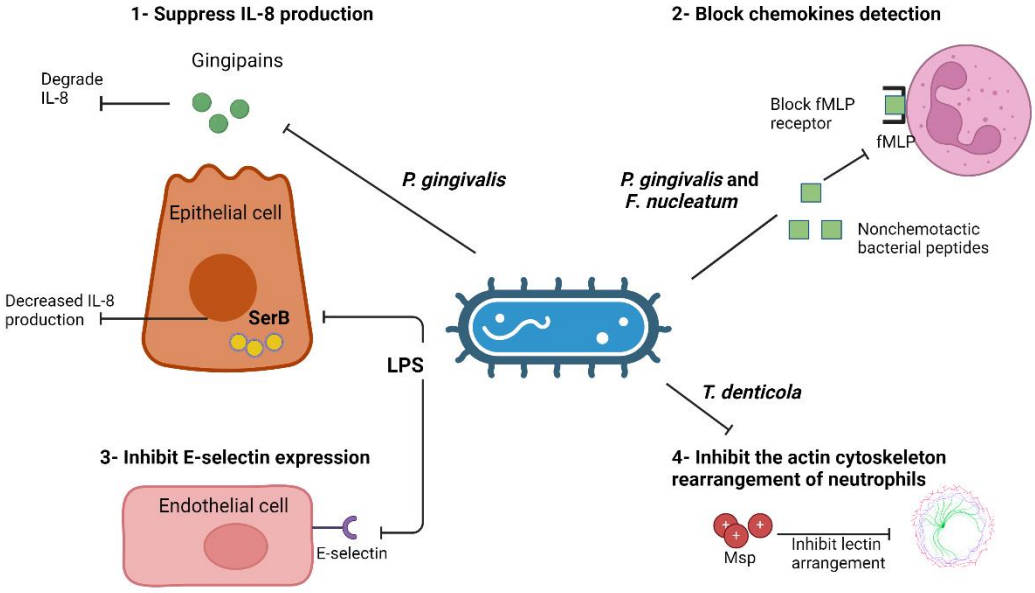

Figure 1.9: Mechanisms by which periodontal pathogens can impair neutrophil recruitment. *P. gingivalis* invades the epithelial cells and secretes SerB, which inhibits the activation of NF-κB, resulting in decreased IL-8 production. The gingipains secreted by *P. gingivalis* can degrade IL-8. *P. gingivalis* and *F. nucleatum* can inhibit fMLP-induced chemotaxis by binding nonchemotactic bacterial peptides to fMLP receptors. The LPS of *P. gingivalis* can inhibit E-selectin expression, which is necessary for neutrophil-endothelium interaction. *T. denticola* can suppress the production of IL-8 and degrade IL-8. The major outer sheath protein (Msp) of *T. denticola* can inhibit actin rearrangement, thereby preventing neutrophil recruitment.

1.9 Aims and Objectives:

The hypothesis of this thesis posited that neutrophils may contribute to the initial formation of biofilms *in vitro*, given their destructive nature and DNA production, which could enhance biofilm survival. The relationship between neutrophils and biofilms has been studied extensively (Papayannopoulos, 2019); however, this is not completely understood. Neutrophils are considered a double-edged sword of innate immunity: whilst they orchestrate the antimicrobial actions against biofilms (Hirschfeld, 2014), they also induce tissue damage and pathological changes (Ryder, 2010, Chapple and

Matthews, 2007). Current evidence shows that biofilm eDNA contributes to biofilm's structural integrity, promoting bacterial attachment and growth (Whitchurch et al., 2002, Serrage et al., 2021). However, the knowledge of how neutrophils, as essential immune effector cells, respond to and interact with eDNA within the biofilm remains limited. Accordingly, the main goal of this research was to investigate whether neutrophils have the ability to positively or negatively impact early periodontal biofilm formation *in vitro*, specifically examining changes in biomass, eDNA content, and colony-forming units (CFUs). Additionally, the study aimed to assess how the biofilm influences neutrophil activation and to identify the underlying mechanisms involved.

The first aim of this study was to develop and optimise a protocol to culture an *in vitro* biofilm. In order to address this four main objectives were applied:

1. Biofilm forming bacteria *P. aeruginosa* was used to assess different biofilm growing platforms (static vs dynamic models).
2. Neutrophil survival in different growth media was examined to assess the best media to use for neutrophil viability in this study.
3. The effect of neutrophil exposure to biofilms at different stages of biofilm development was analysed to determine the ideal timing for introducing neutrophils into the model system.
4. The ability of *S. salivarius* to form a mono-species biofilm was evaluated to standardise tested biofilm growth models on an oral bacterial strain.

The second aim of this study was to investigate the role of neutrophils in response to streptococcal species, which have been implicated in the initial stages of periodontal diseases. In order to address this second aim, the following objectives were applied:

1. Biofilm mass was assessed following neutrophil exposure versus isolated NET exposure to determine the effect of NETs on the biofilm.

2. The mechanical properties of biofilms were investigated by assessing the changes in adhesive forces of the biofilm after neutrophil exposure.
3. The biofilm eDNA content was determined to assess the involvement of neutrophils in breaking down biofilm architecture.
4. The generation of reactive oxygen species was measured to investigate how biofilms influence neutrophil antimicrobial activity.

The third aim of this study was to investigate the effect of neutrophils on disease-associated *A. actinomycetemcomitans*. The same objectives as described above were studied.

2 CHAPTER TWO: Materials and Methods

2.1 Bacteria strains and characterisation

2.1.1 Bacterial strains and growth media

Bacteria were provided by the Periodontal Research Group at the University of Birmingham School of Dentistry and originally purchased from the American Type Culture Collection (ATCC). *Streptococcus oralis* (ATCC 9811), *Streptococcus mitis* (ATCC 46456), *Streptococcus intermedius* (ATCC 27335), and *Streptococcus salivarius* (ATCC 13419) were used as representative strains for early colonisers of dental biofilms.

Aggregatibacter actinomycetemcomitans HK1651 was used as a representative periodontitis pathogen, and *Pseudomonas aeruginosa* PA01 to establish the biofilm models due to this bacterium's ability to rapidly form thick biofilms (Ghafoor et al., 2011).

Bacterial strains were grown on TSB (CM0129 Oxoid, UK) or Schaedler's agar (CM0437 Oxoid, UK) and incubated at 37°C + 5% CO_2 overnight. Up to three colonies from overnight cultures were transferred to sterile skimmed milk with 10% glycerol (Saudi Prepared Media Laboratory, SA) and stored at -80°C.

For experiments, up to three bacterial colonies were transferred from bacterial agar medium, inoculated in TSB or Schaedler's broth (CM0497B Oxoid, UK), and incubated overnight at 37°C on a shaking incubator (GFL, Germany) to reach the exponential phase. A fresh overnight culture was diluted (OD_{600} of 0.5 for *Aggregatibacter actinomycetemcomitans* HK1651 and 0.1 for other microorganisms used in this thesis). For multispecies biofilm, all strains were separately adjusted to OD_{600} 0.1, then mixed in equal numbers and cultured as described for single-species biofilm.

2.1.2 Bacterial growth curve

Growth curves were generated to quantify bacterial culture over time. 200 µl of bacterial overnight TSB culture was transferred to each well in a 96-well plates (3788 Corning, USA). Negative controls consisting of uninoculated TSB were used. The multiwell plates were then transferred to Tecan SPARK Multimode Microplate Reader (Spark®, Tecan; software SparkControl, v. 2.3, Tecan), and OD_{600} readings were recorded every 60 min for two days (37°C incubation temperature with agitation every 1 h). Experiments were performed in triplicate and repeated independently three times.

2.1.3 Bacterial deoxyribonuclease (DNase) production

Bacteria were screened for DNase production by culturing on DNA-containing agar (CM0321 Oxoid, UK), which was prepared according to the manufacturer's instructions. Bacteria were cultured on the agar for up to 3 days at 37°C+ 5% CO_2. After incubation, the plate was flooded with 1 N HCl, and positive DNase activity was visualised as clear zones surrounding colonies.

2.2 Neutrophil studies

2.2.1 Selection of donors

This research was conducted in two locations: The College of Applied Medical Sciences at King Saud University (KSU) in Riyadh, Saudi Arabia, and the School of Dentistry at the University of Birmingham (UoB), UK.

At KSU, buffy coats from healthy, unmedicated adult blood bank donors at King Khalid University Hospital (KKUH) were collected. The selection criteria for all KKUH blood donors are based on the Gulf Cooperation Council (GCC) guidelines for blood product

production and quality control. This research project was approved by the Local Research Ethics Committee (project number E-20-4671). Donated blood was separated using the Revos® automated blood processing system (TerumoBCT, Japan), and buffy coats were collected. All protocols included in this chapter were undertaken at KSU using blood bank donors' neutrophils, with the exception of ROS and NET quantification assays. These were completed at UoB (ethics reference BCHCDent 024.2024) with freshly isolated neutrophils from healthy blood donors using two 7ml lithium heparin Vacutainers (BD VACUTAINER®, USA).

2.2.2 Neutrophil isolation reagent preparation:

Neutrophils were isolated from buffy coats at room temperature under sterile conditions using a class II biological safety cabinet (Biolus BSC). Isolation was performed using Percoll gradients described previously (Haslett et al., 1985). All reagents were stored at 4°C and pre-warmed to room temperature before use.

2.2.2.1 Percoll

In a 30 ml centrifuge tube, 6 ml of 1.098 Percoll was carefully layered underneath 6 ml of 1.079 Percoll. The following **Table 2.1** details the Percoll composition. Materials were: Percoll 1.13 g/ml (17-0891-01 GE Healthcare), distilled sterile water, and 1.5 M NaCl in distilled sterile water (S9625 Merck, Germany). The percoll solution was stored at 4°C until it was used.

Table 2.1: Percoll gradient separation method composition

Density	**1.079**	**1.098**
Percoll	19.70 ml	24.82 ml
Water	11.79 ml	6.68 ml
NaCl	3.5 ml	3.5 ml

2.2.2.2 Erythrocytes lysis buffer

Blood samples were treated with a buffer solution to purify isolated neutrophils and remove erythrocyte contamination. Cell lysis buffer generates an osmotic disequilibrium and induces erythrocyte cell lysis. One litre of lysis buffer was prepared by adding 8.3 g NH_4Cl (A9434 Merck, Germany), 1 g $KHCO_3$ (P9144 Merck, Germany), 0.04 g Na_2 EDTA $2H_2O$ (E5134 Merck, Germany) and 2.5 g bovine serum albumin (BSA; A4530 Merck, Germany) to 1 litre of distilled water and stored at 4°C until use.

2.2.3 Trypan blue preparation

0.4 g of trypan blue powder (23850 Lobachemie, India) was diluted in 80 ml of PBS and heated to boiling point. Then 20 ml of PBS was added to achieve a total volume of 100 ml.

2.2.4 Method for isolation of neutrophils

Blood was layered onto Percoll density gradients in a 30 ml centrifuge tube, then centrifuged (Hettich MIKRO 200 R, Germany) for 8 minutes (min) at 150 relative centrifugal force (rcf) and for 10 min at 1200 rcf at 4°C. The plasma, lymphocyte and monocyte layers were carefully removed and discarded by manual aspiration using a disposable Pasteur pipette. The neutrophil layer directly above the red blood cell layer was transferred to a 15 ml centrifuge tube containing 10 ml lysis buffer. The centrifuge tube was gently inverted to mix and incubated at room temperature for 5-10 min until red blood cells had lysed. This solution was then centrifuged for 6 min at 500 rcf to pellet the neutrophils. The supernatant was removed, the pellet washed in 2 ml PBS, and centrifuged once more for 6 min at 500 rcf before re-suspension in 2 ml PBS. Cells

were counted using a haemocytometer (Marienfeld-superior, Germany), and viability was assessed by trypan blue exclusion (1:1 mix of cells with trypan blue) and visualisation by light microscopy using an OLYMPUS CK40 microscope (Olympus, Japan).

2.3 Neutrophil survival assay

2.3.1 Neutrophil survival in different growth media

After neutrophil isolation and counting, $2x10^5$ cells were suspended in 1 ml of each media type and incubated for 4 hours (h) at 37°C in 5% CO_2. The media tested are listed in **Table 2.2**. All samples were counted under a microscope using a haemocytometer after staining with trypan blue. RPMI + 10% was used as a positive control, and distilled H_2O as a negative control.

Table 2.2: Neutrophil survival assay - media tested

Media	Supplements	manufacturer
RPMI	RPMI 1640 medium	RPMI: 1640 Gibco, USA FBS: 10099141 Gibco, USA Glucose: TC130 Himedia YE: LP0021 Oxoid, UK TSB: CM0129 Oxoid, UK SB: CM0497B Oxoid, UK
RPMI + 10% FBS	RPMI 1640 medium Fetal bovine serum	
RPMI + 2% G	RPMI 1640 medium Glucose	
RPMI + 2% G + 0.5% YE	RPMI 1640 medium Glucose Yeast extract	
TSB	Tryptic Soy Broth	
TSB + 2% G	Tryptic Soy Broth Glucose	
TSB + 2% G + 0.5% YE	Tryptic Soy Broth Glucose Yeast extract	
SB	Schaedler anaerobe broth	
SB + 2% G	Schaedler anaerobe broth Glucose	
SB + 2% G + 0.5% YE	Schaedler anaerobe broth Glucose Yeast extract	
Artificial saliva	2.5 g porcine stomach mucins 0.2 g sodium chloride 0.2 g calcium chloride dehydrate 0.2 g Yeast extract 1.0 g Lab Lemco powder 5.0 g protease peptone	M177 Merck, Germany 102415K VWR, USA 007103020 VWR, USA LP0021 Oxoid, UK L29 Oxoid, UK L85 Oxoid, UK

Artificial saliva components in **Table 2.2** were combined, and sterile H_2O was added to give 1 L. The suspension was autoclaved at 121°C for 15 min. After autoclaving, 1.25 ml of 40% urea (SR20 Oxoid, UK) was added to artificial saliva. The media was aliquoted and stored at 4°C.

2.3.2 Neutrophil survival in low pH

Because the bacterial biofilm pH was shown to decline to 4.5 during biofilm growth, the ability of neutrophils to survive in low pH was evaluated. RPMI media containing 10%

FBS pH was adjusted to pH 4.5 using 1N HCL. Then $1x10^6$ neutrophils were suspended in 1 ml of pH-adjusted RPMI media and incubated at 37°C + 5% CO_2 for one hour. The trypan blue exclusion assay was performed to validate neutrophil survival after incubation.

2.3.3 Assay of neutrophil survival using trypan blue

Light microscopy at 20X magnification was used to assess cell viability. 100 µl of cell suspension was mixed with 100 µl of trypan blue dye (prepared as described in **Section** 2.2.3), and 10 µl of the mixture was loaded into a haemocytometer chamber. The trypan blue exclusion assay was used to measure viability, which identifies the fraction of cells with an intact outer membrane not permeable to the Trypan blue dye as being viable. Blue-stained cells were considered dead or dying due to their outer membrane being damaged. The number of viable cells was counted and multiplied by the dilution factor.

2.4 Neutrophil stimuli

Non-physiological and non-bacterial components stimuli that activate neutrophils without engaging with surface receptors were used in this investigation. PMA is a well-studied neutrophil activator that activates the PKC pathway to imitate the action of various physiological mediators (Fuchs et al., 2007), and HOCl is a product of the ROS cascade that has been demonstrated to promote NET formation (Palmer et al., 2012).

2.4.1 Phorbol 12-myristate, 13-acetate

A stock solution of 1.62 mM PMA corresponding to 1 mg/ml was prepared by dissolving 1 mg PMA powder (P8139 Merck, Germany) in 1 ml DMSO (D2438 Merck, Germany).

Further dilutions with PBS were made to achieve a working concentration of 50 mM in PBS. PMA solutions were aliquoted in a dark container and stored at -20°C. The PMA concentration used was 50 nm for NET and ROS stimulation.

2.4.2 Hypochlorous acid

HOCl was prepared by diluting sodium hypochlorite solution (425044 Merck, Germany) at a 1:10 ratio with PBS. HOCl 0.2% concentration was used to induce NETs. This dilution was made fresh as needed.

2.5 Biofilm culture

A dilution of a fresh overnight culture was used to initiate bacterial biofilms. The biofilm *A. actinomycetemcomitans* had a starting OD_{600} of 0.5, and the other microorganisms in this study had an OD_{600} of 0.1. *A. actinomycetemcomitans*' starting concentration was higher than that of other organisms in this study because of its slow growth rate, as identified by the growth curve shown in **Section** 2.1.2.

For multispecies biofilms, *S. oralis, S. mitis,* and *S. intermedius* strains were separately adjusted to OD_{600} 0.1, mixed in equal numbers and cultured as described for the single-species biofilms. For the *P. aeruginosa* biofilm, 25% BHI (CM1135 Oxoid, UK) was used according to the literature (Moormeier et al., 2014). Schaedler's broth was used for *S. salivarius* and multispecies biofilm culture. TSB was used to culture *A. actinomycetemcomitans* and *S. oralis* biofilms to create comparable biofilms in different studies.

2.5.1 Static biofilm model: multiwell plate

2.5.1.1 Sterilisation of coverslips

Circular 12 mm and 10 mm coverslips were placed in a jar containing 1 molar HCl (Scharlau) and immersed for 24 h. After carefully decanting the acid, coverslips were washed with sterile distilled water, rinsed with 100% ethanol (Merck, Germany), and dried on sterile filter paper prior to use.

2.5.1.2 Static biofilm protocol

Untreated transparent 24-well plates (Nunclon, Germany) were used to grow biofilms. A 12 mm sterile coverslip was placed into each well. In triplicate, aliquots of 1 ml of diluted bacterial suspension were introduced to each well, while wells containing 1 ml sterile growth media served as negative controls. Plates were incubated for 1-3 days at 37°C. The media was changed every 24 h by placing the plate at an angle to allow the media to collect. The old broth was carefully aspirated without disturbing the biofilm, and 1 ml of fresh sterile pre-warmed broth was slowly added to the side of the well to prevent biofilm detachment.

For 96-well plate biofilm, 200 µl from the bacterial suspensions was inoculated into a 96-well plate in triplicate and incubated at 37°C, 5% CO_2 for 24 h. Media were then carefully replaced, and the biofilms were further incubated for an extra 24 h to reach 48 h total incubation time. The media was then removed without disturbing the biofilm, and the biofilms were carefully washed three times with 1x PBS and allowed to dry at room temperature.

2.5.2 Evaluation of biofilm growth in different bacteriological growth media

This experiment was conducted to find the most suitable media for *S. oralis* biofilm culture. The same media and supplements tested for neutrophil survival assay are outlined in **Section** 2.3. were investigated. Biofilms were grown for 48 h in a 96-well plate following the biofilm growing protocol described in **Section** 2.5.1.

2.5.3 Dynamic biofilm models: the flow cell and flow chamber

2.5.3.1 Flow cell

The FC-275 flow cell system (BioSurface Technologies, USA) containing two chambers, each equipped with three glass coupons (**Figure 2.2**), was used. The FC-275 is intended to facilitate biofilm development research by providing precise control over biofilm growth conditions, such as flow rates, nutrient supply and temperature. It has multiple channels for biofilm comparisons using optical glass viewing panes. It is suitable for the majority of microscope objectives and is fully autoclavable and reusable.

Prior to using the flow cell settings shown in **Figure 2.1**, 70% ethanol was run through the system for 1 h for sterilisation, followed by sterilised distilled water being permeated for an additional 1 h to clear the ethanol from the system.

To grow the flow cell biofilm, the bacteria were injected through the injection port with 1 ml of the diluted overnight culture and incubated at 37°C from 1 h to overnight to allow cells to adhere. The flow cell was placed onto a heating plate at 37°C, and growth media were driven through the system using a peristaltic pump (Ismatec REGLO Digital 78017-12, UK) at a speed of 0.25 ml/min (**Figure 2.1**). The flow speed was selected to mimic the oral cavity saliva flow rate under resting conditions (Dawes, 1987). The flow cell was stopped after the desired time period (1 – 5 days), and sterile

distilled water was fed into the system to wash off unattached planktonic cells. The flow cell was then disassembled, the coverslip was used for staining, and coupons were used for biofilm measurements.

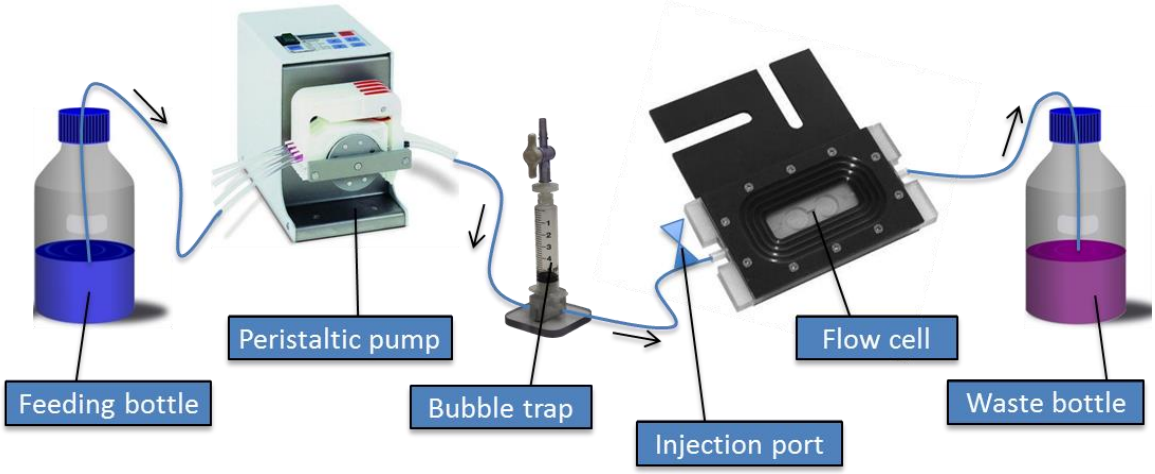

Figure 2.1: Setup of the flow cell. Arrows indicate the flow direction from the feeding bottle to the flow cell. The injection port is where the bacterial suspension is introduced into the flow cell to create the desired biofilms.

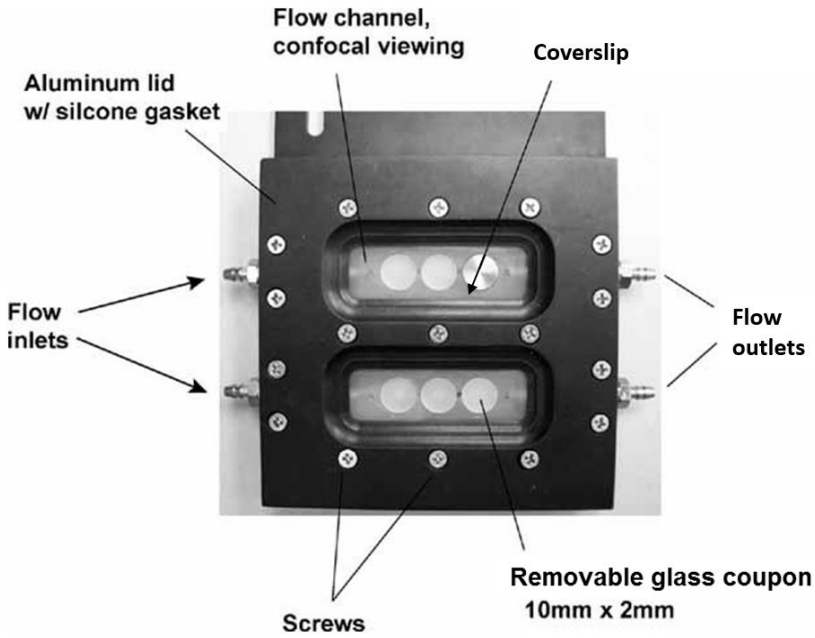

Figure 2.2: BioSurface Technologies (USA) flow cell.(Lauderdale et al., 2010)

2.5.3.2 Etching of glass coupons to improve bacterial attachment

The FC-275 flow cell system is equipped with 10 mm glass coupons to grow the biofilm on its surface (**Figure 2.2**). The coupons were etched using a glass etching cream (Armour Etch, USA) to increase the adhesive surface. Coupons were covered with the cream, incubated at room temperature for 2.5 h, and then washed with distilled water. To evaluate the efficiency of glass etching, 5-day flow cell biofilms were grown from *P. aeruginosa* at a concentration of OD_{600}=0.1 and 0.25 ml/min flow speed in 25% BHI broth diluted in distilled water to reduce aggregation and promote the formation of a more uniform biofilm. Flow speed and media concentration were used according to protocols previously published (Moormeier et al., 2014). Initially, 1 ml of the bacterial suspension was injected into each compartment of the flow cell and incubated at 37°C overnight. The following day, the flow cell was placed over a 37°C heating plate and connected to the biofilm tubing system, as shown in **Figure 2.1** and the flow was started for 5 days for biofilm development. Feeding bottles are filled regularly during biofilm growth, and waste bottles are decanted. The CV technique was used to evaluate biofilm mass.

2.5.3.3 Flow chamber

The flow chamber, also known as flow cells, contained three channels with individual dimensions of 1x4x40 mm (DTU Bioengineering, Technical University of Denmark, DK) and was assembled according to the manufacturer's instructions (**Figure 2.3**). The flow chamber channels have different dimensions compared with the flow cell, which can affect the flow dynamics and shear forces encountered by the biofilm. This, in turn, can have an impact on the biofilm's growth and structure.

The system was assembled by sealing the flow chamber over a glass slide using silicon layering. After the silicon had solidified, the flow chamber was connected to the dynamic biofilm setting, as shown in **Figure 2.4**. 70% ethanol was driven through the system for 1 h to sterilise the flow chamber and the tubing, followed by sterilised distilled water for an additional 1 h before using the biofilm settings.

For biofilm growth, the flow chamber was injected with 1 ml of diluted overnight culture and placed in a 37°C incubator overnight. The following day, the flow chamber was placed on a 37°C heating rack and connected to the dynamic flow system similar to the flow cell settings. After the experiment was completed, the flow was stopped, and the covering slide was disassociated for examination, such as staining and microscopy analysis.

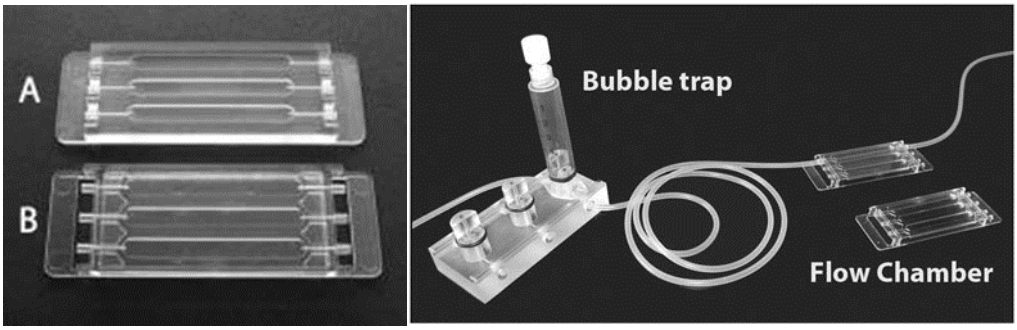

Figure 2.3: Flow chamber design with the bubble trap. The flow chamber and bubble trap are provided by DTU Bioengineering, Technical University of Denmark, DK. The picture on the left (A) illustrates the flow chamber exterior and (B) interior, which attaches to the glass slide. The picture on the right shows the assembly of the flow chamber and the bubble trap.

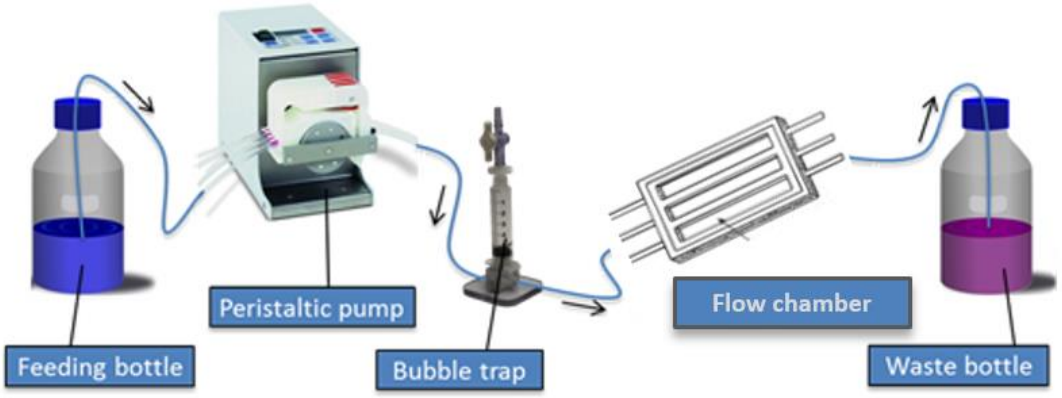

Figure 2.4: Flow chamber dynamic biofilm growth apparatus. Black arrows show the directions of flow from the feeding bottle through the peristaltic pump.

2.6 Biofilm-neutrophil interactions

Neutrophils were isolated according to the protocol described in **Section** 2.2.4, and their concentration was adjusted to $1x10^6$ cells/ml in TSB. In the dynamic models, the flow was stopped, and 1 ml of neutrophil suspension was injected into the injection port and allowed to adhere for 1 h. Subsequently, the flow was continued. For the static biofilm, the biofilm was washed once with 1 ml PBS, and then 1 ml of neutrophils suspension was added and incubated for 2 h.

2.6.1 Determination of the number of unattached neutrophils in static biofilm samples

Neutrophil ability to attach to biofilms was investigated by counting the number of unattached neutrophils in the supernatant of static biofilms after 2 h of incubation. Neutrophils were isolated from three donors and tested in triplicates in a 24-well plate after incubation with 48 h old biofilms at 37°C. The collected supernatant was stained

with trypan blue, and cells were counted using a haemocytometer (Paul Marienfeld GmbH & Co, Lauda-Königshofen Germany).

2.6.2 Imaging of interactions between biofilms and neutrophils

Several imaging techniques have been reported in the literature to analyse biofilms, each with advantages and disadvantages. Light microscopy, confocal laser scanning microscopy (CLSM), and scanning electron microscopy (SEM) are among the most commonly used techniques. Although many researchers favour light microscopic techniques, they have limited resolution and may not be ideal for observing microscopic cellular features or distinguishing between individual cells and the EPS. CLSM, on the other hand, generates high-resolution three-dimensional images of biofilms. CLSM enables imaging of specific components within the biofilm matrix, such as bacterial cells, EPS, or other components, by applying fluorescent dyes or stains. This method is beneficial for investigating biofilm structure, composition, and spatial organisation. SEM allows structural investigations by producing detailed, high-resolution images. The surface topography and delicate structures of biofilms, as well as the morphology of individual cells, can be revealed using this approach (Relucenti et al., 2021). Hematoxylin and eosin (H&E) staining was utilised in this study to visualise the biofilm and neutrophils retained in the culture system. Fluorescent labelling was used to distinguish between living and dead bacteria within the biofilm, biofilm thickness using Z-stack images, neutrophil adherence markers, and NET production. SEM was utilised to capture high-resolution images of neutrophil interactions with bacterial biofilms.

2.6.2.1 H&E staining

In dynamic biofilms (flow cell and flow chamber), the flow was halted, and the coverslip or glass slide, respectively, was retrieved and washed with PBS to remove planktonic cells and allowed to dry. The same procedure was used for the static biofilm, and the coverslip containing the biofilm was washed with PBS and allowed to dry. Biofilms were stained in Harris's haematoxylin solution (Y25086D TBS, USA) for 8 min, washed with running tap water for 5 min, and differentiated in 1% acid ethanol for 30 sec. An additional washing step with running tap water for 1 min was performed, followed by bluing in 0.2 % ammonia water (105431 Merck, Germany) for 1 min and washing with running tap water for 5 min. The coverslip or glass slide was then rinsed by immersion into 95% ethanol ten times. Next, counterstaining in eosin-phloxine (3801602 Leica) solution for 1 min was undertaken, with subsequent dehydration in 95% ethanol, twice for 5 min each. This was followed by a clearing step in xylene, twice for 5 min each. Finally, coverslips were mounted with a xylene-based mounting medium (24176 Polysciences).

2.6.2.2 Immunofluorescence and fluorescent microscopy

For fluorescent imaging, a confocal microscope (Zeiss Imager Z2 microscope with LSM 780 CLSM and Zeiss Zen 2012 Software [Zeiss, Germany]) and a Zeiss Axiovert inverted 200M Fluorescence/Live cell Imaging Microscope (Zeiss, Germany) were used. Z-stacks were imaged with CLSM and using a 20x objective at 488/500 nm. The maximum thickness of the biofilms was estimated by obtaining z-stack horizontal images at 1 μm intervals.

2.6.2.2.1 Paraformaldehyde (PFA) 4%

40 g of PFA (P-6148 Merck, Germany) was dissolved in 800 mL of PBS in a glass beaker and mixed on a stirring plate in a vented fume hood to generate 1 L of 4% PFA. The solution was heated to 60°C while being agitated. After cooling, the solution was aliquoted and stored at -20°C after passing through 0.22 µm sterile filter unit (430513 Corning, USA).

2.6.2.2.2 Fluorescent stain preparation and dilution

Anti-histone H3 (ab5103 Abcam, UK) was conjugated to the fluorescent dye Dylight 550 using the conjugation kit (Fast)-Lightning-link (ab201800 Abcam, UK). Conjugation was carried out according to the manufacturer's instructions, and 1:100 dilution in PBS was used to reach the working concentration.

Anti-CD11b Alexa Fluor 488 conjugated antibody (ab197701 Abcam, UK) was diluted 1:100 in PBS according to the manufacturer's instructions to achieve the working concentration. Nuclear dyes used for counterstaining were Hoechst 33342 (H1398 Invitrogen, USA) or SYTO 9 (S34854 Invitrogen, USA).

2.6.2.2.3 Biofilm (immuno) fluorescence microscopy

Biofilms were fixed in 4% PFA at room temperature for 20 min before being rinsed with PBS. Subsequently, blocking buffer (1% BSA + 10% FBS in PBS) was added for 1 h at room temperature. Anti-CD11b and anti-triple-citrullinated histone H3 antibodies were added, and the biofilms were stored overnight at 4°C and kept in the dark at all times to protect their spectral integrity. The following day, the stains were removed, washed with PBS, and the DNA stain Hoechst 33342 was added and incubated for 20 min before being rewashed with PBS. Finally, the coverslip was placed onto a glass

slide using a glycerol-based mounting medium. Some experiments also used SYTO 9 to stain the bacterial biofilm for 20 min prior to staining with antibodies.

Biofilm live/dead imaging was performed after fixation with 4% PFA, using live/dead biofilm Filmtracer™ LIVE/DEAD™ Biofilm Viability Kit (L10316 Invitrogen, USA), and staining was conducted according to the manufacturer's instructions. Imaging was performed using 40x oil immersion objective (Zeiss Objective EC Plan-Neofluar 40X/1.30 Oil DIC M27, FWD = 0.21 mm). The two stains were first imaged separately to control for any cross-bleed between channels. The excitation/emission was at 488 nm/<550 nm for SYTO® 9 and 555 nm/>550 nm for propidium iodide (PI). The percentage of neutrophil viability within the sample was calculated by the rate of neutrophils of red/yellow colour versus green cells with a diameter of 9-15 µm in four different images taken from each corner of the biofilm.

2.6.2.3 Scanning electron microscopy (SEM)

After 20 min of 4% PFA fixing, samples were fixed for 24 h at 4°C using a primary fixative of 2.5% glutaraldehyde (0396502500 Lobachemi, India). PBS was used to wash the samples three times for 15 min each. 1% Osmium tetroxide (secondary fixative) was applied for 1 h, followed by three 15 min washes with PBS. The samples were then dried for 15 min with ethanol concentrations ranging from 50% to 100%. Before imaging, the samples were air-dried then the coverslips containing the biofilm were placed on to 25 mm aluminium stubs (G3024 Agar Scientific, UK) with carbon conductive tabs and coated in gold for 90 sec (Denton Vacuum Desk II). The biofilms were examined using The JEOL JSM-7610F SEM (JEOL LTD, Japan) at an accelerating voltage 15 kilovolts (kV).

2.6.3 Biofilm and neutrophil eDNA production analysis: SYTOX Green assay

This method quantified DNA by digesting it from the neutrophils and bacterial cells in the biofilm and then measuring it fluorometrically in a multiwell plate reader (Köckritz-Blickwede et al., 2010, Palmer et al., 2012). The main advantage of this method over microscopy was that it allowed DNA analysis without the requirement for sample preparation steps such as fixation and washing, which might impact the results. Furthermore, this method allowed the analysis of a greater number of samples (de Buhr and von Köckritz-Blickwede, 2016).

Prior to use, 96-well plates were blocked with 1% BSA in PBS overnight at 4°C and subsequently rinsed with PBS. In triplicate, wells were inoculated with 200 µl of bacterial suspension in Schaedler broth or TSB and incubated for 48-72 h (37°C, 5% CO_2). The supernatant was removed after incubation, and the biofilm was washed with PBS. Subsequently, 100 µl of RPMI was added to each well. 100 µl of RPMI containing 10^5 neutrophils was added to the biofilm-containing wells. For positive control wells, 1 µl of PMA stock solution (50 mM) was added to 1 ml of 10^6 neutrophils in an Eppendorf tube to achieve a final concentration of 50 nM; 100 µl from this mixture was added to each well. Following stimulation, the plate was incubated for 2 h at 37°C at 5% CO_2. Then, 15 µl of 14.3 units/ml of DNase (89836 Thermo Fisher, USA) in PBS was added to each well. Alternatively, 15 µl of 14.3 units/ml micrococcal nuclease (MNase) solution (88216 Invitrogen, USA) was used. Each wells contents were gently mixed and incubated at 37°C for 10 min. Plates were centrifuged at 1800 rcf for 10 min. Then, 150 µl of the supernatant was transferred (without disturbing the pellet) to the wells of a black 96-well plate, and 15 µl of 10 µM SYTOX Green (S7020 Invitrogen, USA) was applied to each well. Neutrophils with no stimulant were solely measured as a negative control. PMA and 0.2% HOCl were used as positive controls for NET formation.

Fluorescence was recorded as arbitrary fluorescent units (AFU) using a microplate reader (Spark®, Tecan; software SparkControl, v. 2.3, Tecan) at an excitation of 485 nm and emission of 525 nm. This assay quantifies both bacterial and mammalian extracellular DNA.

2.6.4 NET production in response to biofilms

In a 96-well plate, 48 h *S. oralis* bacterial biofilms were grown in TSB, and neutrophils suspended in RPMI were introduced as described in **Section** 2.6.3. After 2 h, each sample was mixed by pipetting and used for enzyme-linked immunosorbent assay ELISA. A negative control with no neutrophils and a positive control containing neutrophils with 0.2% HOCl was used. An ELISA kit (501620 Cayman, USA) for detection of the NET marker citrullinated Histone H3 (Clone 11D3) was employed according to the manufacturer's instructions, 9 test samples were performed in triplicate, and plate reading was performed at 450 nm using a Biotek plate reader (ELx800, BioTek). The experiment was carried out in two technical replicates.

2.7 Comparison protocol for the different biofilm models

In this experiment, two models of biofilm culture were tested: the dynamic model, which included the flow cell and flow chamber, and the static model, which utilised 24-well plates. The comparison protocols and flow chart are shown in **Table 2.3** and **Figure 2.5**.

Table 2.3: Protocols used in the comparison between different biofilm models

Protocol number	Timing	Method details
protocol 1	5-day biofilm, neutrophils were introduced on day 3	Biofilms were grown for 120 h, the flow stopped, and neutrophils were added to the biofilms and allowed to adhere for 2 h. Flow resumed for another 48 h.
Protocol 2	3-day biofilm, neutrophils were introduced on day 3	Biofilms were grown for 72 h, and then neutrophils were added and allowed to adhere for 2 h.
Protocol 3	2-day biofilm, neutrophils on day 0	Biofilms were grown for 12 h, the flow was stopped, and neutrophils were added and allowed to adhere for 2 h. Then, the biofilm was extracted for further manipulation.

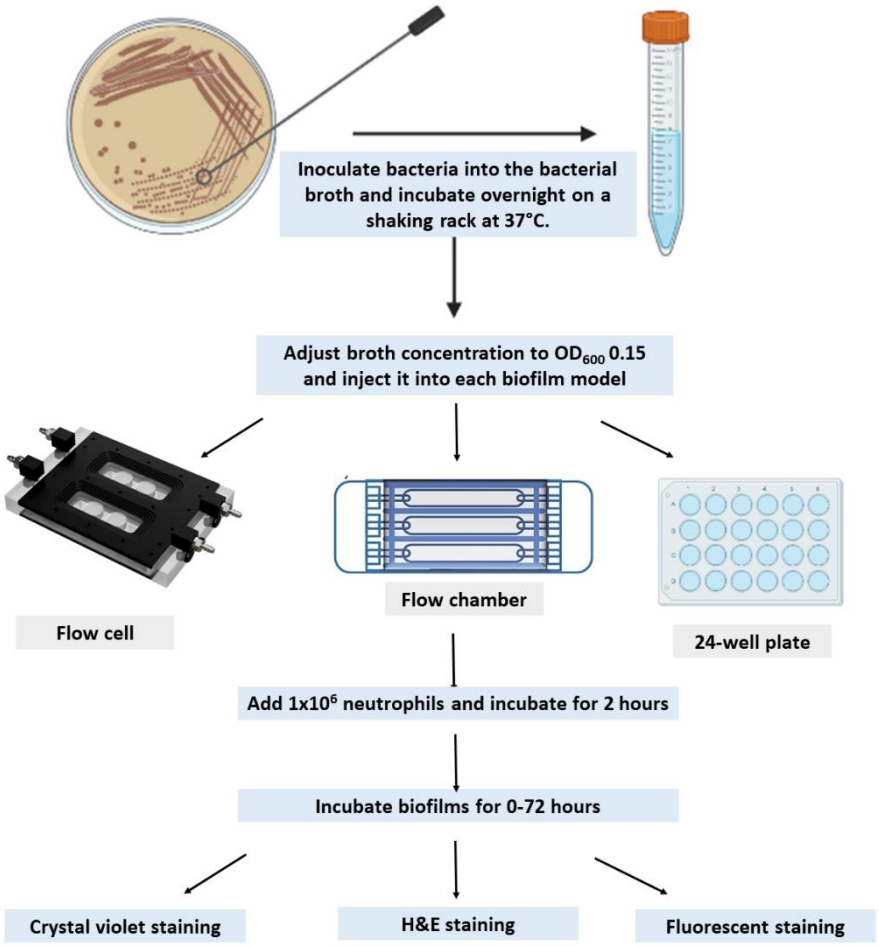

Figure 2.5: Flowchart summarising the comparison between static and dynamic biofilm culture (flow cell and flow chamber). The bacterial strains were inoculated in broth and incubated in a shaking incubator overnight. The bacteria concentration was then adjusted to 0.15 at OD_{600} and inoculated in the different biofilm growing platforms (flow cell, flow chamber, and 24-well plate). After biofilm incubation, neutrophils were added and incubated. Several tests were performed, including crystal violet staining, H&E staining, and fluorescent staining.

2.7.1 Biofilm biomass assessment using crystal violet (CV) staining

2.7.1.1 CV stock solution preparation

To prepare a 0.1% CV stock solution, 0.1 g of CV powder (42555 Lobachemi, India) was dissolved in 2 ml ethanol. The volume was adjusted to 100 ml with distilled water.

2.7.1.2 Biofilm biomass assessment by CV protocol

Static biofilm assessment was performed by removing the 12 mm coverslips containing the bacterial biofilm into a new well in the 24-well plate. Coverslips were carefully washed three times with distilled water to remove planktonic cells, and the coverslips were air-dried. The adherent biomass was then stained with 1 ml of 0.1% CV solution (prepared as described in **Section** 2.7.1.1) and incubated for 30 min at room temperature. After discarding the CV dye, the adhered biofilm was rinsed three times with distilled water and air-dried again. Subsequently, 1 ml of 30% acetic acid was added to each well, and the plate was placed on a rotary shaker (Thermo Scientific™ Titer Plate Shakers, Langenselbold, Germany) for 20 min. The suspension was then transferred to a plate reader to measure absorbance at OD_{600}.

For the flow cell biofilms, coupons were removed from the flow cell, placed into 24-well plates, and treated using the same procedure as described for the static biofilm. For the flow chamber biofilm assessment, the covering slide was detached from the flow chamber, washed with distilled water three times, and allowed to dry overnight. Then, 5 ml of CV solution was added and incubated for 30 min. The slide was washed 3 times with distilled water and allowed to dry overnight. Five ml of 30% acetic acid was added and incubated for 20 min on a rotary shaker. The suspension was then collected and read in the spectrophotometer at OD_{600}.

2.7.2 pH as a measure of metabolic activity analysis

The pH of bacteria following culture in TSB was measured in this experiment. The media's pH before adding bacteria was considered time-point zero. The bacterial concentration was set to 0.1 OD_{600}. The supernatant in the static biofilm (explained in 2.5.1 and the waste medium collected from the dynamic biofilms (explained in **Section** 2.5.2) were compared. The pH was recorded daily using an Orion 2 Star pH meter (Thermo Fisher, USA).

2.7.3 Evaluating biofilm surface adhesion to different surfaces and coating materials

Coverslips were coated to improve bacterial and neutrophil adhesion. In addition to coating glass surfaces, other surfaces were compared. The coating agents and surfaces used are listed in **Table 2.4**.

Table 2.4: Coating materials and surfaces used to evaluate adhesion

		Manufacturer
Coating material	1% BSA in PBS	A4530 Merck, Germany
	0.01% Poly-L-lysine	A005, Merck, Germany
	3 mg/ml Collagen	A1048301, Invitrogen, USA
Surface	Thermanox TMX treated coverslip	150067, NUNC
	Sandblasted coverslips	
	Un-treated ethanol-washed coverslips	

Coverslips were coated by dripping 150 µl of coating solution onto each coverslip and incubating for 1 h for 1% BSA and collagen and 5 min for poly-L-lysine at room temperature. The coating material was then aspirated, and collagen-coated coverslips were rinsed with PBS. All the coverslips were allowed to dry before use. Coverslip sandblasting was performed by treating each coverslip for 5 s with aluminium oxide

(25 µm grit size, 1.2 mm nozzle) using a Basic Quattro sandblasting unit (Renfert, Hilzingen, Germany).

All coverslips were sterilised for 30 min using UV light before use. Tested coverslips were placed in a 24-well plate and inoculated with bacterial suspension in Schaedler's broth. Biofilms were cultured for three days. The CV technique was then used to determine the thickness of the biofilm generated.

2.7.4 Biofilm dry weight assessment

Biofilm dry weight measurement was undertaken to evaluate the change in biofilm weight after adding neutrophils. Coupons containing bacterial biofilm only and coupons containing biofilm with neutrophils were removed from the flow cell biofilm and washed once with PBS before being air-dried for 24 h. The dry weight was recorded and compared with un-inoculated coupons. For static biofilm weight, the coverslips were removed from the wells, washed with PBS, and air-dried for 24 h before weighing. Weighing was undertaken using a Mettler Toledo analytical digital balance (XPR226DR, Zürich, Switzerland).

2.7.5 Biofilm adhesion measurement

Adhesive strength describes the interaction between the biofilm and the surface to which it is attached. Biofilm adhesion was assessed for possible changes after interaction with neutrophils. *S. oralis* biofilms grown for 48 h with and without neutrophils (protocol described in **Section** 2.5.1) were stained with CV for 10 min, followed by washing once with distilled water. The biofilm was then transferred to a new well, and 1 ml of distilled water was added. The 24-well plate was then placed on a rotary shaker (Thermo Scientific™ Titer Plate Shakers, Langenselbold, Germany) at

200 rpm for one min. The distilled water was replaced every min, and an OD_{600} reading of detached biofilm was recorded. These shear forces were applied for a total of 10 min. The sum of all biofilm detachment and remaining biofilm on the coverslip was considered time point zero.

2.7.6 Quantification of viable bacterial cells in biofilms

S. oralis biofilms were grown in a 24-well plate for 48 h as described 2.5.1. When the biofilm was developed, media was removed from all wells and the formed biofilms were washed once with 1 ml PBS. Next, 1 ml of TSB was added to wells containing biofilm, and biofilm cells were fully disrupted and suspended by vigorous pipetting. The suspended biofilm was transferred to a new 24-well flat bottom microplate followed by 10-fold dilutions prepared in PBS. 100 µL of 10^{-5} dilution was plated onto TSA agar plates. Colony forming units (CFU) were enumerated after 24 h of incubation at 37 °C. The experiment was performed twice with three replicates.

2.8 Bacterial strain validation

2.8.1.1 Gram stain

Gram stain was used to reassure the microscopic purity of biofilms at various growth stages. A drop of biofilm supernatant was added onto a clean slide and allowed to air dry. The slide was stained with crystal violet (CV) for 1 min, iodine for 1 min, acetone for 7 sec, and safranin for 1 min. After each step, the slide was washed with distilled water. The slide was allowed to dry before being examined under a light microscope (Olympus, Japan).

2.8.1.2 Matrix-Assisted Laser Desorption Ionisation Time-of-Flight (Maldi/TOF)

MALDI MS analysis was performed to validate the bacteria used to create the multispecies biofilm. A fresh overnight-grown bacterial colony of each species was combined with a single drop of matrix solution (411071 VITEK MS-CHCA MATRIX), an energy-absorbent organic substance, and dried for 1 min. When the matrix crystallises after drying, the sample entrapped within it also crystallises. In an automated mode, a laser beam ionises the sample within the matrix. The protonated ions are then accelerated and separated according to their mass-to-charge ratio (m/z). The m/z ratio of an ion is measured during MALDI-TOF (Vitek MS, BioMerieux). analysis by calculating the time required for it to travel the length of the flight. A characteristic spectrum known as peptide mass fingerprint (PMF) for analytes in the sample is generated based on the TOF information (Singhal et al., 2015). The results were analysed using MyLA® Middleware Solution software (MyLa, bioMérieux, France). The sample workflow is shown in **Figure 2.6**.

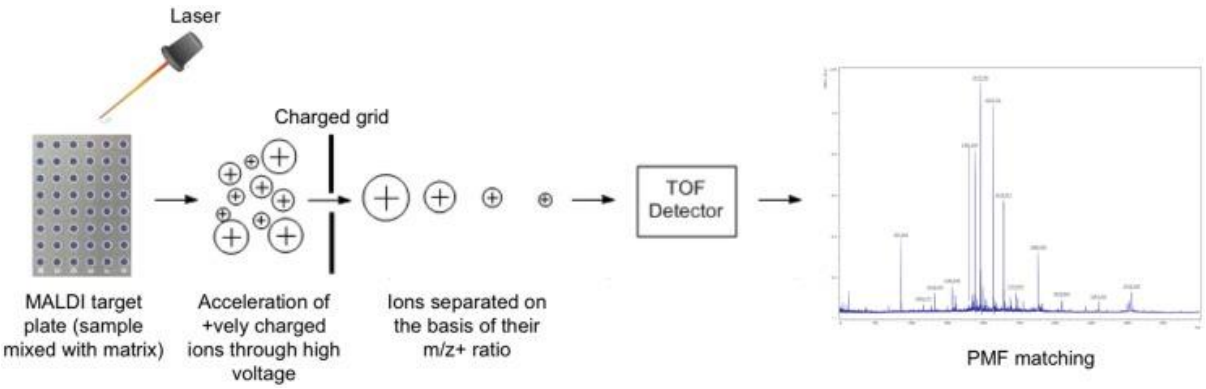

Figure 2.6: Sample workflow used in MALDI-TOF MS (Singhal et al., 2015).

2.8.1.3 Shotgun whole-genome sequencing (WGS)

Shotgun WGS was used to further validate the three bacterial species used in the multispecies biofilm: *S. oralis*, *S. mitis*, and *S. intermedius*. Shotgun sequencing is a technique used to determine the DNA sequence of an organism's genome. The method involves randomly fragmenting the bacterial genome into small, sequenced fragments. A computer program searches for DNA sequence overlaps and uses them to reassemble the fragments correctly to reconstruct the genome. 1 ml of 0.1 OD_{600} adjusted overnight cultured of each bacteria was prepared. All three bacterial suspensions were mixed, and 200 µl from the mixture was inoculated into a 96-well plate as in **Section** 2.5.1.2. After the final biofilm washing, 200 µl of TSB was added to each well and mixed to disassociate the biofilm. The mixture was then transferred to a 1 ml Eppendorf tube with 200 µl of DNA/RNA Shield (R1100-50 Zymo Research, USA) and delivered to the CosmosID®'s CLIA-certified, GCP-compliant facility (Germantown, MD, USA) for DNA isolation and sequencing.

2.9 NET isolation

The study followed a published protocol (Najmeh et al., 2015). In brief, neutrophils were stimulated with 10 µl of 10 mM of PMA (per 10 ml of neutrophil solution) and incubated in a 25 mm flat tissue culture flask for 2 h at 37°C 5% CO_2 to allow NETosis to occur. After incubation, the media was discarded, leaving the layer of NETs and neutrophils adhered to the bottom. Flasks were washed with 5 ml of cold PBS without calcium and magnesium by pipetting the PBS to lift all adherent material from the bottom surface. The washing solution was transferred to a 15 ml conical tube and centrifuged at 450 g at 4°C. The supernatant was divided into 1.5 ml microcentrifuge tubes and centrifuged for 10 min at 18,000 rcf at 4°C. After centrifugation, the

supernatant was discarded, and the pellet was resuspended in ice-cold PBS to a concentration corresponding to $2x10^7$ neutrophils per 100 µl of PBS. The DNA concentration was measured using the Qubit™ dsDNA Quantification Assay Kits (Q32851 Invitrogen, USA) by Qubit 2.0 Fluorometer (Invitrogen, Singapore).

2.10 ROS quantification

2.10.1.1 Luminol

Luminol was prepared by dissolving 0.5 g luminol (A8511 Merck, Germany) in 94.05 ml of 1 mM NaOH to achieve 30 mM stock solution. The stock solution was foil-wrapped and stored for up to 6 months at 4°C prior to use. The working solution was prepared on the day by diluting 1 ml of stock solution with 9 ml of PBS, and the pH was adjusted to 7.3 using a Beckman 40 pH meter.

2.10.1.2 Isoluminol

Isoluminol was prepared by dissolving 0.5 g isoluminol (A8264 Merck, Germany) in 94.05 ml of 1 mM NaOH to achieve a 30 mM stock solution. The stock solution was foil-wrapped and stored for up to 6 months at 4°C. The working solution was prepared on the day by diluting 1 ml of stock solution with 9 ml PBS, and the pH was adjusted to 7.3.

2.10.1.3 ROS quantification protocol

ROS production of neutrophils in response to biofilms was determined using chemiluminescence (Lundqvist and Dahlgren, 1996, Hirschfeld et al., 2017). White flat bottom non-treated white 96-well plates (3912 Costar) were blocked with 1% BSA in PBS overnight at 4°C and washed with PBS prior to use. Each well was inoculated with 200 µl per well of bacterial suspension in TSB and incubated for 48 h (37°C, 5%

CO_2) to form biofilms. After incubation, the suspension was removed, and biofilms were washed once PBS. 100 µl of $1x10^5$ of freshly isolated neutrophils in gPBS (PBS supplemented with 1.8 g/L glucose (Merck, Germany), 0.15 g/L $CaCl_2$ (10070 BDH, UK), and 1.5 ml of 1M $MgCl_2$ (22093 BDH, UK) were added to each well. GPBS was added to negative control wells not containing neutrophils, and 50 nM PMA was added to positive control wells. Luminol (3 mM) was used to quantify total (intra- and extracellular) ROS. Isoluminol (3 mM), together with 1.5 units/µl of horseradish peroxidase (HRP: P8415 Merck, Germany), were used to quantify extracellular ROS only. Luminol and isoluminol were purchased from Merck. For intracellular ROS measurement, 15,000 units/ml of SOD (S9697 Merck, Germany) and 2000 units/ml of catalase (E3289 Merck, Germany) were added to each well-containing luminol. These enzymes reduce ROS levels by catalysing the conversion of ROS into less harmful substances. These conversions occur in the extracellular environment, effectively reducing the level of ROS that illumination-based techniques could potentially detect. However, these enzymatic activities do not affect intracellular ROS, leaving them intact for subsequent measurement. Luminescence was measured in a luminometer (Berthold Tristar2; Berthold Technologies, Harpenden, UK, with MikroWin 2000 software; Informer Technologies, Madrid, Spain). Luminescence was recorded every 3 min for 120 min at 37°C. All readings were expressed as relative light units (RLUs).

2.11 Interaction of neutrophils with bacterial DNA

2.11.1 Bacterial DNA extraction

Bacteria were grown in TSB overnight in a shaking incubator, as previously detailed. QIAamp DNA extraction mini kit (QIAGEN, Valencia, CA) and lysozyme enzyme

(89833 Thermo Scientific, Germany) were used to isolate DNA. The extraction was performed according to the kit's instructions, and the DNA concentration was determined using the Qubit™ dsDNA Quantification Assay Kits (Q32851 Invitrogen, USA) by Qubit 2.0 Fluorometer (Invitrogen, Singapore). *S. oralis* DNA was stained with PI from the Live/Dead biofilm viability kit for 20 min with 3 µg/ml working concentration. DNA was washed twice with PBS and centrifuged for 2 min at 1600 rcf.

2.11.2 Flow cytometry analysis of neutrophils

Neutrophils were isolated and adjusted to $1x10^6$ cells/ml in gPBS and then stained with 1 µg/ml Hoechst 33258 for 20 min, followed by washing twice in gPBS and centrifugation at 1600 rcf for 2 min. 100 µl of stained neutrophils were added to 100 µl of 1 µg/ml stained DNA (isolated as described in **Section** 2.11.1) and incubated at 37°C on a shaking rack. The mixture was transferred to round bottom polystyrene FACS tubes and analysed using FACS Canto II (BD Biosciences, FL2 and UV wavelength) with a medium flow with an event acquisition rate of 10,000 events. Flow cytometry data were analysed using associated FACSDiva software (BD Biosciences). The neutrophil gate was determined by forward (FSC) and side scatter (SSC), representing the cells distribution in the light scatter based on size and intracellular composition, respectively.

2.11.3 Fluorescent imaging of neutrophil interaction with bacterial DNA

Part of the neutrophil-bacterial DNA mixture (5 µl) described in **Section** 2.11.2 was transferred to a glass slide and examined under Zeiss Axiovert inverted 200M Fluorescence/Live-cell Imaging Microscope (Zeiss, Germany), using a 20x objective (Zeiss objective EC Plan-Neofluar 20x/0.50 M27, FWD = 2.0 mm). The two stains were

first imaged separately to control for any cross-bleed between channels. The excitation/emission was 488 nm/<550 nm for SYTO 9 and 555 nm/>550 nm for PI.

2.12 Statistical analysis

Microsoft Excel for Windows or GraphPad InStat 9.5.1. (Graphpad Inc.) were used for all statistical analyses. Normal distribution of data was tested using the Shapiro–Wilk normality test. Subsequently, the tested groups were compared using paired or un-paired, two-tailed t-testing and by analysis of variance (ANOVA) with post hoc analysis using Tukey's test or Dunnett's multiple comparisons test versus controls. All parametric data are shown as mean values ± standard deviations (SD), while non-parametric data are shown as medians and ranges. At $P \leq 0.05$, all results were considered statistically significant.

3 CHAPTER THREE Results: Establishment of an *in vitro* biofilm model for co-culture of biofilms and neutrophils

3.1 Introduction

To explore fundamental questions about biofilms and to better understand their complex and dynamic nature, it is vital to construct reliable *in vitro* models that adequately replicate *in vivo* biofilm environments (Fernández et al., 2017). *In vitro* biofilm models have many advantages, including low cost, high throughput potential, relative ease of replication, and the capacity to change conditions as necessary. The disadvantage of *in vitro* models is that they lack the complexity of the *in vivo* environment; the absence of the host immune response is particularly significant (Gabrilska and Rumbaugh, 2015). This chapter aimed to identify the *in vitro* biofilm method that best mimics the *in vivo* environment. In order to achieve this, two dynamic biofilm models were tested, i.e. a flow cell (FC-275, BioSurface Technologies, USA) and a flow chamber (DTU Bioengineering, Technical University of Denmark, DK), and one static model using a multiwell plate. The FC-275 device was explicitly chosen for direct CLSM examination of the resultant biofilms; moreover, this model was compatible with the Zeiss CLSM inverted microscope used in this study. Furthermore, the FC-275 system has the capacity to examine biofilm formation on a variety of materials and surfaces (Rzhepishevska et al., 2013). However, the flow cell has limitations: each experiment requires a substantial volume of the growth medium, and only two biofilms can be studied per experiment because the flow cell has two biofilm-growing chambers, each of which contains three biofilm growing coupons (Moormeier and Bayles, 2014). The flow chamber was evaluated because it has three biofilm-growing compartments and allows for direct, non-destructive inspection of growing biofilms. The flow chamber has been optimised for direct microscopy, and it can be attached to a glass slide for observation.

Additionally, it maintains the flexibility to be coupled with other materials as needed, expanding its versatility for various microscopy applications. Two of the flow chamber's disadvantages are insufficient capacity and a lack of direct access to the biofilm-growing compartments. A common disadvantage of dynamic biofilm models is that their setup and maintenance are more complex and costly than those of static models. They require specialised equipment, such as pumps and flow cells, and often require more time and technical expertise than static models.

Pseudomonas aeruginosa was used as a biofilm-generating bacterium because it is well-known for its ability to form biofilms (Ghafoor et al., 2011). It can create robust biofilms on various surfaces, including medical devices like catheters and implants (Thi et al., 2020). This makes it an excellent model bacterium to verify the biofilm-growing models examined in this thesis.

The oral streptococci on which this study focused—*S. salivarius*, *S. oralis*, *S. mitis*, and *S. intermedius*—represent the yellow complex, and they account for more than 80% of early biofilm constituents (Socransky et al., 1998, Kreth et al., 2009). All the *Streptococcus* species in this complex are members of the human oral microbiome and are capable of opportunistic pathogenicity (Socransky et al., 1998).

3.2 Assembly of dynamic biofilm models

The system was assembled as described in **Section** 2.5.3 (**Figure 3.1**), and an ethanol wash cycle followed by sterile distilled water was performed, as explained in 2.5.3.1.

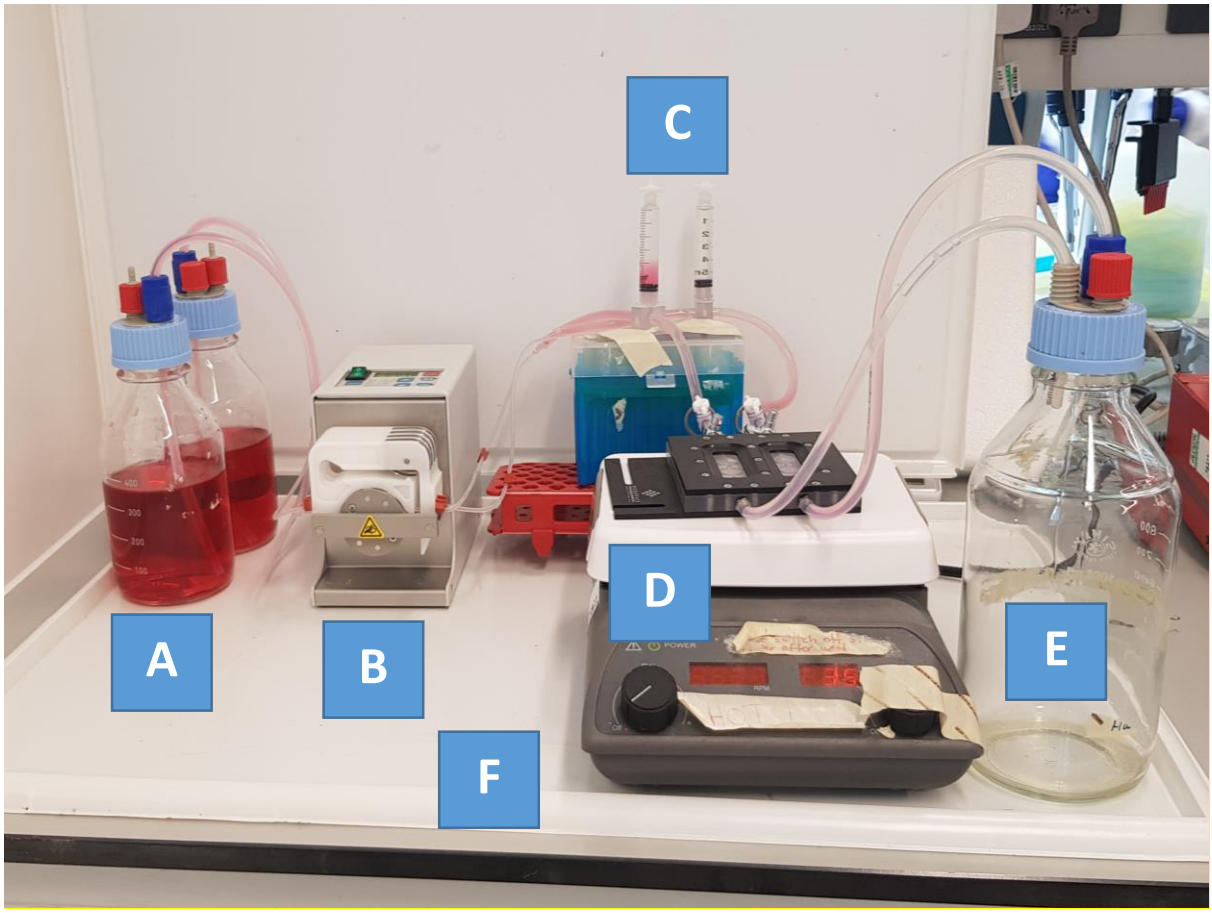

Figure 3.1: Flow cell apparatus used in the laboratory. This image, which equipment used in the early stages of system optimisation, shows (A) RPMI media in the feeding bottles, (B) peristaltic pump, (C) bubble trap on top of the rack and tip box, (D) flow cell on the heating plate, (E) waste bottle. All the system components are on a spillage tray (F).

Although all the system components were autoclaved before use, the ethanol washing cycle was crucial as it decontaminated the system after assembly. The flow cell had to be assembled by placing the coupons in their corresponding chambers, placing the coverslip on top of each chamber, and then installing the flow cell's outer cover, tightening the screws with caution and care to ensure that the coverslip glass did not crack, which would have led to leakage of the media during incubation. The flow chamber was affixed to a glass slide using silicon according to the protocol described

in 2.5.3.3. and displayed in **Figure 3.2.** The flow chamber had to be tested for appropriate liquid flow and checked for leakage after silicon solidification.

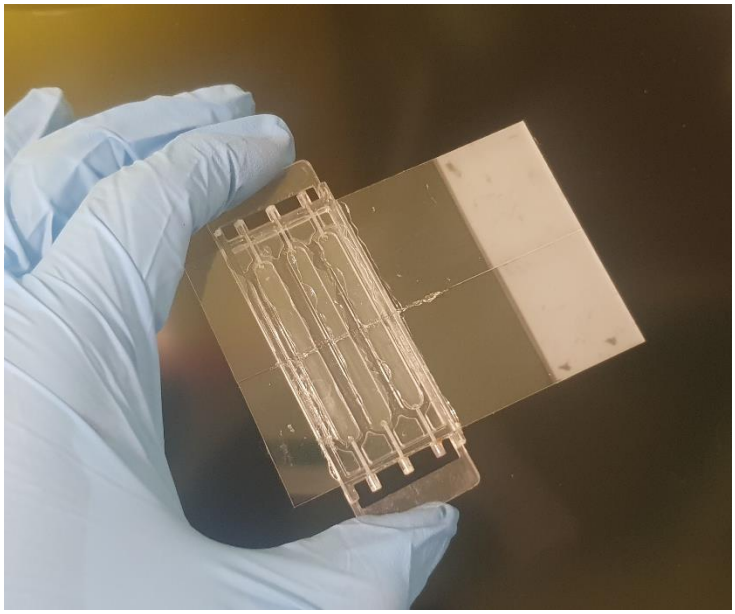

Figure 3.2: Flow chamber fixation to slides using silicon sealing.

The dynamic systems can leak media if any of the tubing connections are improperly assembled. To avoid this problem, the flow had to be observed clearly in the first few hours of running to ensure the absence of leakage. Sealing the connection ports, which were adjoined to the tubes with parafilm, mitigated this problem.

3.2.1 Airlock formation

Biofilms in closed flow systems are prone to airlock formation, which disrupts biofilm development and results in their detachment from the glass surface (Gómez-Suárez et al., 2001). Air lock formation may be due to changes in fluid pressure as the media flows through different diameters of the tubing (Crusz et al., 2012). Tubings of two distinct diameters were used as the devices required different tubing sizes. The peristaltic pump (Ismatec REGLO Digital 78017-12, UK) required 0.51-mm three-stop

Ismatec tubing, whereas the flow cell required 3-mm tubing. The tubing of different sizes was connected using 10-µl pipette tips, as shown in **Figure 3.3**. These connections were potentially a source of air lock formation because air could escape into the tubing if the connections were not fully sealed. To prevent the escape of air and the resulting contamination, the tube connections were encased in parafilm disinfected with 70% ethanol.

Figure 3.3: Peristaltic pump (Ismatec REGLO Digital 78017-12, UK). The 0.51-mm three-stop Ismatec tubing required by the pump was connected to the 3-mm tubing required by the flow cell using 10-µl pipette tips.

The bubble trap was used to capture air in the medium and release it before it contacted the biofilm (Tolker-Nielsen and Sternberg, 2011). It was observed that the bubble trap itself could cause airlock formation as air entered the system through the trap's air-release port. When the bubble traps were elevated above the system (by placement on a tube rack or any other object, as **Figure 3.1** shows), their ability to trap bubbles increased, and their likelihood of introducing air into the system decreased.

3.2.2 Bacterial inoculation and temperature settings

After the decontamination cycle was completed, the flow cell and flow chamber were disconnected. The connection ports were disinfected with 70% ethanol and resealed with parafilm. The bacterial suspension was prepared according to the methodology described in 2.1.1 and injected through the flow cell's injection port. The flow chamber had no injection port, so the bacterial suspension was injected through the connection port. The devices were maintained in a 37°C + 5% CO_2 incubator overnight, as explained in the protocol presented in **Section** 2.5.3.1. Overnight incubation without flow was performed to facilitate the attachment of bacteria to the surface because the shear stress can prevent bacterial attachment and biofilm formation. The devices were subsequently connected to the system to grow dynamic biofilms, and the flow was resumed.

Because of the system's resulting size it was too large to be housed in the incubator; therefore, to ensure the biofilm was maintained a 37°C incubation temperature was achieved by positioning the flow cell and flow chamber on a heating plate (**Figure 3.1**). After the heating plate's temperature was adjusted to 37°C, the devices did not reach the desired temperature, as the open lab environment resulted in heat loss. The temperature was measured by placing a thermometer above the flow cell and flow chamber. The heating plate's temperature was then increased to 45°C to compensate for the heat loss, and the flow cell and flow chamber reached the desired temperature of 37°C. Although this approach was functional, it failed to supply the 5% CO_2 required for optimal growth of the oral bacteria used in this thesis.

3.2.3 Introduction of neutrophils into the model system

Neutrophils were isolated and suspended as described in **Section** 2.2.4, and the suspension was injected into the biofilm-containing flow cell through the injection port. It was observed that the injection port limited the flow of neutrophils to the biofilm as the suspension flowed vertically and that some of the neutrophils were trapped in the port and did not contact the biofilm. The neutrophil suspension flow was investigated by adding brilliant blue FCF (E133; 0.5%) to the suspension to observe liquid flow characteristics, as shown in **Figure 3.4**.

Figure 3.4: Neutrophil entrapment in the flow cell injection port. Neutrophils, suspended in a 0.5% brilliant blue FCF (E133) solution in RPMI 1460, were introduced into the injection port (white arrow) designated for compartment (A). Despite the blue colouration of the suspension, it remained localised in the injection port, failing to permeate to the biofilms within compartment (A). This observation suggests the entrapment of neutrophils within the injection port environment.

To overcome this problem, neutrophils were injected through the connection port, which enabled the fluid to flow horizontally to the biofilm and improved the neutrophils' access to the biofilm.

3.2.4 Disconnecting the dynamic models and collecting the biofilms for analysis

To collect cultured biofilms, the flow cell was disconnected and unscrewed to collect the coupons containing the biofilm. In some cases, more biofilm was found in the coverslip that was aimed for visualising the biofilm than in the coupon itself. Caution must be taken to ensure the coupon side facing the coverslip is the one to be tested to ensure standard biofilm forming conditions. For the flow chamber, The operation of the flow chamber was time-consuming and complicated. The silicon layering, which had to be removed to disconnect the glass slide from the device for biofilm manipulation, was challenging to remove (**Figure 3.5**). Disconnecting the glass slide required some force, which could have resulted in the fracturing of the glass slide or the loss of some of the produced biofilms.

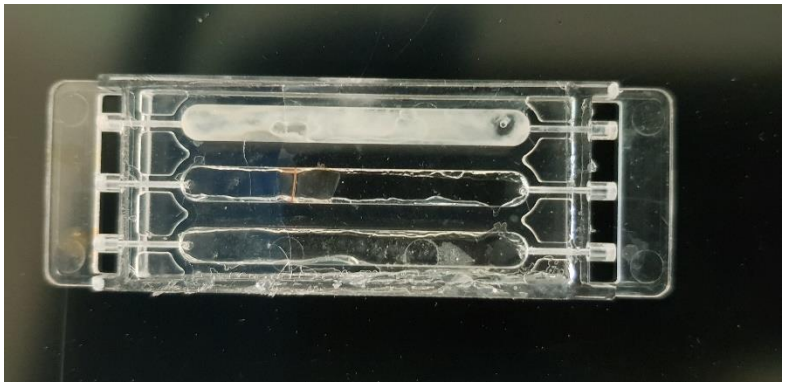

Figure 3.5: Biofilm formation in the flow chamber before detachment of the silicon layering and the glass slide. The biofilm is cultured in the first compartment of the flow chamber, and white biofilm growth is visualised.

3.2.5 Cleaning of the biofilm apparatus

After each biofilm-growing cycle, the system was cleaned by disconnecting all the system components and then autoclaving them. The silicone connecting tubes (Masterflex™ L/S™, Thermofisher, USA) were usually filled with biofilm because silicone is prone to biofilm development (Karlan et al., 1980). Before autoclaving, the

tubes were cleaned with a nylon bristle brush to detach the bacterial aggregates. Upstream growth was detected during the cultivation of *P. aeruginosa* biofilm (**Figure 3.6**); previous research has reported this growth pattern (Heydorn et al., 2002, Kaya and Koser, 2012). The growth increased the difficulty of cleaning the tubes after each trial.

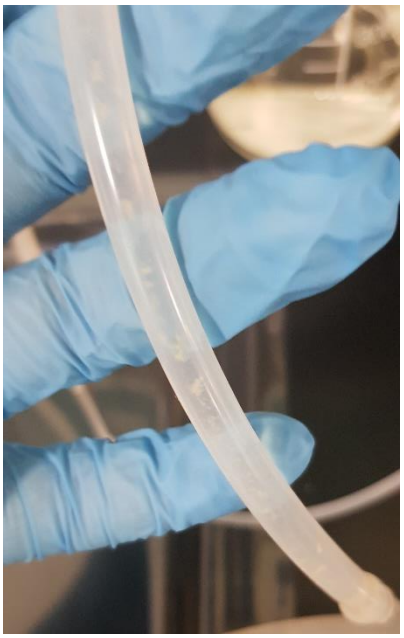

Figure 3.6: *P. aeruginosa* biofilm upstream growth within tubing during dynamic biofilm growth.

3.3 Standardisation of the neutrophil isolation protocol

3.3.1 Neutrophil survival rate after Percoll gradient separation

This test was performed to evaluate the percentage of live neutrophils after separation from whole blood. The trypan blue exclusion test indicated that immediately after isolation, the neutrophil viability was at least 98.9% (**Table 3.1**). Three donors were tested for neutrophil survival. Participants selection, ethics and consents are described in 2.2.1.

Table 3.1: Number of live and dead neutrophils separated using the Percoll isolation protocol (n=3).

Blood samples	1	2	3	Average	SD
Percentage of live neutrophils	98.8%	98.9%	99.16%	98.95	0.18
Percentage of dead neutrophils	1.2%	1.1%	0.84%	1.05	0.16

3.4 Development of *P. aeruginosa* biofilm

3.4.1 Standardisation of flow cell biofilm using *P. aeruginosa*

The first biofilm-growing model tested was the flow cell. The model was tested using *P. aeruginosa,* which was cultured for up to six days, and the biofilm biomasses of different days were compared using the CV assay described in 2.7.1. The broth used was 25 % BHI in distilled water, and the flow speed was 0.25 ml/min. The flow-speed and media-concentration selection followed the method developed by (Jesaitis et al., 2003, Wijesinghe et al., 2018). This protocol was performed to evaluate the efficiency of the device. **Figure 3.7** shows a significant increase in biofilm mass when the biofilm was incubated for four days without a significant increase on the fifth day.

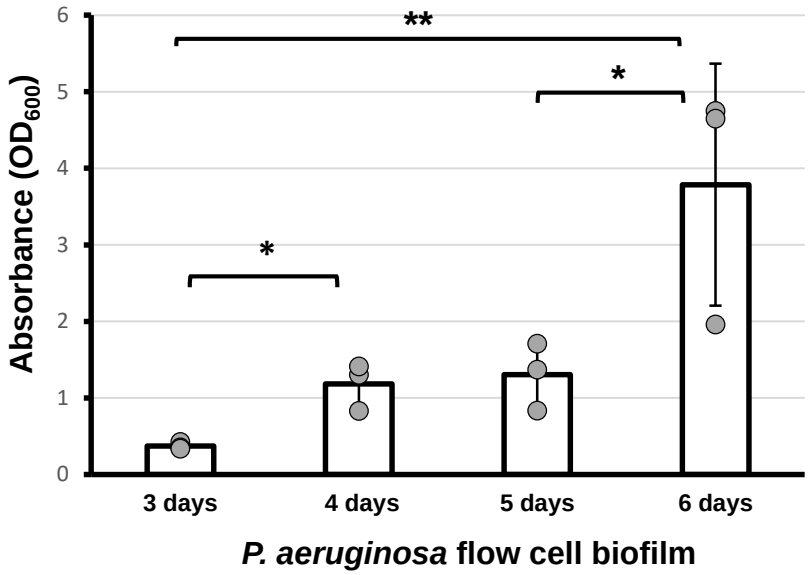

Figure 3.7: *P. aeruginosa* biofilm biomass after three to six days of biofilm culture. P. aeruginosa dynamic biofilm grown on glass coupons inserted in the flow cell device and injected with BHI broth. CV assay was used to measure the biofilm biomass**.** Bars show average values from triplicate coupons n=3 and SD.*P<0.05, **P≤0.01 (calculated using one-way ANOVA).

Based on these results, four days was selected as the incubation period for further analysis with the *P. aeruginosa* biofilm. Although six days of incubation significantly increased the biofilm mass, a six-day period was not selected, as elongated incubation periods make biofilms prone to contamination.

3.4.1.1 Enhancing flow cell biofilm attachment using etched glass coupons

This experiment was performed to improve bacterial attachment to the glass and hence to increase the mass of *P. aeruginosa* biofilm. Etched and nonetched coupons (the etching protocol is explained in 2.5.3.2) were placed into different compartments of the FC-275 flow cell, as shown in **Figure 3.8**.

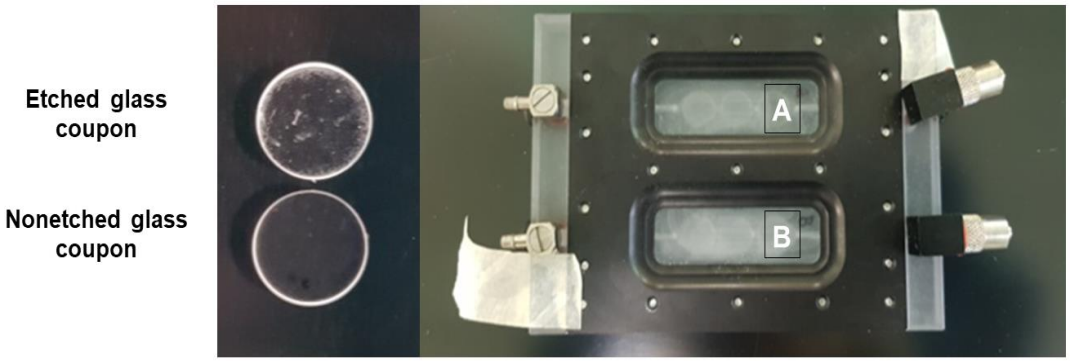

Figure 3.8: Etching of the flow cell glass coupons. The coupons were etched using a glass etching cream (Armour Etch, USA) to increase the adhesive surface. The right-hand side of the figure shows the placement of the coupons inside the flow cell (FC-275) with etched coupons in compartment A and nonetched coupons in compartment B.

All three replicates of the etched-glass coupon contained less biofilm mass than the nonetched coupons in **Figure 3.9**. Despite this decrease, there was no significant difference between the etched and nonetched coupons (P=0.08).

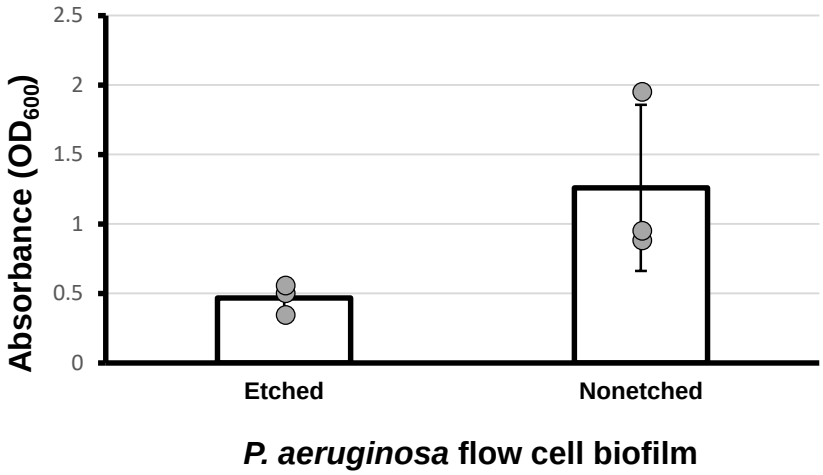

Figure 3.9: Assessing the capability of etched and non-etched flow cell glass coupons to promote dynamic biofilm biomass using *P. aeruginosa* five-day biofilm. CV assay was used for biofilm biomass quantification. Bars show average values from triplicate coupons and SD. P>0.05 (calculated using two-tailed unpaired t-test).

3.4.1.2 Comparison between dynamic flow cell and static 24-well-plate *P. aeruginosa* biofilm biomass and dry weight.

The first biofilm comparison conducted in this work is to compare the dynamic flow cell model with the static multiwell plate for its ability to promote biofilm formation. Four day *P. aeruginosa* biofilm was used in this comparison and the biofilm biomass and dry weight were analysed in **Figure 3.10**.

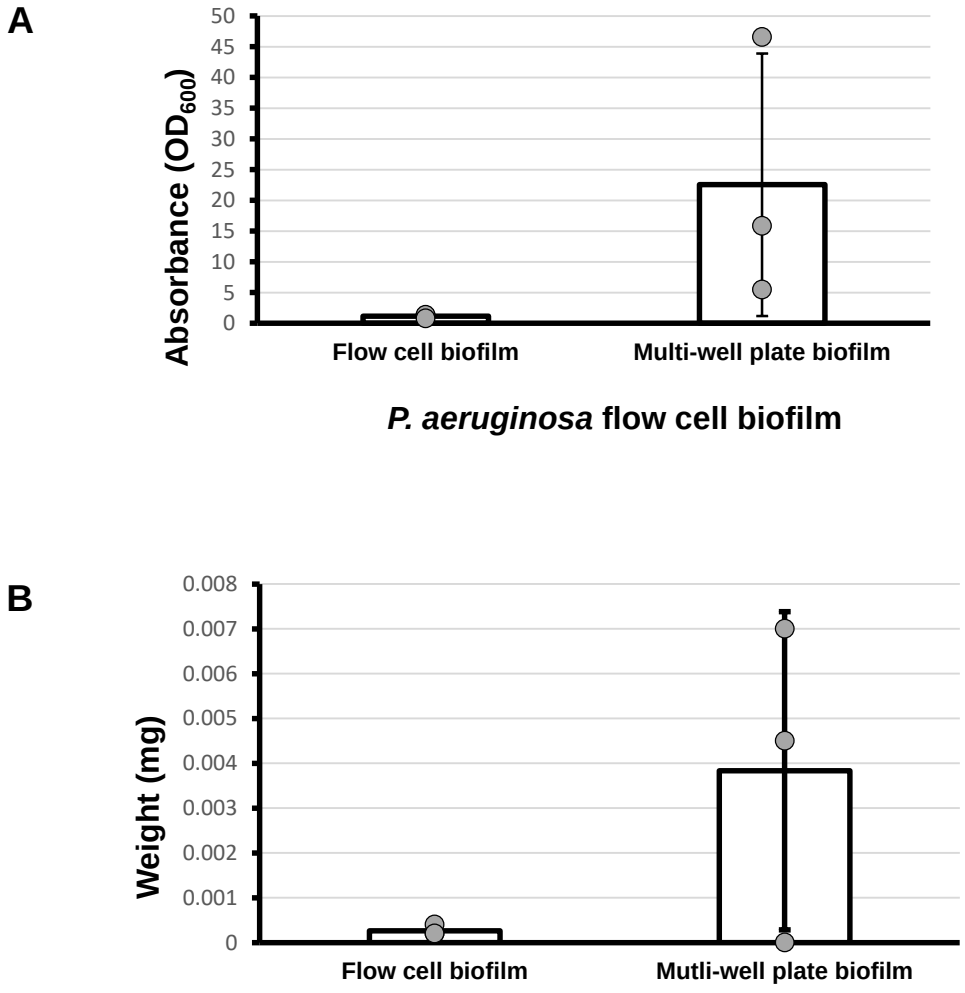

Figure 3.10: Comparison between multiwell-plate and flow cell in their ability to aid in biofilm formation using *P. aeruginosa biofilms* incubated for four days. A: Biofilm biomass was measured by OD_{600} absorbance of the CV biofilm staining. The graph shows mean values ± SD. P>0.05 (calculated using two-tailed t-test). B: Difference in dry-weight analysis between flow cell and multiwell plate *P. aeruginosa* biofilms incubated for four days. The graph shows mean values ± SD. P>0.05 (calculated using two-tailed unpaired t-test), n=3 in triplicate.

Figure 3.10A shows that the static biofilm had more biomass than the flow cell biofilm after four days of incubation, although the difference was not statistically significant. These studies were conducted in triplicate wells in a 24-well plate and in a flow cell with three coupons.

Figure 3.10B presents a comparison of each biofilm model's dry weight. The weight of the multiwell static biofilm was higher than that of the flow cell dynamic biofilm however, this difference was not statistically significant.

There was considerable variation between 24-well plate biofilm repeats due to the development of skills required for the successful handling of the static biofilm model. These biofilms were susceptible to detachment and loss during washing, and need to be handled with the utmost care. Mastering this technique prevented this variation in the studies described in the following section.

3.5 Increasing the attachment of bacteria to the coverslip by coating the coverslip with Schaedler agar in the static biofilm model

To improve bacterial attachment, a thin coating of the coverslips with Schaedler agar before solidification was attempted. Using a coating agent to improve biofilm adhesion to glass surfaces has been shown to be an effective strategy (Walker and Horswill, 2012, Stap et al., 2000). The coating procedure consisted of dripping 100 µl of the melted agar onto each coverslip. However, this procedure led to a surface distribution of agar that was thick, uneven, and incomplete; for example, the agar did not spread to the margins of the coverslip. Furthermore, the agar readily detached during the subsequent washing steps, as shown in **Figure 3.11**. In addition, the Schaedler agar absorbed the CV stain, leading to false positive results in the biofilm biomass assays. Therefore, this coating procedure was not used in further studies.

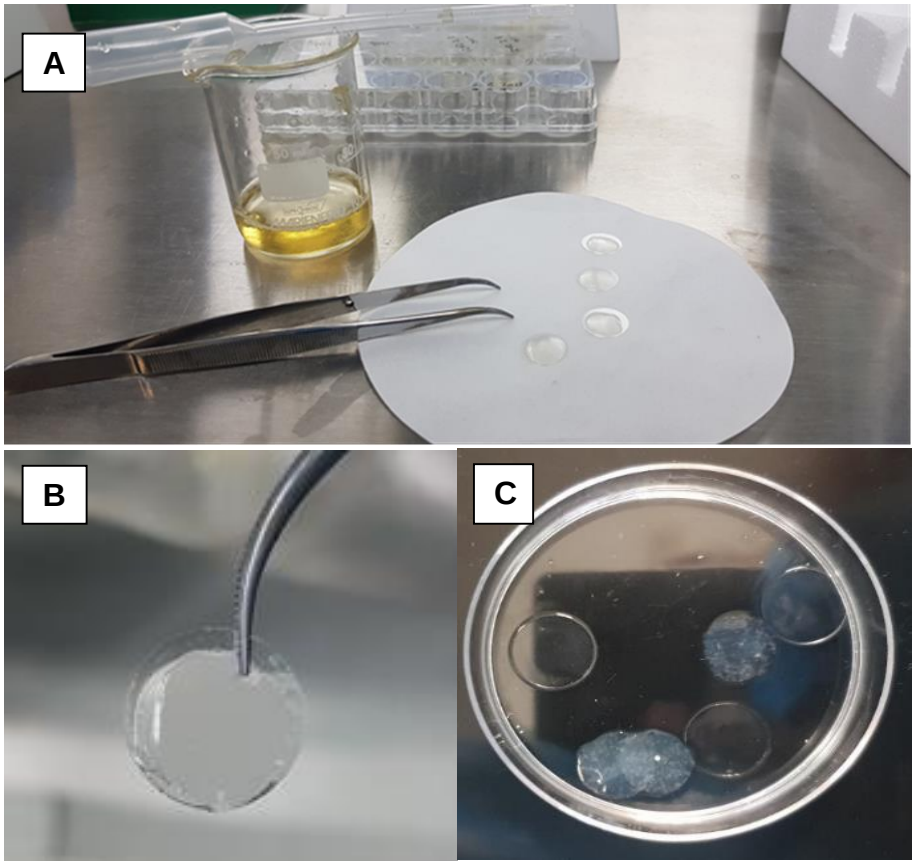

Figure 3.11: Coverslip coating with Schaedler agar. A: Coating of the coverslip with melted Schaedler agar. B: Uneven and incomplete distribution of Schaedler media. C: Detachment of Schaedler agar coating during incubation with bacterial suspension.

3.6 Comparison between flow cell, flow chamber, and 24-well plate biofilm using *S. salivarius*

After initial standardisation using *P. aeruginosa*, the oral commensal *S. salivarius* was utilised as an oral biofilm former. *S. salivarius* was used to investigate biofilm forming ability using three different setups: multiwell plates, flow cell and flow chamber. The flow chamber was added in this step as an additional dynamic biofilm model. This bacterial species was chosen because of its ability to form a biofilm (Couvigny et al., 2018) and the ease with which it can be cultivated and manipulated. Both of these characteristics make it a good model organism for examining oral biofilm formation. All biofilms were incubated for three days, which was the maximum incubation time under

which the dynamic models could grow *S. salivarius* biofilms without contamination. As **Figure 3.12** illustrates, the static biofilm mass increased significantly from the second to the third day of incubation. The flow cell biofilm mass decreased with prolonged incubation; however, this decrease was statistically non significant. The flow chamber biofilm mass increased after three days of incubation, however this increase was not statistically significant.

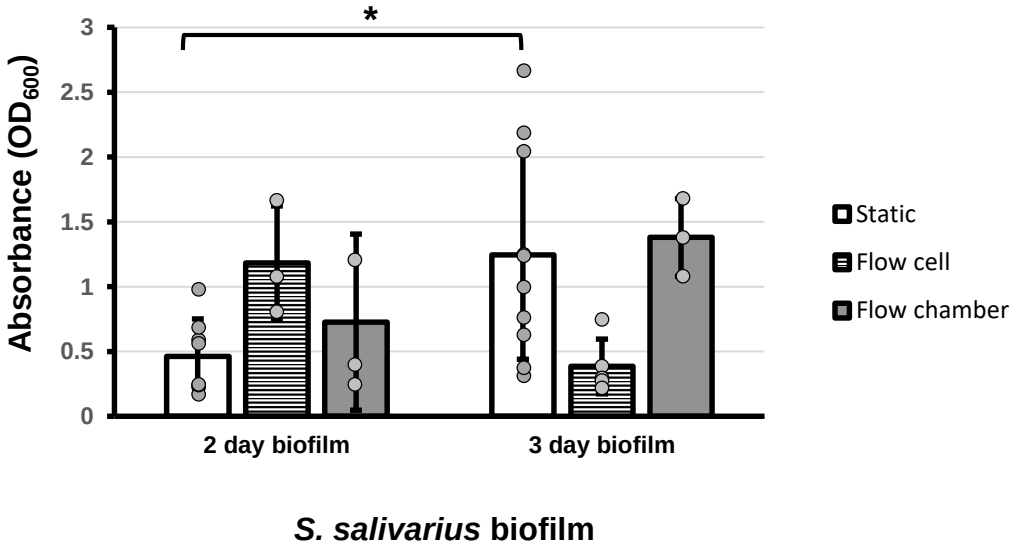

Figure 3.12: *S. salivarius* biofilm biomass in the three biofilm models.Static multiwell plate and dynamic (flow cell and flow chamber) biofilm models were used, and biofilms were cultured for two to three days. Biofilm biomass was measured by OD_{600} absorbance of the CV technique n=3 and in triplicate. Bar graph shows mean values ± SD. *P<0.05 (calculated using two-way ANOVA).

3.7 Retention of neutrophils within biofilm models

3.7.1 H&E staining

An imaging technique was performed to determine whether neutrophils were retained in the different biofilm setups and during biofilm growth. H&E staining was utilised because it provides good contrast and allows for easy identification of neutrophil multi-

lobed nuclei. Neutrophils were added to the biofilm on the first and third days of development. As **Figure 3.13** shows, the static biofilm exhibited only the neutrophils' cytoplasmic membranes, with no visible neutrophil nuclei. The neutrophils retained in the flow cell biofilm exhibited their distinctive nuclear morphology. The flow chamber biofilm exhibited neutrophils with a multilobular nucleus surrounded by *S. salivarius* bacteria. Overall, the images demonstrate neutrophil retention in all tested biofilm models, there was a higher quantity in the static biofilm compared with the two dynamic models.

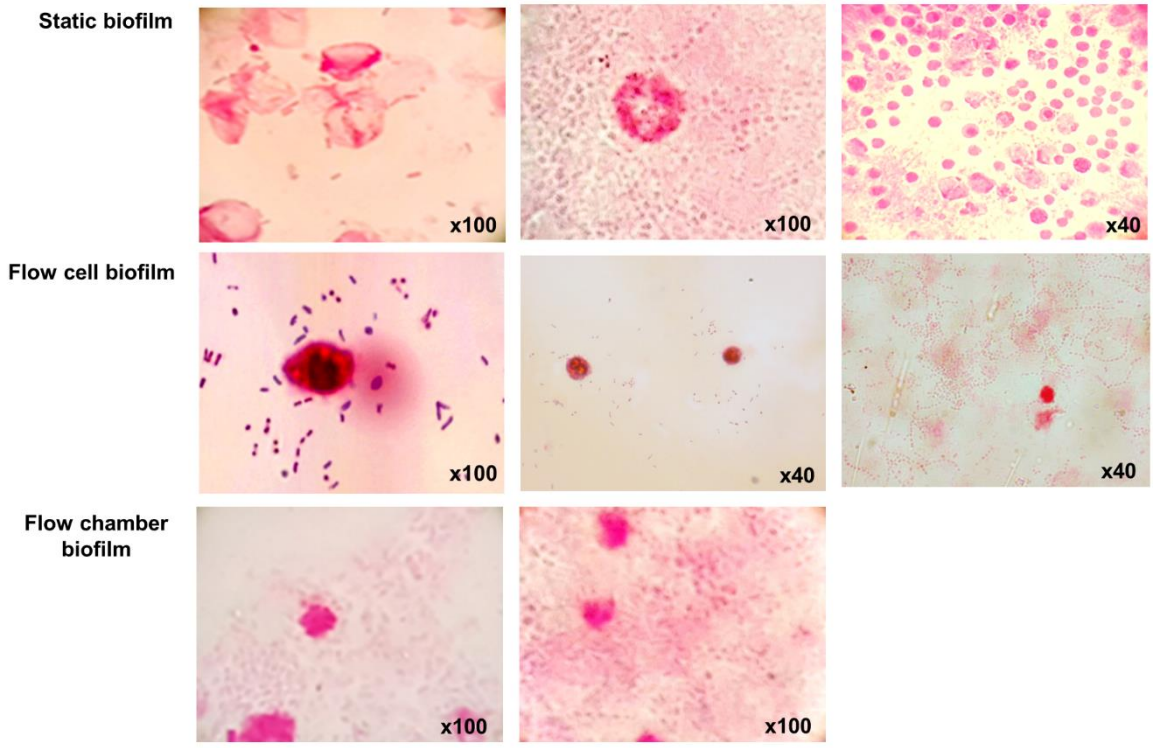

Figure 3.13: Neutrophil retention within *S. salivarius* three-day biofilms in the three biofilm culturing models following H&E staining. *S. salivarius* biofilms were cultured in static multiwell plates, and dynamic (flow cell and flow chamber) biofilm setups. Neutrophils were added to biofilms on the first and third days of biofilm development and incubated for 2 h. Static and flow cell biofilm magnification was 40x and 100x, and flow chamber biofilm magnification was 100x.

3.7.2 Fluorescent staining

3.7.2.1 Multiwell plate and flow cell *S. salivarius* biofilm with neutrophils

Fluorescent staining with SYTO 9 and CLSM imaging was utilised to view the different types of *S. salivarius* three-day dynamic and static biofilms. Neutrophils were added to all models (multiwall plate, flow cell, flow chamber) on days one and three of biofilm development. The static *S. salivarius* 24-well biofilm with added neutrophils was stained using green fluorescence nuclear stain SYTO 9 and examined under a CLSM microscope; representative images are displayed in **Figure 3.14**.

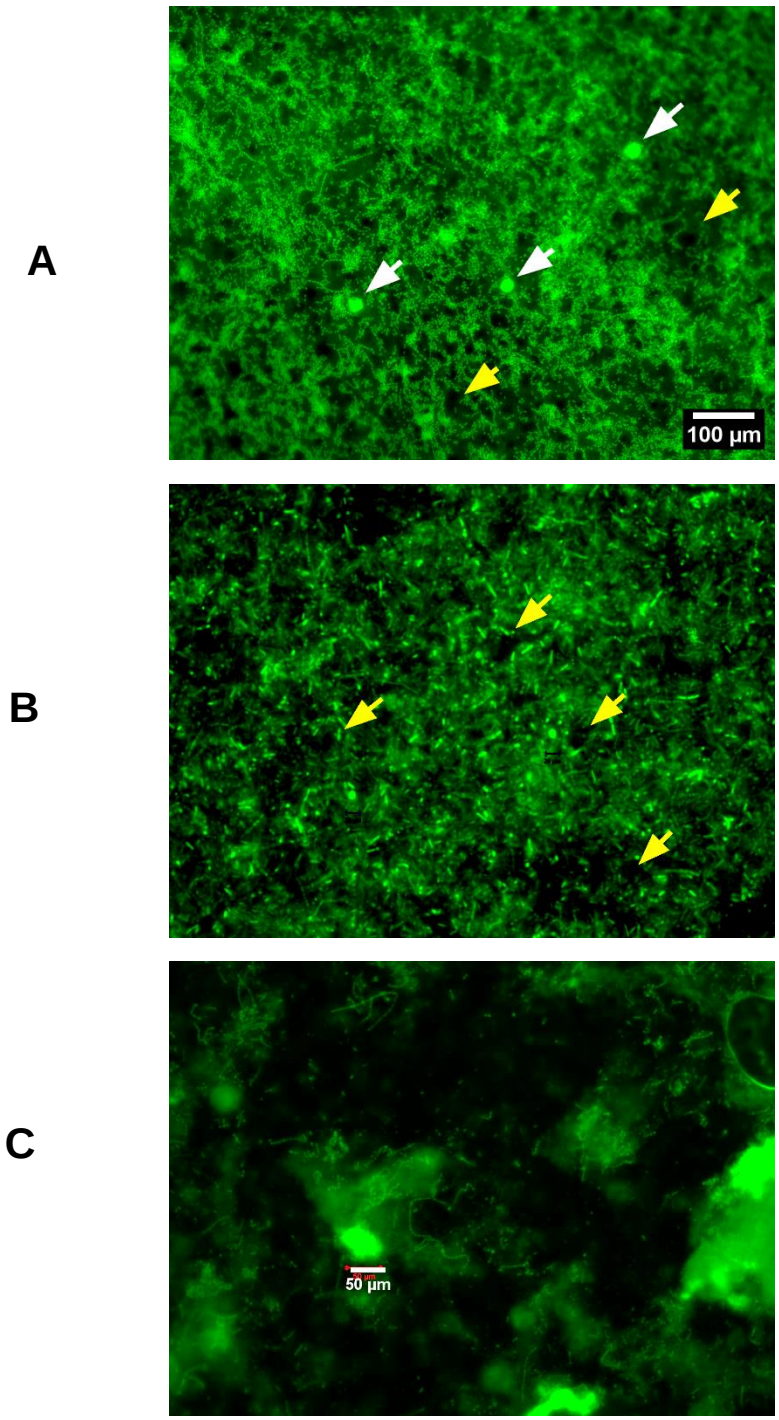

Figure 3.14: Neutrophil retention in *S. salivarius* three-day biofilms in the three biofilm culturing models following SYTO 9 staining and CLSM imaging. *S. salivarius* biofilms were cultured in static multiwell plate, and dynamic (flow cell and flow chamber) biofilm models. Neutrophils were added on the first and third days of biofilm development and incubated for 2 h. A: Multiwell plate biofilm showing long streptococcal chains, which can be seen in some areas. White arrows indicate neutrophil nucleus, and yellow arrows indicate interstitial voids within the biofilm architecture. B: Flow cell biofilm showing streptococcal chains and bacilli contaminants. C: Flow chamber biofilm showing neutrophils along with streptococci chains.

Neutrophils were identified on the basis of their distinguishing features including their morphometric characteristics, specifically, their size. A porous architecture with distinct voids was observed in the biofilm, which is a common structure in dental plaque (Wood et al., 2000). The flow cell biofilm showed a relatively similar structure with less void formation. Some contamination was observed in the flow cell images showing bacterial bacilli shape. The flow chamber did not form homogenous biofilm layering as in the other biofilms. Instead, thick biofilm aggregates with no pores were formed.

3.7.2.2 NET formation in response *S. salivarius* biofilms

The multiwall plate, flow cell, and flow chamber biofilms were stained to observe potential NET formation and expression of CD11b in neutrophils. CD11b is a well-known marker for neutrophil cell adhesion and activation (Repo et al., 1997). As **Figure 3.15** shows, the anti-CD11b marker showed no activity. Instead, needle-like crystals appeared in green in both dynamic models as well as in the static model. These crystals correspond by their physical configuration to those formed by tyrosin. No citrullinated histones in thread-like structures were detected in any of the observational fields. Instead, some distinct, punctate forms scattered over the background matrix were visualised. Neutrophil nuclei, along with *S. salivarius* biofilm were observed in blue.

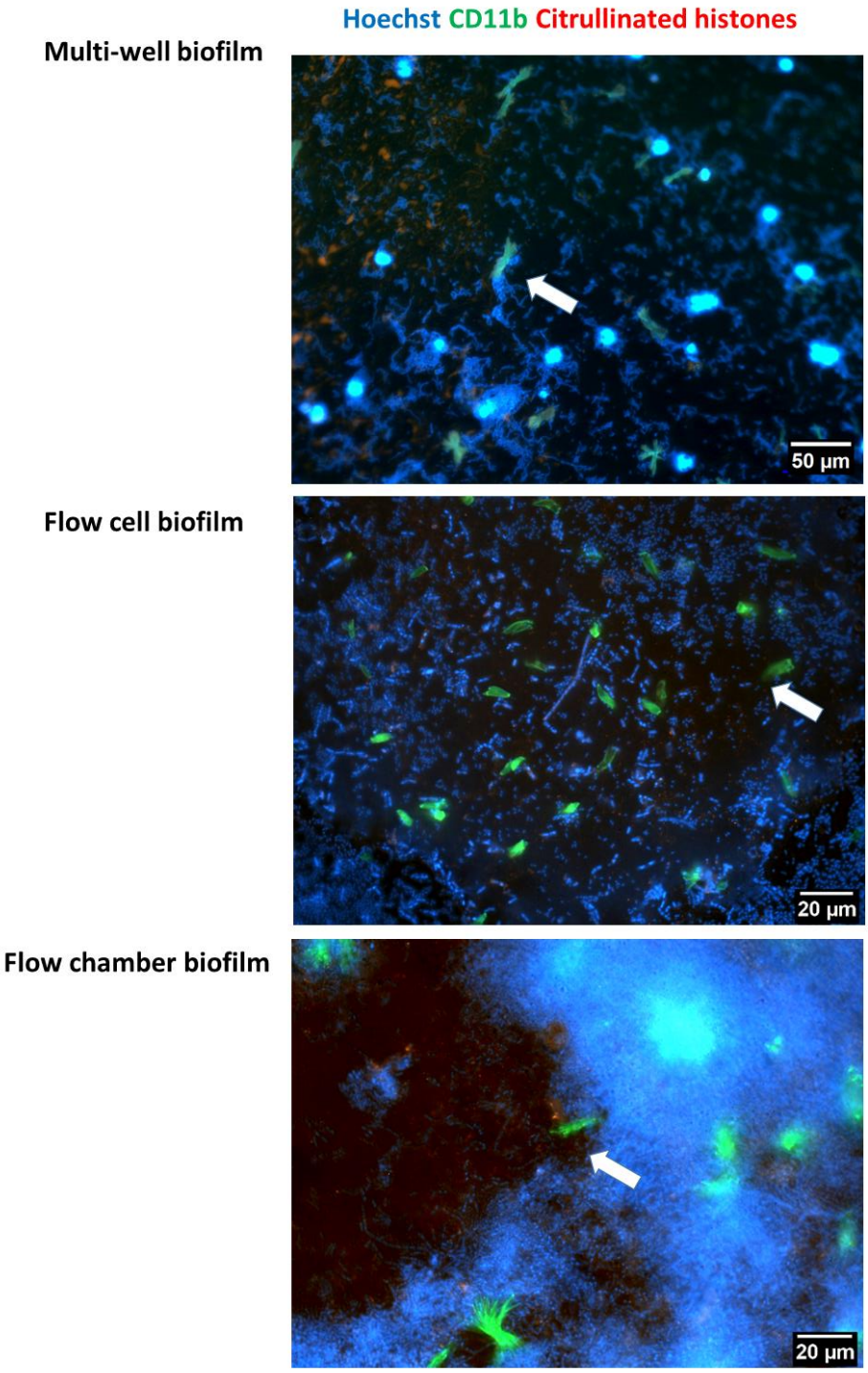

Figure 3.15: NETs specific fluorescent staining and CLSM imaging of *S. salivarius* biofilms with neutrophils at 20x magnification. *S. salivarius* biofilms were cultured in static multiwell plate, and dynamic (flow cell and flow chamber) biofilm models for three days. Neutrophils were added on the first and third days of biofilm development and incubated for 2 h. Biofilms with neutrophils were stained with Hoechst 33258 (blue), anti-CD11b (green), and anti-citrullinated histones (red). White arrows show green crystal formation.

These images also indicated that the static biofilm retained more neutrophils than the two dynamic biofilm models. Higher neutrophil retention was observed in H&E images.

3.7.2.3 Planktonic bacteria with neutrophil staining

Neutrophils were stained with anti CD11b marker for cell adhesion and anti-citrullinated histone H3 fluorescently labelled antibodies to detect NET formation. Citrullinated histone H3 is a key player in the neutrophil release of nuclear chromatin during NET formation (Thålin et al., 2018). The biofilm models did not exhibit effective staining with CD11b and citrullinated histones. To assess the efficiency of the stains used, the neutrophils were incubated with planktonic *S. salivarius* for 2 h. The neutrophils stimulated with bacteria were compared with neutrophils with no bacterial stimulation as a negative control.

As **Figure 3.16** shows, the CD11b surface marker was expressed in most unstimulated neutrophils, with high expression observed in some cells. In stimulated neutrophils, all cells expressed CD11b. Triple-citrullinated histones were expressed in both stimulated and unstimulated neutrophils in a similar pattern. Hoechst 33258 staining revealed enlarged nuclei in stimulated neutrophils, further indicating cell activation (Inozemtsev et al., 2023).

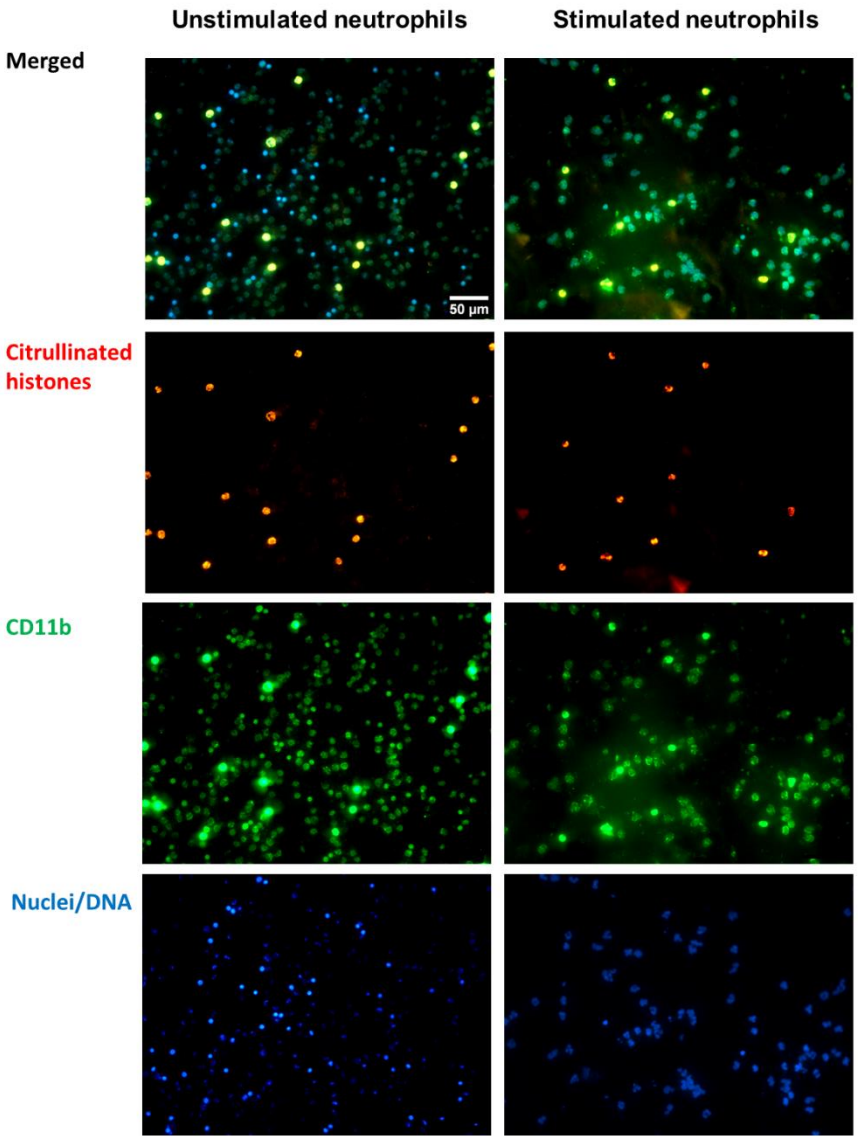

Figure 3.16: NETs specific fluorescent staining and CLSM imaging of *S. salivarius* planktonic bacteria stimulated and unstimulated neutrophils at 20x magnification. Multiplicity of infection [MOI] of neutrophils to bacterial cells is 1:200. Neutrophils were added to the bacterial suspension and incubated for 2 h. Both stimulated, and unstimulated neutrophils were stained with anti-citrullinated histones antibody (red), anti-CD11b (green), and nuclear stain Hoechst 33258 (blue).

3.7.3 SEM imaging

SEM images of the static *S. salivarius* biofilms are presented in **Figure 3.17**. The biofilms were cultured for two, three, and four days. As the static biofilm exhibited low levels of susceptibility to contamination, it could accommodate four-day incubation periods without contamination. All the biofilms displayed interconnecting material

between the bacteria, indicating that an extracellular matrix may have formed within the biofilms. The bacteria exhibited a shape loss in the thicker sections that may have been related to sample preparation (Czerwińska-Główka and Krukiewicz, 2021). Spherical cell shapes with chain arrangement appeared in the thinner sections. Smaller spherical bodies were visible after four days of incubation. Their sizes corresponded with those reported for outer membrane vesicles of streptococci (130 – 160 nm) (Mehanny et al., 2020).

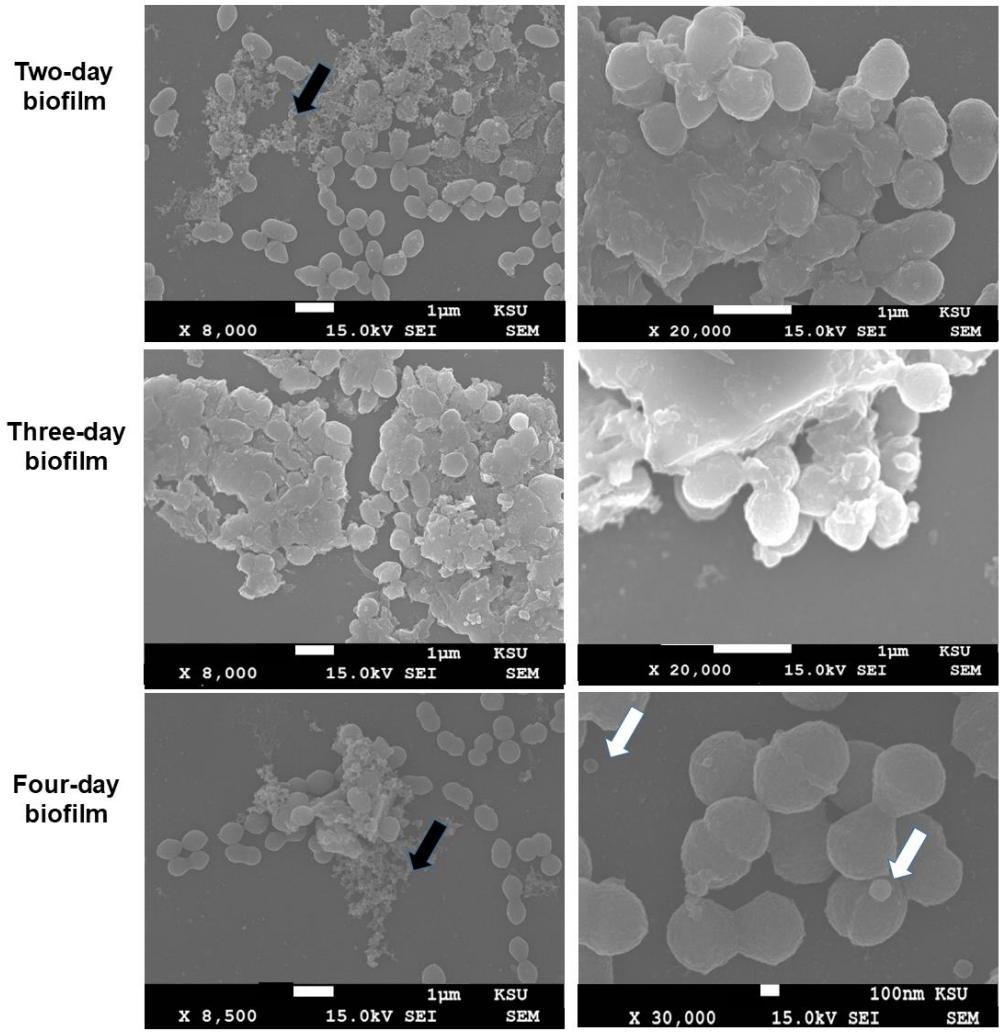

Figure 3.17: *S. salivarius* static biofilm SEM images at various time points during biofilm development. Two-day-, three-day-, and four-day-old biofilms. Matrix material surrounding and interconnecting the bacterial cells is indicated by black arrows, and small spherical bodies are indicated by white arrows. Magnifications and scale bars are displayed below each image.

3.8 Discussion

3.8.1 *P. aeruginosa* biofilm

P. aeruginosa is considered a model organism for growing biofilms (Tuon et al., 2022). For this reason, this study used *P. aeruginosa* to initially develop and validate biofilm-growing models. In the flow cell model, *P. aeruginosa* biofilm growth was directly proportional to the time of incubation. Several issues accompanied the flow cell biofilm growth, including clogging in the tubing and upstream migration of the biofilm. These issues were addressed by massaging the tubes to release the attached biofilm and refilling the feeding bottle with freshly autoclaved broth. When biofilm developed in the tubing could not be dislodged, the tubes were replaced with sterile tubes. Constant observation of the flow cell biofilm was needed to ensure that no leakage, dripping, clogging, or upstream migration occurred.

It is well-documented that the nature of the surface affects biofilm attachment (Feng et al., 2015, Garrett et al., 2008). Etching of the glass coupons was used to increase the attachment of the bacteria and, hence, to increase biofilm biomass. Etched glass coupons did not promote better attachment of cells than nonetched coupons. In fact, nonetched glass coupons provided a thicker biofilm than etched glass. In the literature, inconsistent results have been published regarding the association between biofilm growth and surface roughness (Chatterjee et al., 2019). These differences in study outcomes could be related to differences in the type of surface and the species of microorganism studied. Due to the ineffectiveness of glass etching, BSA-coated coverslips were used instead, as commonly described in the literature (Ma et al., 2020) The flow cell biofilm was compared with the multiwell plate biofilm after its efficiency in growing *P. aeruginosa* biofilm was analysed. The static biofilm had a slightly greater

mass and weight than the flow cell biofilm, although this increase was statistically nonsignificant. The decrease in the flow cell biofilm could have been caused by shear stress, which has been shown to disrupt biofilm growth and consequently limit its development, resulting in decreased biofilm formation (Moreira et al., 2013).

3.8.2 Differences between static and dynamic *S. salivarius* biofilms

Due to its straightforward cultivation requirements, *S. salivarius* was selected as an oral strain for biofilm formation. This strain choice allows for a more efficient and robust performance comparison across biofilm-growing models under investigation. The flow chamber was included as an additional dynamic biofilm-growing model at this point of the study. This study was performed to evaluate different dynamic models' efficiency in forming biofilms. All three models (the multiwell plate, flow cell, and flow chamber) were compared in terms of their ability to form *S. salivarius* biofilms. On the whole, oral biofilms exhibit slow growth rates, which may lead to contamination during the process of biofilm formation (Do et al., 2013). *S. salivarius* biofilm was cultured for three days, which was the maximum period without exhibiting contamination in the dynamic models. Neither of the dynamic biofilms exhibited a significant difference when the incubation time increased from two to three days. On the other hand, the static biofilm exhibited a significant biomass increase when the incubation time increased from two to three days. A comparison of the models demonstrated that the two-day flow cell *S. salivarius* biofilm mass was higher than that of the multiwell plate biofilm. After three days of incubation, the flow cell biofilm mass decreased, whereas the static biofilm mass increased. This may have resulted from the fact that dynamic biofilms initially had better access to nutrients than static biofilms. When the flow cell biofilm was further incubated, shear-stress forces may have negatively impacted the biofilm's mass

because more detachment may have occurred (Moreira et al., 2013). The flow chamber biofilm mass was higher than that of the flow cell and exhibited similar or higher biomass compared to the multiwell plate biofilm. However, despite these differences in the biomasses of the dynamic biofilms, they were not statistically significant due to the considerable variation in biological and technical replicates. These results demonstrate how challenging it can be to ensure consistent and reproducible conditions in dynamic biofilm models (Ramachandra et al., 2023).

The next step was to add neutrophils to the bacterial biofilm to test whether they were retained within the structure. Isolated neutrophils were introduced to *S. salivarius* biofilms suspended in RPMI with 5% FBS, which is commonly used as a base medium in neutrophil studies (Moore et al., 1967). Neutrophils were added to all three biofilm models (the multiwell plate, flow cell, and flow chamber) on the first and third days of biofilm development. Neutrophils were retained in all the tested biofilms, and the dynamic models exhibited lower neutrophil retention compared with the static model. This was confirmed using H&E staining and fluorescent staining. The lower neutrophil retention could be attributed to the failure of neutrophils to attach to the biofilm due to the flow medium sheer forces. In addition, hydrodynamic or sheer forces can cause structural changes in biofilms, making them less layered and more fluffy, affecting the biofilm's ability to trap neutrophils efficiently (Paramonova et al., 2009). Following H&E staining, static biofilm neutrophils and bacteria showed evidence of co-localisation, suggesting potential phagocytic activity. In addition, evidence of cell death was provided by the presence of “empty” cytoplasms and cell-membrane remnants. These indicate the loss of nuclear and other intracellular materials. These neutrophil appearances were not observed in the flow cell or flow chamber biofilms. A possible explanation is that any dead cells were washed away under flow conditions.

Under fluorescent staining, round-shaped voids were observed in the multiwell plate biofilm. These voids appeared in static biofilms, where neutrophils could settle because shear stress was absent. In dynamic biofilms, similar voids were observed in the flow cell biofilm only, which were less uniformed than the static biofilm voids. These voids are presumed to be water channels and were observed with other static oral biofilm *Fusobacterium nucleatum* (Muchova et al., 2022). In the flow chamber, the biofilm formed thick aggregates that attached to the walls, forming clumps and decreasing the space for the medium to flow. The narrowing of the flow channels increases the medium flow forces on the biofilm, leading to possible distortion of the water channels, which could explain the lack of these voids' architecture in the flow chamber (Straub et al., 2020). Voids within the biofilm were potential indications of cell death, which serves as a dispersal mechanism that liberates attached (sessile) resident bacteria from the EPS to the planktonic free-living state during the typical biofilm's development cycle (Webb et al., 2003). The release of bacteria from the biofilm is considered an essential survival strategy to colonise other sites (Socranksy and Haffajee, 2002). While the appearance of voids within the biofilm structure can be attributed to the natural creation of water channels, which is an essential component of biofilm architecture, the observed increase in the frequency of these gaps may not be due exclusively to this typical pattern. It is possible that additional extrinsic or intrinsic elements impact the increase in void frequency. It has been reported that increased void formation within biofilms coincides with antibiofilm treatment (Goodwine et al., 2019). Along with the correspondence between some of the sizes of the voids and that of neutrophils, these previous findings suggest that neutrophil attack may increase void formation.

Needle-like crystals were also observed within the fluorescent-stained biofilm. The morphology of the crystals aligned with the typical characteristics of tyrosine crystals,

which appeared after three days of incubation with TSB. Tyrosine is the primary amino acid in casein, a major component of TSB. Resulting from the action of bacteria causing tyrosine release, casein breakdown causes tyrosine build up and subsequent crystallisation. Tyrosine is known to cross-react with various proteins, including antibodies (Ruyechan and Olson, 1992, Mannironi et al., 2000, Ospina-Villa et al., 2015). Therefore, the binding of anti-CD11b may have led to the appearance of green crystals in fluorescent images. In addition to these observations, anti-citrullinated histone staining showed no obvious NET production in any of the tested biofilm models. Instead, diffuse punctate structures were seen intermittently spread over the backdrop matrix. This form of citrullinated histones diffused pattern was reported to form a scaffold to promote thrombus formation (Fuchs et al., 2010). These dot-like aggregates may be due to the electrostatic bonds between the negatively charged bacterial cells and the positively charged histones in NETs (Watson et al., 1999).

In neutrophils stimulated with planktonic *S. salivarius*, CD11b was highly expressed on some of the unstimulated neutrophils, which indicated their activation (Repo et al., 1997). Even when no stimulation is performed, neutrophils can rapidly become activated. It has been documented that the techniques used for neutrophil isolation from peripheral blood can greatly influence neutrophil activation (Lang et al., 1982, Haslett et al., 1985), especially the expression of cell adhesion molecules like CD11b (Youssef et al., 1995, Macey et al., 1995). Although the use of Percoll gradients is a broadly accepted isolation method that has minimal effects on neutrophil activation (Hu, 2012, Lucas et al., 2013), it has been reported that neutrophil expression of CD11b resulted from subsequent washing by centrifugation (Berends et al., 1994). This could explain the similarity between stimulated and unstimulated neutrophils' expression patterns, with the expression pattern of stimulated neutrophils exhibiting a

slight increase. The upregulation of CD11b induced by *S. salivarius* is consistent with the reported literature (Oveisi et al., 2019). In some neutrophils, citrullinated histones were evident, not in a NET pattern but were associated with the cells. This suggests that the early stage of NET formation may have been captured, which is characterised by hypercitrullination of nuclear histones prior to DNA de-condensation (Wang et al., 2009). As it has been reported that NETs are produced within 2–6 h of incubation with a stimulus, a more extended incubation period may be needed to visualise NET formation (Rada, 2019, Kaplan and Radic, 2012). The time required for NET formation can vary depending on the severity of the stimulation. Strong stimuli, such as pathogenic bacterial infections or robust inflammatory signals, can cause NETosis quickly, often within minutes of contact. This rapid response aids the immune system in rapidly containing and neutralising pathogens. Weaker stimuli, on the other hand, may result in a slower and more extended NETosis process. Sustained low-level stimulation can still cause NET formation, but the process may be slower or less widespread than with greater stimuli (Mikolai et al., 2020, Tatsiy et al., 2021, Parker et al., 2021). *S. salivarius* may not be a robust inducer of NET formation as it is not normally pathogenic under normal conditions. It can, however, cause NETosis under certain situations or in the setting of a dysregulated immunological response. The slower or less robust NET response to *S. salivarius* in this study could be attributed to its status as a comparatively mild stimulus in comparison with more aggressive bacteria (Oveisi et al., 2019).

The static biofilm was relatively easier to reproduce compared with both of the dynamic biofilm systems. The dynamic models required tube cleaning and device autoclaving for every biological replicate. Moreover, the dynamic system was prone to airlock formation. Despite several attempts to prevent air lock formation, bubbles formed due

to changes in shear pressure resulting from different tubing diameters (Crusz et al., 2012). This resulted in the formation of biofilm-free zones due to the liquid–air interface, which leads to biofilm detachment (Sharma et al., 2005). The operation of the flow chamber was time-consuming and complicated. The device is prone to airlock formation and very vulnerable to leakage if not appropriately sealed with silicon. If any leakage occurs during the flow of the medium, the flow cycle has to be stopped, and the flow chamber dried and resealed and left to dry overnight. These artefacts were also addressed in the literature (Tolker-Nielsen and Sternberg, 2014). As a result, the device had poor reproducibility. For these reasons, the flow chamber testing in this study was discontinued.

Choosing the most suitable biofilm model depends on the research question and the experimental approach. Multiwell plate biofilms are simple, inexpensive, and less susceptible to contamination than dynamic models, making them suitable for high-throughput biofilm-formation screening or for assessing the influence of various chemicals on biofilm development. They do not, however, have the flow conditions found in many natural and clinical settings (Azeredo et al., 2017). As a result, they would not be ideal for examining biofilm behaviour in response to fluid dynamics or shear stress. By contrast, dynamic models enable researchers to investigate biofilm formation under dynamic-flow circumstances, which are more representative of clinical settings than static models. They are, however, more challenging to manage, resource-intensive, and susceptible to contamination than static models (Tolker-Nielsen and Sternberg, 2011).

In conclusion, the dynamic mode flow chamber was abandoned due to the difficulty in producing an appropriate biofilm for this study. The flow chamber and the static multi-

well plate approach showed good potential in biofilm formation and were studied further in the following chapter.

3.9 2020 IADR abstract

An abstract titled “Comparison of Three *In Vitro* Models to Assess Biofilm-Neutrophil Interactions” was accepted for a poster presentation at the 2020 International Association for Dental Research (IADR) General Session. Scheduled for March 18–21, 2020, in Washington, DC, the IADR General Session was cancelled due to the COVID-19 outbreak. However, the poster was submitted to the 2020 IADR/AADR/CADR General Session. It became part of IADR’s abstract archive, and it is citable as part of a special issue of *Journal of Dental Research* which is available online at the following web address: **https://iadr.abstractarchives.com/abstract/20iags-3328598/comparison-of-three-in-vitro-models-to-assess-biofilm-neutrophil-interactions**. The abstract is shown in Appendix 1.

3.10 Graphical summary

Evaluation of three biofilm-growing models using *P. aeruginosa* and *S. salivarius*

		Advantages	Neutrophil retention	Disadvantages	Conclusion
Static biofilm model	Multi-well plate 	Simple, inexpensive, and less susceptible to contamination. Suited for investigation of high-throughput biofilm formation or assessments of the influence of chemicals on biofilm development.	Retain a higher number of neutrophils	Lack of flow conditions found in many natural and clinical settings	Lack of flow conditions found in many natural and clinical settings
Dynamic biofilm models	Flow cell 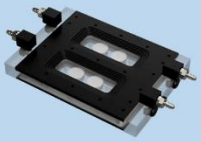 Flow chamber 	Dynamic biofilms Investigate biofilm formation under dynamic flow circumstances, which are more representative of clinical settings	Retain a lower number of neutrophils	Complex, resource intensive, and susceptible to contamination and bubble formation. Only two to three biofilm-growing chambers The flow chamber is difficult to assemble to retrieve the biofilm	The flow cell showed promising results and was further analysed using multispecies oral biofilm in Chapter 4 The flow chamber study was discontinued due to disassembly difficulties

4 CHAPTER FOUR Results: Three-Species Oral Biofilm

4.1 Introduction

Bacteria exist as complex multispecies biofilms in the oral cavity. Whereas Chapter 3 established the biofilm-growing models using a single-species set up, the research presented in Chapter 4 used a multispecies oral biofilm containing *S. oralis*, *S. mitis*, and *S. intermedius*, members of the yellow complex. This biofilm was created to mimic the early biofilms in the oral cavity. Early colonisers can produce an environment that enables other pathogenic organisms to infect the biofilm. Understanding and targeting these early colonisers could aid in preventing or mitigating oral biofilm development. An *S. oralis* monospecies biofilm is documented to induce neutrophil activation, which can change when *S. oralis* is combined with other species (Oveisi et al., 2019). In addition, *S. oralis* and *S. mitis* predominate subgingival plaque, comprising 14.67% and 16.89% of total isolates, respectively (Dhotre et al., 2018). *S. intermedius* was found to rapidly colonise dental implants and reach mature biofilm within 5 hours (Blus et al., 2015). This rapid colonisation is consistent with its ability to establish itself in household contexts shortly after birth (Saijonmaa-Koulumies and Lloyd, 2002). Given the aforementioned considerations, these species were selected for investigation in this chapter.

This chapter investigates two effects: the influence of the three-species biofilm on neutrophils and that of neutrophils on the biofilm. First, the biofilm's influence on neutrophils was assessed by examining its ability to trigger NET formation. Second, the effect of neutrophils on various biofilm models was investigated by measuring biofilm biomass, metabolic activity, and dry weight. During the studies, the bacterial species were examined to ensure that the organisms utilised here had not altered or been contaminated.

4.2 Standardisation

4.2.1 Bacterial growth curve

A growth curve was devised to quantify planktonic bacterial growth and visualise the different stages of bacterial growth over time in TSB. TSB was inoculated to 0.1 OD_{600} from overnight cultures as described in **Section** 2.1.2. The single and three-species growth curves were inoculated with the same cell numbers. The OD_{600} was monitored every 60 min until the cultures reached the stationary phase.

Figure 4.1 demonstrates that *S. oralis* exhibits a faster growth rate when cultured as a single-species compared with its growth together with other species. The stationary phase began after 8 h of culture for all single and mixed-species. The comparison of the growth dynamics of *S. oralis* monospecies and, when mixed with *S. mitis* and *S. intermedius*, revealed unique trends in their respective growth periods. Compared with the three-species culture, *S. oralis* had a more extended logarithmic phase. These data demonstrate that *S. oralis'* growth kinetics are slower, requiring more time to attain the maximal growth rate. Despite the longer duration of the log phase, *S. oralis* had a more pronounced exponential phase than the three-species culture. This suggests that once *S. oralis* reached its development peak, it proliferated faster, resulting in a steeper increase in the exponential portion of its growth curve.

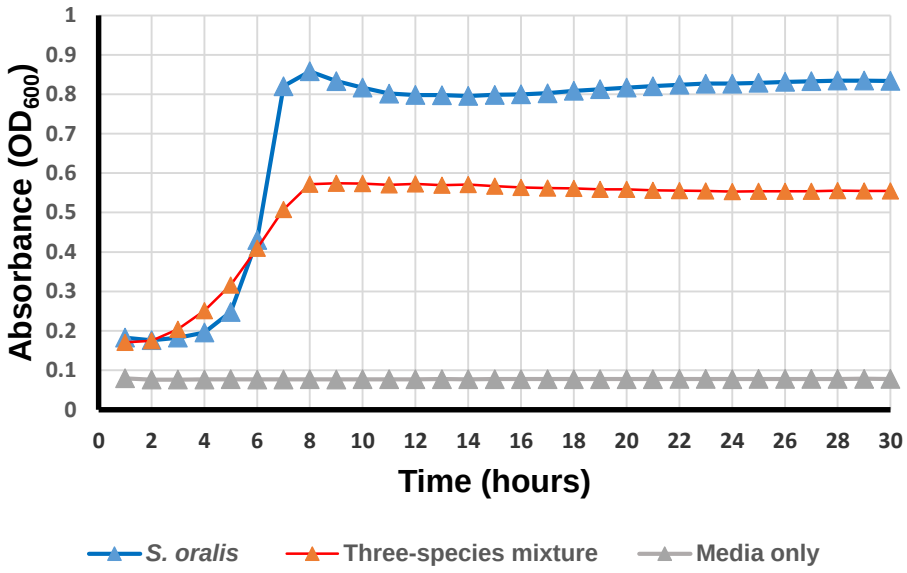

Figure 4.1: Growth curves for planktonic *S. oralis* and the three-species combination in TSB. Readings were obtained every hour for 30 h. Plates were incubated at 37°C for two days. Experiments were performed independently three times.

Both *S. mitis* and *S. intermedius* exhibited a shorter lag phase and a slower exponential phase than *S. oralis*, correlating with the results of the three-species growth curve. OD values for *S. mitis* and *S. intermedius* were found to be lower than those observed for the three species during the exponential phase. *S. intermedius* had the lowest OD among the investigated species, indicating a less robust exponential growth phase.

4.2.2 Detection of potential DNase production by the strains tested and neutrophils

The ability of the bacteria tested to produce the DNase enzyme was assessed to rule out each bacterium's potential to disrupt NETs. In **Figure 4.2**, a clear zone around the bacterial inoculation indicated positive DNase production. No DNase production was detected for any of the tested strains after one day of incubation. After the plates were incubated for three days, weak DNase activity was observed for *S. intermedius* and *S.*

mitis. At no point during the total incubation period did *S. oralis* produce any DNase detectable using this method.

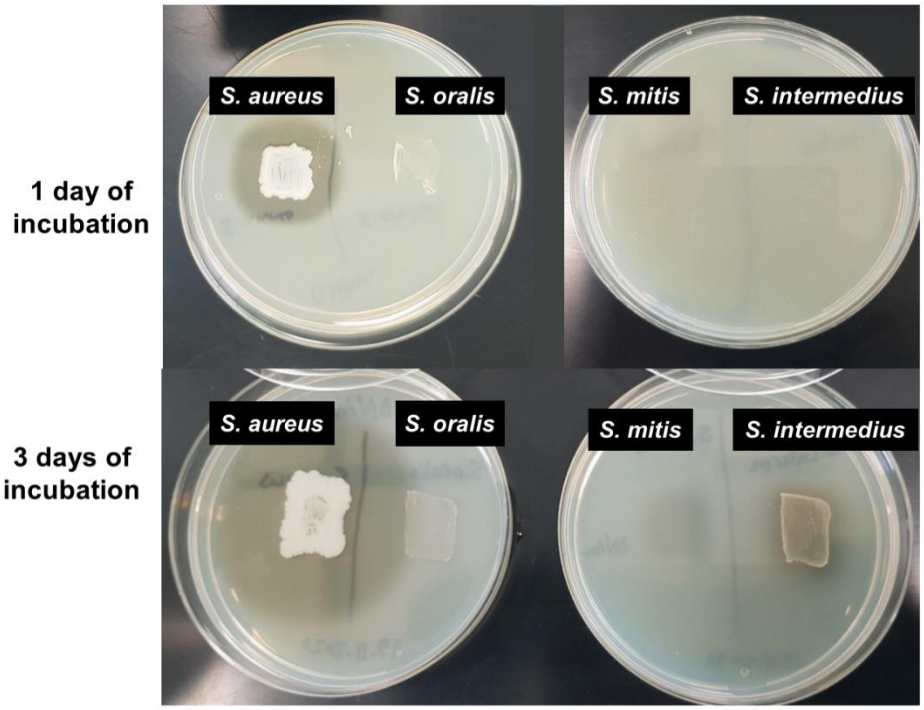

Figure 4.2: Investigation of DNase production in the selected streptococci. A: DNA-containing media after one day and after three days of inoculation of *S. oralis*, *S. mitis*, *S. intermedius*, and *S. aureus* as a positive control. Clear zones around the inoculum after adding HCL to the medium indicate the production of DNA-cleaving enzymes.

Moreover, the potential production of DNase by neutrophils was analysed to investigate whether the neutrophils produced DNA-cleaving enzymes. Three samples containing $1x10^6$ neutrophils suspended in PBS were plated onto DNA-containing agar plates and incubated for one day at 37°C + 5% CO_2. The selection of this short incubation time period was influenced by the average neutrophil half-life of 6 – 8 h (Summers et al., 2010). Several reasons can be advanced to support the use of DNA-containing agar to test neutrophil DNase production. First, this method allows for a direct measurement of DNase activity. Second, the DNA-agar plate approach is simple and inexpensive, making it more accessible and practical compared with alternative

DNase activity evaluation methods, and data interpretation is also relatively straightforward. The number of neutrophils tested was adjusted to equal the number added to the biofilms. Neutrophil samples exhibited no detectable production of DNA-cleaving enzymes.

4.2.3 Assessment of bacterial species present in mixed biofilms

Validating bacterial species during experiments is critical to ensuring that the bacterial strains employed have neither changed nor been contaminated. Even though Gram staining was used to provide continual reassurance of microscopic evidence that streptococcal species were present (**Figure 4.3**), a more precise approach was also used.

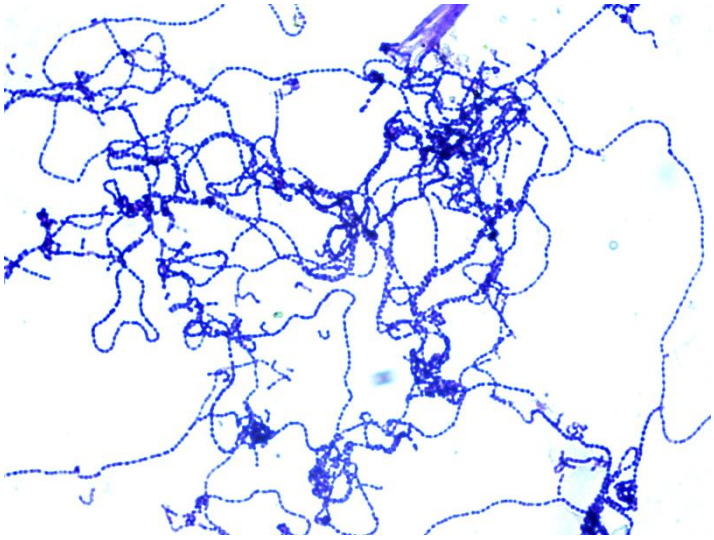

Figure 4.3: Three-species biofilm supernatant Gram stained in 100x magnification showing Gram-positive streptococci in chains. Three-species biofilm was cultured for two days, and the supernatant was aspirated and stained to ensure microscopic purity.

The ability of MALDI-TOF to identify bacterial species within short timeframes, identify a wide variety of bacteria, and provide highly accurate results make it a powerful tool for bacterial identification (Summers et al., 2010). MADLI-TOF is not yet sufficiently

advanced to distinguish between mixed species samples. However, it is optimised for individual species identification. As a result, to aid species identification in this work, each species was cultivated separately and then analysed.

As **Figure 4.4** indicates, *S. intermedius* was identified, but *S. mitis* and *S. oralis* were identified as *S. oralis/S. mitis* because Vitek MS (BioMérieux, Marcy l'Etoile, France) cannot differentiate between these closely related species (Kärpänoja et al., 2014, Angeletti et al., 2015). Therefore, MALDI-TOF proved to be unsuitable to verify this three-species biofilm.

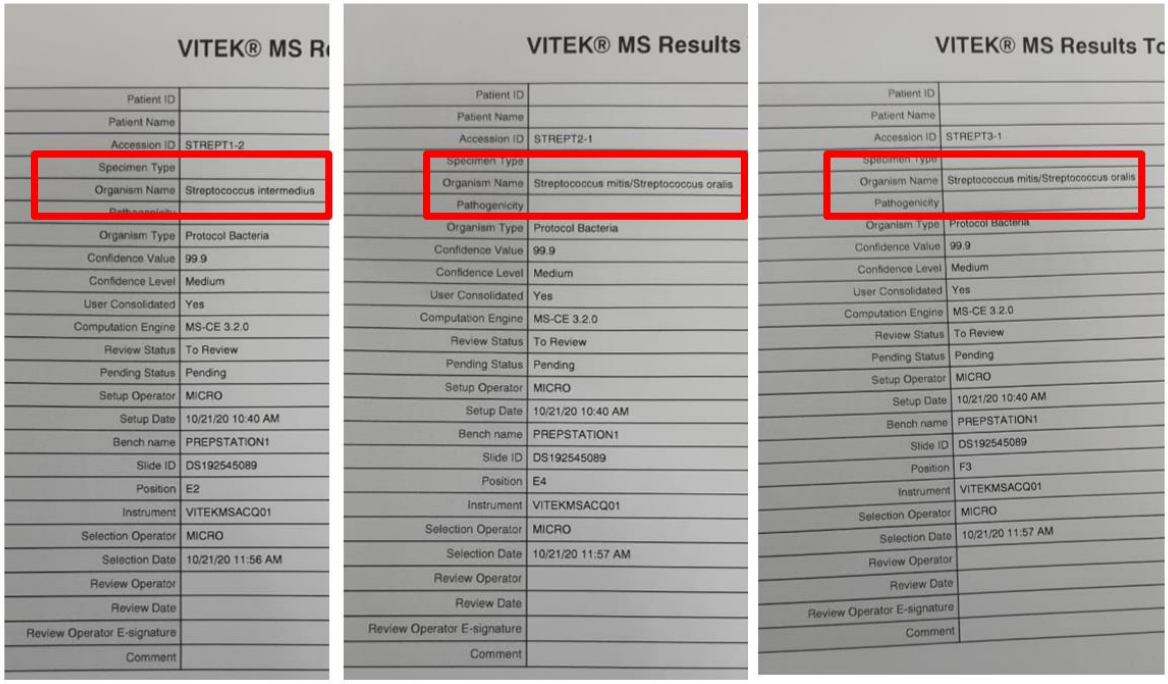

Figure 4.4:MALDI-TOF result sheets for identification of the three species. The strains were cultured separately, and one colony from each culture was analysed. The red boxes highlight the names of the identified organisms.

After the MALDI-TOF approach was deemed inappropriate, a secondary strategy was used, which involved whole-genome shotgun sequencing of the biofilm as a mixed-species community rather than identifying each species individually. Around 6 million reads were generated during the shotgun WGS sequencing. The obtained sequencing data were analysed using two databases, COSMIC ID and Illumina.

Figure 4.5 displays the results of the COSMIC ID database. Streptococci were reliably detected in all replicates. The species abundance was approximately 36% *S. intermedius* and 60% *S. mitis*. Notably, there was no evidence of *S. oralis* being present. This observation could be explained by the large overlap in sequencing reads between *S. oralis* and *S. mitis*, with all overlapped reads likely being ascribed to *S. mitis*. On the other hand, the Illumina database was unable to effectively identify the sequencing data, indicating potential limitations or compatibility issues with this database and the sequencing data obtained from the mixed-species biofilm.

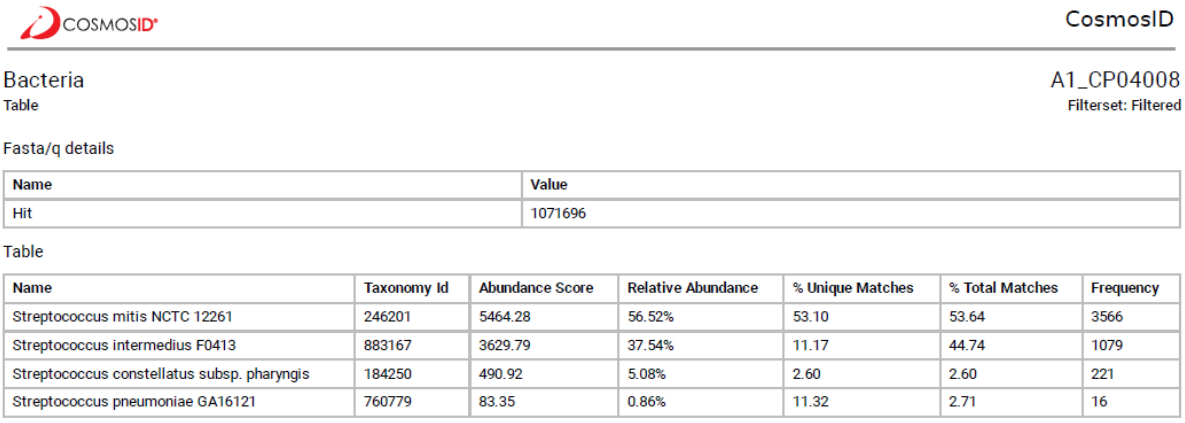

COSMOSID

CosmosID

Bacteria

Table

A1_CP04008

Filterset: Filtered

Fasta/q details

Name	Value
Hit	1071696

Table

Name	Taxonomy Id	Abundance Score	Relative Abundance	% Unique Matches	% Total Matches	Frequency
Streptococcus mitis NCTC 12261	246201	5464.28	56.52%	53.10	53.64	3566
Streptococcus intermedius F0413	883167	3629.79	37.54%	11.17	44.74	1079
Streptococcus constellatus subsp. pharyngis	184250	490.92	5.08%	2.60	2.60	221
Streptococcus pneumoniae GA16121	760779	83.35	0.86%	11.32	2.71	16

Figure 4.5: Shotgun WGS analysis of three-species biofilm in the COSMO ID database. As is indicated in the table, *Streptococcus* species were identified, with *S. mitis* having the highest abundance (n=3).

Overall, the three-species exhibited distinct morphological characteristics and were different in the biofilm-forming capabilities that can be differentiated by visual inspection. **Figure 4.6** shows the differences in their biofilms after three days of incubation.

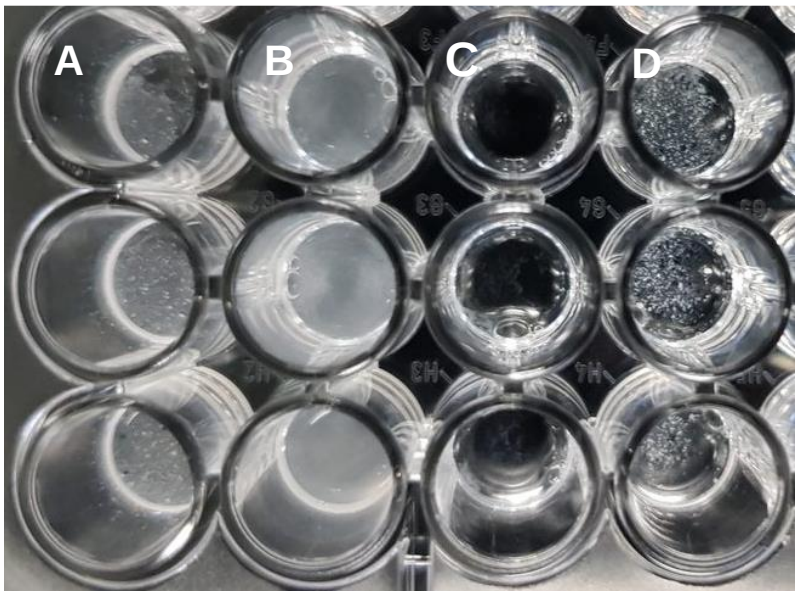

Figure 4.6: Three-species and mono biofilms morphological differences in a multiwell plate. Column A: three-species biofilm, B: *S. oralis* biofilm, C: *S. mitis* biofilm, D: *S. intermedius* biofilm. Biofilms were grown in a 96-well plate for three days and incubated at 37°C + 5% CO_2.

S. intermedium biofilm exhibited a punctate or 'dot-like' morphology rather than a uniform or homogenous structure. *S. mitis* consistently produced a thin biofilm with a low density. *S. oralis*, on the other hand, formed a more homogeneous biofilm structure with a higher density than the other species studied. These observations emphasised the intrinsic differences between species in biofilm development and structural properties.

4.3 Dynamic and static three-species biofilms

The dynamic flow cell with coupons glass or HA discs and the static multiwell plate glass coverslip were used as a platform to create a three-species biofilm containing *S. mitis*, *S. oralis*, and *S. intermedius* (**Figure 4.7**). Regardless of the number of attempts,

the flow cell-generated three-species biofilm was consistently contaminated. The presence of contamination was discerned by Gram staining and SEM imaging.

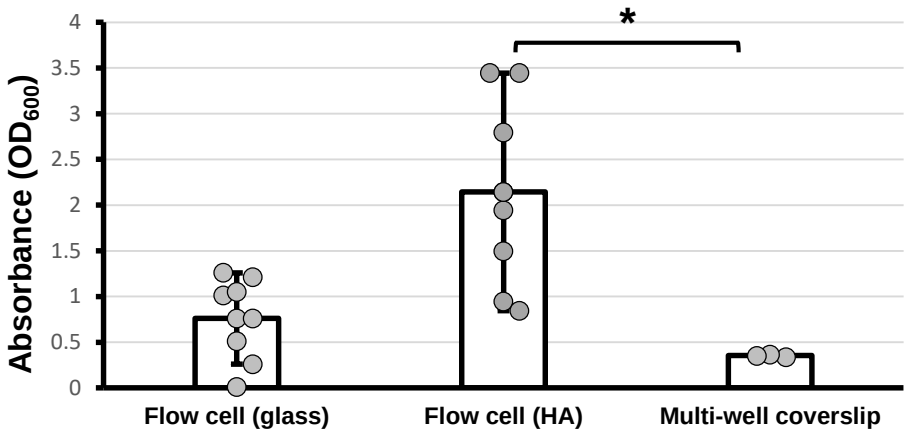

Figure 4.7: Differences in the biomass assessed by CV staining of the three-species biofilms. The biofilms were cultured in the flow cell with glass coupons, flow cell with HA coupons, and the coverslip in multiwell plates (n=3 in triplicates). Biofilm biomass was measured using the OD_{600} absorbance of the CV biofilm staining. Bar graph shows mean values ± SD. P-values were calculated using one-way ANOVA, *P≤0.05

The flow cell with HA coupons produced the biofilm with the highest biomass. The increase in reading, however, may have been obscured by the fact that the HA material appeared to retain the CV stain, which might be related to its surface microroughness. Both of the flow cell surface biofilms were thicker than the static biofilm. However, variability was large due to the described issues with flow cell reproducibility.

4.3.1 pH analysis to determine biofilms metabolic activity

PH was measured to determine the change in metabolic activity of the three-species biofilms, as this reflects the production or consumption of protons during various metabolic processes (Srinivasan and Mahadevan, 2010). The fluid descending from the flow cell was collected over the course of 1 hour, and its pH was measured. The pH of the multiwell plate biofilm was recorded by measuring the media in each well

with a micro pH probe. As **Figure 4.8** illustrates, the pH of the flow cell biofilm decreased from being slightly alkaline to acidic after the first day of incubation and then exhibited a daily decrease of 0.1.

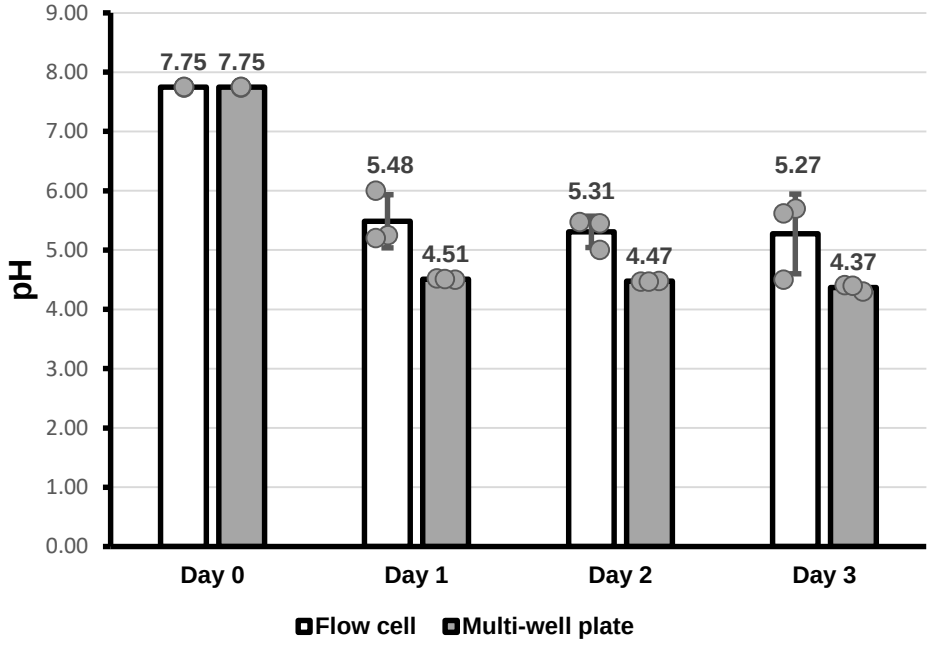

Figure 4.8: The pH values of the three-species biofilms cultured in the flow cell (dynamic) and multiwell plate (static) biofilm models. The flow cell biofilm's pH was recorded by measuring the collected fluid in the waste bottle, while the pH of the multiwell plate was recorded by measuring the biofilm supernatant. Day 0 represents the media pH before bacterial inoculation.

4.3.2 Neutrophil survival at pH 4.5

The survival of neutrophils at pH 4.5 was examined to determine the impact of the pH change induced by the biofilm's metabolic activity on neutrophils within it. Neutrophil survival levels were determined using the trypan blue staining method.

Figure 4.9 demonstrates that 50% of neutrophils survived at pH 4.5 after 1 h compared with their survival at neutral pH. This finding indicated that 50% of neutrophils survive for up to one hour in the three-species biofilm with a pH of 4.5. Although the neutrophils

were always added to the biofilm in fresh media at neutral pH, this ensures the survival of neutrophils at the lowest detected biofilm pH as the biofilm metabolic activity can alter the pH of the media, as indicated by the findings in **Section** 4.3.1.

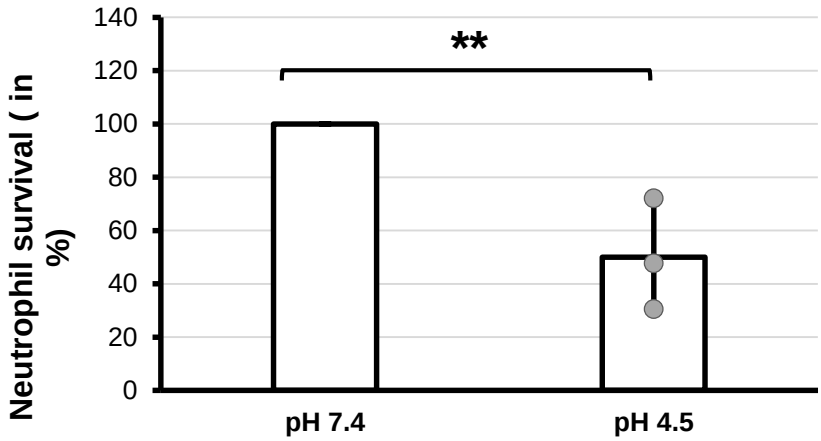

Figure 4.9: Neutrophil survival at pH 4.5. Neutrophils were incubated for 1 h in RPMI + 10% FBS at a pH adjusted to 4.5 (n=3) and compared to neutrophils incubated at pH 7.4. Bar graph shows mean values ± SD. P-values were calculated using Student's t-test. *P=0.01.

4.4 Three-species biofilm with neutrophils added after one day of biofilm development

Neutrophils were added to the biofilm to determine whether the static and dynamic three-species biofilms could retain neutrophils as was seen in the monospecies *S. salivarius* biofilm.

4.4.1 SEM biofilm imaging

SEM imaging was utilised to investigate neutrophil retention in the three-species biofilm. As **Figure 4.10** shows, contamination with Gram-positive rods was detected in the dynamic model only. HA biofilm imaging revealed round cell-like structures that corresponded in size to neutrophils. No neutrophils were detected in the flow cell glass coupon biofilm, which is consistent with the previous findings that neutrophils might

have been washed away due to flow shear stress or, because of their low number, may have detached during the staining process.

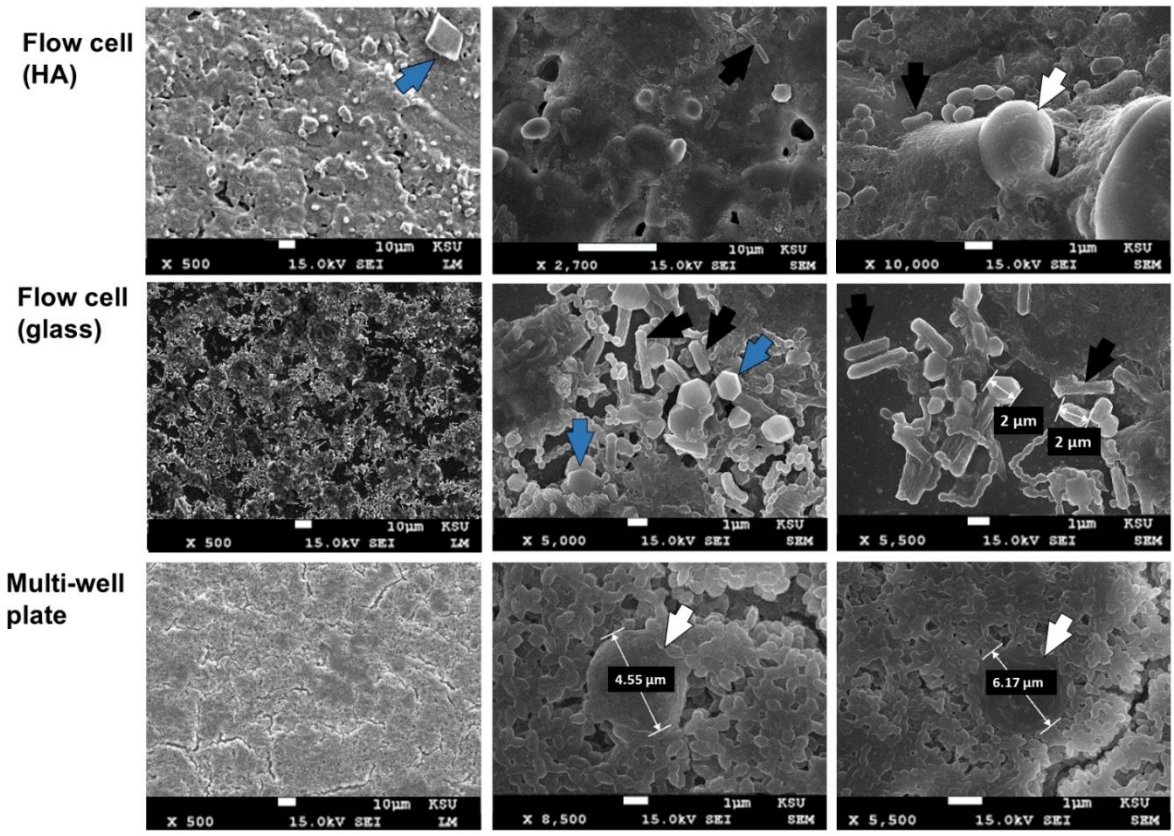

Figure 4.10: SEM of the three-species biofilms with added neutrophils cultured in the flow cell with HA coupons, flow cell with glass coupons, and on glass coverslips in a 24-well plate. Black arrows show bacilli contamination identified by their characteristic rod-like morphology. White arrows show neutrophils within the biofilm texture. Blue arrows show crystals within flow cell biofilms. All biofilm exhibited voids at 500x magnification.

Neutrophils were fully retained in the multiwell plate biofilm and exhibited a rounded morphology. However, these were only visible at higher magnifications. Crystalline structures 1.9–2 µm in diameter appeared only in the flow cell model. The presence of void spaces was discernible within all biofilms. These void spaces may potentially represent biofilm water channels.

4.4.2 CLSM examination of the capacity of the three-species biofilm to activate neutrophils

Fluorescent staining was performed using anti-CD11b for neutrophils, Hoechst 33342 nuclear stain for bacterial biofilms and neutrophil nuclei, and anti-triple-citrullinated histones as an indicator for NET formation.

No neutrophils or NETs were observed in the flow cell with glass coupons in **Figure 4.11**, and, unlike in SEM images, no bacterial biofilms were detected fluorescently in the flow cell. A possible reason for this may be that due to the low number of retained neutrophils they were washed away during sample preparation and staining procedures. Neutrophils were observed in the multiwell plate biofilms, and the CD11b-associated green fluorescent staining indicated neutrophil activation; however, no NETs or citrullinated histones were detected.

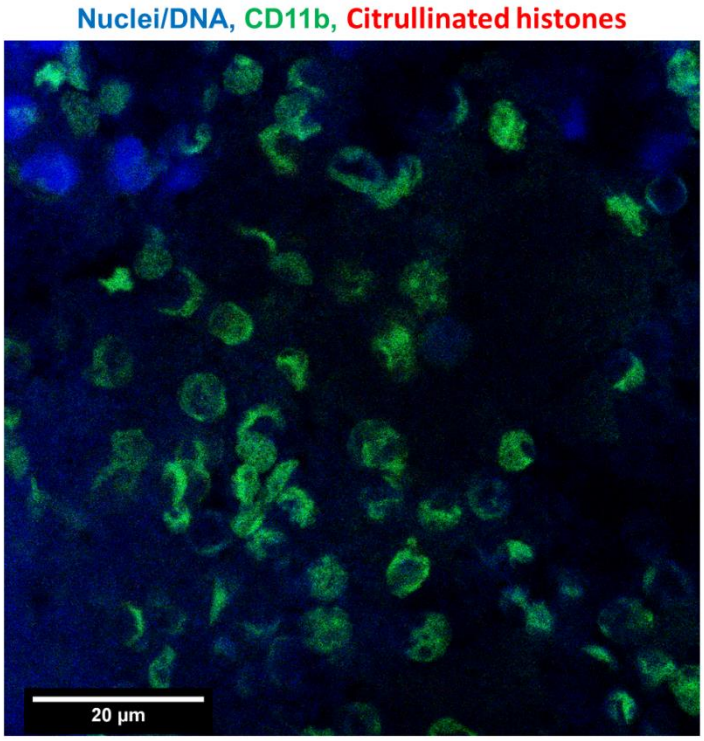

Figure 4.11: NET-specific fluorescent staining and CLSM imaging of the three-species static biofilm with neutrophils. The three-species (*S. oralis*, *S. mitis*, and *S. intermedius*) biofilm was incubated for three days with subsequent neutrophil addition for 2 h. Biofilms were stained with anti-CD11b (green), Hoechst DNA binding stain (blue), and anti-citrullinated histones (red). 100x magnification.

4.5 Multiwell three-species biofilm

As a result of several contaminations, a lack of reproducibility with oral bacteria, and a lack of neutrophil retention, investigations using the flow cell as a dynamic biofilm model were discontinued, and subsequent research was performed using only the static multiwell plate based biofilms.

4.5.1 Analysis of biofilm adhesion to various surfaces and coating materials

The testing of a surface or coating material that promoted attachment of the three-species biofilm was conducted. Three surfaces and three coating materials were investigated, as explained in **Section** 2.7.3. The results, depicted in **Figure 4.12**, showed significant differences in biofilm biomass between untreated wells and all the other tested surfaces and coating materials.

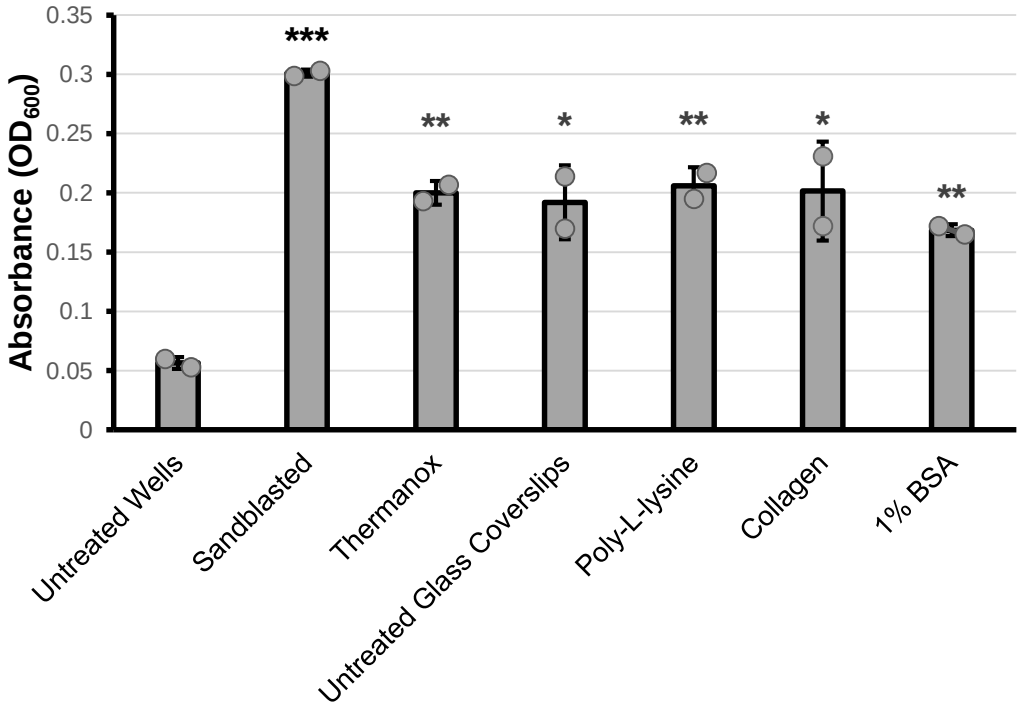

Figure 4.12: The effect of various surfaces and coating agents on the three-species biofilm biomass. The three-species (*S. oralis, S. mitis*, and *S. intermedius*) biofilm was incubated for three days, and the biofilm biomass was assessed using the CV technique. Bar graph shows mean values ± SD. P-values were calculated using one-way ANOVA. *P≤0.05, **p≤0.01, ***p≤0.001 compared to untreated wells.

The sandblasted glass exhibited higher OD_{600} values compared with other surfaces as the CV stain was retained in the microroughness of the glass surface, which was detected on a control sandblasted glass coverslip without bacteria. None of the other tested surfaces or surface treatments led to higher CV retention. Poly-L-lysine coating was used for subsequent experiments as it had one of the highest CV values compared with untreated wells, and it is suitable for fluorescent staining, unlike the thermanox coverslips, which, according to the manufacturer, are not optimal for some types of fluorescent staining due to their inherent autofluorescence. L-lysine's high molecular weight polymers provide an adhesive substrate for neutrophils (Huang et al., 1983). Furthermore, poly-L-lysine is positively charged, which permits it to interact with negatively charged cell membranes, thereby enhancing cell adherence to the surface (Schwieger and Blume, 2007).

4.6 Biofilm biomass

An investigation of the influence of each species on the others in the biofilm and the effect of neutrophils on the biomass of the single-species and three-species biofilms was conducted. All tested single- and three-species biofilms were cultivated in triplicate for three days, as specified in the procedure described in **Section** 2.5.1.2. Neutrophils suspended in RPMI + 10% FBS were introduced into each well and incubated for 2 h at 37°C + 5% CO_2. To investigate the immediate effect of neutrophils on biofilm biomass, neutrophils were added at the end of biofilm development on day three.

When neutrophils were added to the biofilms, the biomass of the multispecies and *S. oralis* biofilms decreased significantly. As **Figure 4.13**A shows, the addition of neutrophils did not have a significant effect on the *S. mitis* or *S. intermedius* biofilm masses.

The *S. oralis* biofilm possessed the highest biomass of any of the investigated single-species biofilms. As the biomass of the *S. oralis* biofilm was not significantly different from that of the three-species biofilm, its contribution to the total biomass of the multispecies biofilm may have been disproportionately strong. Conversely, the biomass of the *S. mitis* and *S. intermedius* biofilms were significantly different than that of the three-species biofilm, indicating that their contribution to the total biomass of the three-species biofilm may have been limited. Furthermore, comparisons of biofilm biomasses among the monospecies exhibit that *S. oralis* biomass was significantly higher than the other two species, indicating that *S. oralis* may have a higher ability to form biofilms. As **Figure 4.13**B illustrates, these differences in the biofilm biomass were also visible after the biofilms were stained with CV.

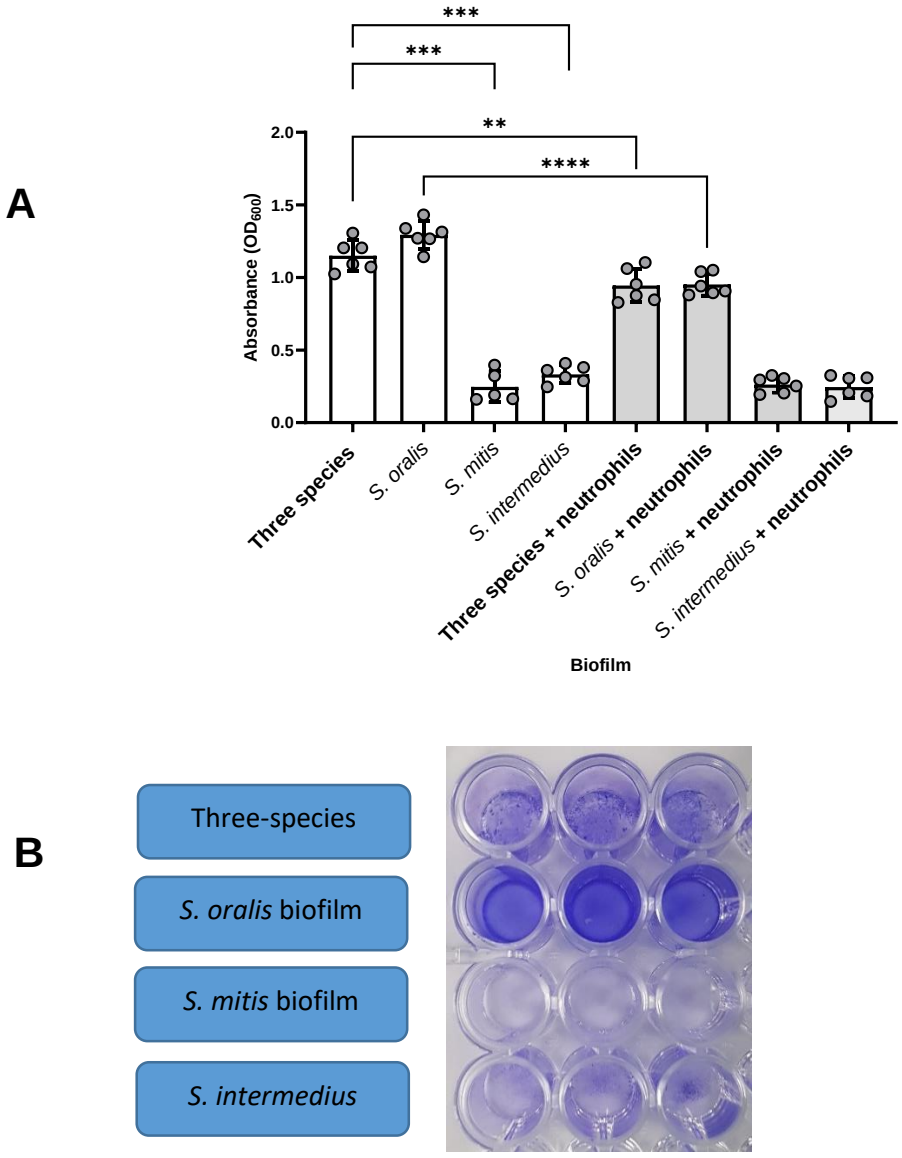

Figure 4.13: Biomass of the three-species and single-species biofilms with and without neutrophils. A: The biomass of three-species (*S. oralis, S. mitis*, and *S. intermedius*) and single-species biofilms were incubated for three days, and neutrophils were added on day 3 for 2 h. The biofilm biomass was assessed using CV technique. P-values were calculated using one-way ANOVA (n=3 in triplicate wells). *P≤0.05, **p≤0.01, ***p≤0.001. B: CV staining of the tested multiwell plate biofilms before decolourising with 99% ethanol.

4.6.1 Effect of isolated NETs on the three-species biofilm

The results presented above showed that neutrophils decreased biofilm biomass. To investigate this finding further, the effect of NETs on biofilm biomass was analysed. NETs were isolated according to the protocol presented in **Section** 2.9, and 150 µl of

0.365 ng/µl (54.75 ng per well) of NETs were added to three-species biofilms. **Figure 4.14** shows the results; as an additional control, $1x10^6$ unstimulated neutrophils suspended in RPMI 1640 media were used.

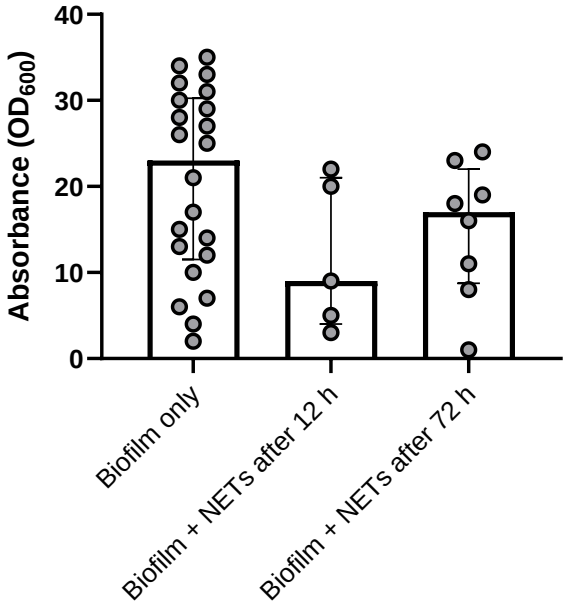

Figure 4.14: Effect of NETs on the biomass of the three-species biofilm after 12 and 72 h of biofilm development. The three-species (*S. oralis, S. mitis*, and *S. intermedius*) were incubated for three days and NETs were added after 12 and 72 h of biofilm growth (n=7 each). Bar graph shows median values and interquartile ranges. Kruskal-Wallis test was used to determine the significance between groups.

Overall, there were no significant differences in biofilm biomass when neutrophils were added 12 h into the biofilm development and 72 h after biofilm development. Indicating that NETs do not add to the biofilm biomass if included in the biofilm at the tested concentration.

Initially, 99 % ethanol was used as a decolourising agent in the CV technique to estimate the biofilm biomass, as outlined in **Section** 2.7.1. However, it was found that whereas ethanol could not fully decolourise the biofilms, it could fully decolourise the neutrophil-only samples. The influence of colour intensity on the absorbance readings

may explain why the samples containing neutrophils exhibited higher OD results than those containing biofilms. This finding is represented in **Figure 4.15**.

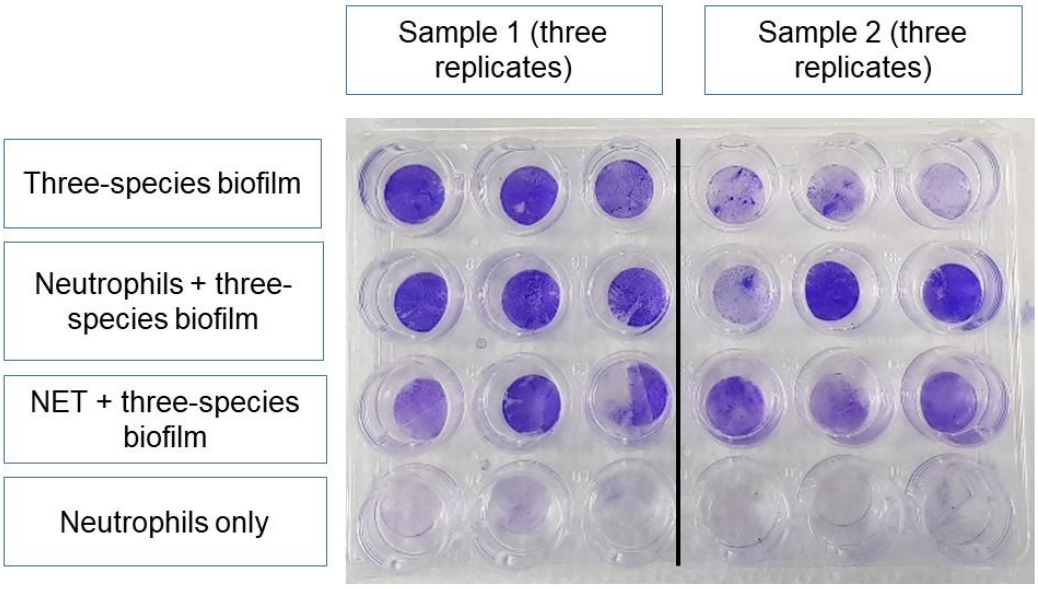

Figure 4.15: CV staining of three-species biofilms after decolourising with 99% ethanol for 20 min on a shaking rack. Neutrophil-containing wells were clear, indicating successful decolourisation. Three-species species (*S. oralis, S. mitis*, and *S. intermedius*) biofilm-containing wells were not completely decolourised.

As the biofilm was not fully decolourised with ethanol, 30% acetic acid was used instead. Acetic acid was found to be more efficient than ethanol in decolourising CV (Merritt et al., 2005).

Figure 4.16 shows that 30% acetic acid decolourised the CV-stained three-species biofilm more effectively than 99% ethanol. Consequently, acetic acid was used as a destaining agent in the subsequent experiments.

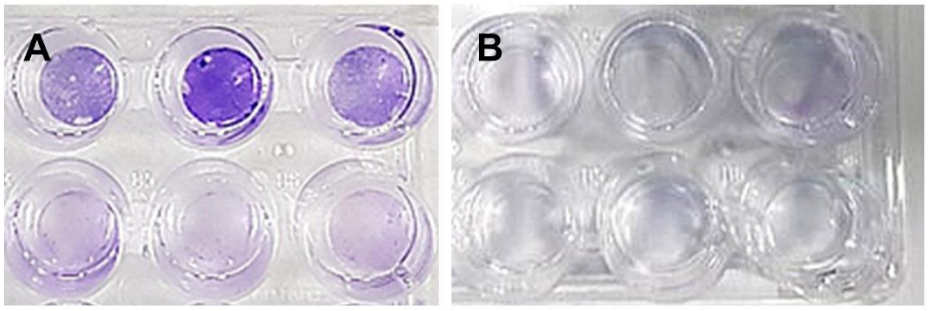

Figure 4.16: The difference in CV stained three-species biofilm after using ethanol and acetic acid as decolourising agents. The three-species (*S. oralis, S. mitis*, and *S. intermedius*) CV stained biofilms were decolourised using 99% ethanol (A) and 30% acetic acid (B).

4.6.2 Examination of the biomass of the three-species biofilm using 30% acetic acid

The effect of the presence of neutrophils on the development of the three-species biofilm was investigated. Neutrophils suspended in RPMI + 10% FBS were added to each well and allowed to adhere for 30 min before the three-species bacterial suspension was added. The medium was aspirated, and the suspension was added and incubated for three days; 30% acetic acid was used as a decolourising agent. Data presented in **Figure 4.17** indicates that the introduction of neutrophils before biofilm formation resulted in a significant decrease in biofilm formation compared to the control.

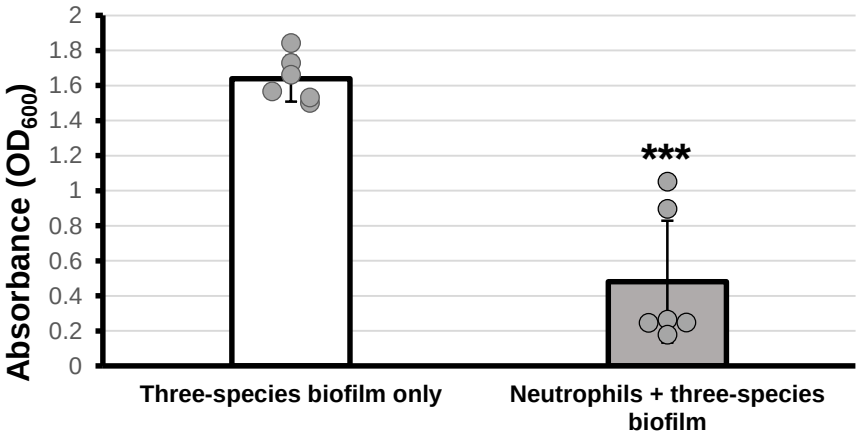

Figure 4.17: The three-species biofilm biomass with and without the addition of neutrophils on day 0. Neutrophils were added to the wells before biofilm development for 2 h. The three-species (*S. oralis*, *S. mitis*, and *S. intermedius*) biofilms were incubated for three days, and the biofilm biomass was assessed using CV technique. Error bars show mean values ± SD. P-value was calculated using Student's t-test, ***p≤ 0.001, n=3 in triplicates. Neutrophil-only readings were subtracted from samples containing both the biofilm and neutrophils.

4.7 Neutrophil survival in various growth media

Biofilm detachment was consistently observed when RPMI + 10 % FBS was added to the wells containing biofilms, which did not occur when adding bacterial growth media. FBS is known to support planktonic bacterial growth; however, it has the ability to inhibit biofilm formation (Abraham and Jefferson, 2010). The use of an alternative medium to suspend neutrophils before introducing them to the biofilms was investigated to replace FBS and, hence, prevent biofilm loss. In addition, it would be ideal to use a single culture medium for the culture of neutrophils and bacterial biofilms to ensure consistency and minimise potential experimental variables. The use of different media may introduce unanticipated variables that may skew the experimental results. As a result, the use of a single medium is expected to produce a more reproducible experimental environment and increase the reliability of the findings. **Figure 4.18** depicts the assessment of neutrophil survival in various growth media that can be used for growing bacterial biofilms.

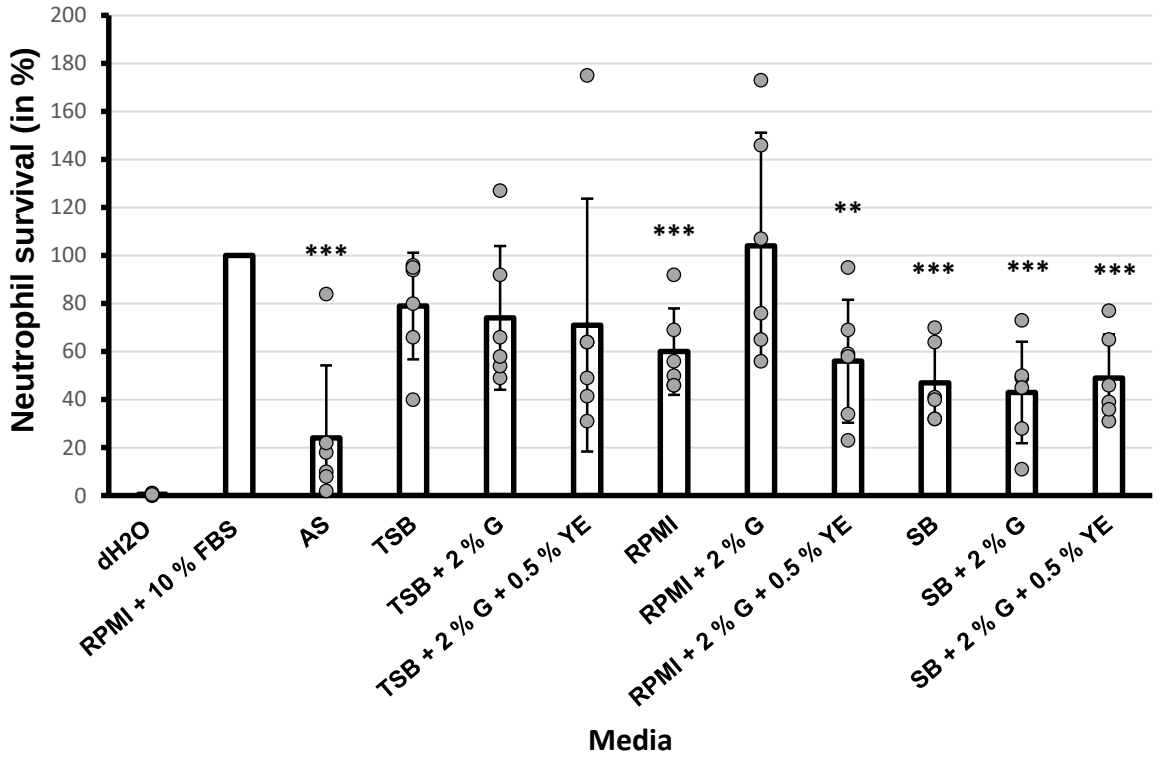

Figure 4.18: Neutrophil survival assays in various media. DH_2O: distilled H_2O (positive control), RPMI + FBS: RPMI 1640 + 10% FBS (negative control), AS: artificial saliva, TSB: tryptic soy broth, G: 2% glucose, YE: 0.5% yeast extract, SB: Schaedler broth. N=6 in triplicate wells. Neutrophil survival in RPMI + 10% FBS was considered a 100% survival rate and compared against the neutrophil survival percentages of other media. Error bars show mean values ± SD. P-values were calculated using one-way ANOVA. **P≤0.01, ***p≤0.001.

Neutrophils exhibited good mean survival rates in RPMI with glucose and in TSB with and without 2% glucose. Poor neutrophil survival in artificial saliva was highly significant compared to the negative control, which indicated that artificial saliva may not be a suitable medium for neutrophil culture. The addition of yeast extract to the media decreased neutrophil survival; this may have resulted in poor neutrophil survival in all tested Schaedler broth-based media, which contain yeast extract as part of their original formulations. Overall, TSB and RPMI enhanced with 2% glucose and TSB alone were the media enabling the highest neutrophil survival rates.

4.8 Imaging of the static three-species biofilms with neutrophils

4.8.1 Fluorescent staining

The anti-citrullinated histone antibody staining protocol visualised the production of NETs only after overnight incubation with the stain. The images in **Figure 4.19** show the web-like formation of NETs in red and neutrophil nuclei in blue. SYTO 9 was added to stain the three-species biofilm. The presented biofilm texture analysis shows voids similar to those in the *S. salivarius* biofilm, as detailed in Chapter 3. In addition to the green biofilm, some neutrophils were stained green, indicating possible phagocytosis of green-stained bacteria.

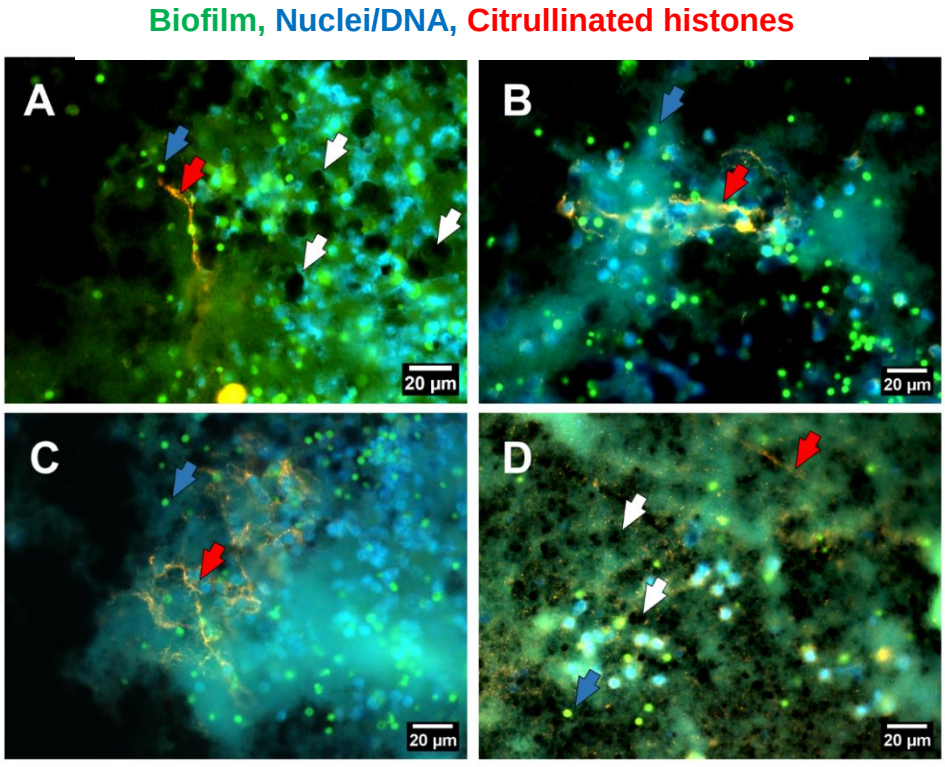

Figure 4.19: Multiple representative views of NETs specific fluorescent staining and CLSM imaging of the three-species static biofilm with neutrophils. The three-species (*S. oralis*, *S. mitis*, and *S. intermedius*) biofilms were incubated for three days and neutrophils were added on day 3 of biofilm development and incubated for 2 h before staining (40x magnification). Bacterial biofilm was pre-stained with SYTO 9 nuclear stain (green) prior to incubation with neutrophils. After incubation, the slides were stained with anti-triple-citrullinated histone (red) overnight, followed by Hoechst 33342 nuclear stain for neutrophils (blue). Voids (white arrows) and some green-stained neutrophils (blue arrows) appear in the biofilm. Red arrows indicate NET formation.

4.8.2 H&E staining

In the H&E staining images of the three-species biofilm (**Figure 4.20**), clear zones surrounding neutrophils may indicate cell shrinkage. H&E stain includes fixation, dehydration, and rehydration. These stages can produce structural changes in cells, particularly white blood cells (leukocytes), such as shrinkage or deformation. This is not specific to H&E staining but is common to many histological and cytological staining methods (Chatterjee, 2014). Activated neutrophils were distinguished by the condensed nucleus positioned to one side of the cell and 'ballooning'. Ballooning alludes to cell swelling linked with inflammatory activity or the early stages of NETosis (Inozemtsev et al., 2023). In addition to these activated neutrophils, eosinophils as well as smaller cells with a single nucleus, indicating the presence of other leukocytes, were observed.

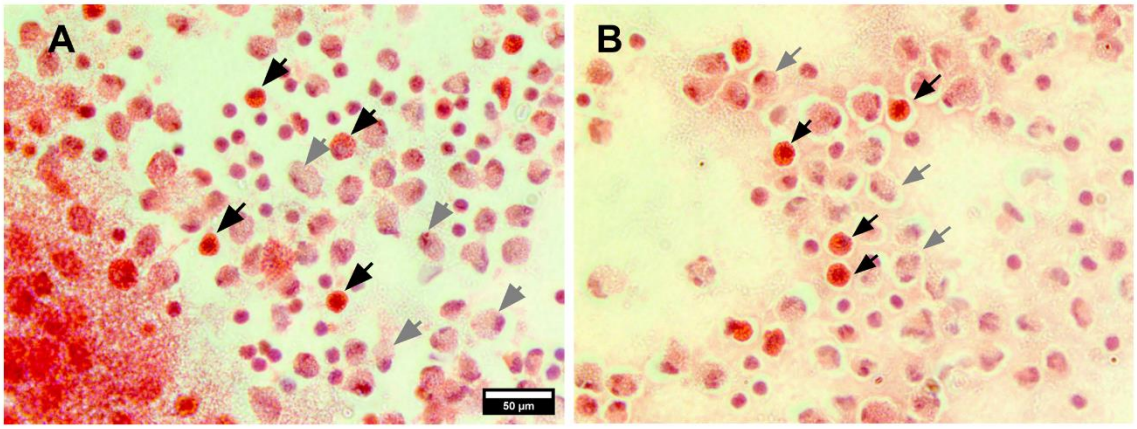

Figure 4.20: H&E staining of the three-species biofilm with neutrophils The three-species (*S. oralis, S. mitis*, and *S. intermedius*) biofilms were incubated for three days and neutrophils were added on day 3 of biofilm development and incubated for 2 h before staining (40x magnification); representative images. Grey arrows show neutrophils exhibiting nuclear fragmentation/condensation and ballooning. Some eosinophils with red/orange-stained granules (black arrows) are present.

The Percoll gradient isolation technique has been tested in this research and yields a high purity for neutrophil isolation. However, like any other biological separation approach, it is susceptible to contamination from other cell types. Despite its efficiency,

additional leukocytes may occasionally be present in the separated sample. This occurs because the concentrations of different leukocyte subtypes can overlap, making it difficult to isolate a 100 % pure neutrophil population (Norouzi et al., 2017).

4.8.3 SEM imaging

The three-species biofilm was examined using high-resolution SEM imaging to enable detailed visualisation of its structure and embedding of neutrophils. **Figure 4.21** reveals cell-like structures with a diameter slightly smaller (up to 7 µm) than that of neutrophils (8–15 µm) (Tigner A, 2021); these were embedded in the structure of the three-species biofilm, indicating the presence of neutrophils in the biofilm after 2 h of incubation. Sample preparation for SEM likely caused specimen shrinkage, leading to smaller measured cell sizes (Ting-Beall et al., 1993, Ting-Beall et al., 1995).

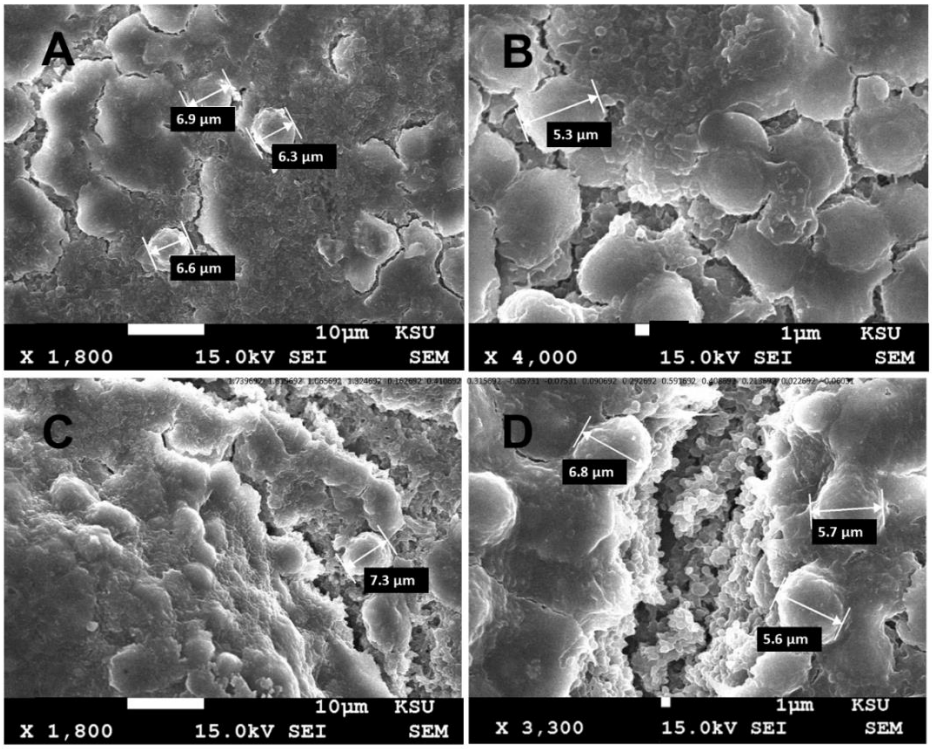

Figure 4.21: Representative SEM images of three-species biofilms and neutrophils. The three-species (*S. oralis*, *S. mitis,* and *S. intermedius*) biofilms were incubated for three days, and neutrophils were added on day 3 of biofilm development and incubated for 2 h before imaging. Neutrophil-like cellular structures were observed within the biofilm matrix. Magnifications and scale bars are displayed below each image.

4.9 Biofilm and neutrophil extracellular DNA

The effect of neutrophils on eDNA content in the biofilm was investigated, as eDNA is a major component of the biofilm matrix, contributing to its biomass and stability (Jakubovics et al., 2013). The COVID outbreak in 2020 caused significant shipping delays and led to a decrease in the supply of reagents, particularly MNase, required for the NETosis assay described in **Section** 2.6.3. Initially, there were attempts to quantify NETs without a nuclease. Subsequently, DNase was utilised as a substitute for MNase. Neither of these attempts to replace MNase was successful. When MNase became available, the MNase-containing experiments were repeated.

4.9.1 Continuous monitoring of NET production over 2 hours of incubation

Neutrophils were added to the three-species biofilm, and the concentration of free DNA was monitored every 15 min for 2 h of incubation at 37°C (**Figure 4.22**). No nuclease was utilised in this assay. The results showed no increased detection of extracellular DNA over time, even in the positive control using PMA. PMA is known to induce NET formation by activating PKC in neutrophils (Damascena et al., 2022). This failure of DNA detection may have been due to the absence of an exogenous nuclease. Slightly higher levels of free DNA were seen in bacteria-containing samples, likely due to bacterial cell death and subsequent DNA release (Jakubovics et al., 2013).

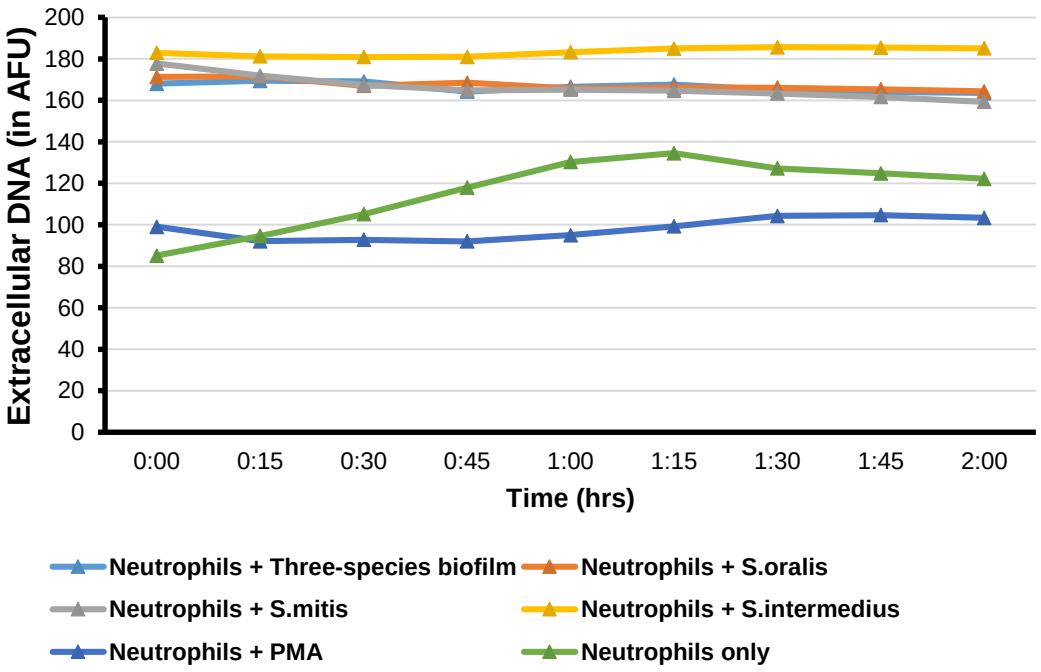

Figure 4.22: Free DNA quantification kinetics after adding neutrophils to three-species biofilms The three-species (*S. oralis*, *S. mitis,* and *S. intermedius*) biofilms were incubated for three days, and neutrophils were added on day 3 of biofilm development and incubated for 2 h (n=2). A SYTOX Green assay was used without any nuclease enzyme. Fluorescence was measured using a SpectraMax plate reader (Molecular Devices, USA). Measurements are reported in Arbitrary Fluorescent Units (AFU). No DNA was quantified using this assay.

4.9.1.1 NET quantification using DNase 1

When the laboratory received the DNase 1 enzyme, the experiment was repeated with some modifications; that is, neutrophils were introduced into the three- and single-species biofilms and incubated at 37°C + 5% CO_2 for 2 h. The endpoint measurements were then performed using two concentrations of the DNase enzyme. A concentration of 4 µl/well DNase 1 nuclease was used as this is the same concentration used for MNase in the SYTOX Green assay in **Section** 2.6.3. As **Figure 4.23** illustrates, the results showed low AFU results. In the second experiment, the DNase concentration was increased following a previously published protocol (Munafo et al., 2009), leading to an increase in AFU. After the addition of neutrophils, there was a significant increase

in the detected DNA content of the three-species and *S. oralis* biofilms. The positive control (PMA) did not induce NET formation.

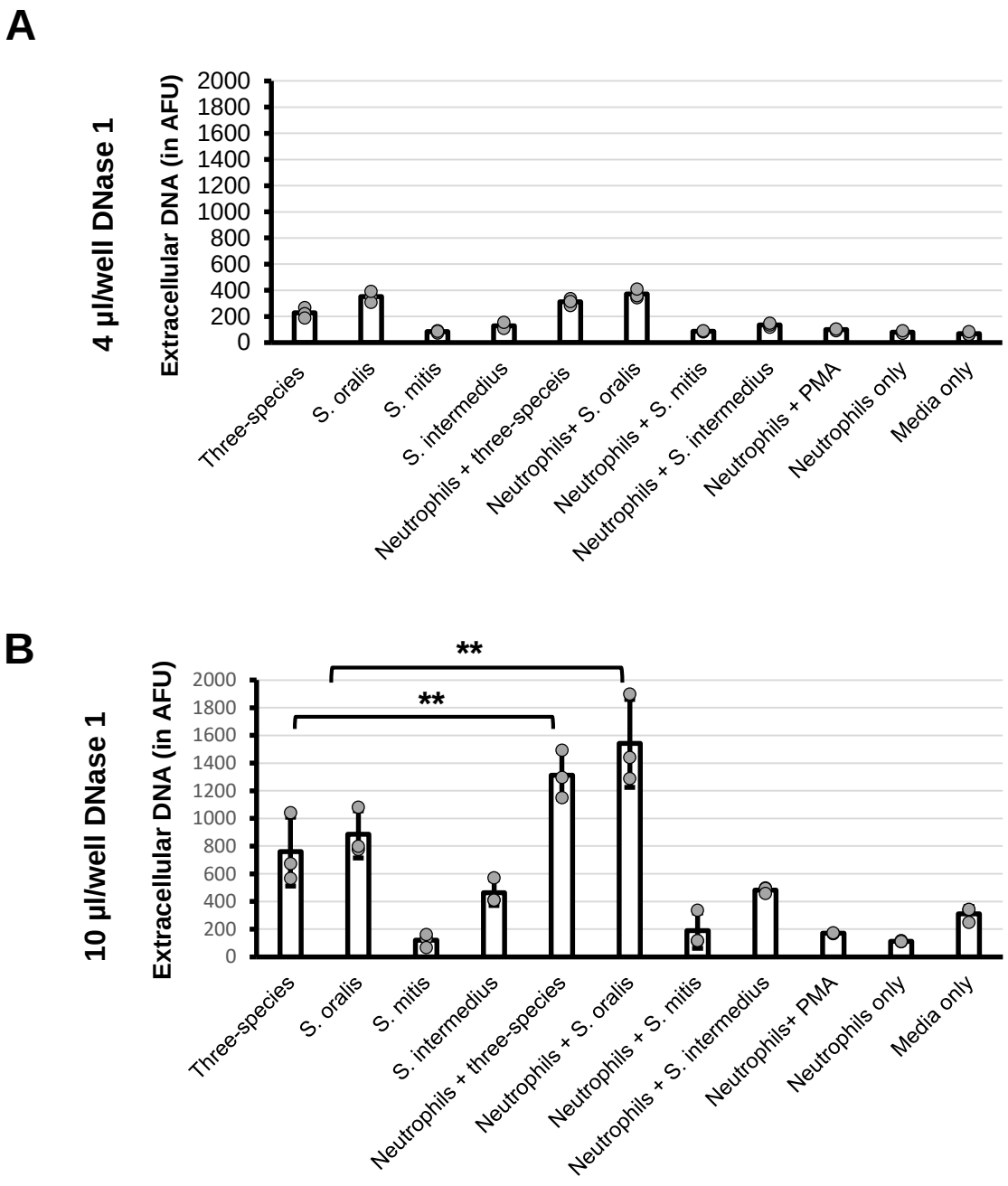

Figure 4.23: Free eDNA quantification using DNase 1 in single- and three-species biofilms with neutrophils.The three-species (*S. oralis*, *S. mitis,* and *S. intermedius*) and single-species biofilms were incubated for three days, and neutrophils were added on day 3 of biofilm development and incubated for 2 h. DNase 1 was used in two concentrations (A)13.4 U/ml (4 µl/well) and (B) 28.6 U/ml (10 µl/well). P-values were calculated using one-way ANOVA. **P<0.005. Values shown are triplicate wells means +/- SD. Measurements are reported in Arbitrary Fluorescent Units (AFU). DNase 1 in 10 µl/well concentration in Figure (B) showed an increased AFU than in 4 µl/well in Figure (A).

4.9.1.2 NET quantification using MNase

After receiving MNase, the NET-quantification process was carried out in accordance with the protocol described in **Section** 2.6.3. **Figure 4.24** shows that using MNase increased the overall readings of all the tested biofilms before neutrophils were added.

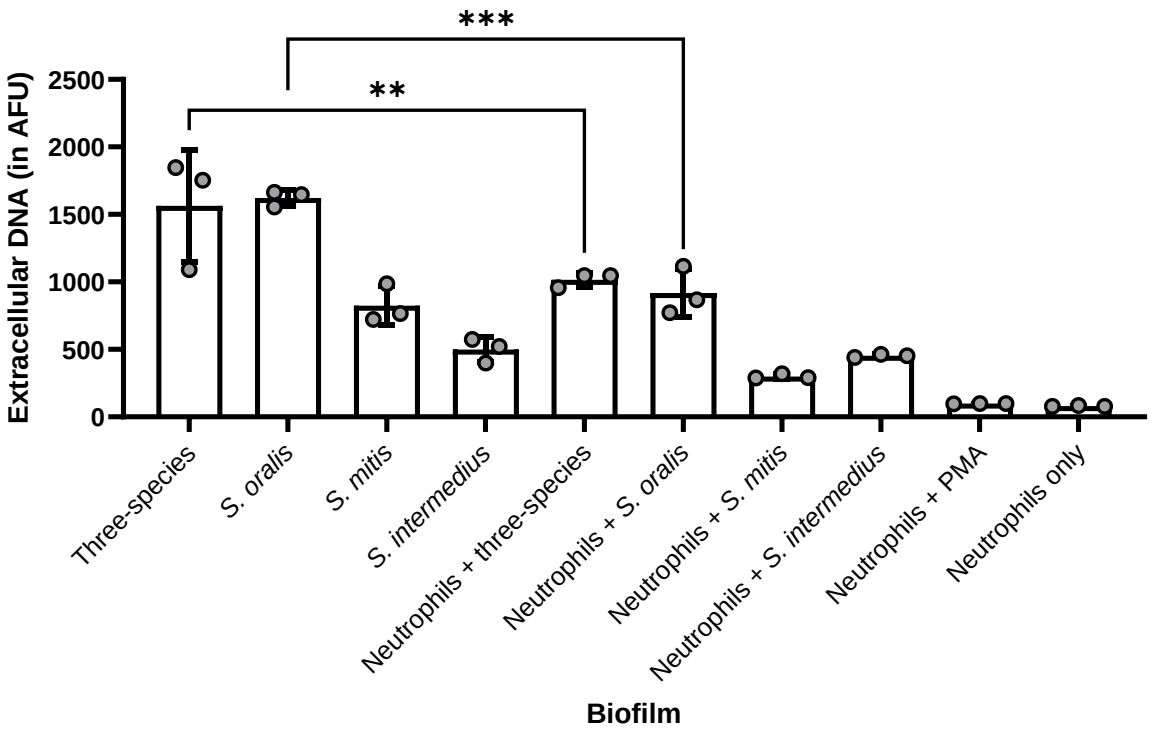

Figure 4.24: Free DNA quantification using MNase in single- and three-species biofilms with neutrophils.The three-species (*S. oralis, S. mitis*, and *S. intermedius*) and single-species biofilms were incubated for three days, and neutrophils were added on day 3 of biofilm development and incubated for 2 h. Bar graph shows mean values ± SD. P-values were calculated using one-way ANOVA *P≤0.05, **p≤0.01, ***p≤0.001 (n=3 in triplicate wells). Measurements are reported in Arbitrary Fluorescent Units (AFU). A significant reduction in the biofilm eDNA content was observed in the three-species and *S. oralis* biofilms after addition of neutrophils.

The eDNA content of the *S. oralis* biofilm was the highest among all the biofilms and was not significantly different from that of the three-species biofilm. The eDNA content of the *S. oralis* and *S. mitis* biofilms decreased significantly when neutrophils were added, indicating biofilm eDNA loss. These results are the opposite of those of DNase

1. MNase and DNase 1 are both nucleases, yet they function differently. DNase 1 cleaves double-stranded DNA non-specifically, producing a mixture of oligonucleotides (Lauková et al., 2020). On the other hand, MNase is sequence-agnostic, meaning it has no preference for any particular sequence. When MNase digests chromatin, this results in the preferential digestion of single-stranded nucleic acids or the formation of mono- and di-nucleosomes (Allan et al., 2012). Due to this variation in DNA cleavage patterns, DNase 1 dissects DNA into smaller fragments than MNase, which may result in more DNA fragments attaching to SYTOX Green and yielding high findings.

While the positive control contained neutrophils with PMA (0.5 µm), it did not exhibit any DNA increase, even though the nuclease was changed to MNase. The highest production of eDNA was observed in the *S. oralis* biofilm without added neutrophils.

4.10 Correlation between eDNA and biofilm biomass

A correlation analysis was conducted to investigate the concordance between the eDNA percentage and biofilm mass percentage after adding neutrophils to the three-species mixed biofilm and the single-species biofilm. As described in **Figure 4.25**, the Pearson correlation coefficients obtained from the analysis reveal that *S. oralis* shows no correlation (- 0.1), indicating no significant relationship between eDNA levels and biofilm mass for this species. The three-species biofilm shows a strong negative correlation (r = - 0.78), indicating a consistent inverse relationship between eDNA levels and biofilm mass. *S. mitis* displays a weak negative correlation (- 0.33). Lastly, *S. intermedius* shows no correlation (- 0.17), indicating no significant association between eDNA levels and biofilm mass.

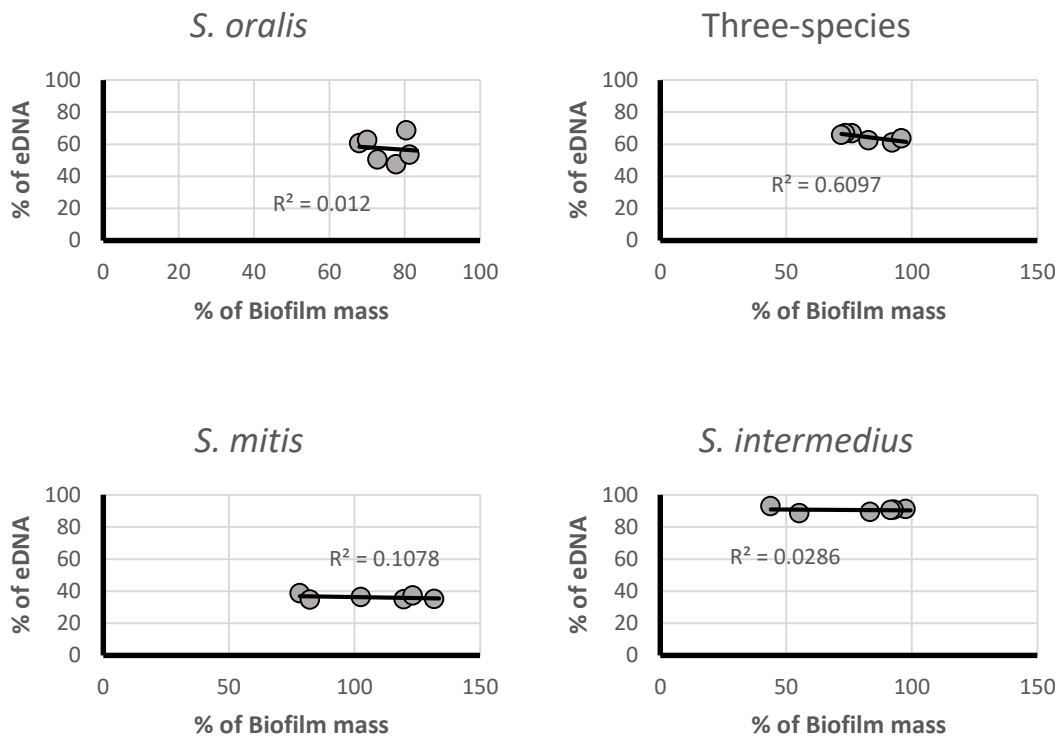

Figure 4.25: Correlation analysis between the percentage change in biofilm mass and eDNA levels after adding neutrophils.The initial biofilm mass and eDNA levels before adding neutrophils were considered 100%. This figure presents the correlation between the percentage reduction in biofilm mass and eDNA within the biofilm post-neutrophil addition. Correlation graphs include trend lines, equations, and R^2 values for six replicates (n=6). The analysis shows no significant correlation in *S. oralis* (r = 0.1) and *S. intermedius* (r = -0.17), a weak negative correlation in *S. mitis* (r = -0.33), and a strong negative correlation in the three-species biofilm (r = -0.78).

4.11 NET generation

The following experiment was performed to determine why PMA did not elicit a positive NET response in the SYTOX Green assay. Different PMA concentrations were used to assess PMA's capacity to induce NETs. Even though PMA is a known concentration-dependent neutrophil activator (Gupta et al., 2005, Damascena et al., 2022), this experiment was performed to validate the test used in this thesis.

As **Figure 4.26** illustrates, NET generation was inversely proportional to the PMA concentration. This was likely related to the known cytotoxicity of PMA at higher concentrations, which leads to rapid cell death rather than NET formation (Geffner et

al., 1991). While 0.1 µM did indeed induce the release NETs, the extent of this release was notably less pronounced than what has been documented in the existing literature (Najmeh et al., 2015).

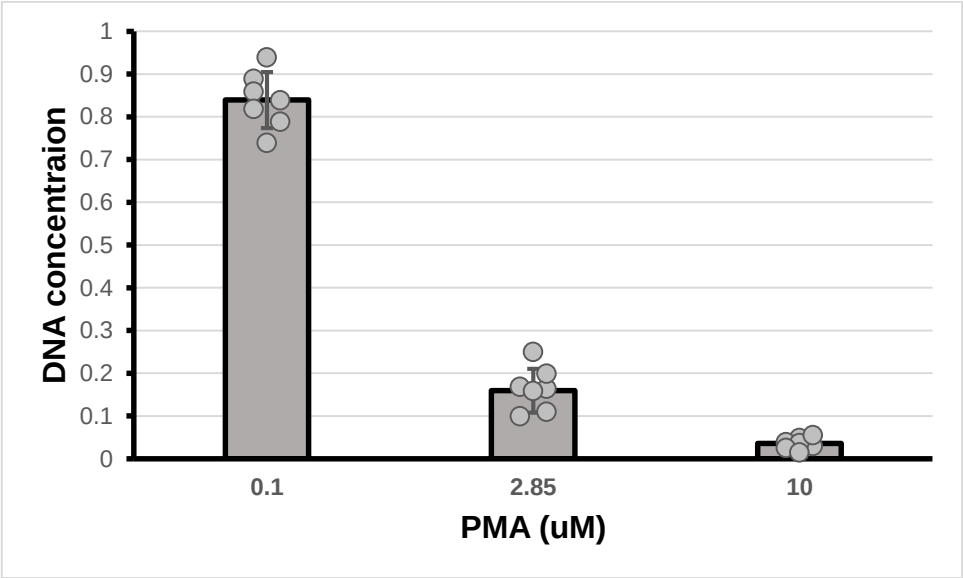

Figure 4.26: NET response to PMA at different concentrations. In a cell-culture flask with PMA, $10x10^6$ neutrophils were incubated for 4 h (n=7). NET production was quantified by Qubit 2.0 Fluorometer (Invitrogen, Singapore). NET generation was inversely proportional to the PMA concentration.

4.12 Discussion

The previous chapter demonstrated that neutrophils were retained in the flow cell *S. salivarius* biofilm. The present chapter showed that the flow cell three-species biofilm did not retain neutrophils and was prone to contamination. The biofilm's biomass may have impacted how neutrophils can attach to it, especially under shear conditions. The heterogeneity in biofilm biomass may precipitate diverse experimental outcomes, and the interaction of distinct bacterial strains with the immune cells may yield different outcomes (Bjarnsholt et al., 2013). The lack of neutrophils in the dynamic model may

have been due to these being washed away by the flow conditions; in the static model, by contrast, neutrophils were retained in the wells.

The growth kinetics of *S. oralis* differed when cultivated in a single-species compared with a mixed three-species culture. The *S. oralis* culture had a longer lag phase than the three-species culture. This could imply that the presence of the other bacterial species in the mixed culture influences the initial adaptation and growth of *S. oralis*, possibly via mechanisms such as quorum sensing (Venturi, 2006, Swift et al., 2001), resource competition or environmental conditions alteration (Pekkonen et al., 2013). Despite the longer lag period, the *S. oralis* culture had a more prominent exponential growth phase than the mixed culture. This suggests that, once it begins to grow, *S. oralis* multiplies at a more rapid pace in the absence of other species, possibly due to a lack of resource competition, antagonistic interactions (Traxler et al., 2012), or other intra-species growth promotion mechanisms (Palmer et al., 2001). These findings highlight the complexities of bacterial relationships and their impact on growth dynamics. It also emphasises the possible impact of microbial community composition on individual bacterial species performance and survival.

Bacterial metabolism was investigated by monitoring pH changes. In the three-species biofilms, the pH changed from alkaline to acidic conditions after the first day of incubation in both the static and dynamic models. Although our tested biological replicates provided reproducible results, biofilm pH *in vivo* can vary; for example, it has been reported that salivary pH ranges from 5.3 to 7.8 (de Almeida Pdel et al., 2008). Moreover, pH varies from 2 to 9 within periodontal pockets, depending on the biological environment, this is attributable to the dynamic composition of the bacterial community over time (Galgut, 2001). Specifically, early colonisers are known to produce acidic byproducts, leading to a lower pH, while late colonisers typically generate alkaline

substances, resulting in a higher pH. Therefore, the temporal shifts in pH can be largely explained by the changing proportions of these two groups of bacteria within the pocket (Schultze et al., 2021). *In vitro* pH changes depend on the media's nutrient composition and buffering capacity (Yeor-Davidi et al., 2020). Furthermore, pH can shift towards alkaline by one pH unit because of gas exchange with the environment, leading to CO_2 loss (Eggert et al., 1991). Other techniques, including the resazurin test (Mariscal et al., 2009), Alamar blue assay (Pettit et al., 2005), or tetrazolium test (Brown et al., 2013), can be used in addition to pH measurements for metabolic-activity monitoring.

Neutrophils were assayed to determine their degree of survival in the biofilm at pH 4.5. It was found that neutrophils moderately tolerated acidity, as evidenced by a 50% survival rate. Interestingly, a previous study reported that extracellular acidification could delay neutrophil apoptosis and alter neutrophil functions (Cao et al., 2015). To better understand the interaction between neutrophils and biofilms, this phenomenon may require further functional assays to be applied.

Neutrophils were also assayed for their ability to produce DNA cleaving enzymes by plating three samples in DNA-containing agar. However, other methods may more sensitively assay DNase production, like the use of fluorescently labelled DNA or spectroscopic DNA quantification. Due to its simplicity and immediate result interpretation, this strategy was selected. The results showed no DNA restriction enzyme production. However, it is essential to note that we are not aware of neutrophil survival in such agar or whether there is toxicity that could cause neutrophil death before they can exhibit any enzymatic activity. Furthermore, neutrophils were evaluated immediately after isolation, with no priming or activation factors added, raising the question of whether adding a priming or activation factor could encourage

neutrophils to generate DNase enzyme, potentially mimicking the physiological situation in the origin of infection.

HA is a mineral type of calcium apatite that occurs naturally and is the major component of dental enamel. It is, therefore, frequently used as a model surface in *in vitro* oral biofilm studies (Liu et al., 2023). In this study, HA was unsuitable for comparison with other biofilm-growing surfaces due to its porous nature, which affected the CV staining findings. The stain appeared to have become trapped in the pores after the rinsing stage, potentially leading to unreliable results.

Although the dynamic model mimics *in vivo* biofilm conditions better than the static model, the former was associated with many difficulties, including its inability to promote optimal growth conditions for bacteria as a result of the device's large size, which prevented it from fitting into a CO_2 incubator. This is in addition to the other disadvantages discussed in Chapter 3, including contamination, laborious system cleaning and sterilisation. Experimental difficulties, including the failure or reduced neutrophil retention and the formation of the crystals, were also discussed. In view of these difficulties, this study used a static biofilm as it provided a cost-effective, reproducible, easy-to-handle system for biofilm growth and manipulation. Coating the cover glass with poly-L-lysine improved bacterial attachment and biofilm formation in the static model.

Neutrophils are the key cells responsible for the innate immune response against oral biofilms. To understand neutrophil responses *in vitro*, suitable media have to be assayed to ensure their survival in biofilm co-incubation models, especially as their life span is estimated to be only 6–12 h *in vivo* (Summers et al., 2010) and less than 24 h *in vitro* (Sawant et al., 2015). When different media were tested, neutrophils showed good overall survival rates in enriched media such as RPMI and TSB with 2% glucose,

compared with RPMI + 10 % FBS media, and these are media of choice for many human cell studies. To date, no published studies have evaluated neutrophil survival in other nutrient-rich culture media. To enrich the media for biofilm-growth enhancement, 2% glucose was added, however a positive effect on neutrophil survival was observed in RPMI media only. Although it was reported that a concentration of 4.24% glucose could induce neutrophil apoptosis (Catalan et al., 2001), our results showed that a 2% glucose concentration positively influenced neutrophil survival in RPMI media, without having any discernible effect when added to TSB or Schaedler broth. TSB enabled the highest neutrophil survival rate among tested media. These findings provided insights for the following work.

To select the optimal media for biofilm formation, the media in which neutrophils survive best was selected. Both TSB and Schaedler media led to protein-crystal formation, which appeared to interfere with fluorescent staining. It is possible that these artefactual crystals were protein crystals because of the paraformaldehyde fixation, which leads to the dissociation of some protein–protein or protein–nucleic acid interaction in living specimens (Li et al., 2015). It is known that protein crystals have the ability to adsorb dyes/antibodies (McPherson and Larson, 2018). Various methods for the identification of formed crystals are available, including face-indexing methods (Wijethunga et al., 2018, Lynch et al., 2019).

In most experiments using static three-species biofilms and ethanol to decolourise CV-stained biofilms, the biofilm biomass increased significantly after the addition of neutrophils. This may be attributed to the limited ability of ethanol to fully destain Gram-positive biofilms compared with the complete destaining seen in neutrophils. After subtracting the neutrophil-only readings, there were no significant differences between the three-species biofilm and the biofilm containing neutrophils. However, when

ethanol was replaced with acetic acid, which completely destains bacteria and neutrophils, absorbance readings altered such that biofilm biomass decreased after the addition of neutrophils. It is essential to note that CV stains protein and DNA, in which a stronger colour intensity is commonly perceived to be directly proportional to bacterial cell numbers in biofilms. However, using other methods to confirm changes in biofilm biomass, such as dry weight measurements or Z-stack measurements obtained by confocal microscopy, can help to confirm these results.

In the three-species static biofilm with neutrophils, the fluorescent images showed that NETs were found in the samples only after they had been treated overnight with the antibodies. Following a 1 h period of incubation with the antibodies, no NET formation was detected. No fixative was used to avoid crystal formation. In addition to the blue-stained neutrophils, some cell-like structures were observed in green. According to (Daniel et al., 2019), inactive or resting neutrophils can have the same size and similar appearance as the green-stained cells observed in the biofilm. Resting neutrophils are neutrophils in a quiescent or non-activated state (Priel and Kuhns, 2019). The green colour of the cell is attributed to possible phagocytosis of the SYTO 9-stained bacteria, which would appear green due to the fluorescent bacteria within their phagosomes. This approach is often used in research to visually confirm phagocytosis and track the internalisation of bacteria by immune cells (Nordenfelt and Tapper, 2011).

To validate the bacterial strains used in this study, no sequence analysis of the 16S rRNA genes was used to discriminate the *viridans* group streptococci due to the 99% similarity in nucleotide composition of 16S rRNA genes in these bacteria (Arbique et al., 2004). For this reason, the three strains used were validated using MALDI-TOF (BioMérieux, Marcy l'Etoile, France), which also failed to distinguish between *S. oralis* and *S. mitis*. Therefore, this study used shotgun-sequencing analysis, which also was

not able to distinguish between these closely related species. The genes were aligned against the database of CosmosID's CLIA-certified, GCP-compliant laboratory (Germantown, MD, USA); however, the bacterial DNA library used may have been limited and failed to distinguish between these species. In addition, the shotgun sequencing data was aligned using the BaseSpace Sequence Hub, provided by Illumina. Illumina is a leading company in the field of genomics whose key technology is next-generation sequencing, and they have developed a range of systems that are used to sequence DNA and RNA (**https://www.illumina.com**). The alignment process was not successful, and it could not distinguish between *S. mitis* and *S. oralis* due to bioinformatics challenges: even following sequencing being completed, bioinformatics analysis may not be able to distinguish between species. For example, many sequencing reads are not uniquely assigned to a single-species, particularly if the reference database used for comparison is incomplete (Quince et al., 2017). The disparity between the expected and actual results acquired from the Illumina database reveals the delicate interplay between data processing approaches, database structures, and the distinct properties of mixed-species biofilms. This problem requires further investigation and refining of bioinformatics tools, database resources, and analytical methodologies adapted to the unique complexities of mixed-species biofilm sequencing data. Such improvements would increase our understanding of microbial communities while also paving the way for more accurate and complete assessments of complex biological systems like the oral cavity.*S. oralis*, as a member of the *S. mitis* group, has been recognised for its phenotypic and genotypic heterogeneity, making the members notoriously difficult to differentiate. Taxonomic classification within this group often presents challenges due to the species' considerable genetic overlap and similar phenotypic characteristics (Jensen et al., 2016, Velsko et al., 2019). The

genetic overlap is attributed to the natural capability of streptococci to absorb DNA from their surroundings and horizontal gene transfer between species (Chi et al., 2007).

Extracellular DNA production within the biofilm was measured for all the tested species, and their ability to elicit a NET response upon interaction with neutrophils was investigated. Despite several changes in the experimental protocol, including the use of different nucleases (DNase and MNase) at different concentrations, the positive controls (PMA-stimulated neutrophils) did not elicit NET responses described in previous studies. This finding warrants further investigation, however a possible reason may be that PMA is prone to degradation and, as a result, loss of action over time. According to the manufacturing company, one crucial factor influencing PMA stability is its sensitivity to light, with ultraviolet radiation being especially harmful. Continuous or prolonged exposure to light can greatly reduce the efficacy of PMA. Furthermore, the stability of PMA is jeopardised by repeated freeze-thaw cycles. Each cycle can contribute to the compound's breakdown, lowering its activity even further.

Overall, the addition of neutrophils to the *S. oralis* biofilm led to the highest NET response among all the tested strains. In addition, DNase production by the tested bacteria was investigated because DNase catalyses the hydrolysis of induced NETs by breaking phosphodiester bonds of DNA (Nishino and Morikawa, 2002). *S. oralis* was the only strain tested that did not produce DNase after three days of incubation, making it a suitable microorganism with which to study the effects of NETs. Although *S. oralis* strain 9811 used in this study did not demonstrate DNase activity when cultured on traditional DNA-containing agar plates, and no reports in the literature indicate DNase activity for this strain, analysis of the genomic sequence available on the ATCC genomic browser **https://genomes.atcc.org** published in December 2021

and updated in May 2024 revealed the predicted presence of a deoxyribonuclease protein product. Notably, the gene encoding this protein remains unannotated. In contrast, other strains of *S. oralis* strain have also shown no evidence of DNase activity on DNA-containing agar plates; however, DNase activity was detected using gel electrophoresis, although the concentration of DNase was relatively low compared to other periodontal bacteria (Palmer et al., 2012). This suggests a discrepancy between phenotypic assays, literature findings, and genomic data that warrants further investigation.

The decrease in the biofilm mass did not correlate with the decrease in *S. oralis, S. mitis*, *S. intermedius*, and the three species biofilm, suggesting no substantial relationship between eDNA and biofilm mass. However, Adding more replicates to the study would provide further insight into these correlations, enhancing the reliability of these findings and potentially revealing subtler trends among the species.

In summary, the results have advanced the development and optimisation of a static neutrophil–biofilm co-incubation model. The dynamic models were discontinued due to their complex handling requirements and a lack of reproducibility. The three-species multiwell plate biofilm retained neutrophils, and its biofilm biomass was less than that of the *S. oralis* single-species biofilm. In addition, *S. oralis* did not produce any DNA-restriction enzymes compared with the other tested species. Therefore, the *S. oralis* biofilm model was employed for further co-incubation experiments, as described in Chapter 5.

4.13 Graphical summary

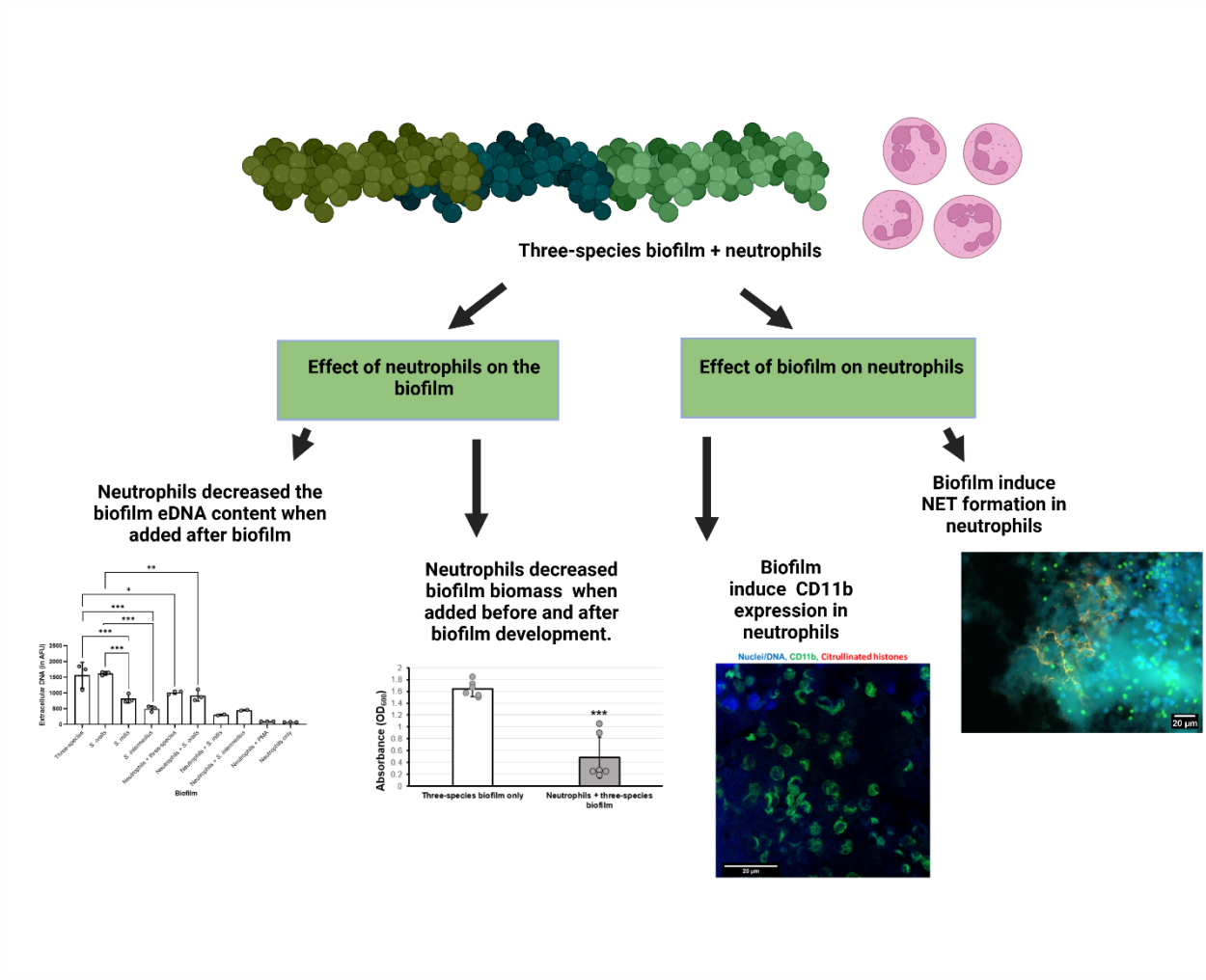

5 CHAPTER FIVE Results: Interactions between *Streptococcus oralis* biofilms and neutrophils

5.1 Introduction

In complex multispecies microbial communities, the behaviour of a single-species can be changed by other species in the community to behave differently than when alone (Luo et al., 2022). In the previous chapter, *S. oralis* growth rate and population number were found to decrease when mixed with the other tested species. In addition, *S. oralis* produced the thickest biofilm and the highest amount of eDNA without producing nuclease restriction enzymes.

Little is known about neutrophils' individual responses to bacterial species grown in biofilms. The majority of previous studies evaluated oral planktonic bacterial species and their interaction with neutrophils, which does not reflect their biological biofilm state *in vivo*. This chapter describes the interactions between *S. oralis* biofilms and neutrophils. *S. oralis* was used as a model microorganism of early periodontal colonisers to understand how neutrophils may affect early biofilm development. Neutrophil NET production, ROS release and phagocytosis in response to *S. oralis* biofilms were investigated. The knowledge of how neutrophils combat oral biofilms to maintain homeostasis can also contribute to the understanding of gingival diseases, leading to potential new avenues for prevention and treatment.

The evidence from the studies performed in Chapter 4 indicated that *S. oralis* yielded thicker biofilms and produced the highest eDNA content among all three tested early coloniser species. For these reasons, in this chapter, further research was conducted on *S. oralis* as a single-species model of early periodontal colonisation, and its interaction with neutrophils was explored in detail.

5.2 Standardisation of *S. oralis* biofilm growth

5.2.1 Biofilm biomass in different growth media

The assay was performed to evaluate the optimal media to use to promote optimum *S. oralis* biofilm growth. Although this analysis was performed on a three-species biofilm in Chapter 4, single-species may behave differently regarding their growth and nutrient requirements (Wijesinghe et al., 2018). RPMI-based media were analysed because of their ability to survive neutrophils. As analysis investigates a medium that supports both the survival and growth of neutrophils and *S. oralis* biofilm, the best performing RPMI-based media were included in the assay along with different bacteriological growth media. Different media were tested with and without additional glucose and yeast extract. Biofilms were cultured for 2 days at 37°C + 5% CO_2 on a 12-mm glass coverslip coated with poly-L-Lysine placed inside a 24-well plate.

Schaedler broth with added glucose supported the most optimal biofilm growth, as evidenced by the data presented in **Figure 5.1**. TSB enabled the best growth conditions for *S. oralis*, with no significant difference compared with Schaedler broth. Based on these findings and the neutrophil survival assay data presented in Chapter 4, TSB was used to suspend both bacteria and neutrophils, as it was the most appropriate to also sustain neutrophil survival.

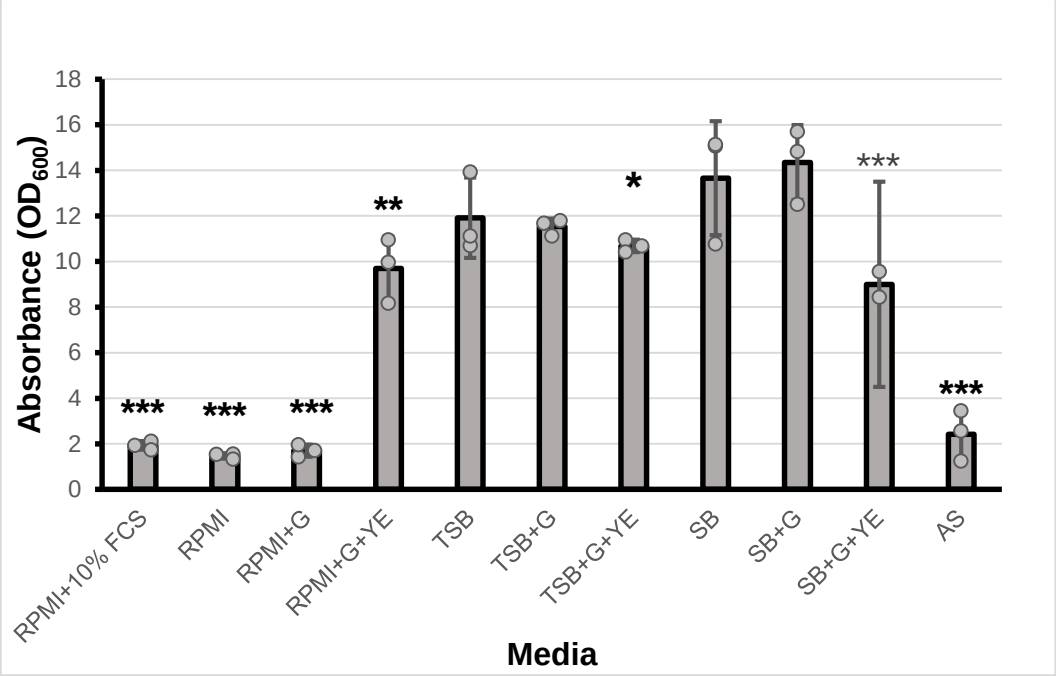

Figure 5.1: The biomass of *S. oralis* two-day biofilm grown in different bacteriological media. RPMI+ FBS: RPMI 1640 +10% FBS, AS: artificial saliva, TSB: tryptic soy broth, G: 2% glucose, YE: 0.5% yeast extract, SB: Schaedler broth (n=3 in triplicate wells). CV assay was used to measure the biofilm biomass. All tested media were compared with SB+G, which gave the highest growth rate. Bar graph shows mean values ± SD. P-values were calculated using one-way ANOVA. *P≤0.05, **p≤0.01, ***p≤0.001.

5.2.2 pH measurement as a metabolic activity indicator

After determining the pH of the three-species biofilm in Chapter 4, the pH of *S. oralis* mono-species biofilm was analysed in two different culture media to understand the possible influence of different media on biofilm metabolism (Behbahani et al., 2022). *S. oralis* biofilm pH was determined every hour for 8 h, then after 24 h. pH was found to decrease to 4.5-4.8 after 8 h of incubation and subsequently remained constant. The data presented in **Figure 5.2** is consistent with that presented in Chapter 4 pertaining to the pH of three-species biofilms.

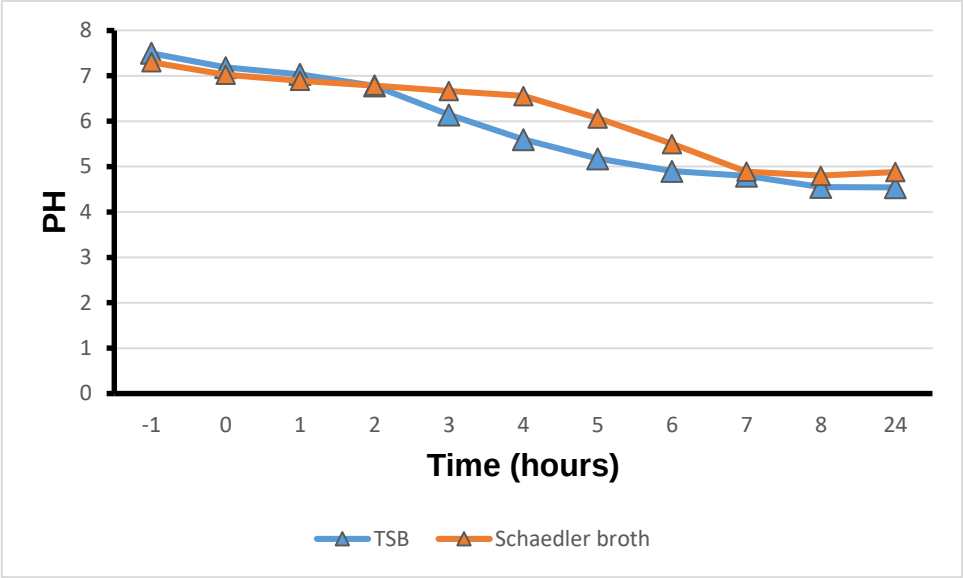

Figure 5.2: *S. oralis* biofilm pH changes during 24 h incubation in TSB and Schaedler broth. Time -1 is the broth pH without inoculating bacteria; time 0 is the pH at the time of bacterial inoculation (n=3 in triplicate wells). PH was decreased to 4.5-4.8 during 8 h of incubation and subsequently remained constant.

5.2.3 Neutrophil ability to attach to *S. oralis* biofilms

The neutrophils' ability to attach to *S. oralis* biofilms was investigated by measuring the number of unattached neutrophils in the supernatant after 2 h of incubation with the biofilm. Neutrophils were isolated from three blood samples and tested in triplicates in a 24-well plate after incubation with two-day-old *S. oralis* biofilms. The collected supernatant was stained with trypan blue, and cells were counted. Unattached neutrophils were at a concentration of 4.3 x 10^4 per ml, which indicated that 4.3 % of neutrophils failed to attach to *S. oralis* biofilms.

5.3 Biofilm biomass assessment after including neutrophils at different time-points of biofilm development

5.3.1 Addition of neutrophils to a 4-day biofilm

Neutrophils were added to *S. oralis* biofilms at various stages of development, and biofilm biomass was investigated using the CV assay. **Figure 5.3** shows the significant variations in biofilm development when neutrophils were introduced at different stages of culture. The exception was when neutrophils were added on day 2 of biofilm development, with no significant decrease in biofilm mass being evident.

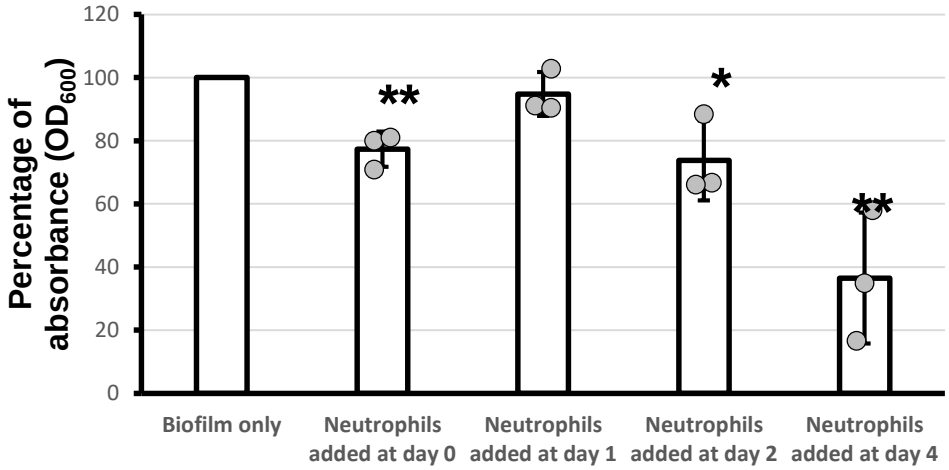

Figure 5.3: The biomass of *S. oralis* biofilm with neutrophils added at different points of biofilm development. Neutrophils-only wells were subtracted from neutrophils and *S. oralis* values. CV assay was used to measure the biofilm biomass. Biofilm only was considered a 100% survival rate and compared to the biofilm with added neutrophils percentages. Bar graph shows mean values ± SD. Statistical analysis was conducted within groups by t-test, *P≤0.05, **p≤0.01, (n=3 in triplicate wells). Day 0: Neutrophils were added before biofilm development. Day 1: Neutrophils were added after one day of biofilm development. Day 2: Neutrophils were added after two days of biofilm development. Day 4: Neutrophils were added after four days of biofilm development and incubated for 2 h. All biofilms were assessed after 4 days, along with control wells containing neutrophils only. A significant reduction in biofilm biomass was observed when neutrophils were added before, at days 2 and 4 of biofilm growth.

In addition, the neutrophil effect on mature biofilms began after the addition of neutrophils to a 2 day biofilm. Consequently, for the purposes of this study, the biofilm incubation duration was limited to 2 days.

5.3.2 Addition of neutrophils to a two-day biofilm culture

This investigation was intended to determine whether the neutrophils' diminishing effect on biofilm mass was limited by the age of the biofilm or by the time of neutrophil exposure. Neutrophils were introduced into *S. oralis* biofilms at various stages of growth over a two day period.

Observations indicated that RPMI + 10% FBS resulted in biofilm detachment, which may overcome any possible effect caused by neutrophils. Therefore, neutrophils were suspended in TSB, which was previously determined as an appropriate medium for neutrophil survival in Chapter 4. Biofilm mass was found to decrease after adding neutrophils. This decrease was significant only when neutrophils were added to a fully developed biofilm grown for two days, and the biofilm mass was measured after 2 h of neutrophil interaction (**Figure 5.4**). Additionally, a non-significant trend of reduced biofilm mass in those samples containing neutrophils was observed.

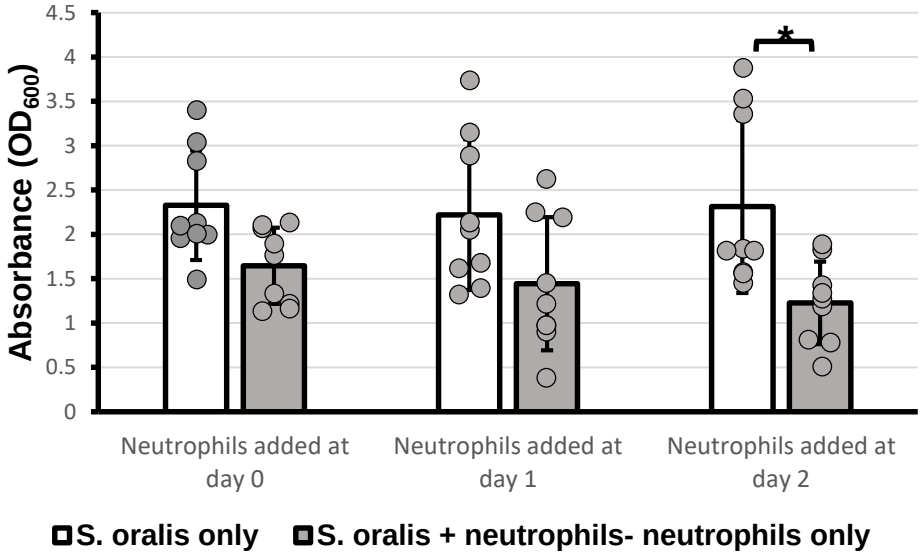

Figure 5.4: The biomass of *S. oralis* biofilm with neutrophils suspended in TSB and added at different time points of biofilm development. CV assay was used to measure the biofilm biomass. Neutrophils-only wells were subtracted from neutrophils and *S. oralis* values (n=9 in triplicate wells). Mean values ± SD are shown, and statistical analysis was calculated by two-way ANOVA, *p<0.005. A significant biomass reduction was observed after adding neutrophils to a 2-day biofilm.

To validate the findings that neutrophils decrease the biofilm biomass, the biofilm mass with non-viable neutrophils was analysed (fixed in 4% PFA). As shown in **Figure 5.5**, fixed neutrophils did not have the same effect as live neutrophils on biofilm biomass formation. Fixed neutrophils did not significantly affect the biofilm biomass even after subtracting neutrophils-only data.

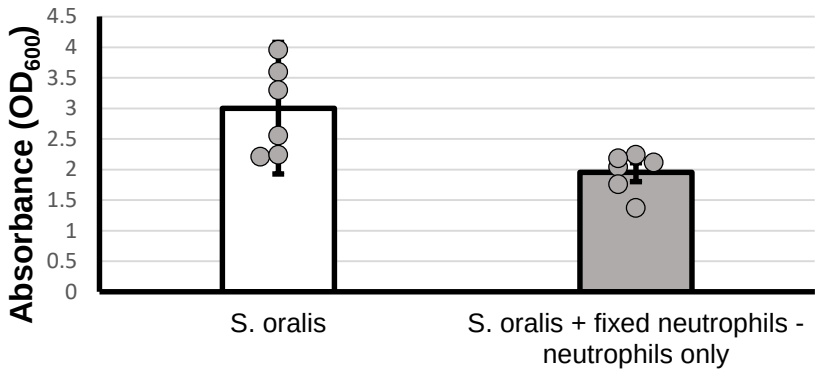

Figure 5.5: Biomass of *S. oralis* two-day biofilm with fixed neutrophils added for 2 h. There is no significant difference between biofilms with and without fixed neutrophils. CV assay was used to measure the biofilm biomass. Neutrophil-only wells were subtracted from neutrophils and *S. oralis* well data. Mean values ± SD are shown, and statistical analysis was completed by a t-test, p>0.05, (n=6 in triplicate wells).

5.4 Imaging of *S. oralis* biofilms after addition of neutrophils

5.4.1 CLSM LIVE/DEAD imaging

Bacterial biofilms with neutrophils were imaged to determine their interplay using CLSM. The biofilms were stained according to the manufacturer's instructions for the Filmtracer™ LIVE/DEAD™ biofilm viability kit. Live/dead imaging uses fluorescence labelling to distinguish between living and dead cells inside the biofilm. Live cells are stained with SYTO 9, which penetrates all bacterial cells and fluoresces green, demonstrating that the cell membranes are intact. Dead cells are labelled with propidium iodide, which only penetrates damaged membranes and fluoresces red.

Figure 5.6 shows a possible decrease in viable biofilm when neutrophils were present, as shown by decreased green staining of the biofilm. However, this could not be quantified due to the high number of stained neutrophils in these samples.

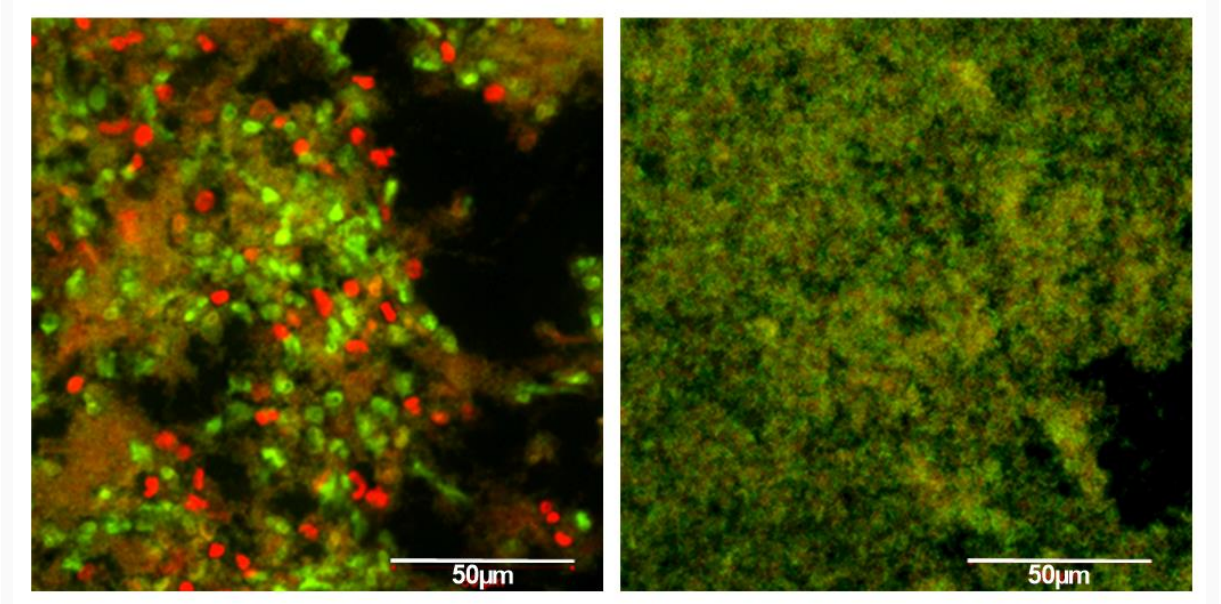

Figure 5.6: Live/Dead CLSM imaging of *S. oralis* biofilm with and without neutrophils.*S. oralis* biofilm was cultured for two days, and neutrophils were added subsequently for 2 h. Biofilms were stained with red propidium iodide (PI) and green SYTO 9 with (left) and without neutrophils (right). Images are shown at 40x magnification.

Neutrophils showed 29.57% death rate after incubation with the biofilm for 2 h. The percentage of neutrophil viability within the sample was calculated by the rate of neutrophils of red colour compared with those stained with green colour in four different images taken from the periphery of the biofilm.

LIVE/DEAD staining Z-stack images (**Figure 5.7**) showed no difference in biofilm thickness when Z-stacks were quantified using ZEN 2012 software. There was no significant difference between neutrophil-treated and untreated biofilm thickness.

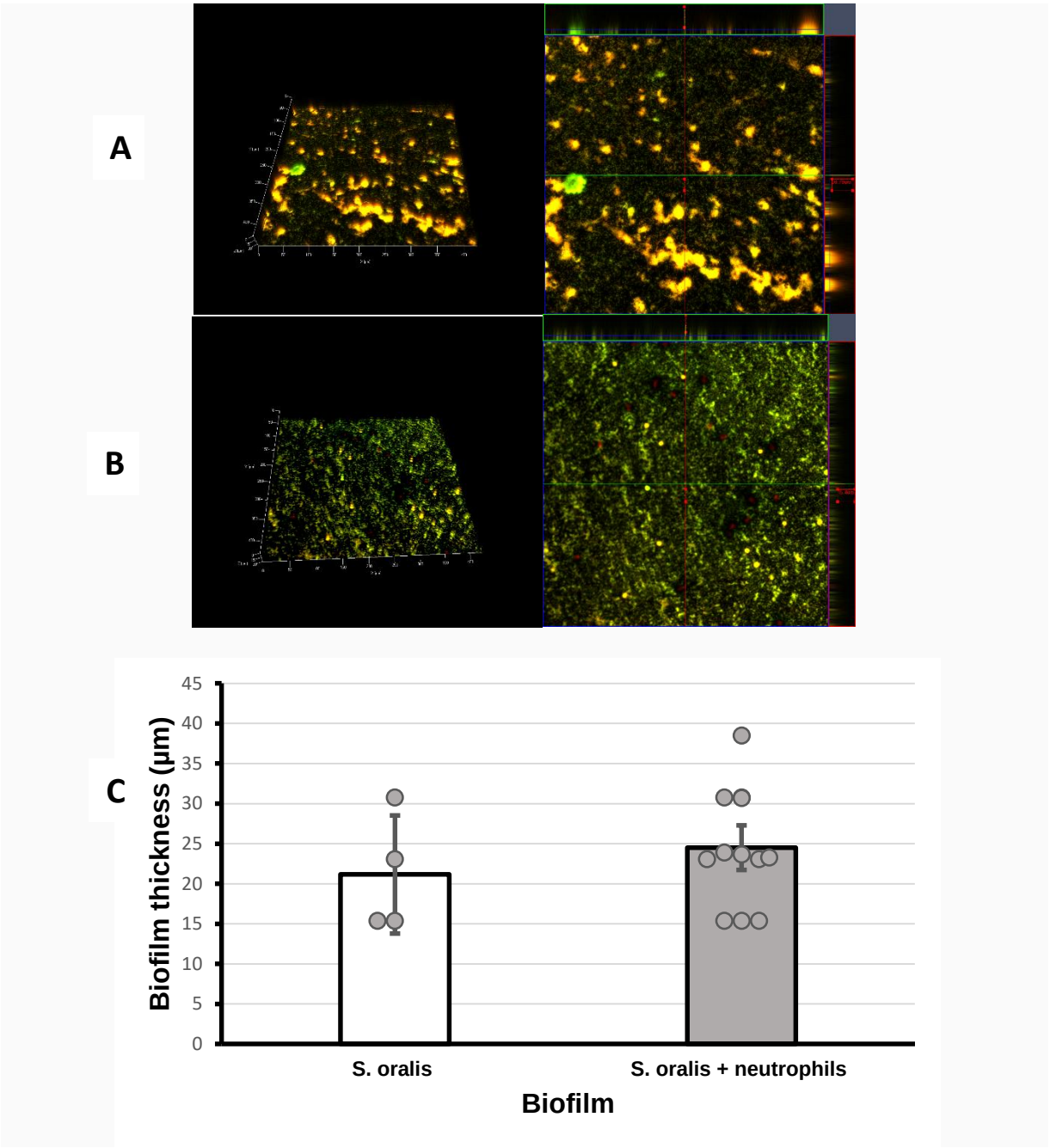

Figure 5.7: *S. oralis* biofilm thickness visualisation (representative images) and quantification after incubation with neutrophils using CSLM. A) *S. oralis* two-day biofilm thickness was determined by ortho-representation of the confocal Z-stacks throughout the entire thickness of single-species biofilms grown on a poly-L-lysine-coated 12-mm coverslip. SYTO 9 and PI were used for biofilm fluorescent staining. B) *S. oralis* biofilm with added neutrophils (for 2 h), Z-stack images. C) Image quantification of bacterial biofilm thickness: quantification was performed using Z-stack CLSM images of bacterial biofilms with and without added neutrophils (n=3 each). Each biofilm was performed in 2 replicates and two Z-stack images were taken from the top and bottom of the biofilm. The thickness of the biofilm was calculated based on the intensity of the live/dead staining, with measurements in micrometres. No significant difference was found in imaging between the neutrophils that were treated and untreated with biofilms. Bar graph shows mean values ± SD, and statistical analysis was calculated using t-test. No significant difference in biomass between biofilms was observed.

5.4.2 SEM imaging of biofilms

SEM biofilm images are displayed in **Figure 5.8**; neutrophils were seen embedded in the bacterial biofilm in the top row. Bacteria were observed surrounding the neutrophil's surface at higher magnifications. Neutrophil structures possibly resembling pseudopodia were observed in several images.

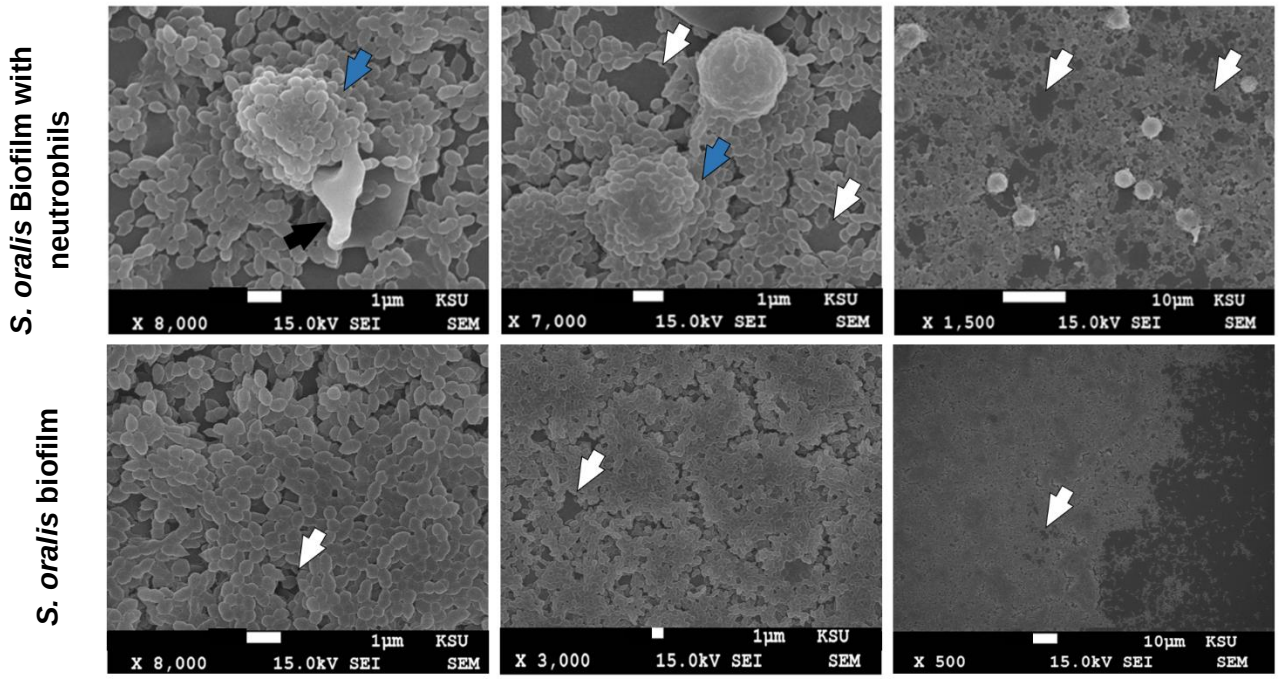

Figure 5.8: Multiple SEM images of two-day *S. oralis* biofilms with and without neutrophil inclusion. White arrows show void formation within the biofilm. Blue arrows display neutrophils coated with bacteria, and black arrows show a projection possibly resembling pseudopodia. Magnifications and scale bars are displayed below each image.

5.5 Neutrophil ROS production in response to *S. oralis* biofilms

ROS plays an essential role in neutrophil antimicrobial activities, making them a vital component for investigation in the context of neutrophil-bacteria interaction (Hirschfeld et al., 2017). Neutrophil interaction with bacteria often involves the production of ROS both within the cell (intracellular) and outside the cell (extracellular). The balance and

distribution of ROS in these compartments provide insight into neutrophil function and the immune response against bacterial infections.

ROS release was measured over 2 h after the addition of neutrophils to two-day *S. oralis* biofilms. ROS production was measured in biofilm-stimulated neutrophils and compared with neutrophils alone as well as to PMA-stimulated neutrophils.

Total ROS increased significantly (**Figure 5.9**A) but not extracellular ROS (**Figure 5.9**B). An increase in intracellular ROS may indicate phagocytosis (Fialkow et al., 2007) (**Figure 5.9**C). ROS responses occurred within the first 20 min, followed by a decrease to baseline levels over the course of 2 h. *S. oralis* biofilms alone exhibited no detectable production of ROS. The positive control, PMA, effectively stimulated the production of ROS within the neutrophil population. Total and extracellular ROS assays were conducted using the same cell population on the same days. However, the intracellular ROS assay was carried out subsequently with neutrophils from different pool of donors. This discrepancy is likely to account for the elevated levels of intracellular ROS in the positive control, exceeding those of total ROS in the positive control. In addition, HRP was added to enhance the chemiluminescent signal in extracellular ROS protocol, which helps enable the detection of ROS at nanomolar concentrations (Díaz et al., 1996). This increased sensitivity enables the measurement of even low amounts of extracellular ROS generation, which may result in higher detection of extracellular ROS levels (Zhu et al., 2016).

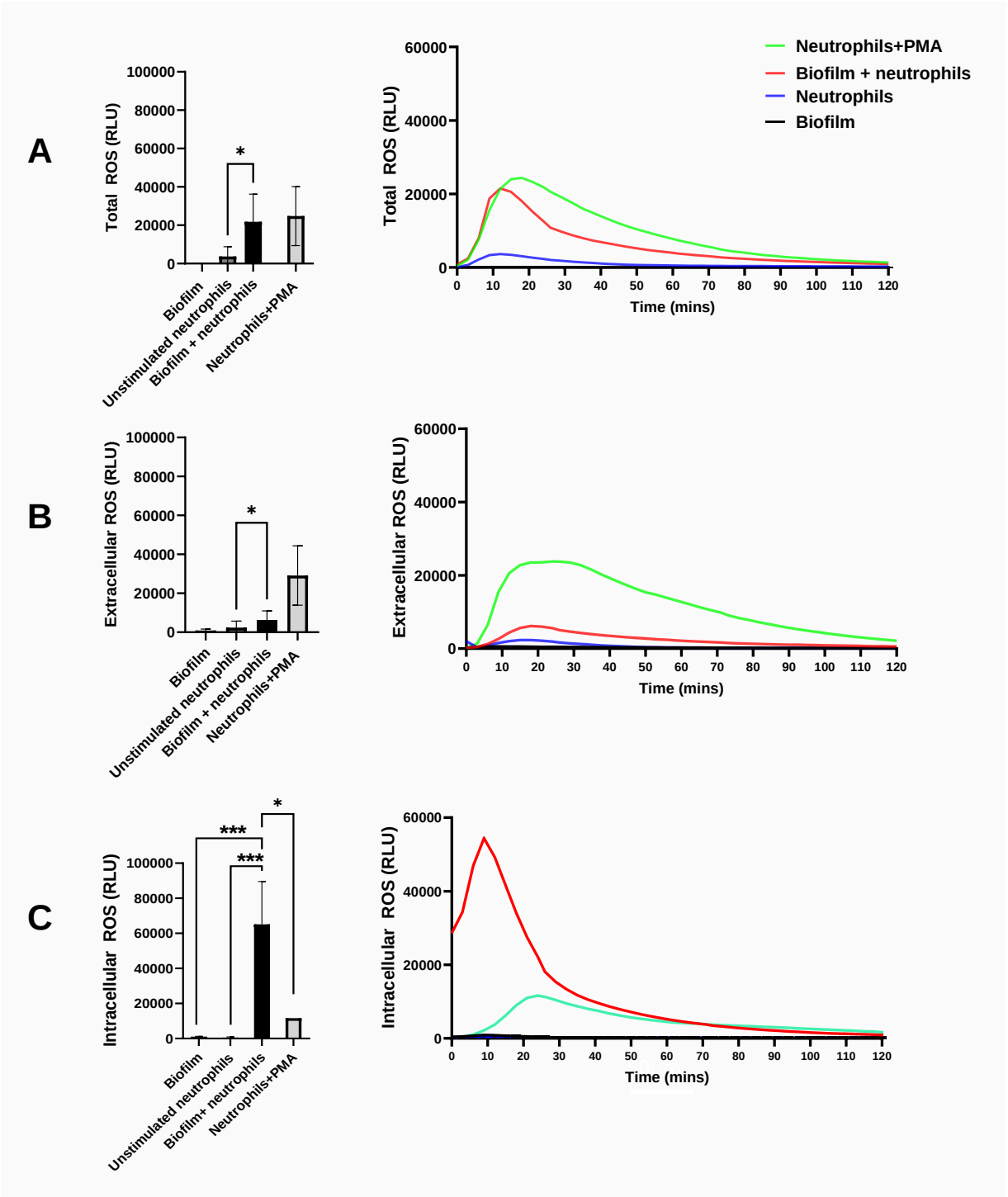

Figure 5.9: Neutrophil ROS release in response to 2-day *S. oralis* biofilms. Enhanced chemiluminescence was measured over 120 min, shown representatively in time curves and shown as relative luminescence units (RLU) of peak values in bar graphs. A) Total ROS, B) extracellular ROS and C) intracellular ROS production. 50 nM PMA was used as the positive control for neutrophil ROS stimulation, and unstimulated neutrophils were used as the negative control (n=6 in triplicate wells). The bar chart shows peak values with error bars displaying mean values ± SD; statistical analysis was calculated using one-way ANOVA, *p<0.05, **p<0.01, ***p<0.001.

5.6 Influence of neutrophils on biofilm adhesive strength

Biofilm adhesive strength was used to determine any potential changes in biofilm surface attachment strength. *S. oralis* biofilm was cultivated for 2 days, the biofilm was then stained with CV, as described in **Section** 2.7.5. The sum of all biofilm detachment and remaining biofilm on the coverslip was considered time-point zero. *S. oralis* alone biofilm detachment was not significantly different from biofilms containing neutrophils, as displayed in **Figure 5.10**.

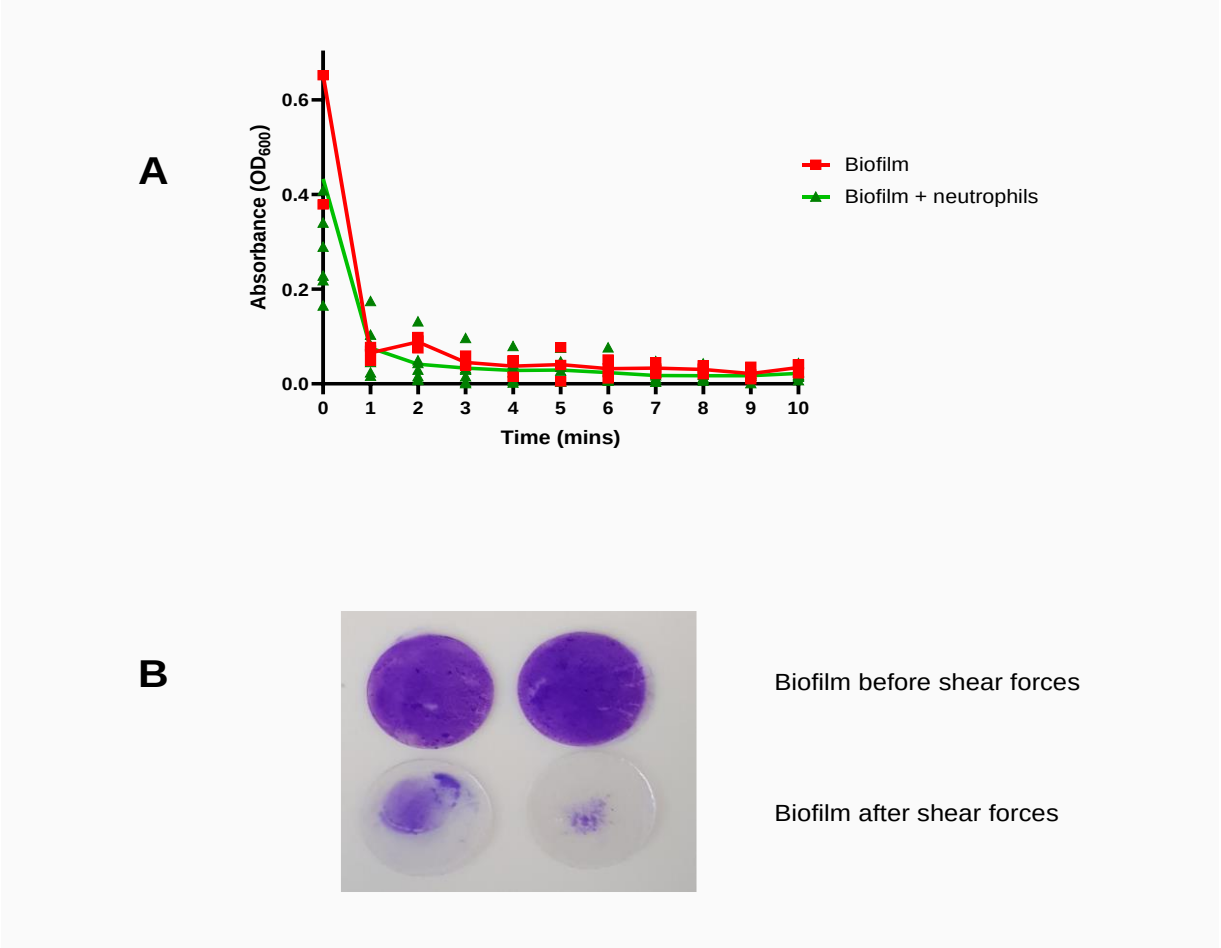

Figure 5.10: Changes in *S. oralis* biofilm adhesive strength in response to neutrophils. *S. oralis* biofilms were cultured for two days, then neutrophils were added to test biofilms for 2 h. Biofilms were stained with CV, and shear stress was applied to them. The OD_{600} reading of detached biofilm was recorded before adhesive strength was determined (n=7 in triplicate wells). A) biofilm detachment kinetics. Medians and ranges of measured absorbance are shown. Differences between the groups were analysed using the Mann-Whitney test. No significant difference in attachment between biofilms was observed. B) Two coverslips containing biofilm stained with CV showing biofilm before and after subjecting coverslips to shear forces.

5.7 Extracellular DNA/NET production by neutrophils and biofilms

In Chapter 4, *S. oralis* three-day biofilm eDNA was reduced after contact with neutrophils. This observation was studied further in this chapter by adding live or inactivated (fixed) neutrophils to a two-day biofilm and determining free extracellular DNA. Data is presented in **Figure 5.11**.

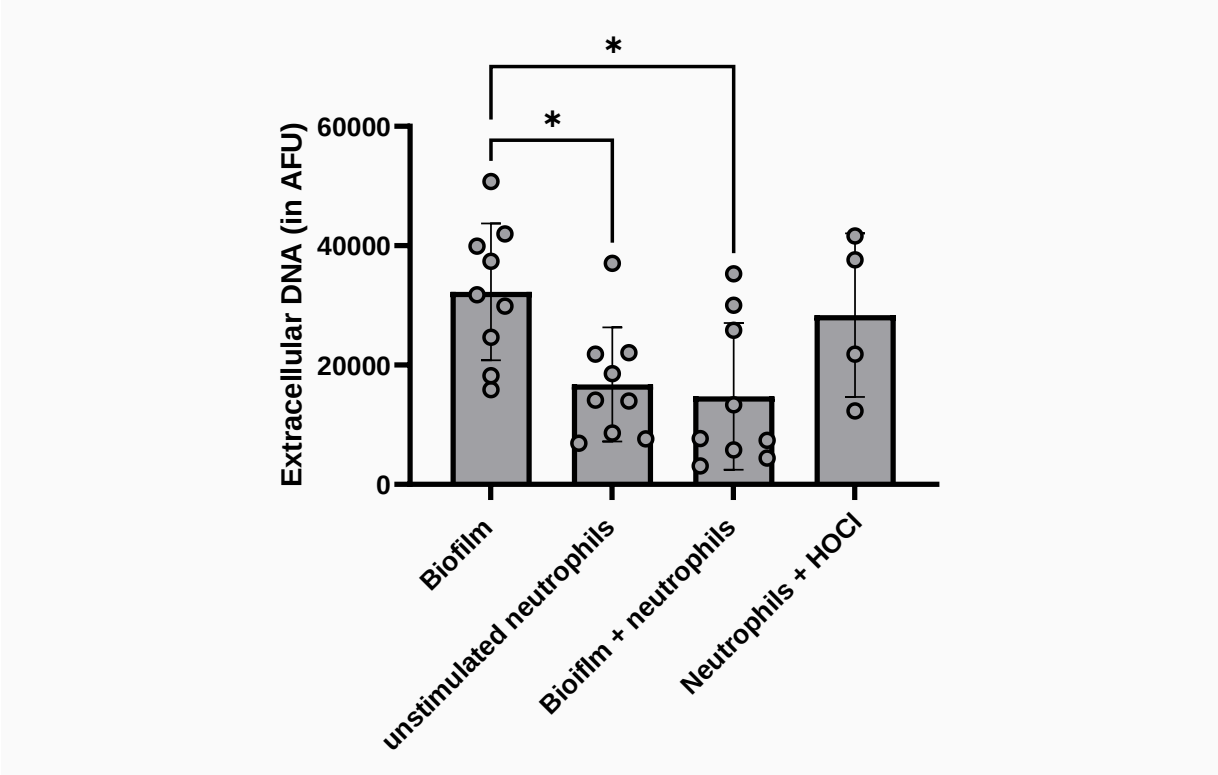

Figure 5.11: Quantification of extracellular DNA of *S. oralis* biofilms with neutrophils (including NET release). Two-day *S. oralis* biofilms were incubated with neutrophils for 2 h and compared with biofilms or neutrophils alone, as well as with a positive control for NET release. The bar graph shows mean values ± SD. Statistical analysis was calculated by one-way ANOVA, *p≤0.05 (n=9 in triplicate wells). Measurements are reported in arbitrary fluorescent units (AFU). A significant decrease in biofilm eDNA content following neutrophil addition was observed.

As observed in **Figure 5.11**, there was a significant decrease in the biofilm DNA content when neutrophils were included. This approach detected the presence of extracellular DNA without discriminating between DNA originating from NETs and eDNA present within the biofilm matrix.

5.8 Detection of neutrophil citrullinated histones in response to *S. oralis* biofilms

NET formation in response to *S. oralis* biofilms was investigated using two techniques: anti-citrullinated histone immunofluorescence and ELISA. These methods were used to enable the selective detection of NETs.

5.8.1 Fluorescent staining of citrullinated histones

Neutrophils were added to *S. oralis* biofilms, incubated for 2 h and detected with fluorescent stains. Triple-citrullinated histone was used as a marker for NET production (red) and cell-permeant Hoechst 33342 live stain (blue) was used as a counterstain. DNA fibres forming the NET strands were observed throughout the samples shown in **Figure 5.12**, which is consistent with the findings of our previous staining experiments showing three-species biofilm inducing NET production (see Chapter 4).

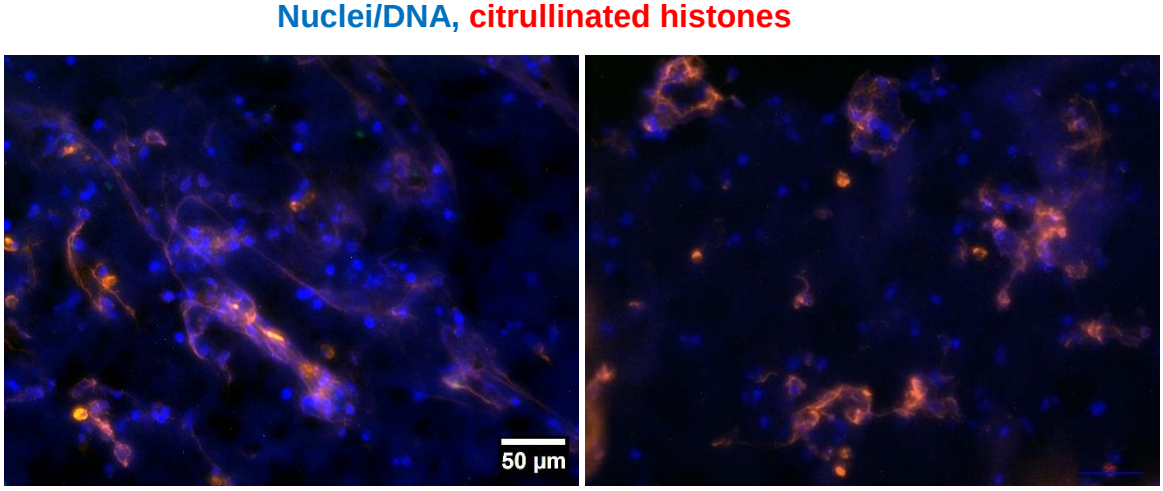

Figure 5.12: NET-specific fluorescent staining and CLSM representative images of neutrophils stimulated with *S. oralis* biofilms. *S. oralis* biofilms were incubated for two days. Neutrophils were added on day 2 of biofilm development and incubated for 2 h. Neutrophils were stained with Hoechst (blue) before they were added to biofilms; citrullinated histone (red) was stained after co-incubation of neutrophils and biofilm. Magnification: 20x. Scale bar is shown. Thread-like red fluorescence indicates the production of NETs containing citrullinated histones in all images.

5.8.2 Anti-citrullinated histone ELISA

To quantify the NET formation seen in microscopic images, NET formation was analysed using an anti-citrullinated histone ELISA. NET formation was not detected in response to *S. oralis* biofilms or by HOCl (NET inducer) by ELISA. The experimental results were below the lower detection limit despite using undiluted samples (**Figure 5.13**).

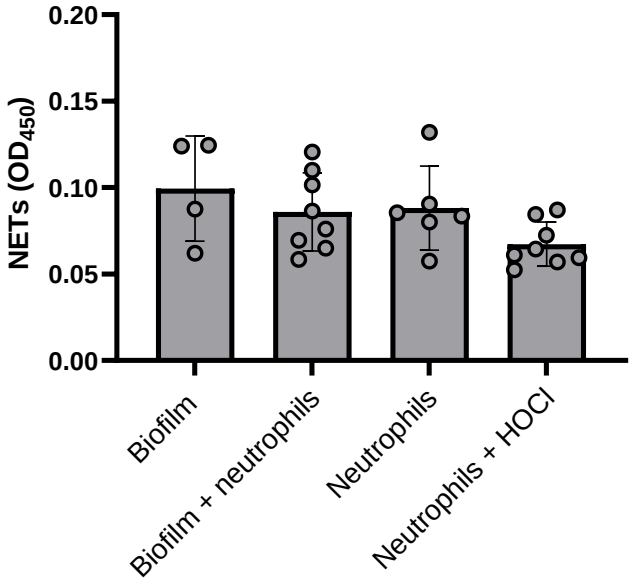

Figure 5.13: Quantification of citrullinated histones in *S. oralis* biofilms with neutrophils by ELISA. *S. oralis* biofilms were incubated for two days. Neutrophils were added on day 2 of biofilm development and incubated for 2 h. The target protein remained below the lowest detection limit of 0.1. Hypochlorous acid (HOCl) was used as a positive control for NET induction. Bar graph show mean values ± SD. Statistical analysis was calculated using one-way ANOVA, and no significant differences were observed.

5.9 Neutrophil interaction with bacterial DNA

The interaction of neutrophils with extracted bacterial DNA was performed to investigate whether neutrophils can take up *S. oralis* DNA, as a decrease in biofilm eDNA had been observed after neutrophils were added to biofilms (see **Section** 5.5). This possible interaction was analysed by fluorescent microscopy and flow cytometry.

5.9.1 Fluorescent staining of bacterial DNA and neutrophils

Neutrophils were tested for their ability to phagocytose bacterial DNA. 1 µg/ml of *S. oralis* genomic DNA was isolated and stained with PI, mixed with neutrophils pre-stained with Hoechst. DNA concentration was selected according to prior evidence, suggesting that 0.2-3.2 µg/ml of *Escherichia coli* DNA can elicit neutrophil activation and delay apoptosis (József et al., 2004). The isolated bacterial DNA co-localised with neutrophil surfaces observed in **Figure 5.14** suggested a possible DNA attachment to the neutrophil cell membrane.

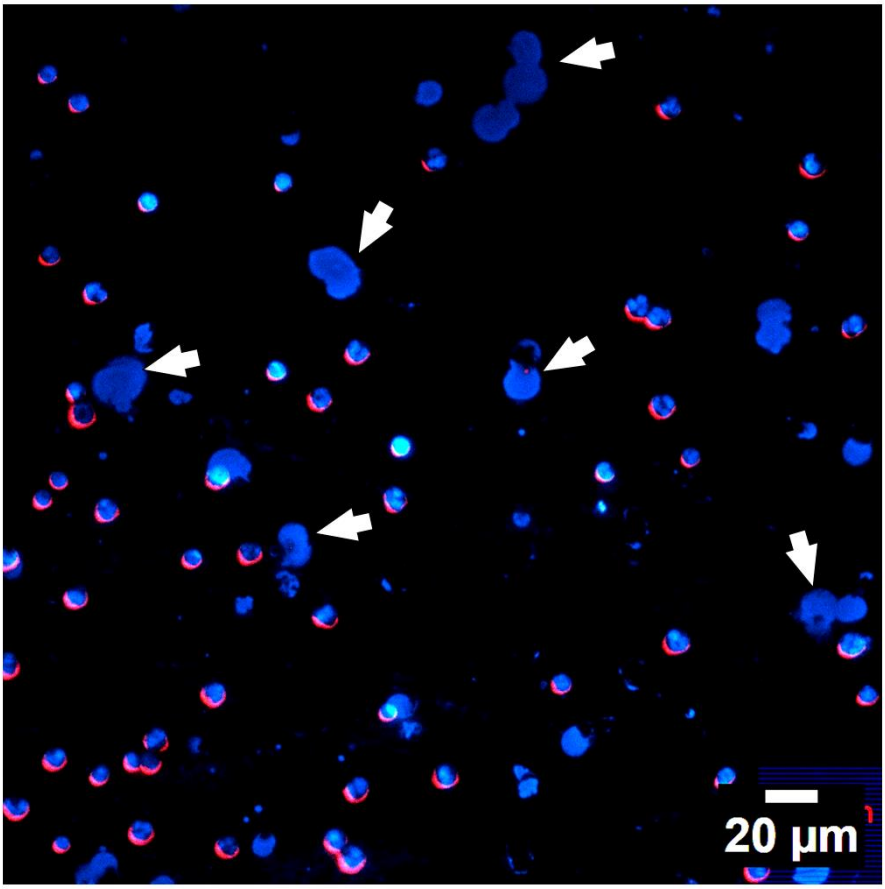

Figure 5.14: Representative fluorescent microscopy image of bacterial isolated DNA co-localising with neutrophils. Magnification is 20x. Neutrophils pre-stained with Hoechst (blue) and incubated with isolated *S. oralis* DNA (PI, red). White arrows show an enlarged nucleus with no co-localisation with bacterial DNA.

Nonetheless, considering the fluorescent microscopy two-dimensional image basic properties, which only visualise cells extracellularly, the possibility of internalisation cannot be completely disregarded. Some neutrophils exhibited a change in nuclear morphology accompanied by an enlarged nucleus. These deformed neutrophils were not co-localised with bacteria DNA. Neutrophils co-localised with DNA were counted in three replicates, and these data indicated that 74.07% of neutrophils exhibited this phenomenon.

5.9.2 Flow cytometer analysis of *S. oralis* DNA interaction with neutrophils

For flow cytometer analysis, the analyses were performed in 5 mL round bottom polystyrene FACS tubes, using FACS Canto II (BD Biosciences) equipped with FACSDiva software (BD Biosciences).

Flow cytometry analysis in **Figure 5.15** revealed a detectable shift in the neutrophil population after bacterial DNA exposure within the gated region. This shift suggested changes in neutrophil physical and optical properties, which were quantified by changes in FSC and SSC indices.

The observed change in FSC and SSC values indicated a change in neutrophil shape and internal structure, which is compatible with increased cellular activity (Ustyantseva et al., 2019) or can be due to the binding of the fluorescently labelled DNA to the neutrophil surface, increasing particle size. In the histogram, a rightward shift after neutrophil stimulation indicates an increase in the fluorescence intensity. This change is generally viewed as an indication of cellular activation or reaction (Lakschevitz et al., 2016). Thus, the rightward shift provides a measurable proxy for neutrophil activation, with larger shifts indicating more robust cellular responses.

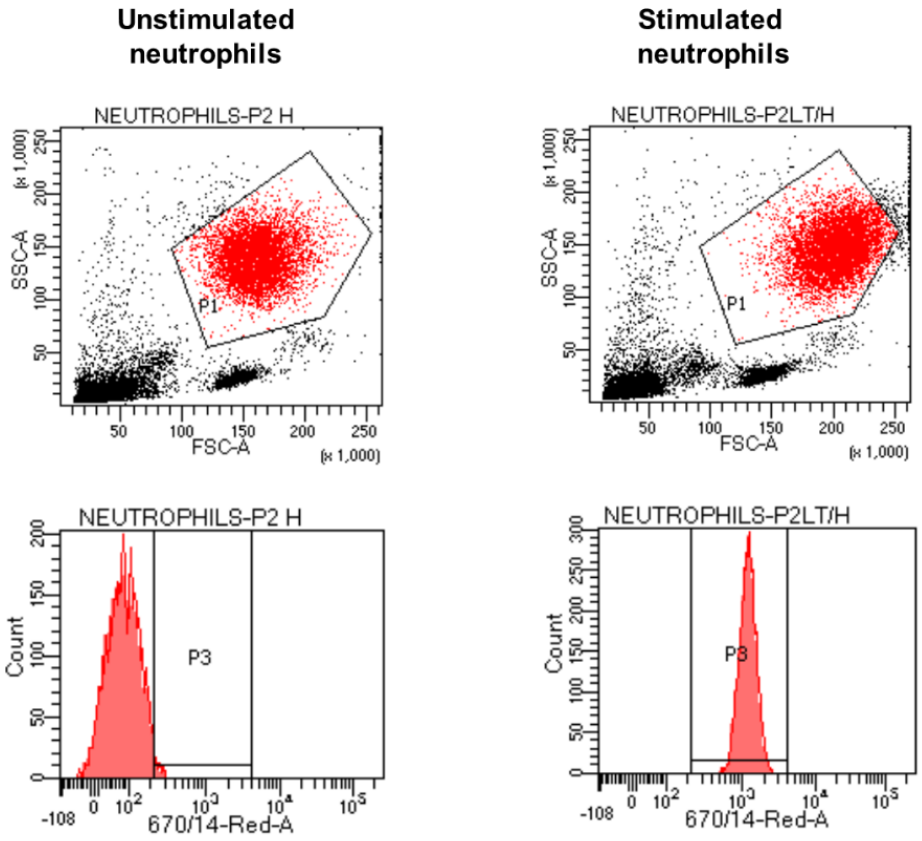

Figure 5.15: Analysis of neutrophil interaction with isolated bacterial DNA by flow cytometry. Neutrophils pre-stained with Hoechst (blue) and incubated with isolated *S. oralis* DNA (PI, red). Top: Flow cytometry scatter plots. Neutrophil gating was based on forward (FSC, size) and side (SSC, granularity) light scattering. Bottom: Flow cytometry histogram. A rightward shift in the histogram following neutrophil stimulation.

5.10 Impact of neutrophils on colony forming units (CFUs) within biofilms.

The amount of viable bacteria within the biofilm was examined to better understand the influence of neutrophils on the bacterial viability within the biofilm. When neutrophils were added to the biofilm, there was a significant increase in the number of live bacteria, as shown in **Figure 5.16**. This unexpected increase in CFU was studied further by introducing inactivated (fixed) neutrophils into the biofilm. Fixed neutrophils had no influence on the CFUs derived from the biofilms.

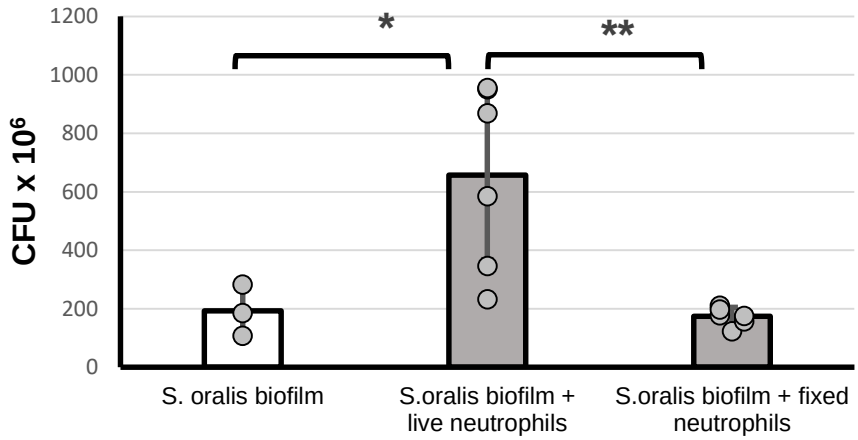

Figure 5.16: *S. oralis* biofilm CFUs with and without live and inactivated (fixed) neutrophils.The *S. oralis* biofilms were incubated for two days, and neutrophils were added on day 2 of biofilm development and incubated for 2 h. Bar graph shows mean values ± SD. Statistical analysis was performed using one-way ANOVA: *p<0.05, **p<0.01 (n=6 in triplicate wells). There was a significant increase in biofilm CFU after live neutrophil interaction, but no significant difference occurred when fixed neutrophils (dead) were added.

5.11 Discussion

Preventing oral bacterial biofilms can be accomplished by understanding the factors that aid in its formation and its interactions with the immune system. Neutrophil-biofilm interactions in the oral cavity are documented but not well understood (Shapira et al., 2000, Mikolai et al., 2020, Hirschfeld, 2014, Hirschfeld et al., 2015). Therefore, the aim of this chapter was to investigate the dynamics of neutrophil engagement with the periodontal biofilm early colonising bacterium, *S. oralis*.

To enable co-culture of biofilms and neutrophils, different media were tested to determine the medium most suitable for both (outlined in **Section** 4.5.2.). Glucose and yeast extract positivity influenced *S. oralis* development but was unsuitable for neutrophil survival. TSB was suitable for both biofilms and neutrophils. When *S. oralis* was cultured with TSB, the pH decreased during the first two hours by one pH unit,

which is the total incubation period of neutrophils with the biofilm in this study; this acidosis may have increased neutrophil survival, as their apoptotic cell death was reported to be delayed when incubated in slightly acidic media (Cao et al., 2015). Furthermore, neutrophil acidosis may amplify acute inflammatory reactions by activating neutrophils, delaying spontaneous death, and increasing neutrophil functional lifespan (Trevani et al., 1999, Martínez et al., 2006). These findings indicate that the decrease in pH within the incubation time intensified the neutrophil response to *S. oralis* biofilm.

One of the aims of this thesis was to investigate the role of NETs in bacterial biofilms. The working hypothesis was that if the biofilm-integrated bacterial eDNA provides structural stability (Okshevsky and Meyer, 2015), then neutrophil-produced DNA in the form of NETs may either have anti-biofilm properties or inadvertently contribute to the biofilm scaffold and therefore aid biofilm development. The observed significant reduction in *S. oralis* biofilm following the incubation with neutrophils was in conflict with this hypothesis. The enhancement of neutrophils in biofilm structures detected by CV biofilm staining was reported in *P. aeruginosa* strain PAO1 found in cystic fibrosis (Parks et al., 2009). While the authors indicated that this increase in CV result is directly related to the biofilm biomass, it is possible that an alternative analysis could yield a divergent outcome. In the findings of Perks et al., there were no negative control containing neutrophils only. Data indicate that neutrophils have a high affinity to be stained by CV, hence the increase in the biofilm biomass may be related to neutrophil remnants within the biofilm but not the biofilm itself. In addition, Parks et al. found that F-actin and DNA polymers were incorporated into the bacterial biofilm (Parks et al., 2009). F-actin and DNA polymers may also be present but do not contribute to the biofilm mass.

Fluorescent 3D-biofilm images showed no significant difference in biofilm thickness, however this is not consistent with the reduction in biofilm biomass detected by CV. This could be attributable to neutrophils contributing to the biofilm intensity. This finding was implied based on the high neutrophil retention in *S. oralis* biofilm and neutrophils were retained in the biofilm, with only 4.3% of neutrophils released into the supernatant. This high affinity of neutrophils to attach to dental biofilms has been reported previously (Shapira et al., 2000). Interestingly, the majority of adhered neutrophils were found to be covered by a bacterial layer in SEM images. This layer may serve as a protective barrier for the biofilm, shielding it from neutrophil-produced antimicrobial components, such as H_2O_2 and myeloperoxidase (Jesaitis et al., 2003). The presence of bacteria-covered neutrophils within a biofilm has important implications for our understanding of host-pathogen interactions and biofilm growth dynamics. Bacteria in biofilms can express surface chemicals that increase neutrophil adherence, potentially as an immunological evasion strategy. *S. aureus*, for example, can produce protein A, which binds to the Fc region of antibodies, potentially enabling the bacteria to 'wrap' themselves with host factors that bind to neutrophils (Rigby and DeLeo, 2012).

Furthermore, due to the high density of bacteria and the protective nature of the biofilm's EPS, neutrophils may have decreased phagocytic function when covered with bacteria. This can result in a state of 'frustrated phagocytosis,' in which neutrophils cannot efficiently engulf and eliminate bacteria (Sadowska et al., 2013). In addition, interaction with biofilms can change neutrophil lifespan by prolonging their activity through delayed apoptosis or inducing necrosis due to an overwhelming bacterial load (Kobayashi et al., 2017). SEM images also showed neutrophil shrinkage, which was likely attributed to their drying during sample preparation (Ting-Beall et al., 1993, Ting-

Beall et al., 1995). After interacting with *S. oralis* biofilm, neutrophils were found to have a 29.57% decrease in their viability, as demonstrated by LIVE/DEAD imaging and cell counting.

A reduction in *S. oralis* biofilm DNA content accompanied the mass decrease in biofilm. It was hypothesised here that neutrophils might phagocytose bacterial DNA. This hypothesis was tested by fluorescently investigating the engagement of neutrophils and isolated bacterial DNA. Instead of the hypothesised phagocytosis, DNA and neutrophil co-localisation was visualised using fluorescent microscopy. The DNA of *S. oralis* was exhibited adjacent to the neutrophil surfaces. Several parameters, including the position and focus of the laser, can influence the detection of a fluorescent signal and its localisation on the cell while undertaking the fluorescence imaging. If the laser is not properly centred or focused, it might cause uneven illumination, making fluorescence appear brighter in one section of the cell than another. Another factor that may influence the apparent distribution of fluorescence is the angle at which the detector (e.g., camera or photomultiplier tube) captures the signal. The fluorescence signal may appear asymmetric if the detector is not positioned perpendicular to the plane of the cell. These reasons could explain the unilateral fluorescence distribution. Notably, as bacterial DNA adhesion to neutrophils was found in this investigation, DNA internalisation cannot be extrapolated. Approximately, 74% of neutrophils showed a close proximity to DNA. Cells not exhibiting this phenomenon were expanded with a ‘bloating’ effect comparable to NETosis, with a 26% percentage corresponding to the existing literature (Fuchs et al., 2007). These neutrophils undergoing NETosis correlate with the NET detection in the fluorescent imaging. These enlarged neutrophils may represent NETosis activity in response to bacterial DNA. In addition, bacterial DNA has been shown to cause neutrophil size transition in this study, as evidenced by a shift in

the stimulated neutrophil population towards the upper right of the flow cytometry gate. Neutrophils are known to change size and granularity when activated *in vitro* (Pember et al., 1983, Ustyantseva et al., 2019). Our findings suggest that the neutrophil density and size transition were caused by bacterial DNA, as their density is altered by *in vitro* stimulation or by activation in disease (Hassani et al., 2020). Alternatively, these changes could potentially result from the simple attachment of fluorescently labelled DNA to neutrophil surfaces, thus increasing particle size. However, it is unlikely that neutrophils do not become activated upon bacterial DNA binding, as bacterial DNA stimulation enhances neutrophil functions such as adhesion, migration, and cytokine production (El Kebir et al., 2009). Neutrophil activation could be studied further by selecting markers known to increase during activation, such as CD62L (L-selectin), CD11b, and CD66b (Ley et al., 2007, Ross, 2002, Yoon et al., 2007).

TLR9 in human neutrophils recognises unmethylated-CpG motifs in bacterial DNA (Akira et al., 2006). However, the receptor was understood to exist intracellularly in neutrophils and could not be activated unless DNA became internalised (Ishii et al., 2014). Subsequent investigations have revealed that TLR-9 can be located on the surface of neutrophils and can sense bacterial DNA via an endocytosis-independent process, leading to neutrophil activation (Miyake and Onji, 2013). Other studies reported that DNA attachment to neutrophils can cause neutrophil activation, which does not require DNA internalisation, revealing that this process is driven through a CpG- and TLR9-independent mechanism (Fuxman Bass et al., 2008, Trevani et al., 2003, Alvarez et al., 2006). This study's visualisation of DNA and neutrophil co-localisation suggests that neutrophil activation is unrelated to endosomal TLR-9 activation. However, the precise pathways by which neutrophils recognise and possibly bind to eDNA are poorly understood. It has been proposed that in low pH, negatively

charged eDNA creates electrostatic interactions with positively charged cell membrane-anchored lipoproteins, facilitating their attachment (Dengler et al., 2015). While there have been some receptor studies on DNA attachment (Trevani et al., 2003), future experiments should be conducted to characterise bacterial DNA recognition by using specific inhibitors or activators of DNA sensors like the TLR9 receptor or cGAS-STING signalling pathway to understand further innate immune responses and the mechanisms of inflammation and infection resolution.

The ability of *S. oralis* biofilms to elicit NET release was tested. The characteristic web-like structure of NETs was observed by fluorescent imaging using a conjugated anti-citrullinated histone antibody (Brinkmann et al., 2004) which correlated with the work of Oveisi (Oveisi et al., 2019), showing the induction of citrullinated histones by *S. oralis* biofilms using flow cytometry. However, NET release was not detected by DNA quantification assay. A possible explanation was that NETs may have been below the minimum detectable level of this assay. NETs in response to *S. oralis* biofilms have been described in the literature but only in small amounts compared with other oral species (Mikolai et al., 2020).

A *S. oralis* biofilm is known to produce DNABII proteins. The DNABII protein family, which consists of an integration host factor and a histone-like protein, has been reported in the EPS matrix of other streptococcal biofilms, such as *S. mitis* and *S. gordonii* (Rocco et al., 2018, Rocco et al., 2017). These proteins are understood to be involved in creating and maintaining the EPS matrix, as antiserum directed against this protein was shown to cause eDNA to lose its structural stability, resulting in the biofilm disintegrating (Brockson et al., 2014). DNABII have a high affinity for binding and bending DNA (Swinger and Rice, 2004). They are assumed to bind and change eDNA from the normal physiological right-handed, low-energy configuration that is sensitive

to nuclease degradation to the Z-form, which has a left-handed configuration with distinct nucleotide geometry and is resistant to nuclease degradation (Buzzo et al., 2021). The formed Z-from DNA accumulates as the biofilm matures (Swinger and Rice, 2004, Buzzo et al., 2021). By functioning as keystone proteins to maintain the cross-stranded structure of eDNA, DNABII proteins functionally imitate Holliday junctions within the EPS to support the biofilm's unique architecture (Devaraj et al., 2019). In contrast, DNA in NETs is a de-condensed form of DNA associated with citrullinated histones, antimicrobial peptides and enzymes; it occupies three to five times the volume of condensed chromatin (Delgado-Rizo et al., 2017). Because of the structural variabilities between bacterial eDNA and NETs, Serrage and colleagues suggested that for a DNA to successfully support biofilm EPS, it must change shape (Serrage et al., 2021). This eDNA structure change occurs as the biofilm matures and becomes more resistant to DNases (Deng et al., 2022). These enzymes have been shown to induce significant reductions in early (<8 h) biofilm formation. However, as the biofilm matures and gets more structurally complex, it becomes less susceptible to DNase activity (Schlafer et al., 2017, Deng et al., 2022). The reported change in susceptibility to DNases during biofilm maturation is consistent with the structural changes in eDNA inside the biofilm matrix. Furthermore, these findings suggest that the reason NETs may not play a role in the biofilm structure in the current study was that they lack the architecture required to construct a DNA lattice network.

S. oralis biofilms stimulated neutrophils to produce total and intracellular ROS higher than the reported total ROS stimulated by planktonic *S. oralis* (Hirschfeld et al., 2017), whilst there was no difference in extracellular ROS production in neutrophils stimulated by biofilm and planktonic bacteria. ROS extracellular release is due to the assembly of NADPH oxidase at the plasma membrane (Boyle et al., 2011). The increase in total

ROS may be attributed either to the higher bacterial numbers in biofilms or to biofilm-produced stimulatory agents such as EPS (Campoccia et al., 2023, Dapunt et al., 2016, Dapunt et al., 2020). Intracellular ROS was at a high value at time zero. This was due to the ability of neutrophils to respond rapidly to stimuli. ROS formation can begin within 30 seconds once activating chemicals are exposed (Nguyen et al., 2017). Neutrophils were already in contact with the biofilm before the measurement began, which may have resulted in elevated ROS levels at time zero. The decrease in ROS after a 20 min peak back to baseline levels was attributed to the ability of *S. oralis* to stimulate the activation of a transcription factor for antioxidants (nuclear factor erythroid 2-related factor, Nrf2) in neutrophils in combination with enhanced ROS production (Oveisi et al., 2019). This mechanism balances the excess ROS production to maintain oral health (Chiu et al., 2017). PMA was used as a positive control, as it is known to induce the extracellular release of ROS with some intracellular ROS production in non-phagosomal compartments (Bylund et al., 2010, Karlsson et al., 2000). Indeed, this ROS activation pattern was observed in our assay. The generation of extracellular ROS by neutrophils in response to dental biofilms can disturb microbial populations and prevent infection, but excessive ROS can damage oral tissues and contribute to inflammatory disorders such as periodontitis. Intracellularly, neutrophil-produced ROS are critical for destroying phagocytosed bacteria, aiding in the maintenance of oral health by controlling biofilm-related infections. A persistent or excessive neutrophil response, on the other hand, can cause chronic inflammation and tissue damage, emphasising the need of balance in the immune response to oral biofilms (Oveisi et al., 2019).

As an early coloniser, *S. oralis* produces surface dextrans that facilitate attachment to the tooth surface (Banas and Vickerman, 2003). Adhesive strength analysis revealed

that detachment in *S. oralis* biofilms with and without neutrophils was similar, suggesting that although neutrophils reduce biofilm mass, biofilm adhesive strength may not be affected. As well as dextrans, eDNA may also increase adhesion capacity, as is reported for other species, along with improving mechanical strength (Hu et al., 2012). Thus, if neutrophils indeed interfere with eDNA, biofilm adhesive forces may not be affected, if other adhesion-mediating components of the biofilm matrix, such as dextran, are also present.

In addition to the measured eDNA loss, the number of viable bacterial cells unexpectedly increased within the biofilm after neutrophil contact, which was observed in all biological replicates. In a previous study, biofilms were subjected to ultrasonication, resulting in CFU increases (Pitt and Ross, 2003). The authors hypothesised that ultrasonic forces could enhance the rate of oxygen and nutrient transfer to bacterial cells while increasing the rate of transport of waste products away from cells, hence enabling cell growth. Indeed, Melaugh and colleagues reported that cells outside of bacterial aggregates grow more rapidly than those in the central regions as they have better access to nutrients (Melaugh et al., 2016). Chebotar and colleagues reported similar findings; as there was an increase in live bacteria in *S. aureus* biofilm supernatant, with a 2 % biofilm destruction rate after neutrophil interaction (Chebotar et al., 2012). These findings lend empirical support to the outcomes of this study, suggesting that a loss of eDNA may cause less structural integrity, allowing more nutrients into the biofilm and thus supporting bacterial growth. However, it was also observed here that there was a decreased biofilm mass when it was subjected to neutrophils, which appears to contradict the hypothesis of enhanced bacterial growth. This could be explained by the ability of neutrophils to generate ROS that disturb the biofilm matrix (Sarangapani and Jayachitra, 2018) and deploy NETs,

which can entrap and kill bacteria while potentially interfering with biofilm structure (Yang et al., 2023), and both have been detected in this study. Furthermore, neutrophils release antimicrobial peptides and enzymes that degrade the biofilm, release EPS, and kill the bacteria within it (Reeves et al., 2002). Finally, neutrophils may disrupt bacterial communication pathways that are critical for biofilm maintenance (Roy et al., 2018). Despite these effects, some biofilms can resist and even thrive in the presence of neutrophils by causing chronic inflammation, which can paradoxically increase biofilm resilience.

In the same context, the decrease in biofilm eDNA content could be attributable to biofilm breakdown and EPS release into the supernatant. Although as only eDNA was assessed, future research should be conducted to investigate the context of neutrophil-induced biofilm biomass loss.

This study used a commensal bacterium to elucidate processes of neutrophil-bacterial interaction in the early phases of oral biofilm development, and it highlighted the influence of neutrophils on the oral biofilm, producing lower biomass and eDNA content. In addition, the biofilm has an effect on neutrophils by activating them to produce ROS and causing NETosis. More research should be undertaken to better understand this reaction.

5.12 Graphical summary

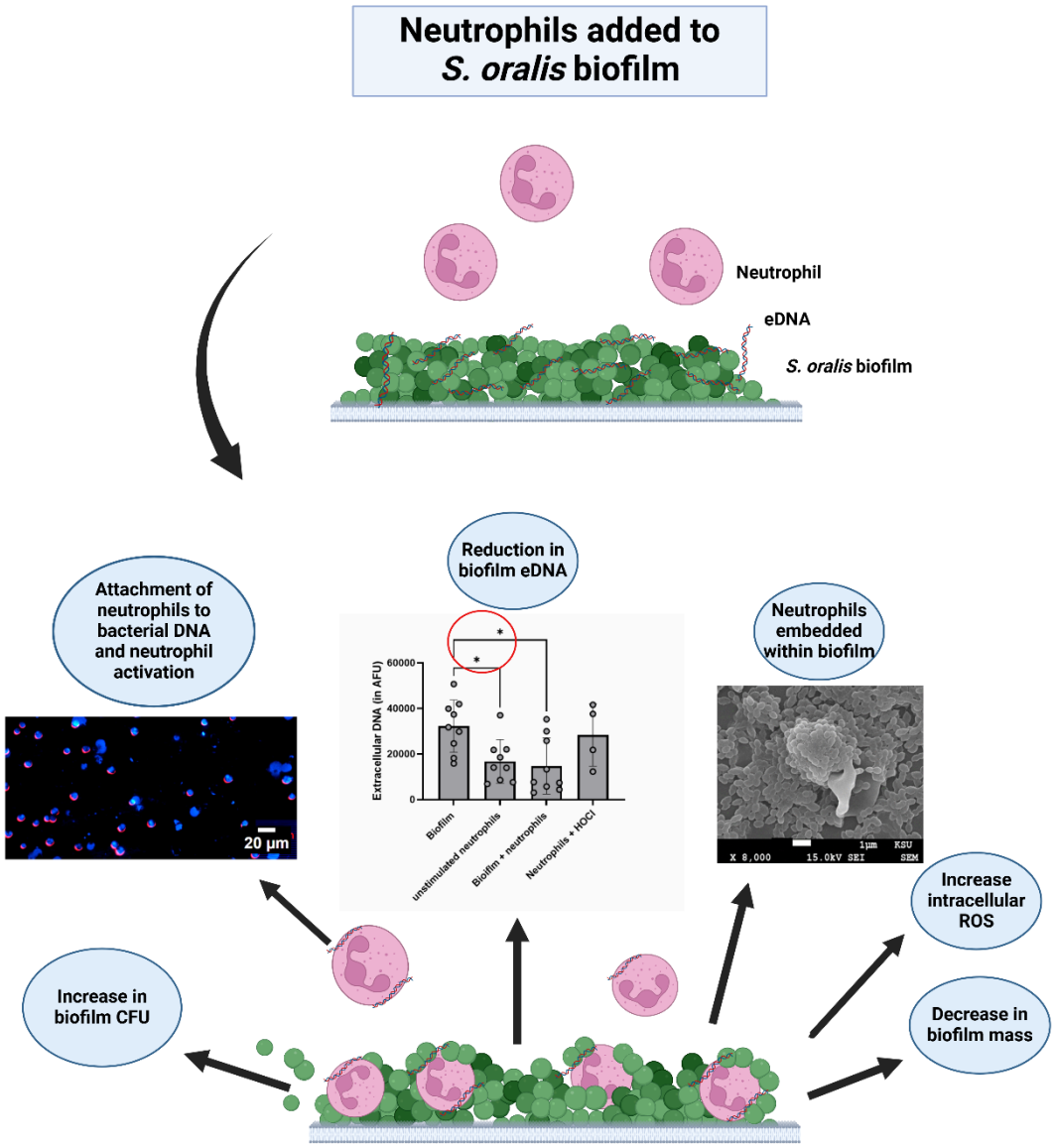

6 CHAPTER SIX Results: Interactions between *Aggregatibacter actinomycetemcomitans* biofilms and neutrophils

6.1 Introduction

The preceding chapters explored how neutrophils interact with biofilms formed by commensal oral bacteria, which are known to be early colonisers in periodontal biofilms. This chapter aims to explore how neutrophils interact with biofilms formed by the periodontal pathogen *A. actinomycetemcomitans*. *A. actinomycetemcomitans* has been linked to rapidly progressing forms of periodontitis occurring at a relatively young age (Fine et al., 2007). In addition, this pathogen has been associated with diseases that are not confined to the oral cavity, including infective endocarditis, soft tissue abscesses, pneumonia and osteomyelitis (Homsi and Kapila, 2020). This study used the *A. actinomycetemcomitans* strain HK 1651 due to its ability to promote NET formation in a concentration-dependent manner (Hirschfeld et al., 2016). This strain was discovered to have LtxA, an *A. actinomycetemcomitans* virulence factor with lytic action against leukocytes, including neutrophils (Baehni et al., 1981).(Hirschfeld et al., 2016). This chapter investigates the interaction of *A. actinomycetemcomitans* biofilms with neutrophils to explore whether these are comparable with those observed in the commensal biofilm model using *S. oralis*.

6.2 DNase enzyme production by *A. actinomycetemcomitans*

DNase production by *A. actinomycetemcomitans* was assessed to determine whether this bacterium produced NET-degrading enzymes. No DNase production was detected after three days of incubation, as shown in **Figure 6.1**.

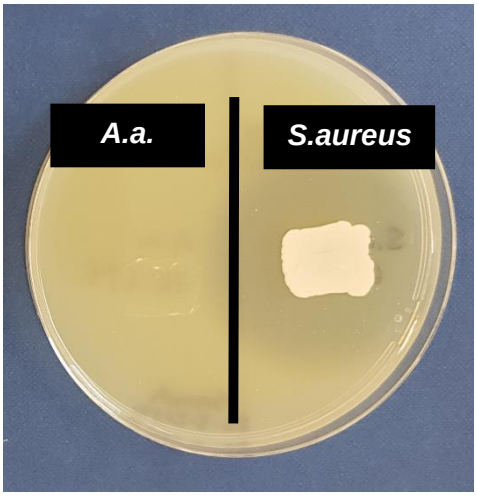

Figure 6.1: Investigation of DNase production in *A. actinomycetemcomitans* (*A. a.*) and *S. aureus* on DNA-containing agar.After three days of incubation, there was a clear area around the positive control S. aureus growth, indicating DNase production. The lack of a clear zone around *A. actinomycetemcomitans* after adding HCL to the medium indicated a lack of DNase production.

6.3 Biomass assessment of *A. actinomycetemcomitans* biofilm interaction with neutrophils

The influence of neutrophils on the biomass of *A. actinomycetemcomitans* biofilms was investigated by adding neutrophils to a two-day biofilm and incubating this co-culture for 2 h. The biomass of the biofilm was assessed using the CV technique as previously described. The biofilm incubation time was chosen to be similar to that for streptococci. **Figure 6.2** shows no significant difference between neutrophil-treated and non-treated biofilms, even after subtracting neutrophil-only values.

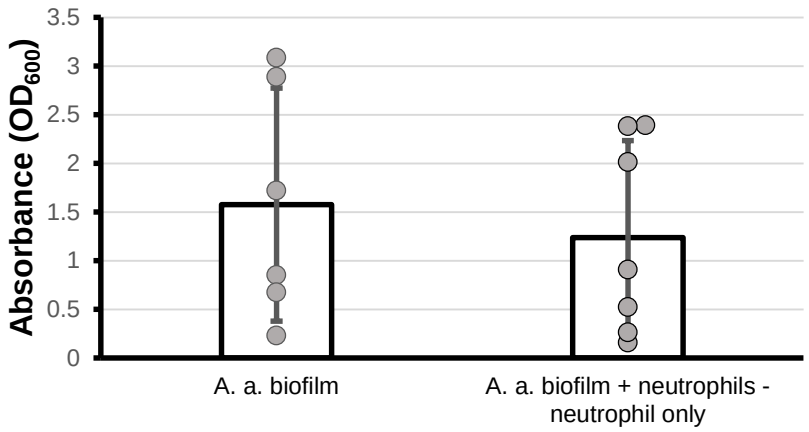

Figure 6.2: The biomass of *A. actinomycetemcomitans* (*A.a.*) biofilms before and after adding neutrophils. *A. actinomycetemcomitans* biofilms were cultured for two days then neutrophils were added subsequently for 2 h. Neutrophil-only containing wells were subtracted from neutrophils and *A. actinomycetemcomitans* biofilm values. Bar graph shows the mean values ± SD. Statistical analysis was calculated using t-test (n = 7 in triplicate wells).

6.4 eDNA production

In Chapter 5, *S. oralis* eDNA content was reduced after adding neutrophils to a two-day biofilm. The effect of neutrophils on *A. actinomycetemcomitans* eDNA content was investigated to explore potential differences between pathogenic and commensal biofilms.

Figure 6.3 illustrates that there was no change in *A. actinomycetemcomitans* biofilm eDNA content after adding neutrophils. *A. actinomycetemcomitans* had more eDNA content than the commensal bacteria *S. oralis* biofilm. The eDNA content of the biofilm did not change when neutrophils were added.

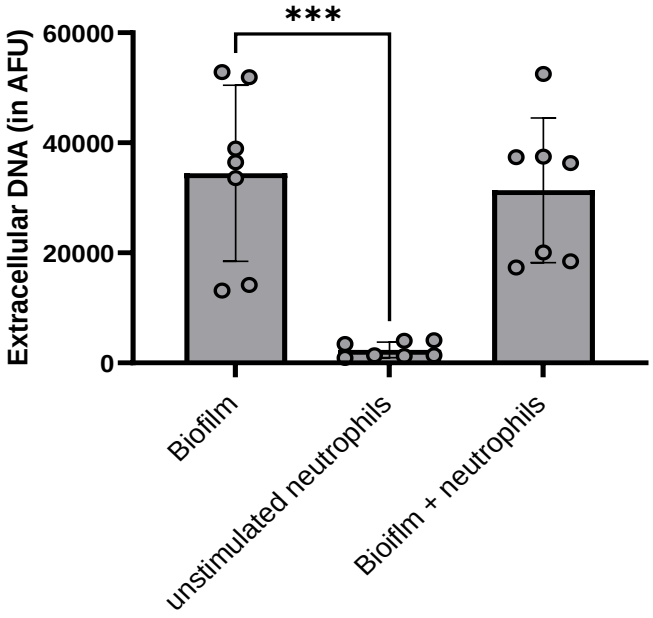

Figure 6.3: Extracellular free DNA quantification of *A. actinomycetemcomitans* biofilms with neutrophils. *A. actinomycetemcomitans* biofilms were cultured for two days then neutrophils were subsequently co-incubated for 2 h (n = 7 in triplicate wells). Bar graph shows the mean values ± SD. Statistical analysis was completed by one-way ANOVA, ***p<0.001. There was no significant difference in DNA production between the neutrophil-treated and non-treated biofilms.

6.5 ROS production

ROS production was measured in biofilm-stimulated neutrophils compared with neutrophils alone and PMA-stimulated neutrophils, as shown in **Figure 6.4**. Within the first 10 min, there was a relatively small increase in total and intracellular ROS production from neutrophils exposed to biofilms, followed by a rapid decrease to baseline levels after approximately 30 min. This was likely due to neutrophil death from LtxA. *A. actinomycetemcomitans* biofilms alone did not produce detectable amounts of ROS.

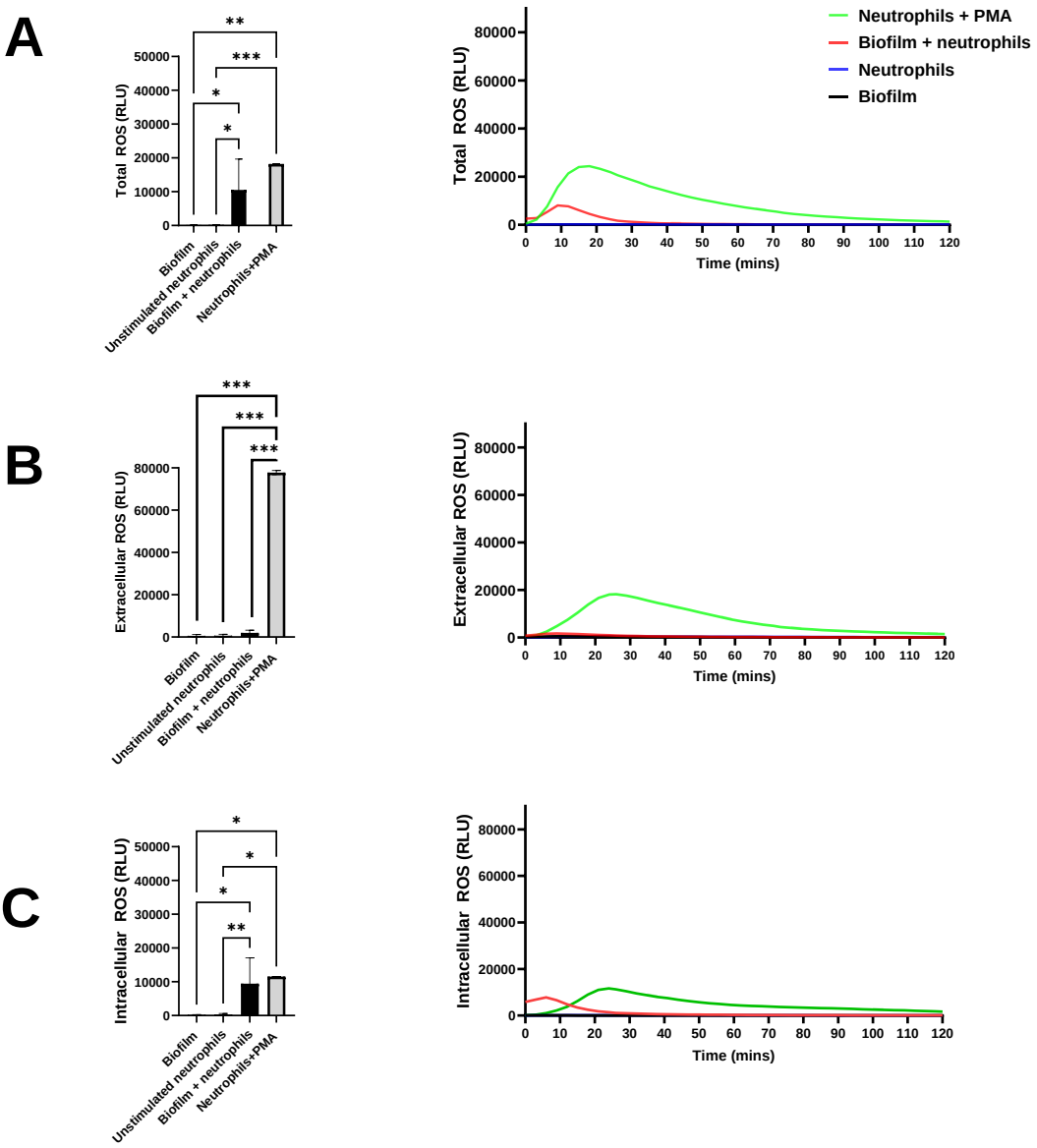

Figure 6.4: Neutrophil ROS release in response to *A. actinomycetemcomitans* two-day biofilms. Enhanced chemiluminescence was measured over 120 min and is shown as relative luminescence units (RLU). A) Total ROS. B) Extracellular ROS. C) Intracellular ROS. Additionally, 50 nM PMA was used as the positive control, and unstimulated neutrophils were used as the negative control (n = 7 in triplicate wells). The bar chart shows peak values, with error bars showing mean values ± SD. Statistical analysis was calculated using one-way ANOVA: *p < 0.05, **p < 0.005 and ***p < 0.001.

6.6 Imaging of *A. actinomycetemcomitans* biofilms after neutrophil exposure

6.6.1 CLSM LIVE/DEAD imaging

The interaction of neutrophils with bacterial biofilms was imaged using a CLSM. After adding neutrophils to the *A. actinomycetemcomitans* biofilm, the biofilm in **Figure 6.5** showed no visual signs of decrease. *S*ome neutrophils appeared in yellow/orange due to transmitting both green and red fluorescence, suggesting dying/dead cells (Stiefel et al., 2015). Neutrophils showed a 96.34 % death rate after incubation with the biofilm for 2 h. The Z-stack images of these biofilms in **Figure 6.6** showed no difference in biofilm thickness.

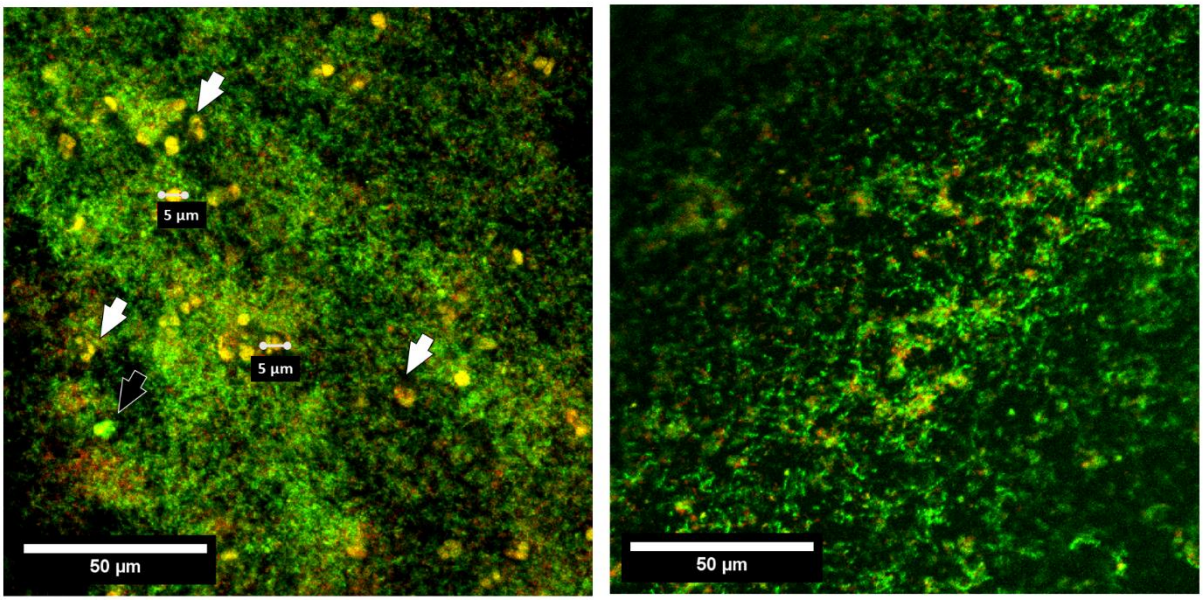

Figure 6.5: Live/Dead CLSM imaging of *A. actinomycetemcomitans* biofilm with neutrophils. *A. actinomycetemcomitans* biofilm was cultured for two days, and neutrophils were added subsequently for 2 h. Biofilms were stained with propidium iodide (PI; red) and SYTO 9 (green). Images are shown at 40x magnification. Left: *A. actinomycetemcomitans* biofilm with neutrophils, showing some neutrophils in yellow (white arrows) and some in green (black arrow). Right: *A. actinomycetemcomitans* biofilm without neutrophils.

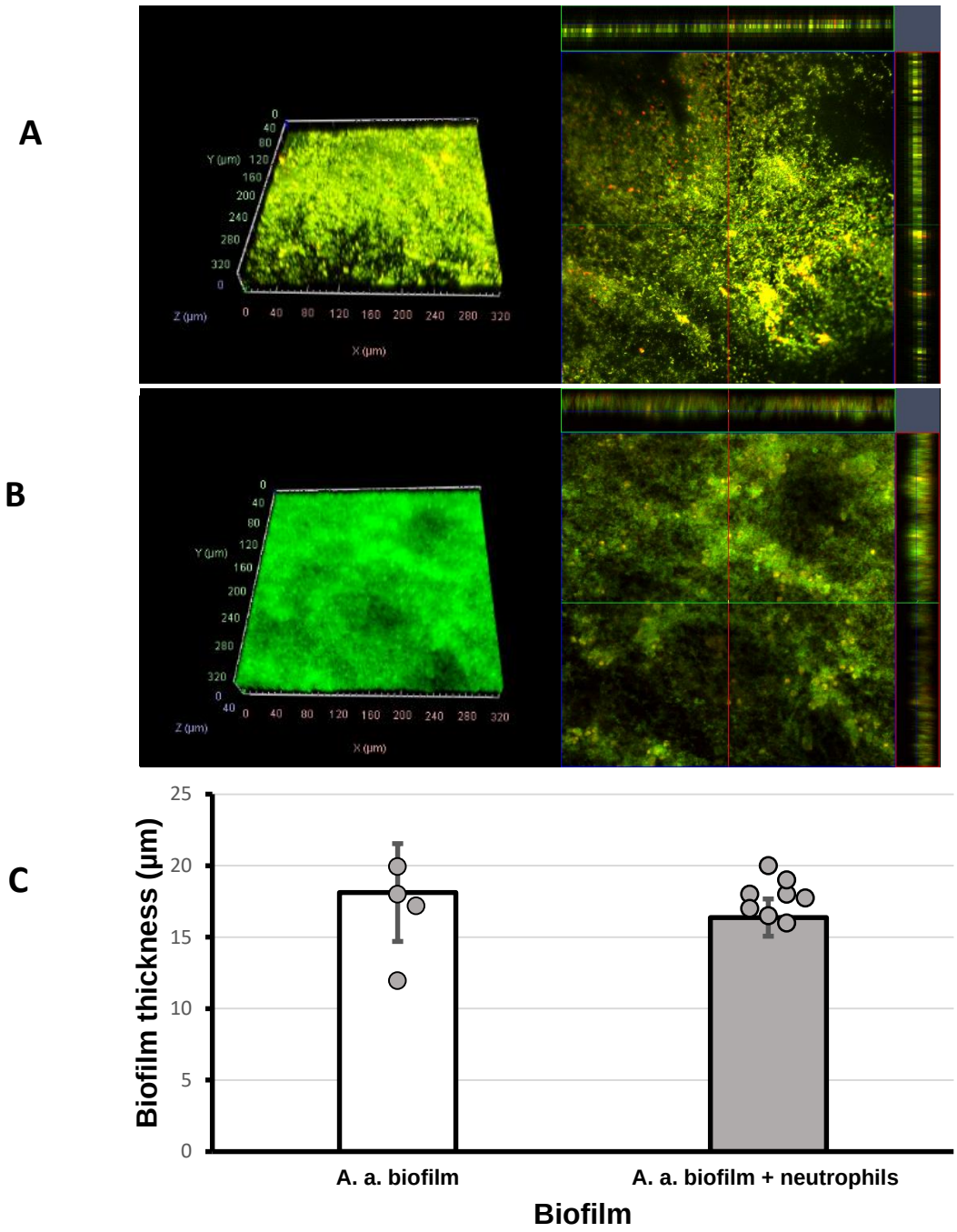

Figure 6.6: *A. actinomycetemcomitans* (*A. a.*) two-day biofilm thickness after incubation with neutrophils using CSLM. (A) ortho-representation of the confocal Z-stacks throughout the entire thickness of single-subspecies biofilms grown on poly-L-lysine-coated 12 mm coverslips. SYTO 9 and PI were used for biofilm fluorescent staining. B) Biofilm Z-stack images after adding neutrophils for 2 h. C) Image quantification of bacterial biofilm thickness. The thickness of the biofilm was calculated based on the intensity of the live/dead staining, with measurements in micrometres. Quantification was performed using Z-stack CLSM images of bacterial biofilm with and without added neutrophils (n = 3). Each biofilm was replicated twice, and two Z-stack images were taken from two sides of the biofilm. No significant difference was found between neutrophil-treated and untreated biofilms. Bar graph show mean values ± SD. Statistical analysis was completed using t-test.

6.6.2 SEM imaging of biofilms and neutrophils

SEM images were captured to characterise the interaction of neutrophils within *A. actinomycetemcomitans* biofilm. The SEM images in **Figure 6.7** show neutrophils embedded in the biofilm matrix, displaying a rounded morphology. The immobilisation and rounding of neutrophils after contact with biofilms has previously been documented (Jesaitis et al., 2003). There was a difference in neutrophil colour when they were exposed to the biofilm. Neutrophils appeared light-grey when imaged separately, and they showed a darker appearance after incubation with the biofilm. Neutrophil-only images showed projections of pseudopodia, facilitating neutrophil surface adherence and migration (Lämmermann and Sixt, 2009). These projections were not observed when neutrophils were embedded in the *A. actinomycetemcomitans* biofilm. Biofilm only images showed channels that were presumed to be water transmitting, which were reported in other biofilm structures (Muchova et al., 2022).

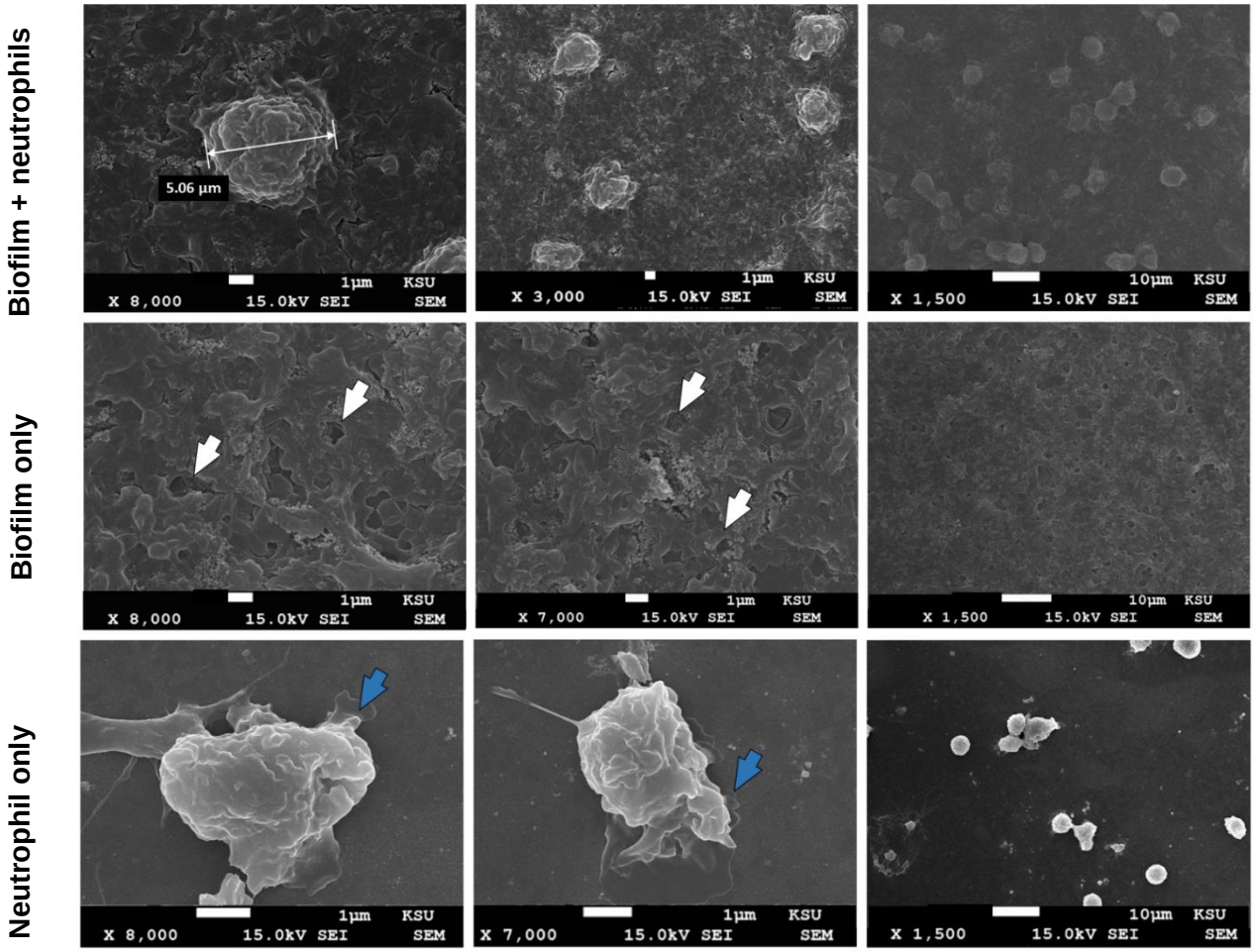

Figure 6.7: SEM images of two-day *A. actinomycetemcomitans* biofilms with neutrophils as well as neutrophil-only controls. White arrows show channels within the biofilm. The blue arrows show neutrophil projections. Magnifications and scale bars are displayed below each image.

6.7 CFU analysis

The quantity of live bacteria in biofilms was estimated using CFU counts. Neutrophil addition did not affect the number of live bacteria when added to the *A. actinomycetemcomitans* biofilm, as shown in **Figure 6.8**.

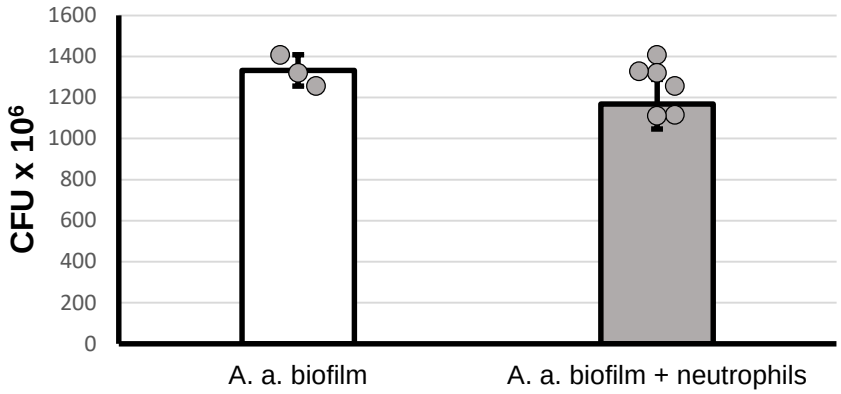

Figure 6.8: *A. actinomycetemcomitans* (*A. a.*) biofilm CFU before and after neutrophil interaction.The *A. actinomycetemcomitans* biofilms were incubated for two days, and neutrophils were added on day 2 of biofilm development and incubated for 2 h. The bar graph shows mean values ± SD; differences were analysed by t-test (n = 6 in triplicate). There was no significant difference in biofilm CFU when neutrophils were added.

6.8 Discussion

Streptococcus spp. and *Actinomyces* spp. dominate the oral health-associated multispecies biofilm, with *S. oralis* dominating the early developmental stage (Hajishengallis, 2015, Jenkinson and Lamont, 2005). In periodontitis, mature biofilms are composed of higher numbers of pathogenic bacteria than is seen in periodontal health, such as *A. actinomycetemcomitans* (Papapanou et al., 2018, Ramos Perfecto et al., 2010). The classification of *A. actinomycetemcomitans* serotype b is based on the composition and structure of its outer membrane LPS (Brígido et al., 2014). In addition, the *A. actinomycetemcomitans* HK 1651 strain is known to exhibit resistance to phagocytosis and production of LtxA, causing leukocyte death (Permpanich et al., 2006). Furthermore, *A. actinomycetemcomitans* eukotoxin promotes MMP release and NET formation in a dose-dependent manner (Claesson et al., 2002, Hirschfeld et al., 2016). Most of the published data relating to *A. actinomycetemcomitans*-neutrophil interactions have used the planktonic form of this bacterium, and minimal information is known regarding the effects of biofilms on neutrophils and vice versa. For this reason, a highly leukotoxic (JP2 genotype) *A. actinomycetemcomitans* HK 1651 biofilm

was used in this study. The interaction of neutrophils with *A. actinomycetemcomitans* biofilms was compared with the findings presented in Chapter 5, where commensal *S. oralis* biofilms were studied.

Adding neutrophils to the *A. actinomycetemcomitans* biofilm had no effect on biofilm biomass, thickness, or eDNA content. ROS production is known to vary with different bacterial stimulations (Pleskova et al., 2023). When ROS was measured, the effect *of A. actinomycetemcomitans* on neutrophils was similar to that of *S. oralis* biofilm data presented in Chapter 5, with increased total and intracellular ROS indicating intracellular activity. However, the onset of the increase and decrease patterns were different. ROS increased and decreased earlier in neutrophil response to *A. actinomycetemcomitans* biofilm with lower intracellular and total peaks. Intracellular ROS response declined after 10 min, which was approximately half the time in which ROS was reduced after interaction with the *S. oralis* biofilm. ROS are an essential component of neutrophil defence against infections. The ability of neutrophils to create ROS decreases as they undergo cell death (Kobayashi et al., 2005). This rapid decrease may be due to LtxA activity causing rapid neutrophil death. LtxA kills neutrophils by binding to leukocyte function antigen-1 on their surface (Lally et al., 1997) subsequently resulting in cell lysis by producing pores in the cell membrane (Chacko and Schmitt, 2023). It has been reported that LtxA concentrations higher than 10 ng/ml induced neutrophil swelling and reduced functionality (Hirschfeld et al., 2016). This supports the findings that the level of LtxA production affects the ability of neutrophils to kill bacteria (Johansson et al., 2000). Although the concentration of LtxA produced by *A. actinomycetemcomitans* biofilm was not measured in this study, the rapid loss of neutrophil function regarding their ROS release suggests that LtxA is produced in high concentrations within the biofilm. In addition, LtxA promotes calcium

influx in immune cells (Fong et al., 2006). This increase in intracellular calcium concentration serves as a signal to activate a variety of cellular processes, including ROS formation, degranulation and chemotaxis (Immler et al., 2018). This activation is evident in low concentration of LtxA, with higher LtxA concentrations, neutrophil loss of functionality and thus reduce ROS (Hirschfeld et al., 2016). This likely explains the rapid reduction in ROS release. For the same reason, no NET production was detected with such a high LtxA concentration.

Notably, neutrophils from healthy donors were used in this study. It has been reported that neutrophils from patients suffering from rapidly progressing forms of periodontitis feature different behaviours (Van Dyke et al., 1982). Periodontitis patients' neutrophils were found to be hyperresponsive to stimuli, and this hyperreactivity can result in the overproduction of inflammatory mediators (Matthews et al., 2007b). Therefore, studying the interaction of periodontitis patients' neutrophils with *A. actinomycetemcomitans* biofilms may yield vital insight into host-pathogen dynamics and potentially identify novel treatment targets to combat this common oral disease.

The biofilm morphology in the SEM images differed from that of *S. oralis* due to the appearance of bacterial cells. *A. actinomycetemcomitans* single cells within the biofilm were not visible, and there was more homogeneity in the texture than in *S. oralis* biofilms. In the *S. oralis* biofilms, the bacteria surrounded the neutrophils. However, in *A. actinomycetemcomitans* biofilms with neutrophils, this bacterial attachment was not evident. It is possible that this lack of single bacterial cell visibility was due to a higher amount of EPS. This is supported by the finding that EPS production decreases in biofilms with patchiness and roughness (Kreft and Wimpenny, 2001). The loss of shape may also be related to sample preparation and dehydration (Alhede et al., 2012). However, sample preparation for SEM followed the same procedure in both biofilm

studies. In addition, neutrophil membrane protrusions were not seen within the biofilms, compared with neutrophils alone. Given the complex and thick structure of bacterial biofilms, it is possible that such neutrophil protrusions or pseudopodia could be rendered invisible. However, it is more likely that this pathogenic biofilm has affected neutrophil integrity and viability. As a result, typical cellular structures of activated neutrophils, such as pseudopodia, would have been disrupted. This is supported by the findings of Hirschfeld et al., as LtxA in high concentration reduces neutrophil migration and functionality (Hirschfeld et al., 2016). Furthermore, changes in material composition can cause variances in electron backscatter or secondary electron emission in SEM imaging, making specific sections of the sample appear lighter or darker (Timischl and Inoue, 2018). Such variations were exhibited in neutrophils after coming into contact with the biofilm as their colour changed from light to dark grey. These colour changes are ascribed to changes in cell density, which could be induced by the impact of LtxA, which leads to cell death (Kelk P, 2009). Cell death can affect neutrophil physical parameters such as density, size, and surface features (Geering and Simon, 2011), and this can be detected under SEM as cell surface morphology changes. SEM scanning, on the other hand, can indicate the consequences of compositional changes on the structure of the cell rather than the compositional changes themselves.

The number of CFUs within the biofilm was not affected by the presence of neutrophils, and neither was the biofilm mass and thickness. This was likely due to neutrophil death due to the action of LtxA, as supported by the previously discussed shortened ROS responses and the 96% dead cells detected in the fluorescent staining. To improve the precision of evaluating the differences in outcomes seen in the interactions of *S. oralis* and *A. actinomycetemcomitans* biofilms with neutrophils, employing consistent assays

with the same neutrophil population would have enhanced the accuracy of the comparisons, a factor that was not addressed in this study.

In conclusion, *A. actinomycetemcomitans* is a key pathogen as it significantly contributes to periodontitis and other systemic disorders. Its capacity to colonise and form biofilms, as well as its virulence factors and interaction with human leukocytes, makes it a relevant target for periodontal research. This pathogenic biofilm exerted high toxicity and impacted neutrophils increasing their death rate, thereby reducing their ROS production. Due to their impaired functionality, neutrophils did not adversely affect the biofilm mass, or the eDNA content as was identified by the *S. oralis* biofilm. These findings can help to shed light on the initial interaction between *A. actinomycetemcomitans* and the innate immune response. Despite advances in understanding its aetiology, many elements of *A. actinomycetemcomitans* involvement in disease remain undiscovered. More research on *A. actinomycetemcomitans* LtxA is needed to determine its action and to develop more effective preventive and treatment techniques.

6.9 Graphical summary

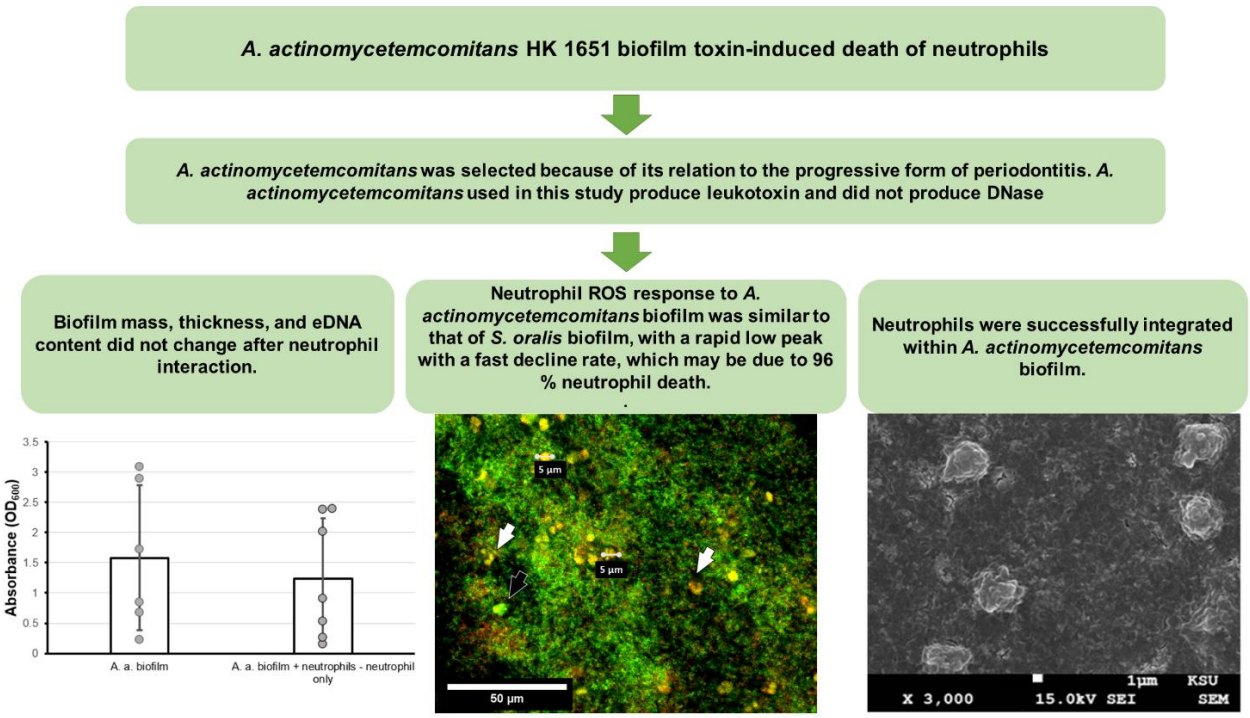

7 CHAPTER SEVEN: Final discussion, study limitations, and future work

7.1 Discussion

This dissertation describes the interactions of neutrophils, a crucial component of the innate immune system, with periodontal biofilm represented by early-colonising streptococci, *S. oralis*, *S. mitis*, and *S. intermedius,* in both single- and mixed-species scenarios. Studies also assessed several models for biofilm formation and evaluated neutrophil retention. Furthermore, analysis of the dynamics between neutrophils and the pathogenic strain *A. actinomycetemcomitans* was reported, comparing outcomes with corresponding findings from the streptococci studied.

7.1.1 The dynamic biofilm models

The evaluated biofilm-culturing methods included two dynamic models (flow cell and flow chamber) and one static model (multiwell plate). The dynamic models were chosen because they effectively simulate the natural conditions and flow of saliva in the oral cavity by allowing for the semi-constant flow of fluids, closely mirroring the physiological environment (Persat et al., 2015). Dynamic systems, which use pumps to imitate saliva or GCF flow, offer a more realistic oral environment than static systems (Blanc et al., 2014, Fernández et al., 2017). They enable the study of shear stress effects on biofilms, continuous nutrient supply, and waste disposal, which better simulates *in vivo* settings (Kim et al., 2016). This arrangement also has an effect on bacterial growth in biofilms, lowering bacterial doubling time and allowing precise control and insights into biofilm development and function in settings more similar to the human mouth.

Notably, the dynamic models were found to be prone to contamination, especially when used with the slow-growing *S. salivarius*; they were less prone to contamination when used with *P. aeruginosa*, a highly adaptable and competitive genus of bacteria

that colonises and dominates various ecological niches (Tuon et al., 2022) (Chapter 3). This bacterium's dynamic nature and fast growth rate made the biofilm less prone to contamination compared with oral bacteria, which was documented using Gram staining, SEM imaging, and fluorescence imaging. Even when combining the three *Streptococcus* species (*S. oralis*, *S. mitis*, and *S. intermedius*) in a multispecies biofilm, their growth rate was relatively slow, and contamination reoccurred (Chapter 4). These bacteria grow slowly, reducing their capacity to compete for space and nutrition. Because faster-growing microorganisms can rapidly colonise available niches and exploit available resources, thereby outcompeting and overwhelming slower-growing microorganisms, these cultures are susceptible to contamination (Yuan et al., 2023). Furthermore, the dynamic model could not fulfil the 5%-CO_2 growth conditions required for *Streptococcus* cultures due to the relatively large and specialised apparatus not fitting within a standard laboratory incubator. The absence of CO_2 in the dynamic models may have contributed to a decrease in competitive conditions for the streptococci, as a CO_2 rich environment has been shown to improve *S. oralis* growth and pathogenicity (Whiley et al., 2015).

The dynamic systems used here also offered some disadvantages despite their susceptibility to contamination. They were, however, more challenging to establish, disinfect, and operate than the static, multiwell system. The complexity of the dynamic systems also made them more vulnerable to defects, such as airlock formation. Furthermore, due to the limited number of separated chambers in the dynamic systems, only a few bacterial species or species combinations could be evaluated in the same experiment, leading to limited replicates and considerable variability.

The flow cell has been playing a prominent role in oral biofilm research. For example, in 2004, Foster and colleagues used the flow cell to test the efficacy of antimicrobials

on *S. gordonii* biofilms (Foster et al., 2004). Later, Foster and Kolenbrander (2004) used the same type of saliva-conditioned flow cell for four-species biofilms and showed that biofilm formation can depend microorganisms forming coaggregates with each other in the planktonic phase (Foster and Kolenbrander, 2004). The flow cell has also been used in studies to test *Streptococcus sanguis* biofilm formation on glass and hydroxyapatite (Elliott et al., 2005). Another study used the flow cell to observe the oral pathogen *Candida albicans* biofilm development in real-time and tested its ability to attach to the flow cell surfaces and develop biomass (McCall and Edgerton, 2017).

In biofilm research, the flow cell terminology has been used to describe any dynamic biofilm growing in small compartments. It only requires a small sample size among flow-fed systems (Luo et al., 2022) and can be imaged during biofilm formation. However, the system's complexity leads to less usage, especially with oral biofilms' slow growth rate as well as nutrient and gas mix requirements. When considering the current literature, few articles were published between 2000 and 2024 examining *S. oralis* biofilm in flow cell devices. Some of these were in-house developed flow cells using glass capillary tubes (Corbin et al., 2011), glass slides (Dorkhan et al., 2012, Dorkhan et al., 2013) or glass coverslip (Periasamy and Kolenbrander, 2010, Periasamy et al., 2009). Ibidi mini flow cells (Boisen et al., 2021, Schlafer et al., 2012) were also used, as well as the University of Denmark flow cell, which was referred to as the flow chamber in this PhD thesis (Wijesinghe et al., 2024). Automated biofilm creation using the Bioflex device (Kristensen et al., 2017) was used in one study in addition to using the Miniature Cell Adhesion Measurement Module (Mini-CAMM) (CARD, University of Bath, UK) in an older study (Saunders and Greenman, 2000). None of these published studies used the flow cell model by Biosurface Technologies applied here. The Biosurface Technologies flow cell model (FC271) device was

successful in culturing pure and reproducible biofilms in many published articles using *P. aeruginosa*, *S. epidermidis, Leuconostoc citreum and Leuconostoc mesenteroides* and *S. aureus* (Boles and Horswill, 2008, Mann, 2010, Yang, 2010, Bernstein et al., 2011, Leathers and Bischoff, 2011, Alkawareek et al., 2012, Miller et al., 2014, Badawy et al., 2015, Nunes et al., 2020). Studies using oral bacteria like *S. mutans* and *S. sobrinus* strains (Leathers et al., 2019) were scarce, and no studies using *S. oralis* in conjunction with this specific device were found. This may be because of the device's design, which contains small compartments, which can increase the liquid pressure and lead to biofilm detachment (Vrouwenvelder et al., 2009). Furthermore, the lack of CO_2 likely negatively impacted the biofilm growth. The flow chamber, which was equipped with larger compartments than the flow cell, supported the 3D structure of the biofilm better, successfully culturing a three-species biofilm. However, contamination occurred, and it was difficult to extract the biofilm for biomass studies. While Wijesinghe and colleagues successfully grew *S. oralis* biofilm in a similar flow chamber, they did not measure the biofilm mass. Their experiments necessitated detaching the device (Wijesinghe et al., 2024), which was challenging to accomplish in the present study. These findings indicate that although the biofilm dynamic model is essential in oral research, the models used in this thesis did not fulfil some essential criteria to support single or multi-species biofilms. Multiple alterations are needed to make these devices functional for slow growing *Streptococcus* species,

Oral biofilms differ from biofilms found elsewhere in the human body because of their specific location, dynamic behaviour, development, and composition (Mosaddad et al., 2019). The oral environment’s complexity makes developing a dynamic model that effectively mimics the semi-constant flow of fluids and the altering supply of nutrients as well as changes in pH and temperature in the oral cavity challenging. The presence

of mechanical stressors (such as chewing and speaking), chemical processes (including enzymatic digestion), and biological elements (such as the presence of microbial flora and host molecules) makes it a complex system to replicate *in vitro* (Darrene and Cecile, 2016). Moreover, salivary-flow rate varies substantially between individuals or even within the same individual under different environmental conditions, with variations of up to 45% in salivary flow rate being considered as normal salivary variation (Ghezzi et al., 2000). Notably, salivary-flow rate varies with age and gender; a younger age is associated with higher flow rates, and men tend to have higher flow rates than women (Fenoll-Palomares et al., 2004). Furthermore, saliva is a complex fluid that contains a wide range of enzymes, proteins, and other components that interact with each other as well as with the oral tissues and the microbial flora. It is challenging to replicate these interactions with precision in a dynamic laboratory model. To address this, some studies have recommended using pooled human saliva as a source of nutrients because it contains certain physical–chemical components and nutrients; compared with artificial media. Biofilms generated in pooled human saliva reportedly better replicate *in vivo* development (Martínez-Hernández et al., 2023, Ahn et al., 2008, Palmer Jr et al., 2001). However, due to the variable composition of saliva, the results of studies that use it can exhibit limited reproducibility (Xu et al., 2019). Some biofilm studies have utilised artificial salvia to eliminate the variability in the composition of natural saliva (Silva et al., 2012, Shellis, 1978, Mei et al., 2013). Artificial saliva was investigated in this thesis; however, it failed to support the survival of neutrophils compared with RPMI + 10% FBS culture media. In addition, it did not support biofilm growth compared to bacteriological culture media. Finally, as this study observed, shear stress can cause bacterial detachment in a dynamic model, especially as *S. oralis* and *S. mitis* have low adhesion forces, ranging from -0.60 to -

0.80 nN; in contrast, single *P. aeruginosa* cells were able to adhere at up to 3 nN of force on glass in a previous study (Wessel et al., 2014, Cooley et al., 2013).

Compared with the static biofilms, the dynamic biofilm models exhibited low levels of neutrophil attachment, which was likely due to the shear stress. The retention of neutrophils in the biofilm was documented using H&E staining, SEM imaging, and fluorescence imaging (Chapters 3 and 4). Neutrophils were found to have a stronger tendency to attach to the *P. aeruginosa* biofilm than to the tested *Streptococcus* biofilms, which is attributed to the components of the *P.aerugniosa* biofilm EPS that can have adhesive properties that increase the likelihood of PMNs sticking to the biofilm (Rybtke et al., 2020). This correlated with previous findings that neutrophil attachment to biofilms depends upon their composition (Shapira et al., 2000). Our study also revealed that the dynamic model had a greater tendency to develop crystal formations, which interfered with the fluorescent staining. Researchers using a dynamic model to analyse the oral environment should be aware of these limitations. However, these limitations also indicate avenues for further research and technology development that could improve the accuracy and applicability of these biomimetic models.

7.1.2 The three-species biofilm

The oral "yellow complex" members *S. oralis*, *S. mitis*, and *S. intermedius* were chosen as early colonisers, and their formation of a three-species biofilm, interaction with each other, and interaction with neutrophils were examined. In complex multispecies communities, the response of a single-species can be influenced by other species in the community, resulting in behavioural changes dissimilar to those that occur in the corresponding single-species environments (Elias and Banin, 2012, Sadiq et al.,

2021). Indeed, *S. oralis* was reported to have limited biofilm-forming abilities because it lacked certain colonisation factors, such as mannose-sensitive hemagglutination pili and type IV pili, that would have allowed it to adhere to abiotic surfaces (Loo et al., 2000). Its contribution to plaque formation and early colonisation was attributable to its capacity to cooperatively interact with other bacteria, such as *S. gordonii* and *Actinomyces oris* in previous studies (Loo et al., 2000, Choo et al., 2021, Palmer Jr et al., 2001). However, in our study, *S. oralis* formed the highest biofilm biomass and produced the highest eDNA content among the three species. Combining *S. oralis* with *S. mitis* and *S. intermedius* did not enhance biofilm mass and had a negative impact on growth. The outcomes of combining *S. oralis* with other species in a biofilm depend on the type of species and environmental factors applied. For example, *S. oralis* was found to cooperate with *P. aeruginosa* effectively by stimulating its virulence-factor production aerobically, whereas, in an atmosphere containing added CO_2, *S. oralis* became a competitor that antagonised *P. aeruginosa* growth through H_2O_2 production, significantly altering the biofilm population dynamics and appearance (Whiley et al., 2015). Furthermore, Whiley et al. (2015) reported that H_2O_2 production significantly increased with elevated CO_2 levels during incubation, whereas CFU decreased. This indicates that environmental factors play a key role in organism behaviour and indicates why *in vitro* findings may differ from *in vivo* conditions. In the oral cavity, *S. oralis* has a synergistic relationship with *C. albicans*: *S. oralis* increases the pathogenicity of *C. albicans*, and *C. albicans* stimulates the production of *S. oralis* biofilms (Xu et al., 2017). In contrast, when *S. oralis* is co-cultured with *S. mutans*, *S. oralis* antagonises *S. mutans,* leading to decreased biofilm biomass compared to the *S. mutans* single-species biofilm (Thurnheer and Belibasakis, 2018). These findings indicate that the contribution of *S. oralis* to a multispecies biofilm is circumstantial and

depends on the tested parameter. In our research, *S. oralis* had a strong capability for biofilm production, which contradicts prior literature that claimed a more moderate or variable biofilm-forming ability (Coraça-Huber et al., 2020, Moscoso et al., 2006). *S. oralis* biofilm forming capabilities have been supported by research. For example, Palmer et al. (2001) reported that *S. oralis* can form biofilms under particular conditions and identified core genes involved in biofilm production (Palmer et al., 2001). Other findings reported that *S. oralis* can enhance biofilm formation when mixed with other species (Souza et al., 2020). This supports the hypothesis that given the correct conditions, *S. oralis* might be an effective biofilm forming, as demonstrated in our study. Our findings revealed that *S. oralis* provided the majority of the three-species biofilm's mass. This was determined by comparing the mass of the three-species biofilm to that of the *S. oralis* biofilm. The *S. oralis* biofilm not only developed more biomass and produced higher levels of eDNA than the *S. mitis* and *S. intermedius* biofilms but also did not produce any DNA-restriction enzymes, which can potentially cleave DNA, including NETs. In light of these findings, *S. oralis* was selected for further experimentation.

7.1.3 Interplay between neutrophils and oral early colonisers

Neutrophils were cultured with the single-species and three-species biofilms of the selected *Streptococcus* strains to investigate the reciprocal effects between these innate immune cells and the *in vitro* oral biofilms. Using immunofluorescently labelled anti-citrullinated histones, the three-species and *S. oralis* biofilms were found to induce NET formation (Chapters 4 and 5). In addition, neutrophils exhibited increased intracellular ROS in response to the *S. oralis* biofilms, which correlates with the published findings that *S. oralis* biofilm induces a 2-fold ROS increase while other

commensal oral bacteria have no effect (Oveisi et al., 2019, Xu et al., 2014). This increase was not detected with the planktonic bacteria published earlier (Hirschfeld et al., 2017). These results are consistent with previous findings demonstrating that neutrophils exhibit differential responses to planktonic versus biofilm-grown bacteria, and biofilm-associated bacteria exhibit enhanced capabilities to evade host defences compared to their planktonic form (McLaughlin and Hoogewerf, 2006). Oveisi and colleagues proved that specific oral commensal bacteria activate neutrophils as part of a healthy innate immune response by showing that *S. oralis* biofilm upregulates some neutrophil surface receptors and increases Nrf2 production (Oveisi et al., 2019). These findings demonstrate that *S. oralis* biofilm not only activates neutrophil oxidative burst but also inhibits ROS destructive damage by inducing Nrf2. The latter promotes an antioxidant pathway in neutrophils, facilitating neutrophil survival in the oral cavity. Thus, neutrophils may exhibit a proinflammatory response towards *S. oralis* biofilms without causing excessive inflammation (Fine et al., 2016).

One could hypothesise that because these streptococci are commensals, neutrophils do not perceive them as invaders or pathogens and do not interact with them during the biofilm's early colonising state. However, the current findings showed that neutrophils did interact with the commensal biofilm. This reduced reaction *in vivo* could be attributed to other factors, such as the lack of neutrophil recruitment. For example, streptolysin O, which inhibits neutrophil chemotaxis, is produced by *S. pyogenes* (Lin et al., 2009). Although the streptococci this study investigated are not known to generate streptolysin, these species are reported to suppress epithelial IL-8 production, which in turn can reduce neutrophil recruitment (Myers et al., 2021). Furthermore, some strains of *S. oralis* and *S. sanguinis* generate H_2O_2, which promotes cell death and decreases responsiveness in neutrophils (Sumioka et al.,

2017). Collectively, these findings suggest that oral streptococci may have evolved strategies *in vivo* to decrease neutrophil recruitment and promote their survival.

Adding neutrophils to the three-species and single-species *S. oralis* biofilms resulted in a transient biomass reduction. This reduction was consistent with previous findings for *S. aureus* biofilms reporting transient biofilm breakdown after 15 min of biofilm-neutrophils reaction (Chebotar et al., 2012). Nevertheless, this reduction in biofilm mass was not reported with *P. aeruginosa* biofilms, where neutrophils were reported to enhance early biofilm formation (Walker et al., 2005, Parks et al., 2009). Biofilm enhancement was attributed to the incorporation of neutrophil DNA into the bacterial biofilm (Walker et al., 2005). This study's data revealed that neutrophils decreased biofilm mass during early and late stages of biofilm development. However, isolated NETs did not affect the biofilm mass, which is inconsistent with Walker's findings. Although neutrophils were found to decrease the biofilm mass, SEM imaging provided evidence that the biofilm overgrew neutrophils by forming a bacterial coating around them (Chapter 5). This bacterial "coating" may immobilise neutrophils and shield the biofilm from their antibacterial activity. Although immobilisation of neutrophils has been observed in *P. aeruginosa* biofilms, it was attributed to the increased alginate EPS component and the emergence of the mucoid phenotype in CF patients, which exacerbates the clinical prognosis (Jesaitis et al., 2003, Hänsch, 2012). Because of the variations in the nature of commensal streptococci and pathogenic *P. aeruginosa*, these differences in response to the neutrophil effect may be attributable to the virulence of the pathogenic strain. In this study, it is possible that an inhibition of some neutrophil functions may have failed to halt neutrophils from decreasing the biofilm mass. This raises an important question: If neutrophils can affect oral biofilms *in vitro*, why is their capacity reduced *in vivo*?

The oral cavity is a complex environment containing saliva, GCF, and tissue barriers that can affect neutrophils' capacity to access and combat *Streptococcus* biofilms. These conditions cannot easily be replicated *in vitro*. Furthermore, the *in vivo* oral biofilm comprises a diverse microbial community. These microorganisms can cooperate to boost their collective resistance against neutrophil attack. The three *Streptococcus* species examined in this study do not entirely represent oral complexity. Furthermore, neutrophils respond to oral biofilms in a species-specific manner (Mikolai et al., 2020, Oveisi et al., 2019). This indicates that different microbial combinations, in turn, may alter neutrophil responses, demonstrating the complicated nature of neutrophil interactions with the oral biofilm.

7.1.4 Interactions between neutrophils and biofilm eDNA

A reduction in the biofilm eDNA content accompanied the decrease in biofilm mass (Chapters 4 and 5). The decrease in eDNA was measured using the SYTOX Green assay, which detects the presence of eDNA in the samples as it exhibits enhanced fluorescence upon binding to DNA (Thakur et al., 2015). In its molecular sequence, eDNA is indistinguishable from chromosomal DNA (Böckelmann et al., 2006, Steinberger and Holden, 2005); hence, SYTOX Green staining cannot distinguish between different DNA origins. This lack of specificity is a disadvantage in research attempting to distinguish between bacterial eDNA and NET-produced DNA, both of which are present as extracellular DNA in biofilms. Because NETs may contribute to the total eDNA measured by this assay, the extent of the biofilm's eDNA loss may be greater than what this study determined. The assessment of DNA origin within oral biofilms EPS can be done by combining fluorescent labelling of double-stranded DNA with techniques such as fluorescence in situ hybridization (FISH), which allows for

specific labelling of citrullinated histones using fluorescent probes. This Combinatorial Labelling and Spectral Imaging-FISH (CLASI-FISH) have been successfully used in the literature to investigate the spatial distribution of organisms in dental plaque samples (Welch et al., 2016). Integrating these microscopy techniques could help identify the source and dynamics of eDNA release in multispecies communities.

The results of this study suggest neutrophils' ability to disassemble biofilms by reducing their eDNA content. Further research needs to be undertaken to confirm and explain this mechanism, as it may reveal novel approaches to target biofilms and neutrophils therapeutically.

7.1.5 Effect of neutrophils on *S. oralis* biofilm CFU

Conversely, neutrophils were found to increase *S. oralis* biofilm's CFU (Chapter 6). This increase may be attributable to the improved nutrient infiltration into the biofilm due to EPS breakdown, which led to a higher growth rate. Depending on the host, the nutrient supplies of oral bacteria alternate between ‘’feast and famine’’. When the host ingests food, the nutrition supply available to bacteria in the oral cavity is more abundant (feast); however, this occurs for a much shorter period of time than when the host takes no new nutrients (famine). This lack of nutrients causes bacteria in the oral biofilms to enter a slow-growing state (Chávez de Paz et al., 2008). These bacteria may regain their metabolic activity and ability to grow once they are released from the biofilm and, therefore, have improved access to nutrients (Socranksy and Haffajee, 2002). The possible ability of neutrophils to degenerate the biofilm and introduce more nutrients into it may explain the increase in the number of live cells in the biofilm after interaction with neutrophils. In addition, the biofilm contains metabolically inactive non-dividing persister cells, which are genetically identical to the remainder of the bacterial

population of their species. These cells are understood to be responsible for re-seeding biofilms in clinical settings after antibiotic treatment is discontinued (Lewis, 2012). In fact, the *P. aeruginosa* biofilm was found to consume six to eight times more oxygen after encountering neutrophils than before (Jesaitis et al., 2003). This increase in oxygen consumption indicates an increase in metabolic activities, including growth and replication (Riedel et al., 2013). Furthermore, another study found that neutrophils increased *P. aeruginosa* biofilm CFUs (Kaya et al., 2020). The CFU increase was interpreted by Kaya and colleagues as an indication of biofilm enhancement. It should be noted, however, that the researchers did not quantify the biofilm mass throughout their analysis. The absence of this metric prevents a complete understanding of the biofilm dynamics, and further study, including biofilm mass measurement, is required to validate or refine the conclusions proposed.

When biofilms are disturbed, the contained bacteria move from a protected to a more vulnerable planktonic condition, as demonstrated by a CFU increase. This may imply an increased susceptibility to antimicrobial drugs, which could be utilised in clinical settings. Treatment methods may include biofilm destabilisation followed by antibiotic delivery for more successful pathogen eradication. Furthermore, the kinetics of a CFU increase can improve the precision with which therapeutic interventions are timed, enabling the strategic administration of antimicrobials to coincide with the period when bacteria are most vulnerable. This knowledge also supports the optimisation of dosage tactics, ensuring the use of drug concentrations appropriate for attacking the now-susceptible bacteria.

7.1.6 Interactions between neutrophils and *A. actinomycetemcomitans* biofilm.

The present study further introduced an *A. actinomycetemcomitans* biofilm because this bacterium is associated with rapidly progressing forms of periodontitis (Chapter 6) (Fine et al., 2007). The *A. actinomycetemcomitans* 1561 strain used in this study is known to induce NET formation in response to planktonic bacteria (Hirschfeld et al., 2016). Neutrophils died rapidly after exposure to the biofilm form of the bacterium. While neutrophils broke down the commensal streptococcal biofilms studied here, they failed to combat *A. actinomycetemcomitans* biofilms. In view of the virulent nature of the bacterium, this was expected. There was no change in biofilm mass, thickness, or eDNA content after neutrophil engagement. At the neutrophil level, a slight activity in intracellular ROS rapidly decreased and this was attributed to the increased production of LtxA toxin in the biofilm and, therefore, rapid neutrophil death. The low ROS levels could also be attributed to *A. actinomycetemcomitans'* other virulence factors that protect the overall bacterial community. For example, *A. actinomycetemcomitans* expresses SOD, which catalyses the dismutation of superoxides into H_2O_2, producing molecular oxygen and leading to the poor performance of ROS against specific oral diseases (Balashova et al., 2007). In addition, in a study comparing neutrophil responses to the non-leukotoxic *A. actinomycetemcomitans* 275253 strain and LtxA-producing *A. actinomycetemcomitans* JP2 clone, researchers showed that neutrophils from patients infected with the leukotoxic strain produced lower levels of ROS and cytokines, indicating a subdued immune response which is consistent with our findings (Hashai et al., 2022). In fact, the study observed that neutrophils from periodontally healthy individuals are more resistant to necrosis when infected with the planktonic leukotoxic strain. Although we did not test for neutrophil necrosis or leukotoxin concentrations in our study, neutrophil death within 2 h suggests that *in vivo*, neutrophil

death may be dependent upon the abundance of leukotoxic *A. actinomycetemcomitans* within the biofilm.

Furthermore, in a study by Mikolai and colleagues, leukotoxic *A. actinomycetemcomitans* biofilms did not induce NET formation, ROS production, and secretion of MMP-8 and MMP-9 in neutrophils. This corresponds with our findings that *A. actinomycetemcomitans* biofilm did not induce high levels of antimicrobial factors in neutrophils (Mikolai et al., 2020).

On the other hand, some studies have reported that various *A. actinomycetemcomitans* strains can induce a neutrophil response; examples include *A. actinomycetemcomitans* 652 serotype c, where planktonic bacteria can promote azurophilic granule exocytosis by neutrophils as an epinephrine source to provide iron and promote bacterial survival (Ozuna et al., 2021). Another study reported that planktonic *A. actinomycetemcomitans* (SUNY465) increased CD64 to a greater extent than the biofilm form (Oveisi et al., 2019). These responses were not observed in this study using leukotoxic strain biofilms, as neutrophils died rapidly, which highlights the findings that neutrophils respond differentially to planktonic and biofilm-grown bacteria and that the latter may evade host defences more than planktonic bacteria (McLaughlin and Hoogewerf, 2006).

Understanding how *A. actinomycetemcomitans* interact with neutrophils could lead to the development of therapeutics that target the unique components of the pathogen's virulence and thus enable more successful regimens for those colonised with the bacterium and with periodontal disease.

7.1.7 Closing remarks

When neutrophils reach single- or mixed-species biofilms *in vitro*, a dynamic interplay occurs at the microscopic and molecular levels. Neutrophils attempt to penetrate the biofilm's EPS, attaching to its surface and producing ROS to disturb and kill the embedded bacteria and possibly produce NETs to trap and kill the bacteria. The biofilm's mass and eDNA decreased while the number of living bacterial cells within the biofilm increased. The biofilm responded by covering the neutrophils embedded in its matrix, reducing their activity. The pH environment of the biofilm can modify the efficacy of these responses, affecting neutrophilic enzyme activity and the overall immune response. Mixed-species biofilms have more complex interactions due to interspecies communication and the possibility of diverse immune evasion tactics. Translating these findings to *in vivo* conditions, however, requires considering additional aspects such as host tissue features, the presence of serum proteins, and the more complex immune system dynamics, all of which can influence both the biofilm's resilience and the neutrophil's efficiency.

7.2 Limitations of this study and future Recommendations

Based on the guidelines developed in Ramachandra' s 2023 review, this study has used all the qualitative methods recommended for biofilm-assessment studies, including live–dead imaging using confocal and scanning electron microscopy (Ramachandra et al., 2023). For quantitative biofilm assessment, CV assay and CFU analyses were performed. The analysis of changes in biofilm metabolic activity was undertaken using pH measurement instead of 2,3-bis-(2-methoxy-4-nitro-5-sulfophenyl)-2H-tetrazolium-5-carboxanilide inner salt (XTT) assay (Xu et al., 2016) as recommended in the review. The assessment of biofilm DNA content was performed

using the SYTOX green assay. In addition to these tests, an assessment of the effect of the biofilm on neutrophil ROS and ROS production was performed using chemiluminescence, including intracellular-, extracellular-, and total-ROS analyses (Chapters 5 and 6). No genetic evaluation of the expression of biofilm-forming core genes was done.

This study failed to distinguish the multispecies and their contribution to the biofilm using MALDI-TOF and WGS. The FISH approach can be used by employing fluorescently labelled probes that attach to specific DNA sequences, enabling the visualisation of several bacterial species inside the biofilm structure under a microscope.

In this investigation, non-stimulated neutrophils were used as a negative control. In the measurement of extracellular DNA, it may be possible to quantify the exact effect of neutrophils on eDNA if neutrophils are also stimulated in a negative control and subtracting the NET values from the eDNA content. As has been demonstrated, neutrophils produce NETs when stimulated. This stimulation could be performed using biofilm supernatant. In addition, neutrophils were assessed for their nuclease activity under unstimulated conditions but not after stimulation. Furthermore, although neutrophils were obtained from systemically healthy donors, these may have been affected by periodontal inflammation, and this may have influenced their neutrophil (re-)activity (Matthews et al., 2007a).

During the growth curve experiments, the conditions were not optimal due to the plate reader's absence of a CO_2 source. This deviation from ideal growth conditions likely impacted the results of the growth curves. Furthermore, the positive controls did not induce the expected effects on neutrophils in specific assays, including the NET formation and ELISA assay. This may be due to several factors, including degradation,

mainly since HOCl is highly unstable and sensitive to environmental conditions like light, heat, and pH (Parker and Winterbourn, 2012). Additionally, the health and source of neutrophils also play crucial roles; variability in cell viability and donor differences can significantly impact results (Duarte et al., 2019). These factors contribute to the occasional failure of PMA and HOCl to elicit expected responses in neutrophil studies and could have influenced the reliability and interpretation of the assay outcomes.

7.2.1 Future directions

Although discontinued, the dynamic model optimisation utilised in this research provides a foundation for further experiments using this approach. Modifying experimental circumstances can improve it to better replicate human oral environmental factors, such as adding a CO_2 pump to the system, which could positively impact upon bacterial growth, as well as including salivary components like mucins to the growth medium. Furthermore, the experimental setup could be modified so that the flow of nutrients is reduced overnight to imitate the natural drop in salivary flow that occurs during sleep. By reducing the flow rate, biofilms may be able to form under lower shear stress conditions. In addition, using substrates covered with salivary pellicle may provide a more accurate surface for biofilm formation, closely imitating the natural oral cavity and potentially modifying biofilm development and its response to neutrophil activity. These modifications will likely yield more clinically pertinent data and enhance the model's predictive validity.

A comprehensive experimental strategy should be utilised to resolve the inconsistencies in experimental setups, in order to improve comparability of data from different bacterial species and biofilm compositions. To clarify the effects of timing and concentration of neutrophils on *S. oralis* biofilms, a sequential and dose-dependent

study can be performed by subjecting the biofilm to different concentrations of neutrophils at various stages of their growth. Using this approach could identify the crucial periods when neutrophil involvement is most efficacious in disturbing biofilm formations.

The observed decrease in biofilm mass should be examined further using other multispecies biofilms from different Socransky complexes and monitoring variations in EPS using fluorescently labelled lectins that bind specifically to its components and can be monitored under a confocal microscope. Real-time biofilm monitoring using optical coherence tomography (OCT), CLSM, or Electrochemical Impedance Spectroscopy (EIS), which measures changes in biofilm thickness, density, and viability. These technologies outperform classic staining and plating processes by enabling non-invasive, real-time continuous analysis and monitoring of biofilm architecture and dynamics in response to neutrophil-induced stress.

In addition, the effect of neutrophils on biofilm CFU can be further studied by blocking different neutrophil receptors and examining the effect on the biofilm CFU. Using other oral bacteria to examine this phenomenon could provide insight into how neutrophils interplay with oral biofilms and may identify areas for treatment development.

Furthermore, future research could investigate how eDNA levels decrease in *S. oralis* biofilms following interaction with neutrophils by treating the biofilm with DNase before and after the introduction of neutrophils to determine whether decreasing eDNA affects biofilm integrity differently in the presence of neutrophils. In addition, chemical methods could be employed to deplete neutrophils of granule contents to investigate changes in biofilm disruption efficacy.

Distinguishing NETs from eDNA using fluorescent markers can aid in understanding the role of NETs in the biofilm. To dive deeper into the mechanisms behind neutrophil

binding or ingestion of bacterial eDNA, identifying individual receptors and signalling cascades will be crucial. Mechanisms such as receptor-blocking approaches with antibodies or chemical inhibitors could be used to evaluate their function in eDNA detection, binding and possible uptake. These approaches will allow for a more comprehensive understanding of the biological mechanisms by which neutrophils interact with bacterial eDNA, potentially revealing new therapeutic targets for modifying immune responses in infectious diseases.

The results from the *A. actinomycetemcomitans* biofilm experiments could be further investigated by comparing them to low leukotoxic strains of *A. actinomycetemcomitans* or to other periodontal pathogens. Also, the concentration of leukotoxin in both *in vitro* and *in vivo* biofilms could be compared, and dose-dependent neutrophil responses be assessed. Understanding *A. actinomycetemcomitans*-containing biofilms and related immune responses is critical for developing periodontal therapies for affected patients.

7.3 Other work undertaken during the PhD

1. The author participated in the "three-minute thesis" competition at UoB and was nominated for the finals.

2. The author won first place in the "three minutes thesis" competition at King Saud bin Abdulaziz University for Health Sciences, Riyadh, Saudi Arabia.

3. The author participated in the following published studies:

- ABDULLATIF, F. A., **ALMAARIK, B**. & AL-ASKAR, M. 2022. Resolvin E1's antimicrobial potential against *Aggregatibacter actinomycetemcomitans*. *Front Oral Health*, 3 :875047.

- ABUDAWOOD, M., TABASSUM, H., **ALMAARIK, B.** & ALJOHI, A. 2020. Interrelationship between oxidative stress, DNA damage and cancer risk in diabetes (type 2) in Riyadh, KSA. *Saudi J Biol Sci*, 27, 177-183.
- ALJAZAIRY, E. A. A., AL-MUSHARAF, S., ABUDAWOOD, M., **ALMAARIK, B.**, HUSSAIN, S. D., ALNAAMI, A. M., SABICO, S., AL-DAGHRI, N. M., CLERICI, M. & ALJURAIBAN, G. S. 2022. Influence of adiposity on the gut microbiota composition of Arab women: A case-control study. *Biology*, 11, 1586.
- ALRASHOUDI, R. H., ABUDAWOOD, M., MATEEN, A., TABASSUM, H., ALGHUMLAS, N. I., FATIMA, S., **ALMAARIK, B.**, MAQSOOD, F., AL MUSAYEIB, N. M. & AMINA, M. 2023. Characterisation and antimicrobial, antioxidant, and anti-proliferative activities of green synthesised magnesium oxide nanoparticles with shoot extracts of *Plicosepalus curviflorus*. *Asian Pac J Trop Biomed*, 13, 315-324.
- ANSAR, S., TABASSUM, H., ALADWAN, N., ALI, M., **ALMAARIK, B**., ALMAHROUQI, S., ABUDAWOOD, M., BANU, N. & ALSUBKI, R. **2020**. Eco-friendly silver nanoparticles synthesis by *Brassica oleracea* and its antibacterial, anticancer and antioxidant properties. *Sci Rep*, 10, 18564.

8 References

ABRAHAM, N. M. & JEFFERSON, K. K. 2010. A low molecular weight component of serum inhibits biofilm formation in *Staphylococcus aureus*. *Microb Pathog,* 49**,** 388-91.

ABRANCHES, J., ZENG, L., KAJFASZ, J. K., PALMER, S. R., CHAKRABORTY, B., WEN, Z. T., RICHARDS, V. P., BRADY, L. J. & LEMOS, J. A. 2018. Biology of oral streptococci. *Microbiol Spectr,* 6.

AHN, S.-J., WEN, Z. T., BRADY, L. J. & BURNE, R. A. 2008. Characteristics of Biofilm Formation by *Streptococcus mutans* in the Presence of Saliva. *Infect Immun,* 76**,** 4259-4268.

AKIRA, S., UEMATSU, S. & TAKEUCHI, O. 2006. Pathogen recognition and innate immunity. *Cell,* 124**,** 783-801.

ALHEDE, M., KRAGH, K. N., QVORTRUP, K., ALLESEN-HOLM, M., VAN GENNIP, M., CHRISTENSEN, L. D., JENSEN, P. Ø., NIELSEN, A. K., PARSEK, M., WOZNIAK, D., MOLIN, S., TOLKER-NIELSEN, T., HØIBY, N., GIVSKOV, M. & BJARNSHOLT, T. 2011. Phenotypes of Non-Attached *Pseudomonas aeruginosa* Aggregates Resemble Surface Attached Biofilm. *PLOS ONE,* 6**,** e27943.

ALHEDE, M., QVORTRUP, K., LIEBRECHTS, R., HØIBY, N., GIVSKOV, M. & BJARNSHOLT, T. 2012. Combination of microscopic techniques reveals a comprehensive visual impression of biofilm structure and composition. *FEMS Immunol Med Microbiol,* 65**,** 335-42.

ALKAWAREEK, M. Y., ALGWARI, Q. T., LAVERTY, G., GORMAN, S. P., GRAHAM, W. G., O'CONNELL, D. & GILMORE, B. F. 2012. Eradication of *Pseudomonas aeruginosa* biofilms by atmospheric pressure non-thermal plasma. *PLOS One,* 7**,** e44289.

ALLAN, J., FRASER, R. M., OWEN-HUGHES, T. & KESZENMAN-PEREYRA, D. 2012. Micrococcal nuclease does not substantially bias nucleosome mapping. *J Mol Biol,* 417**,** 152-64.

ALLESEN-HOLM, M., BARKEN, K. B., YANG, L., KLAUSEN, M., WEBB, J. S., KJELLEBERG, S., MOLIN, S., GIVSKOV, M. & TOLKER-NIELSEN, T. 2006. A characterisation of DNA release in *Pseudomonas aeruginosa* cultures and biofilms. *Mol Microbiol,* 59**,** 1114-28.

ALUGUPALLI, K., KALFAS, S. & FORSGREN, A. 1996. Laminin binding to a heat-modifiable outer membrane protein of *Actinobacillus actinomycetemcomitans*. *Oral Microbiol Immunol,* 11**,** 326-331.

ALVAREZ, M. E., FUXMAN BASS, J. I., GEFFNER, J. R., FERNÁNDEZ CALOTTI, P. X., COSTAS, M., COSO, O. A., GAMBERALE, R., VERMEULEN, M. E., SALAMONE, G., MARTINEZ, D., TANOS, T. & TREVANI, A. S. 2006. Neutrophil signaling pathways activated by bacterial DNA stimulation. *J Immunol,* 177**,** 4037-46.

AMULIC, B., CAZALET, C., HAYES, G. L., METZLER, K. D. & ZYCHLINSKY, A. 2012. Neutrophil function: from mechanisms to disease. *Annu Rev Immunol,* 30**,** 459-489.

ANDERSON, J. M., RODRIGUEZ, A. & CHANG, D. T. 2008. Foreign body reaction to biomaterials. *Semin Immunol,* 20**,** 86-100.

ANGELETTI, S., DICUONZO, G., AVOLA, A., CREA, F., DEDEJ, E., VAILATI, F., FARINA, C. & DE FLORIO, L. 2015. Viridans group streptococci clinical isolates: MALDI-TOF mass spectrometry versus gene sequence-based identification. *PLoS One,* 10**,** e0120502.

ANNOUS, B. A., FRATAMICO, P. M. & SMITH, J. L. 2009. Scientific status summary: quorum sensing in biofilms: why bacteria behave the way they do. *J Food Sci,* 74**,** R24-R37.

APARNA, M. S. & YADAV, S. 2008. Biofilms: microbes and disease. *Braz J Infect Dis,* 12.

ARAI, Y., NISHINAKA, Y., ARAI, T., MORITA, M., MIZUGISHI, K., ADACHI, S., TAKAORI-KONDO, A., WATANABE, T. & YAMASHITA, K. 2014. Uric acid induces NADPH oxidase-independent neutrophil extracellular trap formation. *Biochem Biophys Res Commun,* 443**,** 556-561.

ARBIQUE, J. C., POYART, C., TRIEU-CUOT, P., QUESNE, G., CARVALHO, M. D. G. S., STEIGERWALT, A. G., MOREY, R. E., JACKSON, D., DAVIDSON, R. J. & FACKLAM, R. R. 2004. Accuracy of phenotypic and genotypic testing for identification of *Streptococcus pneumoniae* and description of *Streptococcus pseudopneumoniae* sp. nov. *J Clin Microbiol,* 42**,** 4686-4696.

ARMSTRONG, D. S., HOOK, S. M., JAMSEN, K. M., NIXON, G. M., CARZINO, R., CARLIN, J. B., ROBERTSON, C. F. & GRIMWOOD, K. 2005. Lower airway inflammation in infants with cystic fibrosis detected by newborn screening. *Pediatr Pulmonol,* 40**,** 500-10.

AZEREDO, J., AZEVEDO, N. F., BRIANDET, R., CERCA, N., COENYE, T., COSTA, A. R., DESVAUX, M., DI BONAVENTURA, G., HÉBRAUD, M., JAGLIC, Z., KAČÁNIOVÁ, M., KNØCHEL, S., LOURENÇO, A., MERGULHÃO, F., MEYER, R. L., NYCHAS, G., SIMÕES, M., TRESSE, O. & STERNBERG, C. 2017. Critical review on biofilm methods. *Crit Rev Microbiol,* 43**,** 313-351.

BACALI, C., VULTURAR, R., BUDURU, S., COZMA, A., FODOR, A., CHIȘ, A., LUCACIU, O., DAMIAN, L. & MOLDOVAN, M. L. 2022. Oral microbiome: Getting to know and befriend neighbors, a biological approach. *Biomedicines,* 10**,** 671.

BADAWY, H., BRUNELLIÈRE, J., VERYASKINA, M., BROTONS, G., SABLÉ, S., LANNELUC, I., LAMBERT, K., MARMEY, P., MILSTED, A. & CUTRIGHT, T. 2015. Assessing the antimicrobial activity of polyisoprene based surfaces. *Int J Mol Sci,* 16**,** 4392-4415.

BAEHNI, P., TSAI, C.-C., MCARTHUR, W., HAMMOND, B., SHENKER, B. & TAICHMAN, N. 1981. Leukotoxic activity in different strains of the bacterium *Actinobacillus actinomycetemcomitans* isolated from juvenile periodontitis in man. *Arch Oral Biol,* 26**,** 671-676.

BALASHOVA, N. V., PARK, D. H., PATEL, J. K., FIGURSKI, D. H. & KACHLANY, S. C. 2007. Interaction between leukotoxin and Cu,Zn superoxide dismutase in *Aggregatibacter actinomycetemcomitans*. *Infect Immun,* 75**,** 4490-7.

BANAS, J. A. & VICKERMAN, M. M. 2003. Glucan-binding proteins of the oral streptococci. *Crit Rev Oral Biol Med,* 14**,** 89-99.

BARAI, P., KUMAR, A. & MUKHERJEE, P. P. 2016. Modeling of mesoscale variability in biofilm shear behavior. *PLoS One,* 11**,** e0165593.

BARROS, S. P., WILLIAMS, R., OFFENBACHER, S. & MORELLI, T. 2016. Gingival crevicular fluid as a source of biomarkers for periodontitis. *Periodontol 2000,* 70**,** 53-64.

BARTON, G. M. 2008. A calculated response: control of inflammation by the innate immune system. *J Clin Invest,* 118**,** 413-20.

BARTON, G. M., KAGAN, J. C. & MEDZHITOV, R. 2006. Intracellular localisation of Toll-like receptor 9 prevents recognition of self DNA but facilitates access to viral DNA. *Nat Immunol,* 7**,** 49-56.

BEHBAHANI, S. B., KIRIDENA, S. D., WIJAYARATNA, U. N., TAYLOR, C., ANKER, J. N. & TZENG, T.-R. J. 2022. pH variation in medical implant biofilms: Causes, measurements, and its implications for antibiotic resistance. *Front Microbiol,* 13**,** 1028560.

BEHZADI, P., GARCÍA-PERDOMO, H. A. & KARPIŃSKI, T. M. 2021. Toll-like receptors: general molecular and structural biology. *J Immunol Res,* 2021**,** 1-21.

BELAMBRI, S. A., ROLAS, L., RAAD, H., HURTADO-NEDELEC, M., DANG, P. M. C. & EL-BENNA, J. 2018. NADPH oxidase activation in neutrophils: Role of the phosphorylation of its subunits. *Eur J Clin Investig,* 48**,** e12951.

BELIBASAKIS, G. N., JOHANSSON, A., WANG, Y., CHEN, C., KALFAS, S. & LERNER, U. 2005. The cytolethal distending toxin induces receptor activator of NF-κB ligand expression in human gingival fibroblasts and periodontal ligament cells. *Infect Immun,* 73**,** 342-351.

BELIBASAKIS, G. N., MAULA, T., BAO, K., LINDHOLM, M., BOSTANCI, N., OSCARSSON, J., IHALIN, R. & JOHANSSON, A. 2019. Virulence and pathogenicity properties of *Aggregatibacter actinomycetemcomitans*. *Pathogens,* 8**,** 222.

BENJAMIN, R. M. 2010. Oral health: the silent epidemic. *Public Health Rep,* 125**,** 158-9.

BERENDS, C., DIJKHUIZEN, B., DE MONCHY, J. G. R., GERRITSEN, J. & KAUFFMAN, H. F. 1994. Induction of low density and up-regulation of CD11b expression of neutrophils and eosinophils by dextran sedimentation and centrifugation. *J Immunol Methods,* 167**,** 183-193.

BERNSTEIN, R., BELFER, S. & FREGER, V. 2011. Bacterial attachment to RO membranes surface-modified by concentration-polarisation-enhanced graft polymerisation. *Environ Sci Technol,* 45**,** 5973-5980.

BESIER, S., SMACZNY, C., VON MALLINCKRODT, C., KRAHL, A., ACKERMANN, H., BRADE, V. & WICHELHAUS, T. A. 2007. Prevalence and clinical significance of *Staphylococcus aureus* small-colony variants in cystic fibrosis lung disease. *J Clin Microbiol,* 45**,** 168-72.

BESIER, S., ZANDER, J., SIEGEL, E., SAUM, S. H., HUNFELD, K. P., EHRHART, A., BRADE, V. & WICHELHAUS, T. A. 2008. Thymidine-dependent *Staphylococcus aureus* small-colony variants: human pathogens that are relevant not only in cases of cystic fibrosis lung disease. *J Clin Microbiol,* 46**,** 3829-32.

BHATTY, M., CRUZ, M. R., FRANK, K. L., GOMEZ, J. A., ANDRADE, F., GARSIN, D. A., DUNNY, G. M., KAPLAN, H. B. & CHRISTIE, P. J. 2015. *Enterococcus faecalis pCF10*-encoded surface proteins PrgA, PrgB (aggregation substance) and PrgC contribute to plasmid transfer, biofilm formation and virulence. *Mol Microbiol,* 95**,** 660-77.

BJARNSHOLT, T., ALHEDE, M., ALHEDE, M., EICKHARDT-SØRENSEN, S. R., MOSER, C., KÜHL, M., JENSEN, P. Ø. & HØIBY, N. 2013. The *in vivo* biofilm. *Trends Microbiol,* 21**,** 466-474.

BJÖRNHAM, O. & AXNER, O. 2010. Catch-Bond Behavior of Bacteria Binding by Slip Bonds. *Biophysical Journal,* 99**,** 1331-1341.

BJÖRNSDOTTIR, H., WELIN, A., MICHAËLSSON, E., OSLA, V., BERG, S., CHRISTENSON, K., SUNDQVIST, M., DAHLGREN, C., KARLSSON, A. & BYLUND, J. 2015. Neutrophil NET formation is regulated from the inside by myeloperoxidase-processed reactive oxygen species. *Free Radic Biol Med,* 89**,** 1024-35.

BLANC, V., ISABAL, S., SANCHEZ, M., LLAMA-PALACIOS, A., HERRERA, D., SANZ, M. & LEÓN, R. 2014. Characterisation and application of a flow system for *in vitro* multispecies oral biofilm formation. *J Periodontal Res,* 49**,** 323-332.

BLUS, C., SZMUKLER-MONCLER, S., ORRÙ, G. & GIANNELLI, G. *In vitro* modelling of *Streptococcus intermedius* biofilm on titanium dental implants. 2015.

BÖCKELMANN, U., JANKE, A., KUHN, R., NEU, T. R., WECKE, J., LAWRENCE, J. R. & SZEWZYK, U. 2006. Bacterial extracellular DNA forming a defined network-like structure. *FEMS Microbiol Lett,* 262**,** 31-38.

BOGINO, P. C., DE LAS MERCEDES OLIVA, M., SORROCHE, F. G. & GIORDANO, W. 2013. The role of bacterial biofilms and surface components in plant-bacterial associations. *Int J Mol Sci,* 14**,** 15838-15859.

BOISEN, G., DAVIES, J. R. & NEILANDS, J. 2021. Acid tolerance in early colonisers of oral biofilms. *BMC Microbiol,* 21**,** 45.

BOISVERT, A. A., CHENG, M. P., SHEPPARD, D. C. & NGUYEN, D. 2016. Microbial biofilms in pulmonary and critical care diseases. *Ann Am Thorac Soc,* 13**,** 1615-23.

BOLES, B. R. & HORSWILL, A. R. 2008. *Agr*-mediated dispersal of *Staphylococcus aureus* biofilms. *PLoS pathog,* 4**,** e1000052.

BORREGAARD, N. 2010. Neutrophils, from Marrow to Microbes. *Immunity,* 33**,** 657-670.

BORREGAARD, N. & COWLAND, J. B. 1997. Granules of the Human Neutrophilic Polymorphonuclear Leukocyte. *Blood,* 89**,** 3503-3521.

BOYLE, K. B., GYORI, D., SINDRILARU, A., SCHARFFETTER-KOCHANEK, K., TAYLOR, P. R., MÓCSAI, A., STEPHENS, L. R. & HAWKINS, P. T. 2011. Class IA phosphoinositide 3-kinase β and δ regulate neutrophil oxidase activation in response to *Aspergillus fumigatus* hyphae. *J Immunol,* 186**,** 2978-89.

BRADSHAW, D. J., MARSH, P. D., WATSON, G. K. & ALLISON, C. 1998. Role of *Fusobacterium nucleatum* and coaggregation in anaerobe survival in planktonic and biofilm oral microbial communities during aeration. *Infect Immun,* 66**,** 4729-4732.

BRANITZKI-HEINEMANN, K., MÖLLERHERM, H., VÖLLGER, L., HUSEIN, D. M., DE BUHR, N., BLODKAMP, S., REUNER, F., BROGDEN, G., NAIM, H. Y. & VON KÖCKRITZ-BLICKWEDE, M. 2016. Formation of neutrophil extracellular traps under low oxygen Level. *Front Immunol,* 7**,** 518.

BRANZK, N., LUBOJEMSKA, A., HARDISON, S. E., WANG, Q., GUTIERREZ, M. G., BROWN, G. D. & PAPAYANNOPOULOS, V. 2014. Neutrophils sense microbe size and selectively release neutrophil extracellular traps in response to large pathogens. *Nat Immunol,* 15**,** 1017-25.

BRÍGIDO, J. A., DA SILVEIRA, V. R., REGO, R. O. & NOGUEIRA, N. A. 2014. Serotypes of *Aggregatibacter actinomycetemcomitans* in relation to periodontal status and geographic origin of individuals-a review of the literature. *Med Oral Patol Oral Cir Bucal,* 19**,** e184-91.

BRINKMANN, V., LAUBE, B., ABED, U. A., GOOSMANN, C. & ZYCHLINSKY, A. 2010. Neutrophil extracellular traps: how to generate and visualize them. *JoVE***,** e1724.

BRINKMANN, V., REICHARD, U., GOOSMANN, C., FAULER, B., UHLEMANN, Y., WEISS, D. S., WEINRAUCH, Y. & ZYCHLINSKY, A. 2004. Neutrophil Extracellular Traps Kill Bacteria. *Science,* 303**,** 1532-1535.

BRINKMANN, V. & ZYCHLINSKY, A. 2007. Beneficial suicide: why neutrophils die to make NETs. *Nat Rev Microbiol,* 5**,** 577-82.

BRINKMANN, V. & ZYCHLINSKY, A. 2012. Neutrophil extracellular traps: is immunity the second function of chromatin? *J Cell Biol,* 198**,** 773-83.

BRITIGAN, B. E., HAYEK, M., DOEBBELING, B. & FICK, R. 1993. Transferrin and lactoferrin undergo proteolytic cleavage in the *Pseudomonas aeruginosa*-infected lungs of patients with cystic fibrosis. *Infect Immun,* 61**,** 5049-5055.

BROCKSON, M. E., NOVOTNY, L. A., MOKRZAN, E. M., MALHOTRA, S., JURCISEK, J. A., AKBAR, R., DEVARAJ, A., GOODMAN, S. D. & BAKALETZ, L. O. 2014. Evaluation of the kinetics and mechanism of action of anti-integration host factor-mediated disruption of bacterial biofilms. *Mol Microbiol,* 93**,** 1246-1258.

BROWN, H. L., VAN VLIET, A. H., BETTS, R. P. & REUTER, M. 2013. Tetrazolium reduction allows assessment of biofilm formation by *Campylobacter jejuni* in a food matrix model. *J Appl Microbiol,* 115**,** 1212-21.

BUZZO, J. R., DEVARAJ, A., GLOAG, E. S., JURCISEK, J. A., ROBLEDO-AVILA, F., KESLER, T., WILBANKS, K., MASHBURN-WARREN, L., BALU, S., WICKHAM, J., NOVOTNY, L. A., STOODLEY, P., BAKALETZ, L. O. & GOODMAN, S. D. 2021. Z-form extracellular DNA is a structural component of the bacterial biofilm matrix. *Cell,* 184**,** 5740-5758.e17.

BYLUND, J., BROWN, K. L., MOVITZ, C., DAHLGREN, C. & KARLSSON, A. 2010. Intracellular generation of superoxide by the phagocyte NADPH oxidase: how, where, and what for? *Free Radic Biol Med,* 49**,** 1834-1845.

BYRD, A. S., O'BRIEN, X. M., JOHNSON, C. M., LAVIGNE, L. M. & REICHNER, J. S. 2013. An extracellular matrix-based mechanism of rapid neutrophil extracellular trap formation in response to *Candida albicans*. *J Immunol,* 190**,** 4136-48.

CAMPOCCIA, D., RAVAIOLI, S., MIRZAEI, R., BUA, G., DAGLIA, M. & ARCIOLA, C. R. 2023. Interactions of neutrophils with the polymeric molecular components of the biofilm matrix in the context of implant-associated bone and joint infections. *Int J Mol Sci,* 24**,** 17042.

CANTIN, A. 1995. Cystic fibrosis lung inflammation: early, sustained, and severe. *Am J Respir Crit Care Med,* 151**,** 939-941.

CAO, S., LIU, P., ZHU, H., GONG, H., YAO, J., SUN, Y., GENG, G., WANG, T., FENG, S., HAN, M., ZHOU, J. & XU, Y. 2015. Extracellular acidification acts as a key modulator of neutrophil apoptosis and functions. *PloS one,* 10**,** e0137221-e0137221.

CARVALHO, L. O., AQUINO, E. N., NEVES, A. C. & FONTES, W. 2015. The neutrophil nucleus and its role in neutrophilic function. *J Cell Biochem,* 116**,** 1831-6.

CATALAN, M. P., REYERO, A. N. A., EGIDO, J. & ORTIZ, A. 2001. Acceleration of Neutrophil Apoptosis by Glucose-Containing Peritoneal Dialysis Solutions: Role of Caspases. *J Am Soc Nephrol,* 12**,** 2442.

CHACKO, F. M. & SCHMITT, L. 2023. Interaction of RTX toxins with the host cell plasma membrane. *Biol Chem,* 404**,** 663-671.

CHANDRA, J. & MUKHERJEE, P. K. 2015. *Candida* Biofilms: Development, architecture, and resistance. *Microbiol Spectr,* 3.
CHANG, A. M., KANTRONG, N. & DARVEAU, R. P. 2021. Maintaining homeostatic control of periodontal epithelial tissue. *Periodontol 2000,* 86**,** 188-200.
CHANG, Z. 2010. Important aspects of Toll-like receptors, ligands and their signaling pathways. *Inflamm Res,* 59**,** 791-808.
CHAPPLE, I. L. 1996. Role of free radicals and antioxidants in the pathogenesis of the inflammatory periodontal diseases. *Clin Mol Pathol,* 49**,** M247-55.
CHAPPLE, I. L. & MATTHEWS, J. B. 2007. The role of reactive oxygen and antioxidant species in periodontal tissue destruction. *Periodontol 2000,* 43**,** 160-232.
CHATTERJEE, S. 2014. Artefacts in histopathology. *J Oral Maxillofac Pathol,* 18**,** S111-6.
CHATTERJEE, S., BISWAS, N., DATTA, A. & MAITI, P. K. 2019. Periodicities in the roughness and biofilm growth on glass substrate with etching time: Hydrofluoric acid etchant. *PLOS ONE,* 14**,** e0214192.
CHÁVEZ DE PAZ, L. E., HAMILTON, I. R. & SVENSÄTER, G. 2008. Oral bacteria in biofilms exhibit slow reactivation from nutrient deprivation. *Microbiol,* 154**,** 1927-1938.
CHEBOTAR, I. V., KONCHAKOVA, E. D. & EVTEEVA, N. I. 2012. [Neutrophil dependent breakdown of biofilms formed by *Staphylococcus aureus*]. *Zh Mikrobiol Epidemiol Immunobiol,* 1**,** 10-5.
CHI, F., NOLTE, O., BERGMANN, C., IP, M. & HAKENBECK, R. 2007. Crossing the barrier: evolution and spread of a major class of mosaic pbp2x in *Streptococcus pneumoniae*, *S. mitis* and *S. oralis*. *Int J Med Microbiol,* 297**,** 503-12.
CHIANG, W.-C., NILSSON, M., JENSEN, P. Ø., HØIBY, N., NIELSEN, T. E., GIVSKOV, M. & TOLKER-NIELSEN, T. 2013. Extracellular DNA shields against aminoglycosides in *Pseudomonas aeruginosa* biofilms. *Antimicrob Agents Chemother,* 57**,** 2352-2361.
CHIU, A., SAIGH, M. A., MCCULLOCH, C. & GLOGAUER, M. 2017. The role of NrF2 in the regulation of periodontal health and disease. *J Dent Res,* 96**,** 975-983.
CHOO, S. W., MOHAMMED, W. K., MUTHA, N. V. R., ROSTAMI, N., AHMED, H., KRASNOGOR, N., TAN, G. Y. A. & JAKUBOVICS, N. S. 2021. Transcriptomic responses to coaggregation between *Streptococcus gordonii* and *Streptococcus oralis*. *Appl Environ Microbiol,* 87**,** e01558-21.
CIEUTAT, A.-M., LOBEL, P., AUGUST, J., KJELDSEN, L., SENGELØV, H., BORREGAARD, N. & BAINTON, D. 1998. Azurophilic granules of human neutrophilic leukocytes are deficient in lysosome-associated membrane proteins but retain the mannose 6-phosphate recognition marker. *Blood,* 91**,** 1044-1058.
CLAESSEN, D., ROZEN, D. E., KUIPERS, O. P., SØGAARD-ANDERSEN, L. & VAN WEZEL, G. P. 2014. Bacterial solutions to multicellularity: a tale of biofilms, filaments and fruiting bodies. *Nat Rev Microbiol,* 12**,** 115-124.
CLAESSON, R., JOHANSSON, A., BELIBASAKIS, G., HÄNSTRÖM, L. & KALFAS, S. 2002. Release and activation of matrix metalloproteinase 8 from human neutrophils triggered by the leukotoxin of *Actinobacillus actinomycetemcomitans*. *J Periodontal Res,* 37**,** 353-9.
CLARK, S. R., MA, A. C., TAVENER, S. A., MCDONALD, B., GOODARZI, Z., KELLY, M. M., PATEL, K. D., CHAKRABARTI, S., MCAVOY, E., SINCLAIR, G. D., KEYS, E. M., ALLEN-VERCOE, E., DEVINNEY, R., DOIG, C. J., GREEN, F. H. & KUBES, P. 2007. Platelet TLR4 activates neutrophil extracellular traps to ensnare bacteria in septic blood. *Nat Med,* 13**,** 463-9.
COLE, M. F., EVANS, M., FITZSIMMONS, S., JOHNSON, J., PEARCE, C., SHERIDAN, M. J., WIENTZEN, R. & BOWDEN, G. 1994. Pioneer oral streptococci produce immunoglobulin A1 protease. *Infect Immun,* 62**,** 2165-2168.
CONDLIFFE, A., KITCHEN, E. & CHILVERS, E. 1998. Neutrophil priming: pathophysiological consequences and underlying mechanisms. *Clin Sci (Lond.),* 94**,** 461-471.
CONRAD, A., KONTRO, M., KEINÄNEN, M. M., CADORET, A., FAURE, P., MANSUY-HUAULT, L. & BLOCK, J.-C. 2003. Fatty acids of lipid fractions in extracellular polymeric substances of activated sludge flocs. *Lipids,* 38**,** 1093-1105.

COOLEY, B. J., THATCHER, T. W., HASHMI, S. M., L'HER, G., LE, H. H., HURWITZ, D. A., PROVENZANO, D., TOUHAMI, A. & GORDON, V. D. 2013. The extracellular polysaccharide Pel makes the attachment of *P. aeruginosa* to surfaces symmetric and short-ranged. *Soft Matter,* 9**,** 3871-3876.

COOPER, P. R., PALMER, L. J. & CHAPPLE, I. L. 2013. Neutrophil extracellular traps as a new paradigm in innate immunity: friend or foe? *Periodontol 2000,* 63**,** 165-197.

CORAÇA-HUBER, D. C., KREIDL, L., STEIXNER, S., HINZ, M., DAMMERER, D. & FILLE, M. 2020. Identification and morphological characterisation of biofilms formed by strains causing infection in orthopedic implants. *Pathogens,* 9.

CORBIN, A., PITTS, B., PARKER, A. & STEWART, P. S. 2011. Antimicrobial penetration and efficacy in an *in vitro* oral biofilm model. *Antimicrob Agents Chemother,* 55**,** 3338-44.

COSTA-ORLANDI, C. B., SARDI, J. C., PITANGUI, N. S., DE OLIVEIRA, H. C., SCORZONI, L., GALEANE, M. C., MEDINA-ALARCÓN, K. P., MELO, W. C., MARCELINO, M. Y. & BRAZ, J. D. 2017. Fungal biofilms and polymicrobial diseases. *J Fungi,* 3**,** 22.

COSTERTON, J. W. 1999. Introduction to biofilm. *Int J Antimicrob Agents,* 11**,** 217-221.

COUVIGNY, B., KULAKAUSKAS, S., PONS, N., QUINQUIS, B., ABRAHAM, A.-L., MEYLHEUC, T., DELORME, C., RENAULT, P., BRIANDET, R., LAPAQUE, N. & GUÉDON, E. 2018. Identification of new factors modulating adhesion abilities of the pioneer commensal bacterium *Streptococcus salivarius*. *Front Microbiol,* 9.

COWBURN, A. S., CONDLIFFE, A. M., FARAHI, N., SUMMERS, C. & CHILVERS, E. R. 2008. Advances in neutrophil biology: clinical implications. *Chest,* 134**,** 606-612.

CRUSZ, S. A., POPAT, R., RYBTKE, M. T., CÁMARA, M., GIVSKOV, M., TOLKER-NIELSEN, T., DIGGLE, S. P. & WILLIAMS, P. 2012. Bursting the bubble on bacterial biofilms: a flow cell methodology. *Biofouling,* 28**,** 835-842.

CURTIS, M. A., ZENOBIA, C. & DARVEAU, R. P. 2011. The relationship of the oral microbiotia to periodontal health and disease. *Cell Host Microbe,* 10**,** 302-6.

CZERWIŃSKA-GŁÓWKA, D. & KRUKIEWICZ, K. 2021. Guidelines for a morphometric analysis of prokaryotic and eukaryotic cells by Scanning Electron Microscopy. *Cells,* 10.

DAHLEN, G., BASIC, A. & BYLUND, J. 2019. Importance of virulence factors for the persistence of oral bacteria in the inflamed gingival crevice and in the pathogenesis of periodontal disease. *J Clin Med,* 8.

DAHLGREN, C. & KARLSSON, A. 1999. Respiratory burst in human neutrophils. *J Immunol Methods,* 232**,** 3-14.

DAMASCENA, H. L., SILVEIRA, W. A. A., CASTRO, M. S. & FONTES, W. 2022. Neutrophil activated by the famous and potent PMA (Phorbol Myristate Acetate). *Cells,* 11.

DANCEY, J. T., DEUBELBEISS, K. A., HARKER, L. A. & FINCH, C. A. 1976. Neutrophil kinetics in man. *J Clin Invest,* 58**,** 705-715.

DANIEL, C., LEPPKES, M., MUÑOZ, L. E., SCHLEY, G., SCHETT, G. & HERRMANN, M. 2019. Extracellular DNA traps in inflammation, injury and healing. *Nat Rev Nephrol,* 15**,** 559-575.

DAPUNT, U., GAIDA, M. M., MEYLE, E., PRIOR, B. & HÄNSCH, G. M. 2016. Activation of phagocytic cells by *Staphylococcus epidermidis* biofilms: effects of extracellular matrix proteins and the bacterial stress protein GroEL on netosis and MRP-14 release. *Pathog Dis,* 74.

DAPUNT, U., PRIOR, B., KRETZER, J. P., GIESE, T. & ZHAO, Y. 2020. Bacterial biofilm components induce an enhanced inflammatory response against metal wear particles. *Ther Clin Risk Manag,* 16**,** 1203-1212.

DARRENE, L.-N. & CECILE, B. 2016. Experimental Mmodels of oral biofilms developed on inert substrates: A review of the literature. *BioMed Res Int,* 2016**,** 7461047.

DAS, T., KROM, B. P., VAN DER MEI, H. C., BUSSCHER, H. J. & SHARMA, P. K. 2011a. DNA-mediated bacterial aggregation is dictated by acid–base interactions. *Soft Matter,* 7**,** 2927-2935.

DAS, T., SHARMA, P. K., KROM, B. P., VAN DER MEI, H. C. & BUSSCHER, H. J. 2011b. Role of eDNA on the adhesion forces between *Streptococcus mutans* and substratum surfaces: influence of ionic strength and substratum hydrophobicity. *Langmuir,* 27**,** 10113-8.
DAWES, C. 1987. Physiological Factors Affecting Salivary Flow Rate, Oral Sugar Clearance, and the Sensation of Dry Mouth in Man. *J Dent Res,* 66**,** 648-653.
DE ALMEIDA PDEL, V., GRÉGIO, A. M., MACHADO, M. A., DE LIMA, A. A. & AZEVEDO, L. R. 2008. Saliva composition and functions: a comprehensive review. *J Contemp Dent Pract,* 9**,** 72-80.
DE BUHR, N. & VON KÖCKRITZ-BLICKWEDE, M. 2016. How neutrophil extracellular traps become visible. *J Immunol Res,* 2016**,** 4604713.
DE KIEVIT, T. R. 2009. Quorum sensing in *Pseudomonas aeruginosa* biofilms. *Environ Microbiol,* 11**,** 279-288.
DE PABLO, P., CHAPPLE, I. L., BUCKLEY, C. D. & DIETRICH, T. 2009. Periodontitis in systemic rheumatic diseases. *Nat Rev Rheumatol,* 5**,** 218-24.
DECOURSEY, T. & LIGETI, E. 2005. Regulation and termination of NADPH oxidase activity. *Cell Mol Life Sci,* 62**,** 2173-2193.
DELGADO-RIZO, V., MARTÍNEZ-GUZMÁN, M., IÑIGUEZ-GUTIERREZ, L., GARCÍA-OROZCO, A., ALVARADO-NAVARRO, A. & FAFUTIS-MORRIS, M. 2017. Neutrophil extracellular traps and its implications in inflammation: an overview. *Frontiers in Immunology,* 8.
DENG, W., LEI, Y., TANG, X., LI, D., LIANG, J., LUO, J., LIU, L., ZHANG, W., YE, L., KONG, J., WANG, K. & CHEN, Z. 2022. DNase inhibits early biofilm formation in *Pseudomonas aeruginosa*- or *Staphylococcus aureus*-induced empyema models. *Front Cell Infect Microbiol,* 12**,** 917038.
DENGLER, V., FOULSTON, L., DEFRANCESCO, A. S. & LOSICK, R. 2015. An electrostatic net model for the role of extracellular DNA in biofilm formation by *Staphylococcus aureus*. *J Bacteriol,* 197**,** 3779-87.
DEVARAJ, A., BUZZO, J. R., MASHBURN-WARREN, L., GLOAG, E. S., NOVOTNY, L. A., STOODLEY, P., BAKALETZ, L. O. & GOODMAN, S. D. 2019. The extracellular DNA lattice of bacterial biofilms is structurally related to Holliday junction recombination intermediates. *Proc Natl Acad Sci,* 116**,** 25068-25077.
DEWHIRST, F. E., CHEN, T., IZARD, J., PASTER, B. J., TANNER, A. C., YU, W. H., LAKSHMANAN, A. & WADE, W. G. 2010. The human oral microbiome. *J Bacteriol,* 192**,** 5002-17.
DHOTRE, S., JAHAGIRDAR, V., SURYAWANSHI, N., DAVANE, M., PATIL, R. & NAGOBA, B. 2018. Assessment of periodontitis and its role in viridans streptococcal bacteremia and infective endocarditis. *Indian Heart J,* 70**,** 225-232.
DÍAZ, A. N., SANCHEZ, F. G. & GARCÍA, J. A. G. 1996. Hydrogen peroxide assay by using enhanced chemiluminescence of the luminol-H2O2-horseradish peroxidase system: Comparative studies. *Analytica Chimica Acta,* 327**,** 161-165.
DIAZ, P. I. & VALM, A. M. 2020. Microbial interactions in oral communities mediate emergent biofilm properties. *J Dent Res,* 99**,** 18-25.
DO, T., DEVINE, D. & MARSH, P. D. 2013. Oral biofilms: molecular analysis, challenges, and future prospects in dental diagnostics. *Clin Cosmet Investig Dent,* 5**,** 11-9.
DOERN, C. D. & BURNHAM, C. A. 2010. It's not easy being green: the viridans group streptococci, with a focus on pediatric clinical manifestations. *J Clin Microbiol,* 48**,** 3829-35.
DOGGETT, R. G. 1969. Incidence of mucoid *Pseudomonas aeruginosa* from clinical sources. *Appl Microbiol,* 18**,** 936-7.
DOGGETT, R. G., HARRISON, G. M. & WALLIS, E. S. 1964. Comparison of some properties of *Pseudomonas aeruginosa* isolated from infections in persons with and without cystic fibrosis. *J Bacteriol,* 87**,** 427-31.
DONLAN, R. M. & COSTERTON, J. W. 2002. Biofilms: Survival Mechanisms of Clinically Relevant Microorganisms. *Clin Microbiol Rev,* 15**,** 167.

DORKHAN, M., CHÁVEZ DE PAZ, L. E., SKEPÖ, M., SVENSÄTER, G. & DAVIES, J. R. 2012. Effects of saliva or serum coating on adherence of *Streptococcus oralis* strains to titanium. *Microbiol* 158**,** 390-397.

DORKHAN, M., SVENSÄTER, G. & DAVIES, J. R. 2013. Salivary pellicles on titanium and their effect on metabolic activity in *Streptococcus oralis*. *BMC Oral Health,* 13**,** 32.

DOROSHENKO, N., TSENG, B. S., HOWLIN, R. P., DEACON, J., WHARTON, J. A., THURNER, P. J., GILMORE, B. F., PARSEK, M. R. & STOODLEY, P. 2014. Extracellular DNA impedes the transport of vancomycin in *Staphylococcus epidermidis* biofilms preexposed to subinhibitory concentrations of vancomycin. *Antimicrob Agents Chemother,* 58**,** 7273-7282.

DORWARD, D. A., LUCAS, C. D., CHAPMAN, G. B., HASLETT, C., DHALIWAL, K. & ROSSI, A. G. 2015. The role of formylated peptides and formyl peptide receptor 1 in governing neutrophil function during acute inflammation. *Am J Pathol,* 185**,** 1172-84.

DOUDA, D. N., KHAN, M. A., GRASEMANN, H. & PALANIYAR, N. 2015. SK3 channel and mitochondrial ROS mediate NADPH oxidase-independent NETosis induced by calcium influx. *Proc Natl Acad Sci,* 112**,** 2817-2822.

DUAN, D., SCOFFIELD, J. A., ZHOU, X. & WU, H. 2016. Fine-tuned production of hydrogen peroxide promotes biofilm formation of *Streptococcus parasanguinis* by a pathogenic cohabitant *Aggregatibacter actinomycetemcomitans*. *Environ Microbiol,* 18**,** 4023-4036.

DUARTE, M., KUCHIBHATLA, M., KHANDELWAL, S., AREPALLY, G. M. & LEE, G. M. 2019. Heterogeneity in neutrophil responses to immune complexes. *Blood Advances,* 3**,** 2778-2789.

DUNNE JR, W. M. 2002. Bacterial adhesion: seen any good biofilms lately? *Clin Microbiol Rev,* 15**,** 155-166.

EGGERT, F. M., DREWELL, L., BIGELOW, J. A., SPECK, J. E. & GOLDNER, M. 1991. The pH of gingival crevices and periodontal pockets in children, teenagers and adults. *Arch Oral Biol,* 36**,** 233-238.

EKE, P. I., THORNTON-EVANS, G., DYE, B. & GENCO, R. 2012. Advances in Surveillance of Periodontitis: The Centers for Disease Control and Prevention Periodontal Disease Surveillance Project. *J Periodontol,* 83**,** 1337-1342.

EL KEBIR, D., JÓZSEF, L., PAN, W., WANG, L. & FILEP, J. N. G. 2009. Bacterial DNA Activates Endothelial Cells and Promotes Neutrophil Adherence through TLR9 Signaling1. *The Journal of Immunology,* 182**,** 4386-4394.

ELIAS, S. & BANIN, E. 2012. Multi-species biofilms: living with friendly neighbors. *FEMS Microbiol Rev,* 36**,** 990-1004.

ELLIOTT, D., PRATTEN, J., EDWARDS, M., CROWTHER, J., PETRIE, A. & WILSON, M. 2005. Bacterial biofilm development on hydroxyapatite-coated glass. *Curr Microbiol,* 51**,** 41-45.

EMERSON, J., ROSENFELD, M., MCNAMARA, S., RAMSEY, B. & GIBSON, R. L. 2002. *Pseudomonas aeruginos*a and other predictors of mortality and morbidity in young children with cystic fibrosis. *Pediatr Pulmonol,* 34**,** 91-100.

FAIRN, G. D. & GRINSTEIN, S. 2012. How nascent phagosomes mature to become phagolysosomes. *Trends Immunol,* 33**,** 397-405.

FAURSCHOU, M. & BORREGAARD, N. 2003. Neutrophil granules and secretory vesicles in inflammation. *Microbes Infect,* 5**,** 1317-1327.

FENG, G., CHENG, Y., WANG, S.-Y., BORCA-TASCIUC, D. A., WOROBO, R. W. & MORARU, C. I. 2015. Bacterial attachment and biofilm formation on surfaces are reduced by small-diameter nanoscale pores: how small is small enough? *npj Biofilms Microbiomes,* 1**,** 15022.

FENOLL-PALOMARES, C., MUÑOZ-MONTAGUD, J. V., SANCHIZ, V., HERREROS, B., HERNÁNDEZ, V., MÍNGUEZ, M. & BENAGES, A. 2004. Unstimulated salivary flow rate, pH and buffer capacity of saliva in healthy volunteers. *Rev Esp Enferm Dig,* 96**,** 773-783.

FERNÁNDEZ-BABIANO, I., NAVARRO-PÉREZ, M. L., PÉREZ-GIRALDO, C. & FERNÁNDEZ-CALDERÓN, M. C. 2022. Antibacterial and antibiofilm activity of carvacrol against oral pathogenic bacteria. *Metabolites* [Online], 12.

FERNÁNDEZ, C., ASPIRAS, M., DODDS, M., GONZÁLEZ-CABEZAS, C. & RICKARD, A. 2017. The effect of inoculum source and fluid shear force on the development of *in vitro* oral multispecies biofilms. *J Appl Microbiol,* 122**,** 796-808.

FIALKOW, L., WANG, Y. & DOWNEY, G. P. 2007. Reactive oxygen and nitrogen species as signaling molecules regulating neutrophil function. *Free Radic Biol Med,* 42**,** 153-164.

FINE, D. H., MARKOWITZ, K., FURGANG, D., FAIRLIE, K., FERRANDIZ, J., NASRI, C., MCKIERNAN, M. & GUNSOLLEY, J. 2007. *Aggregatibacter actinomycetemcomitans* and its relationship to initiation of localised aggressive periodontitis: longitudinal cohort study of initially healthy adolescents. *J Clin Microbiol,* 45**,** 3859-3869.

FINE, D. H., PATIL, A. G. & VELUSAMY, S. K. 2019. *Aggregatibacter actinomycetemcomitans* (Aa) under the radar: Myths and misunderstandings of Aa and Its role in aggressive periodontitis. *Front Immunol,* 10.

FINE, N., HASSANPOUR, S., BORENSTEIN, A., SIMA, C., OVEISI, M., SCHOLEY, J., CHERNEY, D. & GLOGAUER, M. 2016. Distinct oral neutrophil subsets define health and periodontal disease states. *J Dent Res,* 95**,** 931-938.

FINKEL, S. E. & KOLTER, R. 2001. DNA as a nutrient: novel role for bacterial competence gene homologs. *J Bacteriol,* 183**,** 6288-6293.

FLEMMING, H.-C. & WINGENDER, J. 2010. The biofilm matrix. *Nat Rev microbiol,* 8**,** 623-633.

FLEMMING, H.-C., WINGENDER, J., SZEWZYK, U., STEINBERG, P., RICE, S. A. & KJELLEBERG, S. 2016. Biofilms: an emergent form of bacterial life. *Nat Rev Microbiol,* 14**,** 563-575.

FLEMMING, H.-C. & WUERTZ, S. 2019. Bacteria and archaea on Earth and their abundance in biofilms. *Nat Rev Microbiol,* 17**,** 247-260.

FONG, K. P., PACHECO, C. M. F., OTIS, L. L., BARANWAL, S., KIEBA, I. R., HARRISON, G., HERSH, E. V., BOESZE-BATTAGLIA, K. & LALLY, E. T. 2006. *Actinobacillus actinomycetemcomitans* leukotoxin requires lipid microdomains for target cell cytotoxicity. *Cell Microbiol,* 8**,** 1753-1767.

FOSTER, J., PAN, P. & KOLENBRANDER, P. 2004. Effects of antimicrobial agents on oral biofilms in a saliva-conditioned flowcell. *Biofilms,* 1**,** 5-12.

FOSTER, J. S. & KOLENBRANDER, P. E. 2004. Development of a multispecies oral bacterial community in a saliva-conditioned flow cell. *App Environ Microbiol,* 70**,** 4340-4348.

FUCHS, T. A., ABED , U., GOOSMANN , C., HURWITZ , R., SCHULZE , I., WAHN , V., WEINRAUCH , Y., BRINKMANN , V. & ZYCHLINSKY , A. 2007. Novel cell death program leads to neutrophil extracellular traps. *J Cell Biol,* 176**,** 231-241.

FUCHS, T. A., BRILL, A., DUERSCHMIED, D., SCHATZBERG, D., MONESTIER, M., MYERS, D. D., WROBLESKI, S. K., WAKEFIELD, T. W., HARTWIG, J. H. & WAGNER, D. D. 2010. Extracellular DNA traps promote thrombosis. *Proc Natl Acad Sci,* 107**,** 15880-15885.

FUTOSI, K., FODOR, S. & MÓCSAI, A. 2013. Neutrophil cell surface receptors and their intracellular signal transduction pathways. *Int Immunopharmacol,* 17**,** 638-50.

FUXMAN BASS, J. I., GABELLONI, M. L., ALVAREZ, M. E., VERMEULEN, M. E., RUSSO, D. M., ZORREGUIETA, Á., GEFFNER, J. R. & TREVANI, A. S. 2008. Characterisation of bacterial DNA binding to human neutrophil surface. *Lab Invest,* 88**,** 926-937.

GABRILSKA, R. A. & RUMBAUGH, K. P. 2015. Biofilm models of polymicrobial infection. *Future Microbiol,* 10**,** 1997-2015.

GAFFEN, S. L. & HAJISHENGALLIS, G. 2008. A new inflammatory cytokine on the block: re-thinking periodontal disease and the Th1/Th2 paradigm in the context of Th17 cells and IL-17. *J Dent Res,* 87**,** 817-28.

GALGUT, P. N. 2001. The relevance of pH to gingivitis and periodontitis. *J Int Acad Periodontol,* 3**,** 61-7.

GARCIA-MENDOZA, A., LIEBANA, J., CASTILLO, A. M., DE LA HIGUERA, A. & PIEDROLA, G. 1993. Evaluation of the capacity of oral streptococci to produce hydrogen peroxide. *J Med Microbiol,* 39**,** 434-439.

GARRETT, T. R., BHAKOO, M. & ZHANG, Z. 2008. Bacterial adhesion and biofilms on surfaces. *Prog Nat Sci,* 18**,** 1049-1056.
GEERING, B. & SIMON, H. U. 2011. Peculiarities of cell death mechanisms in neutrophils. *Cell Death Differ,* 18**,** 1457-69.
GEFFNER, J. R., FONTÁN, P. A., SORDELLI, D. O. & ISTURIZ, M. A. 1991. Neutrophil Erythrotoxicity Induced by Phorbol Myristate Acetate: Mechanisms Involved in Neutrophil Activation. *J Leukoc Biol,* 49**,** 352-359.
GHAFOOR, A., HAY, I. D. & REHM, B. H. 2011. Role of exopolysaccharides in *Pseudomonas aeruginosa* biofilm formation and architecture. *Appl Environ Microbiol,* 77**,** 5238-5246.
GHEZZI, E. M., LANGE, L. A. & SHIP, J. A. 2000. Determination of Variation of Stimulated Salivary Flow Rates. *J Dent Res,* 79**,** 1874-1878.
GIBBONS, R. J., HAY, D. I., CHILDS, W. C. & DAVIS, G. 1990. Role of cryptic receptors (cryptitopes) in bacterial adhesion to oral surfaces. *Arch Oral Biol,* 35**,** S107-S114.
GIGON, L., YOUSEFI, S., KARAULOV, A. & SIMON, H.-U. 2021. Mechanisms of toxicity mediated by neutrophil and eosinophil granule proteins. *Allergol Int,* 70**,** 30-38.
GLOAG, E. S., TURNBULL, L., HUANG, A., VALLOTTON, P., WANG, H., NOLAN, L. M., MILILLI, L., HUNT, C., LU, J. & OSVATH, S. R. 2013. Self-organisation of bacterial biofilms is facilitated by extracellular DNA. *Proc Natl Acad Sci,* 110**,** 11541-11546.
GOMEZ-SUAREZ, C., BUSSCHER, H. J. & VAN DER MEI, H. C. 2001. Analysis of bacterial detachment from substratum surfaces by the passage of air-liquid interfaces. *Appl Environ Microbiol,* 67**,** 2531-7.
GÓMEZ-SUÁREZ, C., BUSSCHER, H. J. & VAN DER MEI, H. C. 2001. Analysis of bacterial detachment from substratum surfaces by the passage of air-liquid interfaces. *Appl Environ Microbiol,* 67**,** 2531-7.
GOODWINE, J., GIL, J., DOIRON, A., VALDES, J., SOLIS, M., HIGA, A., DAVIS, S. & SAUER, K. 2019. Pyruvate-depleting conditions induce biofilm dispersion and enhance the efficacy of antibiotics in killing biofilms *in vitro* and *in vivo*. *Sci Rep,* 9**,** 3763.
GUPTA, A. K., HASLER, P., HOLZGREVE, W., GEBHARDT, S. & HAHN, S. 2005. Induction of neutrophil extracellular DNA lattices by placental microparticles and IL-8 and their presence in preeclampsia. *Hum Immunol,* 66**,** 1146-54.
HAJISHENGALLIS, G. 2015. Periodontitis: from microbial immune subversion to systemic inflammation. *Nat Rev Immunol,* 15**,** 30-44.
HAJISHENGALLIS, G. & LAMONT, R. J. 2016. Dancing with the stars: How choreographed bacterial interactions dictate nososymbiocity and give rise to keystone pathogens, accessory pathogens, and pathobionts. *Trends Microbiol,* 24**,** 477-489.
HALLETT, M. B. & LLOYDS, D. 1995. Neutrophil priming: the cellular signals that say 'amber' but not 'green'. *Immunol Today,* 16**,** 264-8.
HANCOCK, L. E. & PEREGO, M. 2004. The *Enterococcus faecalis* fsr two-component system controls biofilm development through production of gelatinase. *J Bacteriol,* 186**,** 5629-5639.
HÄNSCH, G. M. 2012. Host Defence against Bacterial Biofilms: “Mission Impossible”? *ISRN Immunol,* 2012**,** 853123.
HASHAI, K., CHAPPLE, I. L., SHAPIRA, L., ASSADI, W., DADON, S. & POLAK, D. 2022. CD18 mediates neutrophil imperviousness to the *Aggregatibacter actinomycetemcomitans* JP2 clone in molar-incisor pattern periodontitis. *Front Immunol,* 13**,** 847372.
HASLETT, C., GUTHRIE, L. A., KOPANIAK, M. M., JOHNSTON, R. B., JR. & HENSON, P. M. 1985. Modulation of multiple neutrophil functions by preparative methods or trace concentrations of bacterial lipopolysaccharide. *Am J Pathol,* 119**,** 101-110.
HASSANI, M., HELLEBREKERS, P., CHEN, N., VAN AALST, C., BONGERS, S., HIETBRINK, F., KOENDERMAN, L. & VRISEKOOP, N. 2020. On the origin of low-density neutrophils. *J Leukoc Biol,* 107**,** 809-818.

HAUBEK, D., ENNIBI, O.-K., POULSEN, K., VÆTH, M., POULSEN, S. & KILIAN, M. 2008. Risk of aggressive periodontitis in adolescent carriers of the JP2 clone of *Aggregatibacter (Actinobacillus) actinomycetemcomitans* in Morocco: a prospective longitudinal cohort study. *Lancet,* 371**,** 237-242.

HENNINGHAM, A., DÖHRMANN, S., NIZET, V. & COLE, J. N. 2015. Mechanisms of group A *Streptococcus* resistance to reactive oxygen species. *FEMS Microbiol Rev,* 39**,** 488-508.

HERRMANN, J. M. & MEYLE, J. 2015. Neutrophil activation and periodontal tissue injury. *Periodontol 2000,* 69**,** 111-127.

HEYDORN, A., ERSBØLL, B., KATO, J., HENTZER, M., PARSEK, M. R., TOLKER-NIELSEN, T., GIVSKOV, M. & MOLIN, S. 2002. Statistical analysis of *Pseudomonas aeruginosa* biofilm development: impact of mutations in genes involved in twitching motility, cell-to-cell signaling, and stationary-phase sigma factor expression. *Appl Environ Microbiol,* 68**,** 2008-17.

HIRSCHFELD, J. 2014. Dynamic interactions of neutrophils and biofilms. *J Oral Microbiol,* 6**,** 26102.

HIRSCHFELD, J. 2019. Neutrophil subsets in periodontal health and disease: A mini review. *Front Immunol,* 10**,** 3001.

HIRSCHFELD, J., DOMMISCH, H., SKORA, P., HORVATH, G., LATZ, E., HOERAUF, A., WALLER, T., KAWAI, T., JEPSEN, S., DESCHNER, J. & BEKEREDJIAN-DING, I. 2015. Neutrophil extracellular trap formation in supragingival biofilms. *Int J Med Microbiol,* 305**,** 453-463.

HIRSCHFELD, J., ROBERTS, H. M., CHAPPLE, I. L., PARČINA, M., JEPSEN, S., JOHANSSON, A. & CLAESSON, R. 2016. Effects of *Aggregatibacter actinomycetemcomitans* leukotoxin on neutrophil migration and extracellular trap formation. *J Oral Microbiol,* 8**,** 33070.

HIRSCHFELD, J., WHITE, P. C., MILWARD, M. R., COOPER, P. R. & CHAPPLE, I. L. C. 2017. Modulation of neutrophil extracellular trap and reactive oxygen species release by periodontal bacteria. *Infect Immun,* 85**,** e00297-17.

HOFFMANN, K., SPERLING, K., OLINS, A. L. & OLINS, D. E. 2007. The granulocyte nucleus and lamin B receptor: avoiding the ovoid. *Chromosoma,* 116**,** 227-35.

HOIBY, N. 1974. Epidemiological investigations of the respiratory tract bacteriology in patients with cystic fibrosis. *Acta Pathol Microbiol Scand B Microbiol Immunol,* 82**,** 541-50.

HØIBY, N., BJARNSHOLT, T., MOSER, C., BASSI, G., COENYE, T., DONELLI, G., HALL-STOODLEY, L., HOLÁ, V., IMBERT, C. & KIRKETERP-MØLLER, K. 2015. ESCMID guideline for the diagnosis and treatment of biofilm infections 2014. *Clin Microbiol Infect,* 21**,** S1-S25.

HOMSI, N. & KAPILA, R. 2020. *Aggregatibacter actinomycetemcomitans* causing empyema necessitans and pyomyositis in an immunocompetent patient. *Cureus,* 12**,** e9454.

HOSHINO, T., KAWAGUCHI, M., SHIMIZU, N., HOSHINO, N., OOSHIMA, T. & FUJIWARA, T. 2004. PCR detection and identification of oral streptococci in saliva samples using gtf genes. *Diagn Microbiol Infect Dis,* 48**,** 195-199.

HU, W., LI, L., SHARMA, S., WANG, J., MCHARDY, I., LUX, R., YANG, Z., HE, X., GIMZEWSKI, J. K. & LI, Y. 2012. DNA builds and strengthens the extracellular matrix in *Myxococcus xanthus* biofilms by interacting with exopolysaccharides. *PloS one,* 7**,** e51905.

HU, Y. 2012. Isolation of human and mouse neutrophils *ex vivo* and *in vitro*. *Leucocytes.* Springer.

HUANG, W., LE, S., SUN, Y., LIN, D. J., YAO, M., SHI, Y. & YAN, J. 2022. Mechanical Stabilisation of a Bacterial Adhesion Complex. *J Am Chem So,* 144**,** 16808-16818.

HUANG, W. M., GIBSON, S. J., FACER, P., GU, J. & POLAK, J. M. 1983. Improved section adhesion for immunocytochemistry using high molecular weight polymers of l-lysine as a slide coating. *Histochemistry,* 77**,** 275-279.

IMLAY, J. A. 2008. Cellular defences against superoxide and hydrogen peroxide. *Annu Rev Biochem,* 77**,** 755-776.

IMMLER, R., SIMON, S. I. & SPERANDIO, M. 2018. Calcium signalling and related ion channels in neutrophil recruitment and function. *Eur J Clin Investig,* 48**,** e12964.

INOZEMTSEV, V., SERGUNOVA, V., VOROBJEVA, N., KOZLOVA, E., SHERSTYUKOVA, E., LYAPUNOVA, S. & CHERNYSH, A. 2023. Stages of NETosis development upon stimulation of neutrophils with activators of different types. *Int J Mol Sci,* 24.

ISHII, N., FUNAMI, K., TATEMATSU, M., SEYA, T. & MATSUMOTO, M. 2014. Endosomal localisation of TLR8 confers distinctive proteolytic processing on human myeloid cells. *J Immunol,* 193**,** 5118-28.

JAILLON, S., GALDIERO, M. R., DEL PRETE, D., CASSATELLA, M. A., GARLANDA, C. & MANTOVANI, A. 2013. Neutrophils in innate and adaptive immunity. *Semin Immunopathol,* 35**,** 377-94.

JAKUBOVICS, N. S. & BURGESS, J. G. 2015. Extracellular DNA in oral microbial biofilms. *Microbes Infect,* 17**,** 531-7.

JAKUBOVICS, N. S., SHIELDS, R. C., RAJARAJAN, N. & BURGESS, J. G. 2013. Life after death: the critical role of extracellular DNA in microbial biofilms. *Lett Appl Microbiol,* 57**,** 467-475.

JAUMOUILLÉ, V. & WATERMAN, C. M. 2020. Physical constraints and forces involved in phagocytosis. *Front immunol,* 11**,** 1097.

JAUREGUI, C. E., WANG, Q., WRIGHT, C. J., TAKEUCHI, H., URIARTE, S. M. & LAMONT, R. J. 2013. Suppression of T-Cell Chemokines by *Porphyromonas gingivalis*. *Infect Immun,* 81**,** 2288-2295.

JENKINSON, H. F. & LAMONT, R. J. 2005. Oral microbial communities in sickness and in health. *Trends Microbiol,* 13**,** 589-595.

JENSEN, A., SCHOLZ, C. F. P. & KILIAN, M. 2016. Re-evaluation of the taxonomy of the Mitis group of the genus *Streptococcus* based on whole genome phylogenetic analyses, and proposed reclassification of *Streptococcus dentisani* as *Streptococcus oralis* subsp. dentisani comb. nov., *Streptococcus tigurinus* as *Streptococcus oralis* subsp. tigurinus comb. nov., and *Streptococcus oligofermentans* as a later synonym of *Streptococcus cristatus*. *Int J Syst Evol Microbiol,* 66**,** 4803-4820.

JESAITIS, A. J., FRANKLIN, M. J., BERGLUND, D., SASAKI, M., LORD, C. I., BLEAZARD, J. B., DUFFY, J. E., BEYENAL, H. & LEWANDOWSKI, Z. 2003. Compromised host defence on *Pseudomonas aeruginosa* biofilms: characterisation of neutrophil and biofilm interactions. *J Immunol,* 171**,** 4329-4339.

JIANG, Q., ZHAO, Y., SHUI, Y., ZHOU, X., CHENG, L., REN, B., CHEN, Z. & LI, M. 2021. Interactions between neutrophils and periodontal pathogens in late-onset periodontitis. *Front Cell Infect Microbiol,* 11**,** 627328.

JOHANSSON, A., CLAESSON, R., HÄNSTRÖM, L., SANDSTRÖM, G. & KALFAS, S. 2000. Polymorphonuclear leukocyte degranulation induced by leukotoxin from *Actinobacillus actinomycetemcomitans*. *J Periodontal Res,* 35**,** 85-92.

JOHANSSON, A., JESAITIS, A. J., LUNDQVIST, H., MAGNUSSON, K.-E., SJÖLIN, C., KARLSSON, A. & DAHLGREN, C. 1995. Different subcellular localisation of cytochrome b and the dormant NADPH-oxidase in neutrophils and macrophages: effect on the production of reactive oxygen species during phagocytosis. *Cell Immunol,* 161**,** 61-71.

JONES, E. A., MCGILLIVARY, G. & BAKALETZ, L. O. 2013. Extracellular DNA within a nontypeable *Haemophilus influenzae*-induced biofilm binds human beta defensin-3 and reduces its antimicrobial activity. *J Innate immun,* 5**,** 24-38.

JÓZSEF, L., KHREISS, T. & FILEP, J. G. 2004. CpG Motifs in Bacterial DNA Delay Apoptosis of Neutrophil Granulocytes. *Faseb J,* 18**,** 1776-8.

KAHL, B. C. 2014. Small colony variants (SCVs) of *Staphylococcus aureus*--a bacterial survival strategy. *Infect Genet Evol,* 21**,** 515-22.

KAPLAN, J. B., PERRY, M. B., MACLEAN, L. L., FURGANG, D., WILSON, M. E. & FINE, D. H. 2001. Structural and genetic analyses of O polysaccharide from *Actinobacillus actinomycetemcomitans* serotype f. *Infect Immun,* 69**,** 5375-5384.

KAPLAN, M. J. & RADIC, M. 2012. Neutrophil extracellular traps: double-edged swords of innate immunity. *J Immunol,* 189**,** 2689-95.

KARLAN, M. S., SKOBEL, B., GRIZZARD, M., CASSISI, N. J., SINGLETON, G. T., BUSCEMI, P. & GOLDBERG, E. P. 1980. Myringotomy tube materials: bacterial adhesion and infection. *Otolaryngol Head Neck Surg,* 88**,** 783-795.

KARLSSON, A., NIXON, J. B. & MCPHAIL, L. C. 2000. Phorbol myristate acetate induces neutrophil NADPH-oxidase activity by two separate signal transduction pathways: dependent or independent of phosphatidylinositol 3-kinase. *J leukoc biol,* 67**,** 396-404.

KÄRPÄNOJA, P., HARJU, I., RANTAKOKKO-JALAVA, K., HAANPERÄ, M. & SARKKINEN, H. 2014. Evaluation of two matrix-assisted laser desorption ionisation–time of flight mass spectrometry systems for identification of viridans group streptococci. *Eur J Clin Microbiol Infect Dis,* 33**,** 779-788.

KAYA, E., GRASSI, L., BENEDETTI, A., MAISETTA, G., PILEGGI, C., DI LUCA, M., BATONI, G. & ESIN, S. 2020. *In vitro* interaction of *Pseudomonas aeruginosa* biofilms with human peripheral blood mononuclear cells. *Front Cell Infect Microbiol,* 10**,** 187.

KAYA, T. & KOSER, H. 2012. Direct Upstream Motility in *Escherichia coli*. *Biophysic J,* 102**,** 1514-1523.

KELK P, A. H., CLAESSON R, SANDSTRÖM G, SJÖSTEDT A, JOHANSSON A 2009. Inflammatory cell death of human macrophages induced by *Aggregatibacter actinomycetemcomitans* leukotoxin. *Cell Death Dis,* 10;2**,** e126.

KENNY, E. F., HERZIG, A., KRÜGER, R., MUTH, A., MONDAL, S., THOMPSON, P. R., BRINKMANN, V., BERNUTH, H. V. & ZYCHLINSKY, A. 2017. Diverse stimuli engage different neutrophil extracellular trap pathways. *Elife,* 6**,** e24437.

KHAN, T. Z., WAGENER, J. S., BOST, T., MARTINEZ, J., ACCURSO, F. J. & RICHES, D. W. 1995. Early pulmonary inflammation in infants with cystic fibrosis. *Am J Respir Crit Care Med,* 151**,** 1075-82.

KHARAZMI, A., GIWERCMAN, B. & HØIBY, N. 1999. [16] Robbins device in biofilm research. *Methods Enzymol.* Elsevier.

KIEDROWSKI, M. R. & HORSWILL, A. R. 2011. New approaches for treating staphylococcal biofilm infections. *Ann N Y Acad Sci,* 1241**,** 104-121.

KIM, M. K., INGREMEAU, F., ZHAO, A., BASSLER, B. L. & STONE, H. A. 2016. Local and global consequences of flow on bacterial quorum sensing. *Nat Microbiol,* 1**,** 15005.

KITCHEN, E., ROSSI, A. G., CONDLIFFE, A. M., HASLETT, C. & CHILVERS, E. R. 1996. Demonstration of reversible priming of human neutrophils using platelet-activating factor. *Blood,* 88**,** 4330-7.

KOBAYASHI, S. D., MALACHOWA, N. & DELEO, F. R. 2017. Influence of microbes on neutrophil life and death. *Front Cell Infect Microbiol,* 7**,** 159.

KOBAYASHI, S. D., VOYICH, J. M., BURLAK, C. & DELEO, F. R. 2005. Neutrophils in the innate immune response. *Arch Immunol Ther Exp (Warsz),* 53**,** 505-17.

KÖCKRITZ-BLICKWEDE, M. V., CHOW, O., GHOCHANI, M. & NIZET, V. 2010. 7 - Visualisation and Functional Evaluation of Phagocyte Extracellular Traps. *In:* KABELITZ, D. & KAUFMANN, S. H. E. (eds.) *Methods Microbiol.* Academic Press.

KOGA, T., OKAHASHI, N., YAMAMOTO, T., MIZUNO, J., INOUE, M. & HAMADA, S. 1983. Purification and immunochemical characterisation of *Streptococcus sanguis* ATCC 10557 serotype II carbohydrate antigen. *Infect Immun,* 42**,** 696-700.

KOLACZKOWSKA, E. & KUBES, P. 2013. Neutrophil recruitment and function in health and inflammation. *Nat Rev Immunol,* 13**,** 159-75.

KOLENBRANDER, P. E., ANDERSEN, R. N., BLEHERT, D. S., EGLAND, P. G., FOSTER, J. S. & PALMER, R. J., JR. 2002. Communication among oral bacteria. *Microbiol Mol Biol Rev,* 66**,** 486-505, table of contents.

KONIG, M. F. & ANDRADE, F. 2016. A critical reappraisal of neutrophil extracellular traps and NETosis mimics based on differential requirements for protein citrullination. *Front Immunol,* 7**,** 461.

KOO, H., FALSETTA, M. & KLEIN, M. 2013. The exopolysaccharide matrix: a virulence determinant of cariogenic biofilm. *J Dent Res,* 92**,** 1065-1073.

KOSTAKIOTI, M., HADJIFRANGISKOU, M. & HULTGREN, S. J. 2013. Bacterial biofilms: development, dispersal, and therapeutic strategies in the dawn of the postantibiotic era. *Cold Spring Harb Perspect Med,* 3**,** a010306.

KRAUS, R. F. & GRUBER, M. A. 2021. Neutrophils—From bone marrow to first-line defence of the innate immune system. *Front Immunol,* 12.

KREFT, J.-U. & WIMPENNY, J. W. 2001. Effect of EPS on biofilm structure and function as revealed by an individual-based model of biofilm growth. *Water Sci Technol,* 43**,** 135-135.

KRETH, J., MERRITT, J. & QI, F. 2009. Bacterial and host interactions of oral streptococci. *DNA Cell Biol,* 28**,** 397-403.

KRIEG, D. P., HELMKE, R. J., GERMAN, V. F. & MANGOS, J. A. 1988. Resistance of mucoid *Pseudomonas aeruginosa* to nonopsonic phagocytosis by alveolar macrophages *in vitro*. *Infect Immun,* 56**,** 3173-9.

KRISTENSEN, M. F., ZENG, G., NEU, T. R., MEYER, R. L., BAELUM, V. & SCHLAFER, S. 2017. Osteopontin adsorption to Gram-positive cells reduces adhesion forces and attachment to surfaces under flow. *J Oral Microbiol,* 9**,** 1379826.

KRSMANOVIC, M., BISWAS, D., ALI, H., KUMAR, A., GHOSH, R. & DICKERSON, A. K. 2021. Hydrodynamics and surface properties influence biofilm proliferation. *Adv Colloid Interface Sci,* 288**,** 102336.

KRZYŚCIAK, W., PLUSKWA, K. K., JURCZAK, A. & KOŚCIELNIAK, D. 2013. The pathogenicity of the *Streptococcus* genus. *Eur J Clin Microbiol Infect Dis,* 32**,** 1361-76.

KULKARNI, M. & MUKHERJEE, A. 2017. Understanding B-DNA to A-DNA transition in the right-handed DNA helix: Perspective from a local to global transition. *Prog Biophys Mol Biol,* 128**,** 63-73.

KUMAR, P. S., GRIFFEN, A. L., MOESCHBERGER, M. L. & LEYS, E. J. 2005. Identification of candidate periodontal pathogens and beneficial species by quantitative 16S clonal analysis. *J Clin Microbiol,* 43**,** 3944-3955.

KUMAR, V. & SHARMA, A. 2010. Neutrophils: Cinderella of innate immune system. *Int Immunopharmacol,* 10**,** 1325-34.

LAHOZ-BENEYTEZ, J., ELEMANS, M., ZHANG, Y., AHMED, R., SALAM, A., BLOCK, M., NIEDERALT, C., ASQUITH, B. & MACALLAN, D. 2016. Human neutrophil kinetics: modeling of stable isotope labeling data supports short blood neutrophil half-lives. *Blood,* 127**,** 3431-3438.

LAKSCHEVITZ, F. S., HASSANPOUR, S., RUBIN, A., FINE, N., SUN, C. & GLOGAUER, M. 2016. Identification of neutrophil surface marker changes in health and inflammation using high-throughput screening flow cytometry. *Exp Cell Res,* 342**,** 200-209.

LALLY, E. T., KIEBA, I. R., SATO, A., GREEN, C. L., ROSENBLOOM, J., KOROSTOFF, J., WANG, J. F., SHENKER, B. J., ORTLEPP, S., ROBINSON, M. K. & BILLINGS, P. C. 1997. RTX toxins recognise a beta2 integrin on the surface of human target cells. *J Biol Chem,* 272**,** 30463-9.

LAM, J., CHAN, R., LAM, K. & COSTERTON, J. W. 1980. Production of mucoid microcolonies by *Pseudomonas aeruginosa* within infected lungs in cystic fibrosis. *Infect Immun,* 28**,** 546-56.

LÄMMERMANN, T. & SIXT, M. 2009. Mechanical modes of 'amoeboid'cell migration. *Curr Opin Cell biol,* 21**,** 636-644.

LAMONT, R. J. & JENKINSON, H. F. 1998. Life below the gum line: pathogenic mechanisms of *Porphyromonas gingivalis*. *Microbiol Mol Biol Rev,* 62**,** 1244-63.

LAMONT, R. J., KOO, H. & HAJISHENGALLIS, G. 2018. The oral microbiota: dynamic communities and host interactions. *Nat Rev Microbiol,* 16**,** 745-759.

LANG, T. A., BERGUM, P. W., LICHTER, J. P. & SPRAGG, R. G. 1982. The labeling of rabbit neutrophils with [111In] oxine. *J Immunol Methods,* 51**,** 293-305.

LAUDERDALE, K. J., MALONE, C. L., BOLES, B. R., MORCUENDE, J. & HORSWILL, A. R. 2010. Biofilm dispersal of community-associated methicillin-resistant *Staphylococcus aureus* on orthopedic implant material. *J Ortho Res,* 28**,** 55-61.

LAUKOVÁ, L., KONEČNÁ, B., JANOVIČOVÁ, Ľ., VLKOVÁ, B. & CELEC, P. 2020. Deoxyribonucleases and their applications in biomedicine. *Biomolecules,* 10.

LAWRENCE, S. M., CORRIDEN, R. & NIZET, V. 2018. The ontogeny of a neutrophil: Mechanisms of granulopoiesis and homeostasis. *Microbiol Mol Biol Rev,* 82.
LEATHERS, T. D. & BISCHOFF, K. M. 2011. Biofilm formation by strains of *Leuconostoc citreum* and *L. mesenteroides*. *Biotechno lett,* 33**,** 517-523.
LEATHERS, T. D., RICH, J. O., BISCHOFF, K. M., SKORY, C. D. & NUNNALLY, M. S. 2019. Inhibition of *Streptococcus mutans* and *S. sobrinus* biofilms by liamocins from *Aureobasidium pullulans*. *Biotechnol Rep (Amst),* 21**,** e00300.
LECUYER, S., RUSCONI, R., SHEN, Y., FORSYTH, A., VLAMAKIS, H., KOLTER, R. & STONE, H. A. 2011. Shear stress increases the residence time of adhesion of *Pseudomonas aeruginosa*. *Biophys J,* 100**,** 341-50.
LEID, J. G. 2009. Bacterial biofilms resist key host defences. *Microbe,* 4**,** 66-70.
LEWIS, K. 2012. Persister Cells: Molecular Mechanisms Related to Antibiotic Tolerance. *In:* COATES, A. R. M. (ed.) *Antibiotic Resistance.* Berlin, Heidelberg: Springer Berlin Heidelberg.
LEY, K., LAUDANNA, C., CYBULSKY, M. I. & NOURSHARGH, S. 2007. Getting to the site of inflammation: the leukocyte adhesion cascade updated. *Nat Rev Immunol,* 7**,** 678-89.
LI, D. & WU, M. 2021. Pattern recognition receptors in health and diseases. *Signal Transduct Target Ther,* 6**,** 291.
LI, M. W., ZHOU, L. & LAM, H. M. 2015. Paraformaldehyde fixation may lead to misinterpretation of the subcellular localisation of plant high mobility group box proteins. *PLoS One,* 10**,** e0135033.
LI, P., LI, M., LINDBERG, M. R., KENNETT, M. J., XIONG, N. & WANG, Y. 2010. PAD4 is essential for antibacterial innate immunity mediated by neutrophil extracellular traps. *J Exp Med,* 207**,** 1853-1862.
LI, Y., WANG, W., YANG, F., XU, Y., FENG, C. & ZHAO, Y. 2019. The regulatory roles of neutrophils in adaptive immunity. *Cell Commun Signal,* 17**,** 147.
LIAO, S., KLEIN, M. I., HEIM, K. P., FAN, Y., BITOUN, J. P., AHN, S. J., BURNE, R. A., KOO, H., BRADY, L. J. & WEN, Z. T. 2014. *Streptococcus mutans* extracellular DNA is upregulated during growth in biofilms, actively released via membrane vesicles, and influenced by components of the protein secretion machinery. *J Bacteriol,* 196**,** 2355-66.
LIN, A., LOUGHMAN, J. A., ZINSELMEYER, B. H., MILLER, M. J. & CAPARON, M. G. 2009. Streptolysin S inhibits neutrophil recruitment during the early stages of *Streptococcus pyogenes* infection. *Infect Immun,* 77**,** 5190-201.
LIU, C., SHAO, C., ZHANG, L. & HUANG, Q. 2023. Chapter 3 - Biomaterials and MSCs composites in regenerative medicine. *In:* ZHANG, L., HAN, Z., WANG, J., LI, Z. & HUANG, Q. (eds.) *Mesenchymal Stem Cells.* Academic Press.
LIU, T., CHENG, Y. F., SHARMA, M. & VOORDOUW, G. 2017. Effect of fluid flow on biofilm formation and microbiologically influenced corrosion of pipelines in oilfield produced water. *J Petrol Sci Eng,* 156**,** 451-459.
LO, S. K., VAN SEVENTER, G. A., LEVIN, S. M. & WRIGHT, S. D. 1989. Two leukocyte receptors (CD11a/CD18 and CD11b/CD18) mediate transient adhesion to endothelium by binding to different ligands. *J Immunol,* 143**,** 3325-9.
LOESCHE, W. J. & GROSSMAN, N. S. 2001. Periodontal Disease as a Specific, albeit Chronic, Infection: Diagnosis and Treatment. *Clin Microbiol Rev,* 14**,** 727.
LOO, C. Y., CORLISS, D. A. & GANESHKUMAR, N. 2000. *Streptococcus gordonii* biofilm formation: identification of genes that code for biofilm phenotypes. *J Bacteriol,* 182**,** 1374-82.
LUCAS, C. D., ALLEN, K. C., DORWARD, D. A., HOODLESS, L. J., MELROSE, L. A., MARWICK, J. A., TUCKER, C. S., HASLETT, C., DUFFIN, R. & ROSSI, A. G. 2013. Flavones induce neutrophil apoptosis by down-regulation of Mcl-1 via a proteasomal-dependent pathway. *FASEB J,* 27**,** 1084-1094.
LUND-PALAU, H., TURNBULL, A. R., BUSH, A., BARDIN, E., CAMERON, L., SOREN, O., WIERRE-GORE, N., ALTON, E. W., BUNDY, J. G. & CONNETT, G. 2016. *Pseudomonas aeruginosa* infection in

cystic fibrosis: pathophysiological mechanisms and therapeutic approaches. *Expert Rev Respir Med,* 10**,** 685-697.

LUNDQVIST, H. & DAHLGREN, C. 1996. Isoluminol-enhanced chemiluminescence: A sensitive method to study the release of superoxide anion from human neutrophils. *Free Radic Biol Med,* 20**,** 785-792.

LUO, T. L., VANEK, M. E., GONZALEZ-CABEZAS, C., MARRS, C. F., FOXMAN, B. & RICKARD, A. H. 2022. *In vitro* model systems for exploring oral biofilms: From single-species populations to complex multi-species communities. *J Appl Microbiol,* 132**,** 855-871.

LYNCH, A., VERMA, V., ZEGLINSKI, J., BANNIGAN, P. & RASMUSON, Å. 2019. Face indexing and shape analysis of salicylamide crystals grown in different solvents. *CrystEngComm,* 21**,** 2648-2659.

MA, G. J., FERHAN, A. R., JACKMAN, J. A. & CHO, N.-J. 2020. Conformational flexibility of fatty acid-free bovine serum albumin proteins enables superior antifouling coatings. *Commun Mater,* 1**,** 45.

MACEY, M., MCCARTHY, D., VORDERMEIER, S., NEWLAND, A. & BROWN, K. 1995. Effects of cell purification methods on CD11b and L-selectin expression as well as the adherence and activation of leucocytes. *J Immunol Methods,* 181**,** 211-219.

MANFREDI, A. A., COVINO, C., ROVERE-QUERINI, P. & MAUGERI, N. 2015. Instructive influences of phagocytic clearance of dying cells on neutrophil extracellular trap generation. *Clin Exp Immunol,* 179**,** 24-9.

MANN, E. E. 2010. *Staphylococcus aureus cid and lrg operons mediate biofilm development under the influence of microenvironment*, University of Nebraska Medical Center.

MANNIRONI, C., SCERCH, C., FRUSCOLONI, P. & TOCCHINI-VALENTINI, G. P. 2000. Molecular recognition of amino acids by RNA aptamers: the evolution into an L-tyrosine binder of a dopamine-binding RNA motif. *Rna,* 6**,** 520-7.

MANSAB ALI, S., NAVINDRA KUMARI, P. & ENG HWA, W. 2018. Alternative approaches to combat medicinally important biofilm-forming pathogens. *In:* SAHRA, K. (ed.) *Antimicrobials, Antibiotic Resistance, Antibiofilm Strategies and Activity Methods.* Rijeka: IntechOpen.

MARISCAL, A., LOPEZ-GIGOSOS, R. M., CARNERO-VARO, M. & FERNANDEZ-CREHUET, J. 2009. Fluorescent assay based on resazurin for detection of activity of disinfectants against bacterial biofilm. *Appl Microbiol Biotechnol,* 82**,** 773-83.

MARTÍNEZ-GARCÍA, R., NADELL, C. D., HARTMANN, R., DRESCHER, K. & BONACHELA, J. A. 2018. Cell adhesion and fluid flow jointly initiate genotype spatial distribution in biofilms. *PLoS Comput Biol,* 14**,** e1006094.

MARTÍNEZ-HERNÁNDEZ, M., REYES-GRAJEDA, J. P., HANNIG, M. & ALMAGUER-FLORES, A. 2023. Salivary pellicle modulates biofilm formation on titanium surfaces. *Clin Oral Investig,* 27**,** 6135-6145.

MARTÍNEZ, D., VERMEULEN, M. N., TREVANI, A. A., CEBALLOS, A., SABATTÉ, J., GAMBERALE, R., ÁLVAREZ, M. A. E., SALAMONE, G., TANOS, T., COSO, O. A. & GEFFNER, J. 2006. Extracellular Acidosis Induces Neutrophil Activation by a Mechanism Dependent on Activation of Phosphatidylinositol 3-Kinase/Akt and ERK Pathways1. *J Immunol,* 176**,** 1163-1171.

MATHELIÉ-GUINLET, M., VIELA, F., ALSTEENS, D. & DUFRÊNE, Y. F. 2021. Stress-Induced Catch-Bonds to Enhance Bacterial Adhesion. *Trends in Microbiology,* 29**,** 286-288.

MATSUI, H., GRUBB, B. R., TARRAN, R., RANDELL, S. H., GATZY, J. T., DAVIS, C. W. & BOUCHER, R. C. 1998. Evidence for periciliary liquid layer depletion, not abnormal ion composition, in the pathogenesis of cystic fibrosis airways disease. *Cell,* 95**,** 1005-15.

MATTHEWS, J., WRIGHT, H., ROBERTS, A., COOPER, P. & CHAPPLE, I. 2007a. Hyperactivity and reactivity of peripheral blood neutrophils in chronic periodontitis. *Clin Exp Immunol,* 147**,** 255-264.

MATTHEWS, J. B., WRIGHT, H. J., ROBERTS, A., LING-MOUNTFORD, N., COOPER, P. R. & CHAPPLE, I. L. 2007b. Neutrophil hyper-responsiveness in periodontitis. *J Dent Res,* 86**,** 718-22.

MAYADAS, T. N., CULLERE, X. & LOWELL, C. A. 2014. The multifaceted functions of neutrophils. *Annual review of pathology,* 9**,** 181-218.
MCCALL, A. & EDGERTON, M. 2017. Real-time approach to flow cell imaging of *Candida albicans* biofilm development. *J fungi,* 3**,** 13.
MCLAUGHLIN, R. A. & HOOGEWERF, A. J. 2006. Interleukin-1β-induced growth enhancement of *Staphylococcus aureus* occurs in biofilm but not planktonic cultures. *Microb Pathog,* 41**,** 67-79.
MCPHERSON, A. & LARSON, S. B. 2018. Investigation into the binding of dyes within protein crystals. *Acta Crystallogr F Struct Biol Commun,* 74**,** 593-602.
MEHANNY, M., KOCH, M., LEHR, C. M. & FUHRMANN, G. 2020. Streptococcal extracellular membrane vesicles Are rapidly internalised by immune cells and alter their cytokine release. *Front Immunol,* 11**,** 80.
MEI, M. L., CHU, C. H., LO, E. C. & SAMARANAYAKE, L. P. 2013. Preventing root caries development under oral biofilm challenge in an artificial mouth. *Med Oral Patol Oral Cir Bucal,* 18**,** e557.
MELAUGH, G., HUTCHISON, J., KRAGH, K. N., IRIE, Y., ROBERTS, A., BJARNSHOLT, T., DIGGLE, S. P., GORDON, V. D. & ALLEN, R. J. 2016. Shaping the growth behaviour of biofilms initiated from bacterial aggregates. *PLoS One,* 11**,** e0149683.
MERRITT, J. H., KADOURI, D. E. & O'TOOLE, G. A. 2005. Growing and analyzing static biofilms. *Curr Protoc Microbiol,* Chapter 1**,** Unit 1B.1.
MEYLE, E., STROH, P., GÜNTHER, F., HOPPY-TICHY, T., WAGNER, C. & HÄNSCH, G. M. 2010. Destruction of bacterial biofilms by polymorphonuclear neutrophils: relative contribution of phagocytosis, DNA release, and degranulation. *Int J Artif Organs,* 33**,** 608-620.
MEYLE, J. & CHAPPLE, I. 2015. Molecular aspects of the pathogenesis of periodontitis. *Periodontology 2000,* 69**,** 7-17.
MIKOLAI, C., BRANITZKI-HEINEMANN, K., INGENDOH-TSAKMAKIDIS, A., STIESCH, M., VON KÖCKRITZ-BLICKWEDE, M. & WINKEL, A. 2020. Neutrophils exhibit an individual response to different oral bacterial biofilms. *J Oral Microbiol,* 13**,** 1856565.
MILLER, J. K., BRANTNER, J. S., CLEMONS, C., KREIDER, K., MILSTED, A., WILBER, P., YUN, Y. H., YOUNGS, W. J., YOUNG, G. & BADAWY, H. T. 2014. Mathematical modelling of *Pseudomonas aeruginosa* biofilm growth and treatment in the cystic fibrosis lung. *Math Med Biol J IMA,* 31**,** 179-204.
MIRALDA, I. & URIARTE, S. M. 2021. Periodontal Pathogens' strategies disarm neutrophils to promote dysregulated inflammation. *Mol Oral Microbiol,* 36**,** 103-120.
MISTRY, D. & STOCKLEY, R. A. 2006. IgA1 protease. *Int J Biochem Cell Biol,* 38**,** 1244-1248.
MIYAKE, K. & ONJI, M. 2013. Endocytosis-free DNA sensing by cell surface TLR9 in neutrophils: Rapid defence with autoimmune risks. *Euro J Immunol,* 43**,** 2006-2009.
MIYAKE, K., SHIBATA, T., FUKUI, R., SATO, R., SAITOH, S.-I. & MURAKAMI, Y. 2022. Nucleic acid sensing by Toll-Like receptors in the endosomal compartment. *Front Immunol,* 13.
MOHANTY, R., ASOPA, S. J., JOSEPH, M. D., SINGH, B., RAJGURU, J. P., SAIDATH, K. & SHARMA, U. 2019. Red complex: Polymicrobial conglomerate in oral flora: A review. *J Family Med Prim Care,* 8**,** 3480-3486.
MOHANTY, T., SJÖGREN, J., KAHN, F., ABU-HUMAIDAN, A. H., FISKER, N., ASSING, K., MÖRGELIN, M., BENGTSSON, A. A., BORREGAARD, N. & SØRENSEN, O. E. 2015. A novel mechanism for NETosis provides antimicrobial defence at the oral mucosa. *Blood,* 126**,** 2128-37.
MOLIN, S. & TOLKER-NIELSEN, T. 2003. Gene transfer occurs with enhanced efficiency in biofilms and induces enhanced stabilisation of the biofilm structure. *Curr Opin Biotechnol,* 14**,** 255-261.
MONDS, R. D. & O'TOOLE, G. A. 2009. The developmental model of microbial biofilms: ten years of a paradigm up for review. *Trends Microbiol,* 17**,** 73-87.
MOORE, G. E., GERNER, R. E. & FRANKLIN, H. A. 1967. Culture of normal human leukocytes. *Jama,* 199**,** 519-24.

MOORMEIER, D. E. & BAYLES, K. W. 2014. Examination of *Staphylococcus epidermidis* biofilms using flow-cell technology. *Methods Mol Biol,* 1106**,** 143-55.
MOORMEIER, D. E., BOSE, J. L., HORSWILL, A. R. & BAYLES, K. W. 2014. Temporal and stochastic control of *Staphylococcus aureus* biofilm development. *mBio,* 5**,** e01341-14.
MOREIRA, J. M., TEODÓSIO, J. S., SILVA, F. C., SIMÕES, M., MELO, L. F. & MERGULHÃO, F. J. 2013. Influence of flow rate variation on the development of Escherichia coli biofilms. *Bioprocess Biosyst Eng,* 36**,** 1787-96.
MOSADDAD, S. A., TAHMASEBI, E., YAZDANIAN, A., REZVANI, M. B., SEIFALIAN, A., YAZDANIAN, M. & TEBYANIAN, H. 2019. Oral microbial biofilms: an update. *Eur J Clin Microbiol Infect Dis,* 38**,** 2005-2019.
MOSCOSO, M., GARCÍA, E. & LÓPEZ, R. 2006. Biofilm Formation by *Streptococcus pneumoniae*: Role of Choline, Extracellular DNA, and Capsular Polysaccharide in Microbial Accretion. *J Bacteriol,* 188**,** 7785-7795.
MOSIER, A. P. & CADY, N. C. 2011. Analysis of bacterial surface interactions using microfluidic systems. *Sci prog,* 94**,** 431-450.
MUCHOVA, M., BALACCO, D. L., GRANT, M. M., CHAPPLE, I. L. C., KUEHNE, S. A. & HIRSCHFELD, J. 2022. *Fusobacterium nucleatum* subspecies differ in biofilm forming ability *in vitro*. *Front Oral Health,* 3**,** 853618.
MULCAHY, H., CHARRON-MAZENOD, L. & LEWENZA, S. 2008. Extracellular DNA chelates cations and induces antibiotic resistance in *Pseudomonas aeruginosa* biofilms. *PLoS pathog,* 4**,** e1000213.
MULLARKY, I., SU, C., FRIEZE, N., PARK, Y. & SORDILLO, L. 2001. *Staphylococcus aureus* agr genotypes with enterotoxin production capabilities can resist neutrophil bactericidal activity. *Infect Immun,* 69**,** 45-51.
MUNAFO, D. B., JOHNSON, J. L., BRZEZINSKA, A. A., ELLIS, B. A., WOOD, M. R. & CATZ, S. D. 2009. DNase I inhibits a late phase of reactive oxygen species production in neutrophils. *J Innate Immun,* 1**,** 527-42.
MYERS, S., DO, T., MEADE, J. L., TUGNAIT, A., VERNON, J. J., PISTOLIC, J., HANCOCK, R. E. W., MARSH, P. D., TRIVEDI, H. M., CHEN, D. & DEVINE, D. A. 2021. Immunomodulatory streptococci that inhibit CXCL8 secretion and NFκB activation are common members of the oral microbiota. *J Med Microbiol,* 70.
NAIK, E. & DIXIT, V. M. 2011. Mitochondrial reactive oxygen species drive proinflammatory cytokine production. *J Exp Med,* 208**,** 417-420.
NAJMEH, S., COOLS-LARTIGUE, J., GIANNIAS, B., SPICER, J. & FERRI, L. E. 2015. Simplified human neutrophil extracellular traps (NETs) isolation and handling. *J Vis Exp*.
NGUYEN, G. T., GREEN, E. R. & MECSAS, J. 2017. Neutrophils to the ROScue: mechanisms of NADPH oxidase activation and bacterial resistance. *Front Cell Infect Microbiol,* 7**,** 373.
NILSSON, L. M., THOMAS, W. E., SOKURENKO, E. V. & VOGEL, V. 2006. Elevated Shear Stress Protects Escherichia coli Cells Adhering to Surfaces via Catch Bonds from Detachment by Soluble Inhibitors. *Applied and Environmental Microbiology,* 72**,** 3005-3010.
NISHINO, T. & MORIKAWA, K. 2002. Structure and function of nucleases in DNA repair: shape, grip and blade of the DNA scissors. *Oncogene,* 21**,** 9022-9032.
NORDENFELT, P. & TAPPER, H. 2011. Phagosome dynamics during phagocytosis by neutrophils. *J Leukoc Biol,* 90**,** 271-84.
NOROUZI, N., BHAKTA, H. C. & GROVER, W. H. 2017. Sorting cells by their density. *PLoS One,* 12**,** e0180520.
NUNES, J., FARIAS, I., VIEIRA, C., RIBEIRO, T., SAMPAIO, F. & MENEZES, V. 2020. Antimicrobial activity and toxicity of glass ionomer cement containing an essential oil. *Braz J Med Biol Res,* 53**,** e9468.
NUSSBAUM, G. & SHAPIRA, L. 2011. How has neutrophil research improved our understanding of periodontal pathogenesis? *J Clin Periodontol,* 38 Suppl 11**,** 49-59.

OETTINGER-BARAK, O., SELA, M., SPRECHER, H. & MACHTEI, E. 2014. Clinical and microbiological characterisation of localised aggressive periodontitis: a cohort study. *Aust Dent J,* 59**,** 165-171.

OKSHEVSKY, M. & MEYER, R. L. 2015. The role of extracellular DNA in the establishment, maintenance and perpetuation of bacterial biofilms. *Crit Rev Microbiol,* 41**,** 341-352.

OLIVER, A., CANTÓN, R., CAMPO, P., BAQUERO, F. & BLÁZQUEZ, J. 2000. High Frequency of Hypermutable *Pseudomonas aeruginosa* in Cystic Fibrosis Lung Infection. *Science,* 288**,** 1251-1253.

OSPINA-VILLA, J. D., ZAMORANO-CARRILLO, A., LOPEZ-CAMARILLO, C., CASTAÑON-SANCHEZ, C. A., SOTO-SANCHEZ, J., RAMIREZ-MORENO, E. & MARCHAT, L. A. 2015. Amino acid residues Leu135 and Tyr236 are required for RNA binding activity of CFIm25 in *Entamoeba histolytica*. *Biochimie,* 115**,** 44-51.

OVEISI, M., SHIFMAN, H., FINE, N., SUN, C., GLOGAUER, N., SENADHEERA, D. & GLOGAUER, M. 2019. Novel assay To characterise neutrophil responses to oral Biofilms. *Infect Immun,* 87.

OZUNA, H., URIARTE, S. M. & DEMUTH, D. R. 2021. The hunger games: *Aggregatibacter actinomycetemcomitans* exploits human neutrophils as an epinephrine source for survival. *Front Immunol,* 12**,** 707096.

PAGANELLI, F. L., WILLEMS, R. J., JANSEN, P., HENDRICKX, A., ZHANG, X., BONTEN, M. J. & LEAVIS, H. L. 2013. *Enterococcus faecium* biofilm formation: identification of major autolysin AtlAEfm, associated Acm surface localisation, and AtlAEfm-independent extracellular DNA Release. *mBio,* 4**,** e00154.

PAGE, R. C., OFFENBACHER, S., SCHROEDER, H. E., SEYMOUR, G. J. & KORNMAN, K. S. 1997. Advances in the pathogenesis of periodontitis: summary of developments, clinical implications and future directions. *Periodontol 2000,* 14**,** 216-48.

PALMER JR, R. J., KAZMERZAK, K., HANSEN, M. C. & KOLENBRANDER, P. E. 2001. Mutualism versus independence: strategies of mixed-species oral biofilms *in vitro* using saliva as the sole nutrient source. *Infect Immun,* 69**,** 5794-5804.

PALMER, L. J., CHAPPLE, I. L., WRIGHT, H. J., ROBERTS, A. & COOPER, P. R. 2012. Extracellular deoxyribonuclease production by periodontal bacteria. *J Periodontal Res,* 47**,** 439-45.

PALMER, R. J., KAZMERZAK, K., HANSEN, M. C. & KOLENBRANDER, P. E. 2001. Mutualism versus independence: Strategies of mixed-species oral biofilms *in vitro* using saliva as the sole nutrient source. *Infect Immun,* 69**,** 5794-5804.

PAPAPANOU, P. N., SANZ, M., BUDUNELI, N., DIETRICH, T., FERES, M., FINE, D. H., FLEMMIG, T. F., GARCIA, R., GIANNOBILE, W. V., GRAZIANI, F., GREENWELL, H., HERRERA, D., KAO, R. T., KEBSCHULL, M., KINANE, D. F., KIRKWOOD, K. L., KOCHER, T., KORNMAN, K. S., KUMAR, P. S., LOOS, B. G., MACHTEI, E., MENG, H., MOMBELLI, A., NEEDLEMAN, I., OFFENBACHER, S., SEYMOUR, G. J., TELES, R. & TONETTI, M. S. 2018. Periodontitis: Consensus report of workgroup 2 of the 2017 World Workshop on the Classification of Periodontal and Peri-Implant Diseases and Conditions. *J Periodontol,* 89 Suppl 1**,** S173-s182.

PAPAYANNOPOULOS, V. 2019. Neutrophils facing biofilms: The battle of the barriers. *Cell Host Microbe,* 25**,** 477-479.

PAPAYANNOPOULOS, V., METZLER, K. D., HAKKIM, A. & ZYCHLINSKY, A. 2010. Neutrophil elastase and myeloperoxidase regulate the formation of neutrophil extracellular traps. *J Cell biol,* 191**,** 677-691.

PAPAYANNOPOULOS, V., STAAB, D. & ZYCHLINSKY, A. 2011. Neutrophil elastase enhances sputum solubilisation in cystic fibrosis patients receiving DNase therapy. *PLoS One,* 6**,** e28526.

PARAMONOVA, E., KALMYKOWA, O. J., VAN DER MEI, H. C., BUSSCHER, H. J. & SHARMA, P. K. 2009. Impact of Hydrodynamics on Oral Biofilm Strength. *J Dent Res,* 88**,** 922-926.

PARKER, H. & WINTERBOURN, C. C. 2012. Reactive oxidants and myeloperoxidase and their involvement in neutrophil extracellular traps. *Front Immunol,* 3**,** 424.

PARKER, H. A., JONES, H. M., KALDOR, C. D., HAMPTON, M. B. & WINTERBOURN, C. C. 2021. Neutrophil NET formation with microbial stimuli requires late stage NADPH oxidase activity. *Antioxidants (Basel),* 10.

PARKS, Q. M., YOUNG, R. L., POCH, K. R., MALCOLM, K. C., VASIL, M. L. & NICK, J. A. 2009. Neutrophil enhancement of *Pseudomonas aeruginosa* biofilm development: human F-actin and DNA as targets for therapy. *J Med Microbiol,* 58**,** 492-502.

PAUL, E., OCHOA, J. C., PECHAUD, Y., LIU, Y. & LINÉ, A. 2012. Effect of shear stress and growth conditions on detachment and physical properties of biofilms. *Water Res,* 46**,** 5499-5508.

PEARCE, C., BOWDEN, G. H., EVANS, M., FITZSIMMONS, S. P., JOHNSON, J., SHERIDAN, M. J., WIENTZEN, R. & COLE, M. F. 1995. Identification of pioneer viridans streptococci in the oral cavity of human neonates. *J Med Microbiol,* 42**,** 67-72.

PEKKONEN, M., KETOLA, T. & LAAKSO, J. T. 2013. Resource Availability and Competition Shape the Evolution of Survival and Growth Ability in a Bacterial Community. *PLOS ONE,* 8**,** e76471.

PEMBER, S. O., BARNES, K. C., BRANDT, S. J. & KINKADE, J. J. 1983. Density heterogeneity of neutrophilic polymorphonuclear leukocytes: gradient fractionation and relationship to chemotactic stimulation. *Blood,* 61**,** 1105-15.

PERIASAMY, S., CHALMERS, N. I., DU-THUMM, L. & KOLENBRANDER, P. E. 2009. *Fusobacterium nucleatum* ATCC 10953 requires *Actinomyces naeslundii* ATCC 43146 for growth on saliva in a three-species community that includes *Streptococcus oralis* 34. *Appl Environ Microbiol,* 75**,** 3250-7.

PERIASAMY, S. & KOLENBRANDER, P. E. 2010. Central role of the early coloniser *Veillonella* sp. in establishing multispecies biofilm communities with initial, middle, and late colonisers of enamel. *J Bacteriol,* 192**,** 2965-72.

PERMPANICH, P., KOWOLIK, M. J. & GALLI, D. M. 2006. Resistance of fluorescent-labelled *Actinobacillus actinomycetemcomitans* strains to phagocytosis and killing by human neutrophils. *Cell Microbiol,* 8**,** 72-84.

PERSAT, A., NADELL, C. D., KIM, M. K., INGREMEAU, F., SIRYAPORN, A., DRESCHER, K., WINGREEN, N. S., BASSLER, B. L., GITAI, Z. & STONE, H. A. 2015. The mechanical world of bacteria. *Cell,* 161**,** 988-997.

PETERSON, B. W., VAN DER MEI, H. C., SJOLLEMA, J., BUSSCHER, H. J. & SHARMA, P. K. 2013. A distinguishable role of eDNA in the viscoelastic relaxation of biofilms. *mBio,* 4**,** e00497-13.

PETTIT, R. K., WEBER, C. A., KEAN, M. J., HOFFMANN, H., PETTIT, G. R., TAN, R., FRANKS, K. S. & HORTON, M. L. 2005. Microplate Alamar blue assay for *Staphylococcus epidermidis* biofilm susceptibility testing. *Antimicrob Agents Chemother,* 49**,** 2612-2617.

PIGMAN, W., ELLIOTT JR, H. C. & LAFFRE, R. 1952. An artificial mouth for caries research. *J Dent Res,* 31**,** 627-633.

PILSCZEK, F. H., SALINA, D., POON, K. K., FAHEY, C., YIPP, B. G., SIBLEY, C. D., ROBBINS, S. M., GREEN, F. H., SURETTE, M. G., SUGAI, M., BOWDEN, M. G., HUSSAIN, M., ZHANG, K. & KUBES, P. 2010. A novel mechanism of rapid nuclear neutrophil extracellular trap formation in response to *Staphylococcus aureus*. *J Immunol,* 185**,** 7413-25.

PITT, W. G. & ROSS, S. A. 2003. Ultrasound Increases the Rate of Bacterial Cell Growth. *Biotechnol Prog,* 19**,** 1038-1044.

PLESKOVA, S. N., EROFEEV, A. S., VANEEV, A. N., GORELKIN, P. V., BOBYK, S. Z., KOLMOGOROV, V. S., BEZRUKOV, N. A. & LAZARENKO, E. V. 2023. ROS production by a single neutrophil cell and neutrophil population upon bacterial stimulation. *Biomedicines,* 11**,** 1361.

PRIEL, D. L. & KUHNS, D. B. 2019. 94 - Assessment of neutrophil function. *In:* RICH, R. R., FLEISHER, T. A., SHEARER, W. T., SCHROEDER, H. W., FREW, A. J. & WEYAND, C. M. (eds.) *Clinical Immunology (Fifth Edition).* London: Elsevier.

PROCTOR, R. A., VON EIFF, C., KAHL, B. C., BECKER, K., MCNAMARA, P., HERRMANN, M. & PETERS, G. 2006. Small colony variants: a pathogenic form of bacteria that facilitates persistent and recurrent infections. *Nat Rev Microbiol,* 4**,** 295-305.

QUINCE, C., WALKER, A. W., SIMPSON, J. T., LOMAN, N. J. & SEGATA, N. 2017. Shotgun metagenomics, from sampling to analysis. *Nat Biotechnol,* 35**,** 833-844.
RADA, B. 2019. Neutrophil extracellular traps. *Methods Mol Biol,* 1982**,** 517-528.
RAGHUPATHI, P. K., LIU, W., SABBE, K., HOUF, K., BURMØLLE, M. & SØRENSEN, S. J. 2018. Synergistic interactions within a multispecies biofilm enhance individual species protection against grazing by a pelagic protozoan. *Front Microbiol,* 8**,** 2649.
RAINEY, K., MICHALEK, S. M., WEN, Z. T. & WU, H. 2019. Glycosyltransferase-mediated biofilm matrix dynamics and virulence of *Streptococcus mutans*. *Appl Environ Microbiol,* 85**,** e02247-18.
RAMACHANDRA, S. S., WRIGHT, P., HAN, P., ABDAL-HAY, A., LEE, R. S. B. & IVANOVSKI, S. 2023. Evaluating models and assessment techniques for understanding oral biofilm complexity. *Microbiologyopen,* 12**,** e1377.
RAMIREZ, T., SHRESTHA, A. & KISHEN, A. 2019. Inflammatory potential of monospecies biofilm matrix components. *Int Endod J,* 52**,** 1020-1027.
RAMOS PERFECTO, D., MOROMI NAKATA, H., MARTÍNEZ CADILLO, E. & MENDOZA ROJAS, A. 2010. *Aggregatibacter actinomycetemcomitans*: Patógeno importante en la periodontitis. *Odontología Sanmarquina,* 13**,** 42-45.
RASHEED, Z. 2008. Hydroxyl radical damaged Immunoglobulin G in patients with rheumatoid arthritis: Biochemical and immunological studies. *Clin Biochem,* 41**,** 663-669.
REEVES, E. P., LU, H., JACOBS, H. L., MESSINA, C. G. M., BOLSOVER, S., GABELLA, G., POTMA, E. O., WARLEY, A., ROES, J. & SEGAL, A. W. 2002. Killing activity of neutrophils is mediated through activation of proteases by K+ flux. *Nature,* 416**,** 291-297.
RELUCENTI, M., FAMILIARI, G., DONFRANCESCO, O., TAURINO, M., LI, X., CHEN, R., ARTINI, M., PAPA, R. & SELAN, L. 2021. Microscopy methods for biofilm imaging: Focus on SEM and VP-SEM pros and cons. *Biology (Basel),* 10.
REPO, H., ROCHON, Y. P., SCHWARTZ, B. R., SHARAR, S. R., WINN, R. K. & HARLAN, J. M. 1997. Binding of human peripheral blood polymorphonuclear leukocytes to E-selectin (CD62E) does not promote their activation. *J Immunol Methods,* 159**,** 943-951.
RICH, A. & ZHANG, S. 2003. Timeline: Z-DNA: the long road to biological function. *Nat Rev Genet,* 4**,** 566-72.
RICHARDS, V. P., PALMER, S. R., PAVINSKI BITAR, P. D., QIN, X., WEINSTOCK, G. M., HIGHLANDER, S. K., TOWN, C. D., BURNE, R. A. & STANHOPE, M. J. 2014. Phylogenomics and the dynamic genome evolution of the genus *Streptococcus*. *Genome Biol Evol,* 6**,** 741-753.
RIEDEL, T. E., BERELSON, W. M., NEALSON, K. H. & FINKEL, S. E. 2013. Oxygen consumption rates of bacteria under nutrient-limited conditions. *Appl Environ Microbiol,* 79**,** 4921-31.
RIGBY, K. M. & DELEO, F. R. 2012. Neutrophils in innate host defence against *Staphylococcus aureus* infections. *Semin Immunopathol,* 34**,** 237-59.
RIJNAARTS, H. H., NORDE, W., BOUWER, E. J., LYKLEMA, J. & ZEHNDER, A. J. 1993. Bacterial adhesion under static and dynamic conditions. *Appl Environ Microbiol,* 59**,** 3255-3265.
RIORDAN, J. R., ROMMENS, J. M., KEREM, B., ALON, N., ROZMAHEL, R., GRZELCZAK, Z., ZIELENSKI, J., LOK, S., PLAVSIC, N., CHOU, J. L. & ET AL. 1989. Identification of the cystic fibrosis gene: cloning and characterisation of complementary DNA. *Science,* 245**,** 1066-73.
ROBERTS, R. E. & HALLETT, M. B. 2019. Neutrophil cell shape change: Mechanism and signalling during cell spreading and phagocytosis. *Int J Mol Sci,* 20.
ROCCO, C. J., BAKALETZ, L. O. & GOODMAN, S. D. 2018. Targeting the HUbeta protein prevents *Porphyromonas gingivalis* from entering into preexisting biofilms. *J Bacteriol,* 200.
ROCCO, C. J., DAVEY, M. E., BAKALETZ, L. O. & GOODMAN, S. D. 2017. Natural antigenic differences in the functionally equivalent extracellular DNABII proteins of bacterial biofilms provide a means for targeted biofilm therapeutics. *Mol Oral Microbiol,* 32**,** 118-130.
RONDA, C., GARCÍA, J. L. & LÓPEZ, R. 1988. Characterisation of genetic transformation in *Streptococcus oralis* NCTC 11427: expression of the pneumococcal amidase in *S. oralis* using a new shuttle vector. *Mol Gen Genet,* 215**,** 53-57.

ROOS, D., VAN BRUGGEN, R. & MEISCHL, C. 2003. Oxidative killing of microbes by neutrophils. *Microbes Infect,* 5**,** 1307-15.
ROSS, G. D. 2002. Role of the lectin domain of Mac-1/CR3 (CD11b/CD18) in regulating intercellular adhesion. *Immunol Res,* 25**,** 219-227.
ROY, R., TIWARI, M., DONELLI, G. & TIWARI, V. 2018. Strategies for combating bacterial biofilms: A focus on anti-biofilm agents and their mechanisms of action. *Virulence*.
RUYECHAN, W. T. & OLSON, J. W. 1992. Surface lysine and tyrosine residues are required for interaction of the major herpes simplex virus type 1 DNA-binding protein with single-stranded DNA. *J Virol,* 66**,** 6273.
RYBTKE, M., JENSEN PETER, Ø., NIELSEN CLAUS, H. & TOLKER-NIELSEN, T. 2020. The extracellular polysaccharide matrix of *Pseudomonas aeruginosa* biofilms Is a determinant of polymorphonuclear leukocyte responses. *Infection and Immunity,* 89**,** 10.1128/iai.00631-20.
RYDER, M. I. 2010. Comparison of neutrophil functions in aggressive and chronic periodontitis. *Periodontol 2000,* 53**,** 124-137.
RZHEPISHEVSKA, O., HAKOBYAN, S., RUHAL, R., GAUTROT, J., BARBERO, D. & RAMSTEDT, M. 2013. The surface charge of anti-bacterial coatings alters motility and biofilm architecture. *Biomaterials Science,* 1**,** 589-602.
SADIQ, F. A., BURMØLLE, M., HEYNDRICKX, M., FLINT, S., LU, W., CHEN, W., ZHAO, J. & ZHANG, H. 2021. Community-wide changes reflecting bacterial interspecific interactions in multispecies biofilms. *Crit Rev Microbiol,* 47**,** 338-358.
SADOWSKA, B., WIĘCKOWSKA-SZAKIEL, M., PASZKIEWICZ, M. & RÓŻALSKA, B. 2013. The Immunomodulatory activity of *Staphylococcus aureus* products derived from biofilm and planktonic cultures. *Arch Immunol Ther Exp,* 61**,** 413-420.
SAIJONMAA-KOULUMIES, LEENA E. & LLOYD, DAVID H. 2002. Colonisation of neonatal puppies by *Staphylococcus intermedius*. *Veterinary Dermatol,* 13**,** 123-130.
SANTOS, D., PIRES, J. G., BRAGA, A. S., SALOMAO, P. M. A. & MAGALHAES, A. C. 2019. Comparison between static and semi-dynamic models for microcosm biofilm formation on dentin. *J Appl Oral Sci,* 27**,** e20180163.
SARANGAPANI, S. & JAYACHITRA, A. 2018. Targeting biofilm inhibition using quercetin – interaction with bacterial cell membrane and ROS mediated biofilm control. *Funct Foods Health Dis*.
SAUER, K., STOODLEY, P., GOERES, D. M., HALL-STOODLEY, L., BURMØLLE, M., STEWART, P. S. & BJARNSHOLT, T. 2022. The biofilm life cycle: expanding the conceptual model of biofilm formation. *Nat Rev Microbiol,* 20**,** 608-620.
SAUNDERS, K. A. & GREENMAN, J. 2000. The formation of mixed culture biofilms of oral species along a gradient of shear stress. *J Appl Microbiol,* 89**,** 564-72.
SAWANT, S. A., SOMANI, S. P., OMANWAR, S. K. & SOMANI, P. R. 2015. Chemical and photocatalytic degradation of crystal violet dye by indian edible chuna (Calcium Oxide/Hydroxide). *J Green Sci Technol,* 2**,** 45-48.
SCHAEDEL, C., DE MONESTROL, I., HJELTE, L., JOHANNESSON, M., KORNFALT, R., LINDBLAD, A., STRANDVIK, B., WAHLGREN, L. & HOLMBERG, L. 2002. Predictors of deterioration of lung function in cystic fibrosis. *Pediatr Pulmonol,* 33**,** 483-91.
SCHARNOW, A. M., SOLINSKI, A. E. & WUEST, W. M. 2019. Targeting *S. mutans* biofilms: a perspective on preventing dental caries. *Medchemcomm,* 10**,** 1057-1067.
SCHLAFER, S., MEYER, R. L., DIGE, I. & REGINA, V. R. 2017. Extracellular DNA contributes to dental biofilm stability. *Caries Res,* 51**,** 436-442.
SCHLAFER, S., RAARUP, M. K., WEJSE, P. L., NYVAD, B., STÄDLER, B. M., SUTHERLAND, D. S., BIRKEDAL, H. & MEYER, R. L. 2012. Osteopontin reduces biofilm formation in a multi-species model of dental biofilm. *PLoS One,* 7**,** e41534.
SCHULTZE, L. B., MALDONADO, A., LUSSI, A., SCULEAN, A. & EICK, S. 2021. The impact of the pH value on biofilm formation. *Monogr Oral Sci,* 29**,** 19-29.

SCHWIEGER, C. & BLUME, A. 2007. Interaction of poly(l-lysines) with negatively charged membranes: an FT-IR and DSC study. *Eur Biophys J,* 36**,** 437-450.
SCOTT, D. A. & KRAUSS, J. 2012. Neutrophils in periodontal inflammation. *Front Oral Biol,* 15**,** 56-83.
SEGAL, A. W., GEISOW, M., GARCIA, R., HARPER, A. & MILLER, R. 1981. The respiratory burst of phagocytic cells is associated with a rise in vacuolar p H. *Nature,* 290**,** 406-409.
SERRAGE, H. J., JEPSON, M. A., ROSTAMI, N., JAKUBOVICS, N. S. & NOBBS, A. H. 2021. Understanding the matrix: The role of extracellular DNA in oral biofilms. *Front Oral Health,* 2**,** 640129-640129.
SHAH, R., THOMAS, R. & MEHTA, D. S. 2017. Neutrophil priming: Implications in periodontal disease. *J Indian Soc Periodontol,* 21**,** 180-185.
SHAPIRA, L., TEPPER, P. & STEINBERG, D. 2000. The Interactions of Human Neutrophils with the Constituents of an Experimental Dental Biofilm. *J Dent Res,* 79**,** 1802-1807.
SHARMA, P., DIETRICH, T., FERRO, C. J., COCKWELL, P. & CHAPPLE, I. L. 2016. Association between periodontitis and mortality in stages 3-5 chronic kidney disease: NHANES III and linked mortality study. *J Clin Periodontol,* 43**,** 104-13.
SHARMA, P. K., GIBCUS, M. J., MEI, H. C. V. D. & BUSSCHER, H. J. 2005. Influence of Fluid Shear and Microbubbles on Bacterial Detachment from a Surface. *App Environ Microbiol,* 71**,** 3668-3673.
SHELLIS, R. 1978. A synthetic saliva for cultural studies of dental plaque. *Arch Oral Biol,* 23**,** 485-489.
SHEN, Y., MONROY, G. L., DERLON, N., JANJAROEN, D., HUANG, C., MORGENROTH, E., BOPPART, S. A., ASHBOLT, N. J., LIU, W.-T. & NGUYEN, T. H. 2015. Role of biofilm roughness and hydrodynamic conditions in *Legionella pneumophila* adhesion to and detachment from simulated drinking water biofilms. *Environ Sci Technol,* 49**,** 4274-4282.
SHESHACHALAM, A., SRIVASTAVA, N., MITCHELL, T., LACY, P. & EITZEN, G. 2014. Granule Protein Processing and Regulated Secretion in Neutrophils. *Front Immunol,* 5.
SILVA, M. P., CHIBEBE JUNIOR, J., JORJÃO, A. L., MACHADO, A. K., OLIVEIRA, L. D., JUNQUEIRA, J. C. & JORGE, A. O. 2012. Influence of artificial saliva in biofilm formation of *Candida albicans in vitro*. *Braz Oral Res,* 26**,** 24-8.
SILVA, M. T. 2010. When two is better than one: macrophages and neutrophils work in concert in innate immunity as complementary and cooperative partners of a myeloid phagocyte system. *J Leukoc Biol,* 87**,** 93-106.
SIMON-SORO, A., REN, Z., KROM BASTIAAN, P., HOOGENKAMP MICHEL, A., CABELLO-YEVES PEDRO, J., DANIEL SCOTT, G., BITTINGER, K., TOMAS, I., KOO, H. & MIRA, A. 2022. Polymicrobial aggregates in human saliva build the oral biofilm. *mBio,* 13**,** e00131-22.
SIMPSON, J. A., SMITH, S. E. & DEAN, R. T. 1988. Alginate inhibition of the uptake of *Pseudomonas aeruginosa* by macrophages. *J Gen Microbiol,* 134**,** 29-36.
SINGH, P. K., YADAV, V. K., KALIA, M., SHARMA, D., PANDEY, D. & AGARWAL, V. 2019. *Pseudomonas aeruginosa* quorum-sensing molecule N-(3-oxo-dodecanoyl)-L-homoserine lactone triggers mitochondrial dysfunction and apoptosis in neutrophils through calcium signaling. *Med Microbiol Immunol,* 208**,** 855-868.
SINGHAL, N., KUMAR, M., KANAUJIA, P. K. & VIRDI, J. S. 2015. MALDI-TOF mass spectrometry: an emerging technology for microbial identification and diagnosis. *Front Microbiol,* 6**,** 791.
SMITH, J. J., TRAVIS, S. M., GREENBERG, E. P. & WELSH, M. J. 1996. Cystic fibrosis airway epithelia fail to kill bacteria because of abnormal airway surface fluid. *Cell,* 85**,** 229-36.
SOCRANKSY, S. S. & HAFFAJEE, A. D. 2002. Dental biofilms: difficult therapeutic targets. *Periodontol 2000,* 28**,** 12-55.
SOCRANSKY, S. S., HAFFAJEE, A. D., CUGINI, M. A., SMITH, C. & KENT, R. L., JR. 1998. Microbial complexes in subgingival plaque. *J Clin Periodontol,* 25**,** 134-44.
SOKURENKO, E. V., VOGEL, V. & THOMAS, W. E. 2008. Catch-Bond Mechanism of Force-Enhanced Adhesion: Counterintuitive, Elusive, but … Widespread? *Cell Host & Microbe,* 4**,** 314-323.

SOUZA, J. G. S., BERTOLINI, M., THOMPSON, A., MANSFIELD, J. M., GRASSMANN, A. A., MAAS, K., CAIMANO, M. J., BARAO, V. A. R., VICKERMAN, M. M. & DONGARI-BAGTZOGLOU, A. 2020. Role of glucosyltransferase R in biofilm interactions between *Streptococcus oralis* and *Candida albicans*. *The ISME Journal,* 14**,** 1207-1222.

SPEERT, D. P., DIMMICK, J. E., PIER, G. B., SAUNDERS, J. M., HANCOCK, R. E. & KELLY, N. 1987. An immunohistological evaluation of *Pseudomonas aeruginosa* pulmonary infection in two patients with cystic fibrosis. *Pediatr Res,* 22**,** 743-7.

SPOERING, A. L. & GILMORE, M. S. 2006. Quorum sensing and DNA release in bacterial biofilms. *Curr Opin Microbiol,* 9**,** 133-137.

SRINIVASAN, K. & MAHADEVAN, R. 2010. Characterisation of proton production and consumption associated with microbial metabolism. *BMC Biotechnol,* 10**,** 2.

STAP, J., VAN MARLE, J., VAN VEEN, H. A. & ATEN, J. A. 2000. Coating of coverslips with glow-discharged carbon promotes cell attachment and spreading probably due to carboxylic groups. *Cytometry,* 39**,** 295-299.

STEINBERGER, R. E. & HOLDEN, P. A. 2005. Extracellular DNA in single- and multiple-species unsaturated biofilms. *Appl Environ Microbiol,* 71**,** 5404-10.

STENBIT, A. E. & FLUME, P. A. 2011. Pulmonary exacerbations in cystic fibrosis. *Curr Opin Pulm Med,* 17**,** 442-447.

STEWART, P. S. & FRANKLIN, M. J. 2008. Physiological heterogeneity in biofilms. *Nat Rev Microbiol,* 6**,** 199-210.

STIEFEL, P., SCHMIDT-EMRICH, S., MANIURA-WEBER, K. & REN, Q. 2015. Critical aspects of using bacterial cell viability assays with the fluorophores SYTO9 and propidium iodide. *BMC microbiology,* 15**,** 1-9.

STOJKOVA, P., SPIDLOVA, P. & STULIK, J. 2019. Nucleoid-associated protein HU: A lilliputian in gene regulation of bacterial virulence. *Front Cell Infect Microbiol,* 9**,** 159.

STOODLEY, P., SAUER, K., DAVIES, D. G. & COSTERTON, J. W. 2002. Biofilms as complex differentiated communities. *Annl Rev Microbiol,* 56**,** 187-209.

STRAUB, H., EBERL, L., ZINN, M., ROSSI, R. M., MANIURA-WEBER, K. & REN, Q. 2020. A microfluidic platform for in situ investigation of biofilm formation and its treatment under controlled conditions. *J Nanobiotechnol,* 18**,** 166.

STROH, P., GÜNTHER, F., MEYLE, E., PRIOR, B., WAGNER, C. & HÄNSCH, G. M. 2011. Host defence against *Staphylococcus aureus* biofilms by polymorphonuclear neutrophils: oxygen radical production but not phagocytosis depends on opsonisation with immunoglobulin G. *Immunobiol,* 216**,** 351-357.

SUDHAKARA, P., SELLAMUTHU, I. & ARUNI, A. W. 2019. Bacterial sialoglycosidases in virulence and pathogenesis. *Pathogens,* 8.

SUMIOKA, R., NAKATA, M., OKAHASHI, N., LI, Y., WADA, S., YAMAGUCHI, M., SUMITOMO, T., HAYASHI, M. & KAWABATA, S. 2017. *Streptococcus sanguinis* induces neutrophil cell death by production of hydrogen peroxide. *PLOS ONE,* 12**,** e0172223.

SUMMERS, C., RANKIN, S. M., CONDLIFFE, A. M., SINGH, N., PETERS, A. M. & CHILVERS, E. R. 2010. Neutrophil kinetics in health and disease. *Trends Immunol,* 31**,** 318-324.

SWAIN, S. D., ROHN, T. T. & QUINN, M. T. 2002. Neutrophil priming in host defence: role of oxidants as priming agents. *Antioxid Redox Signal,* 4**,** 69-83.

SWIFT, S., ALLAN DOWNIE, J., WHITEHEAD, N. A., BARNARD, A. M. L., SALMOND, G. P. C. & WILLIAMS, P. 2001. Quorum sensing as a population-density-dependent determinant of bacterial physiology. *Adv Microb Physiol.* Academic Press.

SWINGER, K. K. & RICE, P. A. 2004. IHF and HU: flexible architects of bent DNA. *Curr Opin Struct Biol,* 14**,** 28-35.

TAKEUCHI, O. & AKIRA, S. 2010. Pattern recognition receptors and inflammation. *Cell,* 140**,** 805-820.

TAKEUCHI, O., HOSHINO, K., KAWAI, T., SANJO, H., TAKADA, H., OGAWA, T., TAKEDA, K. & AKIRA, S. 1999. Differential roles of TLR2 and TLR4 in recognition of gram-negative and gram-positive bacterial cell wall components. *Immunity,* 11**,** 443-451.

TATSIY, O., DE CARVALHO OLIVEIRA, V., MOSHA, H. T. & MCDONALD, P. P. 2021. Early and late processes driving NET formation, and the Autocrine/Paracrine role of endogenous RAGE ligands. *Front Immunol,* 12**,** 675315.

TELES, F. R., TELES, R. P., SACHDEO, A., UZEL, N. G., SONG, X. Q., TORRESYAP, G., SINGH, M., PAPAS, A., HAFFAJEE, A. D. & SOCRANSKY, S. S. 2012. Comparison of microbial changes in early redeveloping biofilms on natural teeth and dentures. *J Periodontol,* 83**,** 1139-48.

THAKUR, S., CATTONI, D. I. & NÖLLMANN, M. 2015. The fluorescence properties and binding mechanism of SYTOX green, a bright, low photo-damage DNA intercalating agent. *Eur Biophys J,* 44**,** 337-348.

THÅLIN, C., LUNDSTRÖM, S., SEIGNEZ, C., DALESKOG, M., LUNDSTRÖM, A., HENRIKSSON, P., HELLEDAY, T., PHILLIPSON, M., WALLÉN, H. & DEMERS, M. 2018. Citrullinated histone H3 as a novel prognostic blood marker in patients with advanced cancer. *PLoS One,* 13**,** e0191231.

THANABALASURIAR, A., SCOTT, B. N. V., PEISELER, M., WILLSON, M. E., ZENG, Z., WARRENER, P., KELLER, A. E., SUREWAARD, B. G. J., DOZIER, E. A. & KORHONEN, J. T. 2019. Neutrophil extracellular traps confine *Pseudomonas aeruginosa* ocular biofilms and restrict brain invasion. *Cell Host Microbe,* 25**,** 526-536. e4.

THI, M. T. T., WIBOWO, D. & REHM, B. H. A. 2020. *Pseudomonas aeruginosa* biofilms. *Int J Mol Sci,* 21.

THOMAS, V. C., THURLOW, L. R., BOYLE, D. & HANCOCK, L. E. 2008. Regulation of autolysis-dependent extracellular DNA release by *Enterococcus faecalis* extracellular proteases influences biofilm development. *J Bacteriology,* 190**,** 5690-5698.

THURLOW, L. R., HANKE, M. L., FRITZ, T., ANGLE, A., ALDRICH, A., WILLIAMS, S. H., ENGEBRETSEN, I. L., BAYLES, K. W., HORSWILL, A. R. & KIELIAN, T. 2011. *Staphylococcus aureu*s biofilms prevent macrophage phagocytosis and attenuate inflammation *in vivo*. *J Immunol,* 186**,** 6585-6596.

THURNHEER, T. & BELIBASAKIS, G. N. 2018. *Streptococcus oralis* maintains homeostasis in oral biofilms by antagonising the cariogenic pathogen *Streptococcus mutans*. *Mol Oral Microbiol,* 33**,** 234-239.

TIGNER A, I. S., MURRAY IV 2021. *Histology, white blood cell*, StatPearls Publishing.

TIMISCHL, F. & INOUE, N. 2018. Increasing compositional backscattered electron contrast in scanning electron microscopy. *Ultramicroscopy,* 186**,** 82-93.

TING-BEALL, H. P., NEEDHAM, D. & HOCHMUTH, R. M. 1993. Volume and osmotic properties of human neutrophils. *Blood,* 81**,** 2774-80.

TING-BEALL, H. P., ZHELEV, D. V. & HOCHMUTH, R. M. 1995. Comparison of different drying procedures for scanning electron microscopy using human leukocytes. *Microsc Res Tech,* 32**,** 357-61.

TOLKER-NIELSEN, T. & STERNBERG, C. 2011. Growing and analyzing biofilms in flow chambers. *Curr Protoc Microbiol,* Chapter 1**,** Unit 1B.2.

TOLKER-NIELSEN, T. & STERNBERG, C. 2014. Methods for studying biofilm formation: flow cells and confocal laser scanning microscopy. *Methods Mol Biol,* 1149**,** 615-29.

TONETTI, M. S., GREENWELL, H. & KORNMAN, K. S. 2018. Staging and grading of periodontitis: Framework and proposal of a new classification and case definition. *J Periodontol,* 89 Suppl 1**,** S159-s172.

TRAXLER, M. F., SEYEDSAYAMDOST, M. R., CLARDY, J. & KOLTER, R. 2012. Interspecies modulation of bacterial development through iron competition and siderophore piracy. *Mol Microbiol,* 86**,** 628-644.

TREVANI, A. A. S., ANDONEGUI, G., GIORDANO, M., LÓPEZ, D. H., GAMBERALE, R., MINUCCI, F. & GEFFNER, J. R. 1999. Extracellular Acidification Induces Human Neutrophil Activation1. *J Immunol,* 162**,** 4849-4857.

TREVANI, A. S., CHORNY, A., SALAMONE, G., VERMEULEN, M., GAMBERALE, R., SCHETTINI, J., RAIDEN, S. & GEFFNER, J. 2003. Bacterial DNA activates human neutrophils by a CpG-independent pathway. *Eur J Immunol,* 33**,** 3164-3174.

TUON, F. F., DANTAS, L. R., SUSS, P. H. & TASCA RIBEIRO, V. S. 2022. Pathogenesis of the *Pseudomonas aeruginosa* biofilm: A review. *Pathogens,* 11**,** 300.

TUSON, H. H. & WEIBEL, D. B. 2013. Bacteria–surface interactions. *Soft Matter,* 9**,** 4368-4380.

URBAN, C. F., LOURIDO, S. & ZYCHLINSKY, A. 2006. How do microbes evade neutrophil killing? *Cell Microbiol,* 8**,** 1687-1696.

USTYANTSEVA, M., KHOKHLOVA, O. & AGADZHANYAN, V. 2019. Innovative Technologies in the evaluation of the neutrophil functional activity in sepsis. *Sysmex J Int,* 29**,** 34-39.

VAN DYKE, T. E., HOROSZEWICZ, H. U. & GENCO, R. J. 1982. The polymorphonuclear leukocyte (PMNL) locomotor defect in juvenile periodontitis. Study of random migration, chemokinesis and chemotaxis. *J Periodontol,* 53**,** 682-7.

VEGA, B. A., BELINKA, B. A., JR. & KACHLANY, S. C. 2019. *Aggregatibacter actinomycetemcomitans* leukotoxin (LtxA; Leukothera(®)): Mechanisms of action and therapeutic applications. *Toxins (Basel),* 11.

VELSKO, I. M., PEREZ, M. S. & RICHARDS, V. P. 2019. Resolving phylogenetic relationships for *Streptococcus mitis* and *Streptococcus oralis* through Core- and Pan-Genome analyses. *Genome Biol Evol,* 11**,** 1077-1087.

VENTURI, V. 2006. Regulation of quorum sensing in *Pseudomonas*. *FEMS Microbiol Rev,* 30**,** 274-291.

VIJAY, G. K. M. 2016. *The role of Toll-like receptor 9 and ammonia in the development of hepatic encephalopathy, brain oedema and immune dysfunction.* PhD, King's College London

VILAIN, S., COSETTE, P., ZIMMERLIN, I., DUPONT, J.-P., JUNTER, G.-A. & JOUENNE, T. 2004. Biofilm proteome: homogeneity or versatility? *J Proteome Res,* 3**,** 132-136.

VITKOV, L., KLAPPACHER, M., HANNIG, M. & KRAUTGARTNER, W. D. 2009. Extracellular neutrophil traps in periodontitis. *J Periodontal Res,* 44**,** 664-72.

VOLLMER, W., JORIS, B., CHARLIER, P. & FOSTER, S. 2008. Bacterial peptidoglycan (murein) hydrolases. *FEMS Microbiol Rev,* 32**,** 259-286.

VOS, T., ABAJOBIR, A. A., ABATE, K. H., ABBAFATI, C., ABBAS, K. M., ABD-ALLAH, F., ABDULKADER, R. S., ABDULLE, A. M., ABEBO, T. A., ABERA, S. F., ABOYANS, V., ABU-RADDAD, L. J., ACKERMAN, I. N., ADAMU, A. A., ADETOKUNBOH, O., AFARIDEH, M., AFSHIN, A., AGARWAL, S. K., AGGARWAL, R., AGRAWAL, A., AGRAWAL, S., AHMADIEH, H., AHMED, M. B., AICHOUR, M. T. E., AICHOUR, A. N., AICHOUR, I., AIYAR, S., AKINYEMI, R. O., AKSEER, N., AL LAMI, F. H., ALAHDAB, F., AL-ALY, Z., ALAM, K., ALAM, N., ALAM, T., ALASFOOR, D., ALENE, K. A., ALI, R., ALIZADEH-NAVAEI, R., ALKERWI, A. A., ALLA, F., ALLEBECK, P., ALLEN, C., AL-MASKARI, F., AL-RADDADI, R., ALSHARIF, U., ALSOWAIDI, S., ALTIRKAWI, K. A., AMARE, A. T., AMINI, E., AMMAR, W., AMOAKO, Y. A., ANDERSEN, H. H., ANTONIO, C. A. T., ANWARI, P., ÄRNLÖV, J., ARTAMAN, A., ARYAL, K. K., ASAYESH, H., ASGEDOM, S. W., ASSADI, R., ATEY, T. M., ATNAFU, N. T., ATRE, S. R., AVILA-BURGOS, L., AVOKPHAKO, E. F. G. A., AWASTHI, A., BACHA, U., BADAWI, A., BALAKRISHNAN, K., BANERJEE, A., BANNICK, M. S., BARAC, A., BARBER, R. M., BARKER-COLLO, S. L., BÄRNIGHAUSEN, T., BARQUERA, S., BARREGARD, L., BARRERO, L. H., BASU, S., BATTISTA, B., BATTLE, K. E., BAUNE, B. T., BAZARGAN-HEJAZI, S., BEARDSLEY, J., BEDI, N., BEGHI, E., BÉJOT, Y., BEKELE, B. B., BELL, M. L., BENNETT, D. A., BENSENOR, I. M., BENSON, J., BERHANE, A., BERHE, D. F., BERNABÉ, E., BETSU, B. D., BEURAN, M., BEYENE, A. S., BHALA, N., et al. 2017. Global, regional, and national incidence, prevalence, and years lived with disability for 328 diseases and injuries for 195 countries, 1990-2013;2016: a systematic analysis for the Global Burden of Disease Study 2016. *Lancet,* 390**,** 1211-1259.

VROUWENVELDER, J. S., HINRICHS, C., VAN DER MEER, W. G. J., VAN LOOSDRECHT, M. C. M. & KRUITHOF, J. C. 2009. Pressure drop increase by biofilm accumulation in spiral wound RO and NF membrane systems: role of substrate concentration, flow velocity, substrate load and flow direction. *Biofouling,* 25**,** 543-555.

WALKER, J. & HORSWILL, A. 2012. A coverslip-based technique for evaluating *Staphylococcus aureus* biofilm formation on human plasma. *Front Cell Infect Microbiol,* 2.

WALKER, T. S., TOMLIN, K. L., WORTHEN, G. S., POCH, K. R., LIEBER, J. G., SAAVEDRA, M. T., FESSLER, M. B., MALCOLM, K. C., VASIL, M. L. & NICK, J. A. 2005. Enhanced *Pseudomonas aeruginosa* biofilm development mediated by human neutrophils. *Infect Immun,* 73**,** 3693-701.

WANG, Y., LI, M., STADLER, S., CORRELL, S., LI, P., WANG, D., HAYAMA, R., LEONELLI, L., HAN, H. & GRIGORYEV, S. A. 2009. Histone hypercitrullination mediates chromatin decondensation and neutrophil extracellular trap formation. *J Cell Biol,* 184**,** 205-213.

WATSON, K., GOODERHAM, N. J., DAVIES, D. S. & EDWARDS, R. J. 1999. Nucleosomes Bind to Cell Surface Proteoglycans *. *J Biol Chem,* 274**,** 21707-21713.

WEBB, J. S., THOMPSON, L. S., JAMES, S., CHARLTON, T., TOLKER-NIELSEN, T., KOCH, B., GIVSKOV, M. & KJELLEBERG, S. 2003. Cell death in *Pseudomonas aeruginosa* biofilm development. *J Bacteriol,* 185**,** 4585-4592.

WELCH, J., ROSSETTI, B., RIEKEN, C., DEWHIRST, F. & BORISY, G. 2016. Biogeography of a human oral microbiome at the micron scale. *Proc Natl Acad Sci U S A*.

WESSEL, S. W., CHEN, Y., MAITRA, A., VAN DEN HEUVEL, E. R., SLOMP, A. M., BUSSCHER, H. J. & VAN DER MEI, H. C. 2014. Adhesion forces and composition of planktonic and adhering oral microbiomes. *J Dent Res,* 93**,** 84-8.

WHATMORE, A. M., EFSTRATIOU, A., PICKERILL, A. P., BROUGHTON, K., WOODARD, G., STURGEON, D., GEORGE, R. & DOWSON, C. G. 2000. Genetic relationships between clinical isolates of *Streptococcus pneumoniae*, *Streptococcus oralis*, and *Streptococcus mitis*: characterisation of "atypical" pneumococci and organisms allied to *S. mitis* harboring *S. pneumoniae* virulence factor-encoding genes. *Infect Immun,* 68**,** 1374-1382.

WHILEY, R. & BEIGHTON, D. 1998. Current classification of the oral streptococci. *Oral Microbiol Immunol,* 13**,** 195-216.

WHILEY, R. A., FLEMING, E. V., MAKHIJA, R. & WAITE, R. D. 2015. Environment and colonisation sequence are key parameters driving cooperation and competition between *Pseudomonas aeruginosa* Cystic Fibrosis strains and oral commensal Streptococci. *PLOS ONE,* 10**,** e0115513.

WHITCHURCH, C. B., TOLKER-NIELSEN, T., RAGAS, P. C. & MATTICK, J. S. 2002. Extracellular DNA required for bacterial biofilm formation. *Science,* 295**,** 1487.

WHITMORE, S. E. & LAMONT, R. J. 2011. The pathogenic persona of community-associated oral streptococci. *Mol Microbiol,* 81**,** 305-14.

WIJESINGHE, G., DILHARI, A., GAYANI, B., KOTTEGODA, N., SAMARANAYAKE, L. & WEERASEKERA, M. 2018. Influence of laboratory culture media on *in vitro* growth, adhesion, and biofilm formation of *Pseudomonas aeruginosa* and *Staphylococcus aureus*. *Med Princ Pract,* 28**,** 28-35.

WIJESINGHE, G. K., NISSANKA, M., MAIA, F. C., ROSSINI DE OLIVEIRA, T. & HÖFLING, J. F. 2024. Inverted amino acids reduce the adhesion and biofilm biomass of early oral colonisers. *Dent Med Probl,* 61**,** 385-390.

WIJETHUNGA, T. K., STOJAKOVIĆ, J., BELLUCCI, M. A., CHEN, X., MYERSON, A. S. & TROUT, B. L. 2018. General method for the identification of Crystal Faces using Raman spectroscopy combined with machine learning and application to the epitaxial growth of Acetaminophen. *Langmuir,* 34**,** 9836-9846.

WILTON, M., CHARRON-MAZENOD, L., MOORE, R. & LEWENZA, S. 2016. Extracellular DNA acidifies biofilms and induces aminoglycoside resistance in *Pseudomonas aeruginosa*. *Antimicrob Agents Chemother,* 60**,** 544-53.

WINTERBOURN, C. C., KETTLE, A. J. & HAMPTON, M. B. 2016. Reactive oxygen species and neutrophil function. *Annu Rev Biochem,* 85**,** 765-792.
WOOD, S. R., KIRKHAM, J., MARSH, P. D., SHORE, R. C., NATTRESS, B. & ROBINSON, C. 2000. Architecture of intact natural human plaque biofilms studied by confocal laser scanning microscopy. *J Dent Res,* 79**,** 21-7.
WU, C., LIM, JI Y., FULLER, GERALD G. & CEGELSKI, L. 2012. Quantitative Analysis of Amyloid-Integrated Biofilms Formed by Uropathogenic *Escherichia coli* at the Air-Liquid Interface. *Biophysic J,* 103**,** 464-471.
WU, Y. & OUTTEN, F. W. 2009. IscR controls iron-dependent biofilm formation in *Escherichia coli* by regulating type I fimbria expression. *J Bacteriol,* 191**,** 1248-57.
XU, F., LAGUNA, L. & SARKAR, A. 2019. Aging-related changes in quantity and quality of saliva: Where do we stand in our understanding? *J Texture Stud,* 50**,** 27-35.
XU, H., SOBUE, T., BERTOLINI, M., THOMPSON, A., VICKERMAN, M. M., NOBILE, C. J. & DONGARI-BAGTZOGLOU, A. 2017. *S. oralis* activates the Efg1 filamentation pathway in *C. albicans* to promote cross-kingdom interactions and mucosal biofilms. *Virulence,* 8**,** 1602-1617.
XU, H., SOBUE, T., THOMPSON, A., XIE, Z., POON, K., RICKER, A., CERVANTES, J., DIAZ, P. I. & DONGARI-BAGTZOGLOU, A. 2014. Streptococcal co-infection augments *Candida* pathogenicity by amplifying the mucosal inflammatory response. *Cell Microbiol,* 16**,** 214-231.
XU, Z., LIANG, Y., LIN, S., CHEN, D., LI, B., LI, L. & DENG, Y. 2016. Crystal violet and XTT assays on *Staphylococcus aureus* biofilm quantification. *Curr Microbiol,* 73**,** 474-482.
YADAV, M. K., SONG, J.-J., SINGH, B. P. & VIDAL, J. E. 2020. Chapter 1 - Microbial biofilms and human disease: A concise review. *In:* YADAV, M. K. & SINGH, B. P. (eds.) *New and future developments in microbial biotechnology and bioengineering: Microbial biofilms.* Elsevier.
YANG, T., YU, J., AHMED, T., NGUYEN, K., NIE, F., ZAN, R., LI, Z., HAN, P., SHEN, H., ZHANG, X., TAKAYAMA, S. & SONG, Y. 2023. Synthetic neutrophil extracellular traps dissect bactericidal contribution of NETs under regulation of α-1-antitrypsin. *Sci Adv,* 9**,** eadf2445.
YANG, X. 2010. Initial adhesion of EPS producing bacteria *Burkholderia cepacia*–the impact of cranberry juice. *Biofouling,* 28**,** 417-31.
YIN, W., WANG, Y., LIU, L. & HE, J. 2019. Biofilms: The microbial "Protective Clothing" in extreme environments. *Int J Mol Sci,* 20.
YIPP, B. G., PETRI, B., SALINA, D., JENNE, C. N., SCOTT, B. N., ZBYTNUIK, L. D., PITTMAN, K., ASADUZZAMAN, M., WU, K., MEIJNDERT, H. C., MALAWISTA, S. E., DE BOISFLEURY CHEVANCE, A., ZHANG, K., CONLY, J. & KUBES, P. 2012. Infection-induced NETosis is a dynamic process involving neutrophil multitasking *in vivo*. *Nat Med,* 18**,** 1386-93.
YOON, J., TERADA, A. & KITA, H. 2007. CD66b regulates adhesion and activation of human eosinophils. *J Immunol,* 179**,** 8454-8462.
YOSHIMOTO, T., FUJITA, T., KAJIYA, M., OUHARA, K., MATSUDA, S., KOMATSUZAWA, H., SHIBA, H. & KURIHARA, H. 2016. *Aggregatibacter actinomycetemcomitans* outer membrane protein 29 (Omp29) induces TGF-β-regulated apoptosis signal in human gingival epithelial cells via fibronectin/integrinβ1/FAK cascade. *Cell Microbiol,* 18**,** 1723-1738.
YOUNG, R. L., MALCOLM, K. C., KRET, J. E., CACERES, S. M., POCH, K. R., NICHOLS, D. P., TAYLOR-COUSAR, J. L., SAAVEDRA, M. T., RANDELL, S. H., VASIL, M. L., BURNS, J. L., MOSKOWITZ, S. M. & NICK, J. A. 2011. Neutrophil extracellular trap (NET)-mediated killing of *Pseudomonas aeruginosa*: evidence of acquired resistance within the CF airway, independent of CFTR. *PLoS One,* 6**,** e23637.
YOUSEFI, S., GOLD, J. A., ANDINA, N., LEE, J. J., KELLY, A. M., KOZLOWSKI, E., SCHMID, I., STRAUMANN, A., REICHENBACH, J., GLEICH, G. J. & SIMON, H. U. 2008. Catapult-like release of mitochondrial DNA by eosinophils contributes to antibacterial defence. *Nat Med,* 14**,** 949-53.

YOUSEFI, S., MIHALACHE, C., KOZLOWSKI, E., SCHMID, I. & SIMON, H. U. 2009. Viable neutrophils release mitochondrial DNA to form neutrophil extracellular traps. *Cell Death Differ,* 16**,** 1438-44.

YOUSSEF, P. P., MANTZIORIS, B. X., ROBERTS-THOMSON, P. J., AHERN, M. J. & SMITH, M. D. 1995. Effects of ex vivo manipulation on the expression of cell adhesion molecules on neutrophils. *J Immunol Methods,* 186**,** 217-224.

YUAN, L., STRAUB, H., SHISHAEVA, L. & REN, Q. 2023. Microfluidics for biofilm studies. *Annu Rev Anal Chem,* 16**,** 139-159.

ZÄHNER, D., GANDHI, A. R., YI, H. & STEPHENS, D. S. 2011. Mitis group streptococci express variable pilus islet 2 pili. *PLoS One,* 6**,** e25124.

ZHOU, H., COVENEY, A. P., WU, M., HUANG, J., BLANKSON, S., ZHAO, H., O'LEARY, D. P., BAI, Z., LI, Y., REDMOND, H. P., WANG, J. H. & WANG, J. 2018. Activation of both TLR and NOD signaling confers host innate immunity-mediated protection against microbial infection. *Front Immunol,* 9**,** 3082.

ZHU, H., JIA, Z., TRUSH, M. A. & LI, Y. R. 2016. A Highly Sensitive Chemiluminometric Assay for Real-Time Detection of Biological Hydrogen Peroxide Formation. *ROS,* 1**,** 216–227.

Appendix: IADR abstract 2020

3569

Comparison of Three in Vitro Models to Assess Biofilm-Neutrophil Interactions

Basmah Almaarik[1,2] , Tariq Khattak[3] , Raid Alakeel[2] , Paul R. Cooper[4] , Michael R. Milward[1] , Josefine Hirschfeld[1]

[1]University of Birmingham, Dental School & Hospital, Birmingham, UK; [2] King Saud University, College of Applied Medical Sciences, Riyadh, SA;
[3]University of Birmingham, School of Biomedical Sciences, Birmingham, UK ; [4]University of Otago, Faculty of Dentistry, NZL

OBJECTIVE

To investigate the best culture media for neutrophil survival.

Use selected culture media to culture *Streptococcus salivarius* biofilm and introduce neutrophils to assess biofilm-neutrophil interaction.

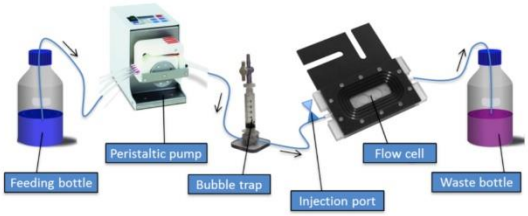

Figure1: *Flow cell setup*

INTRODUCTION

Microbial biofilms are defined as a three-dimensional structure, consisting of multicellular communities embedded in extracellular matrix. Mature biofilms can trigger caries and periodontal diseases. Mimicking oral biofilms *in vitro* remains challenging, due to their complexity and diversity. In addition, the interactions between host immune cells, such as neutrophils, and biofilms are not well understood. This study aimed to develop an *in vitro* model to assess biofilm formation and the interaction with neutrophils.

METHODS

Neutrophil survival was determined in six different bacterial growth media after 4h by trypan blue staining and cell counting. Three different oral streptococcal biofilm models were examined using static (multiwell plates) versus dynamic biofilm systems (flow cell with glass coupons (BioSurface Technologies Corp., USA) (**Fig 1**) and flow chamber with individual channel dimensions of 1x4x40 mm (DTU Bioengineering,Technical University of Denmark, DK) under varying flow conditions) in tryptic soy broth (TSB) supplemented with 2% glucose. Neutrophils were added to biofilms at different stages of maturity (0-3 days) and for different durations (4-48h). Biofilm structure containing neutrophils was assessed using confocal microscopy (Hoechst 33342 (Invitrogen, USA)), as well as H&E staining and light microscopy. Biofilm mass was quantified using crystal violet staining and spectrophotometry. All experiments were performed on duplicate coupons/ in duplicate wells.

RESULTS

Neutrophil survival over 4h was high in the majority of tested growth media (>95%) compared to RPMI + 10% FCS. (**Fig. 2**). Biofilm mass varied between different methods over time. In the flow chamber, thicker biofilms were noted after 5 days of growth than in the other biofilm models (**Fig. 3**). Biofilm thickness was directly proportional to the time of incubation in the static model and flow chamber, whereas the flow cell showed a decrease in biofilm thickness at day 3 of biofilm growth, which may be due to biofilm detachment under shear forces. The optimum flow rate was found to be 0.25ml/min. Neutrophils were observed in all biofilm models and setups, although nuclei appeared enlarged and rounded after incubation times of >4h, indicating cell death (**Fig. 4**).

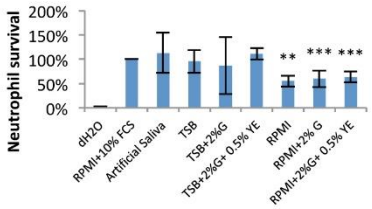

Figure 2: *Neutrophil survival of 3 healthy donors in different culture media (positive control: RPMI + 10% FCS, negative control: dH_2O). TSB = tryptic soy broth, G = glucose. **p=0.001, ***p<0.004 compared to the positive control (Student's t-test).*

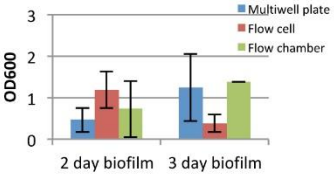

Figure3: *Biofilm mass determined by crystal violet staining, biofilm harvesting and spectrophotometry. After 24h (day 1), insufficient biofilm was available for harvesting and quantification.*

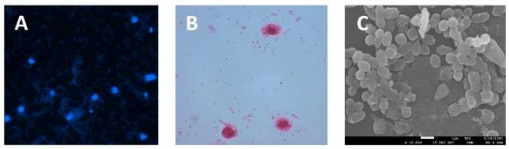

Figure 4: (A) *Fluorescent image showing neutrophils within an S. salivarius biofilm (Blue: Hoechst 33342). (B)* H&E staining of *neutrophils and bacteria (C) SEM of a 48h old S.salivarius static biofilm.*

CONCLUSION

Neutrophils showed good survival in TSB-based bacterial culture media and in artificial saliva

Co-culturing streptococcal biofilms and neutrophils in the same growth media was successful with regard to neutrophil survival and their adherence to biofilms

Dynamic flow devices show a lower neutrophil retention than the static model, but better mimic the conditions found in the gingival crevice. Therefore, the most suitable model will depend on the specific research question and experimental approach.